Mineralisation controls in the Ultramafic Sequence and T Zone of the Waterberg Project, north of the Hout River Shear Zone, Bushveld Complex, South Africa

Sehlabane Aleck Mkhabela

Supervisors:

Dr Marina Yudovskaya & Prof Judith Kinnaird

UNIVERSITY OF THE WITWATERSRAND, JOHANNESBURG

A dissertation submitted to the Faculty of Science, University of the Witwatersrand, Johannesburg in partial fulfilment of the requirements for Master of Science degree in Economic Geology.

21 October 2021

DECLARATION

I, **<u>Sehlabane Aleck Mkhabela</u>** declare that this dissertation is my own work submitted to the University of Witwatersrand, Johannesburg in partial fulfilment for the Master of Science degree in Economic Geology. The document has not been submitted to any other University for any degree or examination.

…………………………………………..

(Signature of candidate)

Date: 21 October 2021 **Location:** University of the Witwatersrand, Johannesburg

ABSTRACT

The Waterberg Project area is separated from the Northern Limb by the Hout River Shear Zone (HRSZ). Unlike the Northern Limb which unconformably overlies the Transvaal Supergroup and Archaean rocks of the Kaapvaal Craton, the Waterberg Project, located to the north of the HRSZ rests unconformably on granite-gneiss of the Southern Marginal Zone of the Limpopo Belt. The 1 100 m - 1 200 m thick magmatic succession strikes SW–NE and dips at 34–38° towards the NW. The 2.06 Ga succession is composed of basal Marginal pyroxenite sills, the Ultramafic Sequence (UmS), the Troctolite–Gabbronorite-Anorthosite sequence (TGA) and the Upper Zone (UZ). The entire succession is covered by thick 2.05 Ga – 1.95 Ga Waterberg Group sediments of the Setlaole (lower) and Makgabeng (upper) formations. Deposition of these sediments took place after an intense total erosion of the roof rocks and partial erosion of the Bushveld succession. The sedimentary succession was later succeeded by intrusions of 1.1 Ga dolerite sills linked to the Umkondo Igneous Province.

Platinum-group element (PGE)-Au-Cu and Ni sulphide mineralisation within the succession is confined to both the lower Ultramafic Sequence (the F zone) and the upper portion of the TGA (the T Zone). This mineralisation is intimately associated with conspicuous blebby and disseminated sulphides, which are predominantly chalcopyrite, pentlandite and pyrrhotite with traces of bornite in places. Within the UmS, the mineralised interval varies from 3 m to 100 m in thickness; with grade occurring in both the lower feldspathic pyroxenite (FP) and the upper feldspathic harzburgite (FH). Based on the grade-thickness attributes, the UmS (F Zone) has been subdivided into five highly mineralised zones/districts. The thinnest and less mineralised F - South, the thickest and well mineralised F - Central, F - Boundary South, F - Boundary North and F - North. In both the F- Central and F – Boundary South, well defined floor embayments seem to have played a crucial role in shaping and defining the thicker mineralisation. The mineralisation in both the F - Boundary North and the F - North seems to have not been controlled by such embayments. Unlike all the four F Zone districts, mineralisation within the F - North is better defined and developed in the FP rather than the FH. The prevalence of FP xenoliths within the FH of the F - Central suggests intense thermo mechanical erosion, entrainment and resorption during multiple FH magma influxes. These xenoliths are less common within the F - North where the FP is well preserved. As for the T Zone, the highest grade mineralisation is within the lower subzone (T2) gabbronorite, transgressing up-dip from west to east and along strike from SW to NE into the Lower Pegmatoidal Anorthosite (LPA). Both the T2 and the LPA are well endowed with mineralisation while the upper subzone (T1) and Upper Pegmatoidal Anorthosite (UPA) mineralisation is inconsistent and spatially sporadic. A well mineralised T0 subzone (*sensu amplo*) has been locally identified in the UZ. This mineralisation transgresses up-dip from west to east and along strike from SW to NE into the upper portion of the UPA converging along strike and up-dip with the T2/LPA mineralisation.

Overall, there is a lack of an upward decrease in tenor (that is PGE content in 100% sulphide) within the UmS. Instead, tenors are lower at the base of the UmS (FP), increasing upwards to higher levels towards the top of the FH. Since the sulphide content is higher than can be dissolved by intercumulus liquid, this implies that multiple UmS magma influxes gained their tenors elsewhere and were already rich in PGE sulphides when entering the resident magma chamber. Unlike in-situ segregation of sulphides observed in the Western Bushveld and T1 of Turfspruit, the sulphides within the UmS were probably transported and deposited as chonolithic crystal mush without undergoing segregation. Both lateral tenor variations and Cu/Pd variations seem to favour a westerly/SW feeder zone for the UmS magma influxes.

There is some degree of variability in both tenors and Cu/Pd trends within the T Zone. However, the trends seem to favour a westerly/SW feeder zone with higher tenors in both T2 and the LPA. Unlike the UmS, there seems to be higher levels of lateral anti-correlations between PGEs and Au tenors; implying that the higher Au content observed within the T Zone were obtained from a different source.

There is some lithostratigraphic and geochemical correlatability between mineralisation of the Waterberg Project and that of the distal Harriet's Wish and far distal Aurora Projects. However, the Waterberg mineralisation is comparable to the Platreef of both Mogalakwena and Turfspruit. In contrast to the western-eastern Bushveld, which is Pt dominant with high rhodium credit, the Waterberg Project is Pd dominant with high gold credit.

ACKNOWLEDGEMENTS

I would like to thank Dr. Marina Yudovskaya for the immense guidance throughout the course of this project. The site visit, the discussions on orthomagmatic processes, and the guidance on how to conduct and interpret PGE tenor calculations were very informative and much appreciated. I thank Professor Judith Kinnaird for guiding me through the process of putting together not only a comprehensive but also a coherent research report.

This project would have not been possible without the funding from my employer Platinum Group Metals (Pty) Ltd. I would therefore like to express my sincere gratitude to Mike Jones. A special thanks to my direct manager Thys Botha for granting me exclusive access to the company data and allowing me to dedicate some time to this work. Thanks to Edwin Matiwane for helping me to extract geological data out of the company's database. Laying out borehole core for logging can be a very strenuous task and I would therefore like to extend my gratitude to Lodwick Kgatla, Andries Ramoroka, Simon Rapheaga and Steven Laka for helping out.

Thanks to the technical staff of the School of Geoscience at the University of the Witwatersrand, particularly Caiphus Majola for assistance with sample preparations for thin sections.

Lastly, I would like to thank my wife Dimakatso Mkhabela for the absolute patience and support during the write-up process. Without your encouragements and support, putting together this project would have been extremely difficult. To my little daughter Hlumelo Mkhabela, thanks for the patience and the encouragement to "go back to work" referring to my write-up desk. I hope this achievement will inspire you and make you proud one day.

TABLE OF CONTENTS

LIST OF FIGURES

LIST OF TABLES

CHAPTER 1

INTRODUCTION

1.1 Preamble

During the year 2011, Platinum Group Metals Ltd. and its joint venture partners embarked on an exploration campaign north of the world-renowned northern limb of the Bushveld Complex. The objective of the campaign was to ascertain as to whether the northern limb together with the associated PGE mineralisation does extend further north of the Hout River Shear Zone, beneath the Waterberg Group sediments, as initially proposed by Van der Merwe (1976). Three boreholes (WB001, WB002 & WB003) were initially drilled, all of which intersected Bushveld Complex rocks. WB003 (the discovery drillhole) intersected mafic and ultramafic rocks endowed with PGEs. A lower and an upper mineralised zones were intersected with the lower mineralised zone referred to as the F Zone and the upper mineralised zone referred to as the T Zone. Since then, a total number of 437 boreholes was drilled in the area to delineate the extent of the mineralisation.

The uniqueness and widely unexpected nature of the deposit (now known as the Waterberg JV Resources) attracted many scholars. To date, intensive studies and publications on the magmatism (Kinnaird et al. 2017), geochronology (Huthmann et al., 2016), geochemistry (Huthman et al., 2017; Huthmann et al., 2018) and PGE mineralisation (McCreesh et al. 2018) have been done.

Although intensive studies with significant progress have been made on the project, a lot of research is still needed to fully understand the deposit. Although it has been shown that the Waterberg Project is endowed with higher palladium and higher gold content (Kinnaird et al., 2017) in comparison to the rest of the Bushveld Complex, the pegmatoidal anorthosites and gabbronorites of the T Zone need to be studied further to determine or account for the higher gold content.

1.2 Aims of the study

The aims of this study are four-fold: -

- To investigate mineralisation controls in the lower ultramafic sequence (F-Zone) and the upper T-Zone.
- To investigate vertical and lateral PGE + Au tenor variations within the two mineralised zones.
- To investigate Cu/Pd ratios with an aim of determining whether the igneous body experienced sulphide segregation or not.
- To compare/correlate the results with the rest of the Bushveld Complex, in particular, from the Aurora Project, Harriet's Wish Project and the distal Turfspruit Reef of the northern limb.

1.3 General Overview of the Bushveld Complex

The Paleoproterozioc Bushveld Complex is the world's largest layered intrusion located in the Republic of South Africa (Lee, 1996). This 2055.91 - 2054.89 Ma intrusion (Zeh et al., 2015) is long known to consist of five limbs (Willemse, 1969): The Western limb with NE dipping rock succession, the Northern and Eastern limb with westerly dipping rock successions, the Far western limb and the Bethal limb (Figure 1.1). According to recent geophysical studies, together with the exploration activities north of the Hout River Shear Zone, the areal extent of the Bushveld Complex is estimated to be > 90 000 km^2 (Finn et al., 2015).

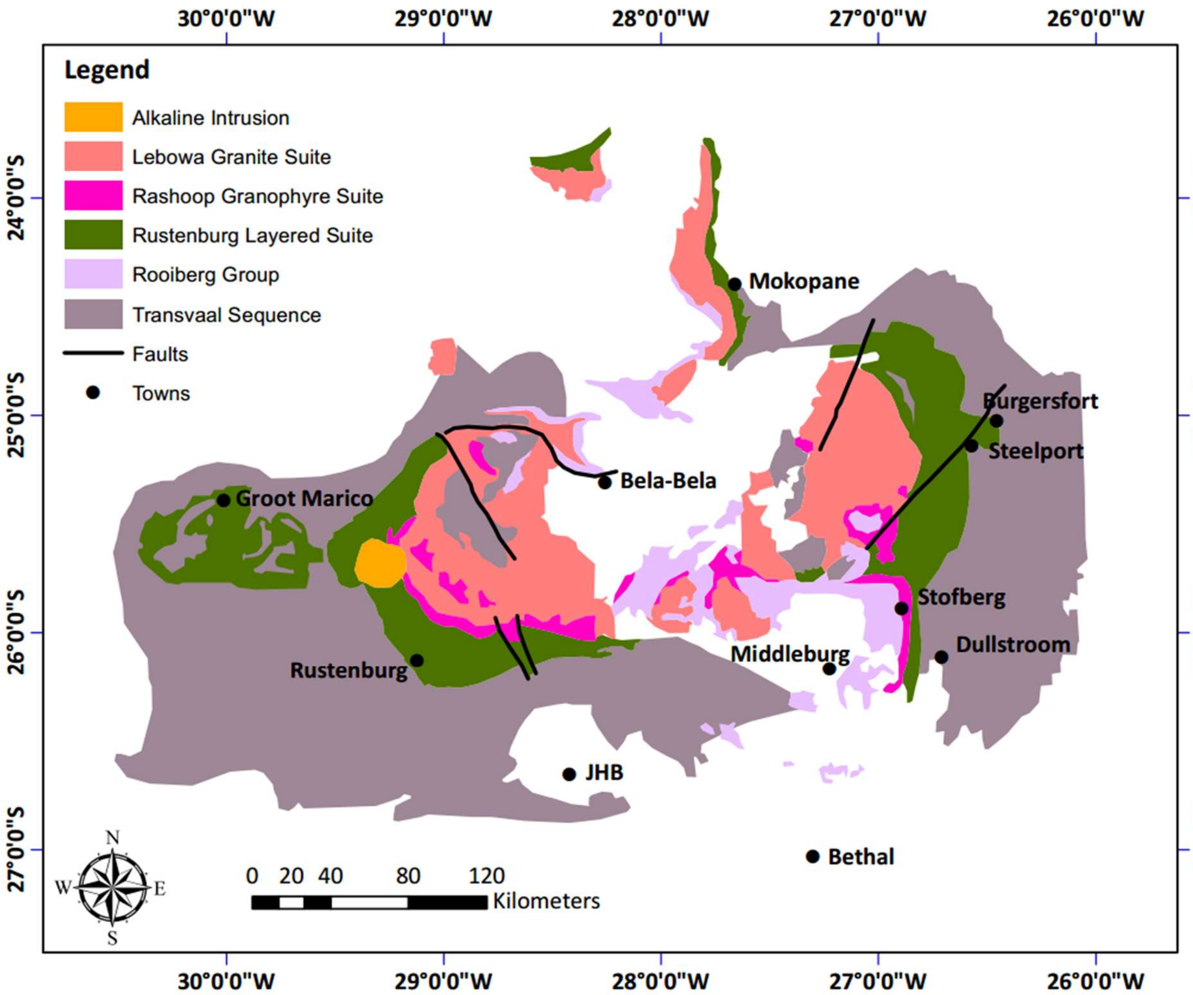

Figure 1.1. Simplified geological map of the Bushveld Large Igneous Province (modified after Kinnaird, 2017).

Although previous interpretations of the Bourgeur gravity anomalies by Meyer and De Beer (1987) suggested that the limbs of the Bushveld Complex are discrete bodies, recent gravity data interpretation suggests that the Western and Eastern limbs might be linked at depth (Finn et al., 2015). The link between the Eastern and Northern limbs is highly contentious due to geochemical and lithostratigraphic variations while the link between the Northern limb and the recently discovered Waterberg deposit is yet to be established. The possible relationship between the Northern limb, the Waterberg deposit and the south-dipping Villa Nora segment (Figure 1.2) have recently sparked an interesting debate (Huthmann et al. 2016, Kinnaird et al. 2017 and McCreesh et al. 2018).

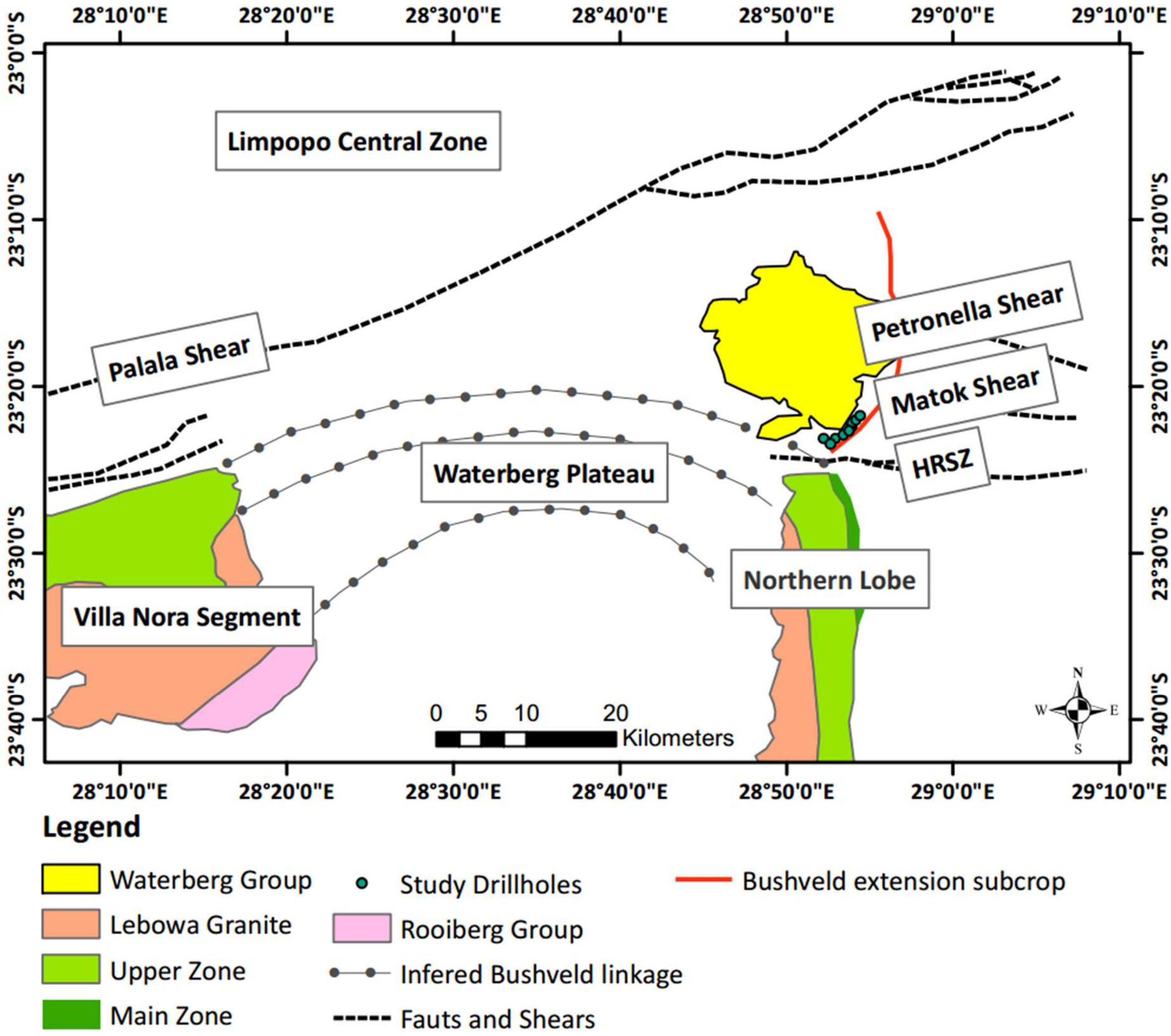

Figure 1.2. A map showing possible links between Northern Limb, the Waterberg Project extent (green dotted line) and the Villa Nora Segment as hypothesised by van der Merwe, (1976), Vermaak and van der Merwe, (1986) and Huthmann et al., (2016).

As initially suggested by SACS (1980) and later modified by Hatton and Schweitzer (1995), the Bushveld Complex is subdivided into the: -

- Lebowa Granite Suite
- Rashoop Granophyre Suite
- Rustenburg Layered Suite

Table 1.1 is a detailed description of the widely accepted subdivision of the Bushveld Complex succession.

Table 1.1. Subdivision and nomenclature of the Bushveld Complex from SACS (1980), Hatton and Schweitzer (1995). Modified by Kekana (2014).

LEBOWA GRANITE SUITE	Nebo, Lease, Makhutso, Klipkloof, Bobbejaankop, Balmoral and Verena Granites	
RASHOOP GRANOPHYRE SUITE	Stavoren and Diepkloof Granophyres, Rooikop Porphyritic Granite, Zwartbank Pseudogranophyre	
RUSTENBURG LAYERED SUITE	Upper Zone	Subzone C (Ol-Ap diorite)
		Subzone B (Ol-Mt gabbronorite)
		Subzone C (Mt gabbronorite)
	Main Zone	Upper Subzone (gabbronorite)
		Lower Subzone (gabbronorite, norite)
	Critical Zone	Upper Subzone (norite, anorthosite, pyroxenite)
		Lower Subzone (pyroxenite)
	Lower Zone	Upper Pyroxenite Subzone
		Harzburgite Subzone
		Lower Pyroxenite Subzone
	Marginal Zone (norite)	
ROOIBERG GROUP	Schrikkloof Formation (flow-banded rhyolite)	
	Kwaggasnek Formation (massive rhyolite)	
	Damwal Formation (dacite, rhyolite)	
	Dullstroom Formation (basaltic andesite)	

According to SACS (1980) and based on studies by von Gruenewaldt et al. (1985), Walraven (1986), Kruger (1994) the 8 km thick Rustenburg Layered Suite is subdivided into the: -

- Upper Zone
- Main Zone
- Critical Zone
- Lower Zone
- Marginal Zone

Table 1.2 is a detailed description of the currently accepted Rustenburg Layered Suite subdivision. In addition, Wilson (2015) described a thick succession of peridotite and pyroxenite that underlies the Marginal Zone in the Clapham trough the eastern limb. This was termed the Basal Ultramafic Sequence of the Bushveld Complex.

Table 1.2. Lithostratigraphic classification of the Rustenburg Layered Suite from SACS (1980), von Gruenewaldt et al. (1985), Walraven (1986), Kruger (1994)). Modified by Kekana (2014).

	Standard zonal subdivision (informal)		Nomenclature recommenced by SACS (1980), including subsequent additions					
	All areas		Eastern limb		Western limb		Northern limb	
RUSTENBURG LAYERED SUITE	Upper Zone	Subzone C	Roossenekal Subsuite[1]	Luipershoek Olivine Diorite		Bierkraal Magnetite Gabbro		Molendraai Magnetite Gabbro[1]
		Subzone B		Ironstone Magnetite Gabbro				
		Subzone A		Magnet Heights Gabbronorite				
	Main Zone	Upper Subzone[4]	Dsjate Subsuite[1]	Mapoch Gabbronorite		Pyramid Gabbronorite		Mapela Gabbronorite[1]
		Lower Subzone		Leolo Mountain Gabbronorite				
				Winnaarshoek Norite-Anorthosite				
	Critical Zone	Upper Subzone	Dwars River Subsuite[1]	Winterveld Norite-Anorthosite	Schilpadnest Subsuite[1]	Mathlagame Norite-Anorthosite		Grasvalley Norite-Anorthosite[1]
		Lower Subzone		Mooihoek Pyroxenite		Ruighoek Pyroxenite		
	Lower Zone[3]	Upper Pyroxenite Subzone	Croydon Subsuite[1]	Serokolo Pyroxenite	Vlakfontein Subsuite[1]	Tweelaagte Pyroxenite	Zoetveld Subsuite[1]	Moorddrift Harzburgite-Pyroxenite[2]
		Harzburgite Subzone		Jagdlust Harzburgite		Groenfontein Harzburgite		Drummondlea Harzburgite[2]
		Lower Pyroxenite Subzone		Rostock Pyroxenite		Makgope Pyroxenite		Volspruit Pyroxenite[2]
				Clapham Pyroxenite		Eerlyk Pyroxenite		
	Marginal Zone			Shelter Norite		Kroondal Norite		
						Kolobeng Norite		

1.3.1 Rooiberg Group

As illustrated in Table 1.1, the Rooiberg Group is divided into different formations based on the chemical and lithological variations. Basaltic andesite and basalt with various pyroclastic and arenaceous layers occur near the base, becoming more felsic towards the top (Schweitzer et al., 1995a). Siliceous volcanic rocks with sandstone and shale intercalations constitute the bulk of the Rooiberg Group succession. The Rooiberg volcanic rocks occur at both the floor and roof of the Bushveld mafic sequence.

The Rooiberg volcanic rocks host minor quantities of epigenetic fluorite and cassiterite (Schweitzer et al., 1995b).

1.3.2 Marginal Zone

The Marginal zone is predominantly comprised of medium-grained norite with minor gabbronorite, pyroxenite and peridotite. The presence of variable amounts of biotite and quartz are indicative of shale assimilation. According to Cawthorn et al. (2006), the unlayered Marginal Zone sequence formed from multiple magma intrusions rather than representing a true chill.

1.3.3 Lower Zone

The Lower Zone is generally divided into the Lower Pyroxenite Subzone, the Harzburgite Subzone and the Upper Pyroxenite Subzone (Table 1.1). These subzones differ slightly with two Lower Pyroxenite Subzone types in both the Eastern and Western Limb (Table 1.2). All the subzones of the western and eastern limbs have modest chromite content of less than 1% whereas the Lower Zone of the northern limb contain economic deposits of high-Cr chromite at Grasvally (Hulbert and von Gruenewaldt, 1985). The ultramafic rocks are locally attenuated propagating into overlying zones. The attenuation is generally attributed to the structural complexities in the sedimentary floor rocks (Uken and Watkeys, 1997).

1.3.4 Critical Zone

The Critical Zone displays conspicuous layering of anorthosite, norite, pyroxenite and chromitite (Cameron, 1980). The UG2 and the Merensky Reef host the world's largest PGE resources. Significant chromite mineralisation occurs within the Lower Group (LG), the Middle Group (MG) and the Upper Group (UG) chromitite layers of the Critical Zone (Schurmann et al., 1998).

The Merensky Reef is the thinnest of all cyclic units with very thin (mm scale) chromitite layers typically above and below a pegmatoidal feldspathic pyroxenite. Although mineralisation ranging from 6 – 8 g/t PGE (Pt, Pd, Rh and Au), 0.3% Ni and 0.15% Cu (Lee, 1996) is associated with sulphides, many PGEs do not occur as or within sulphides. This mineralisation predominantly occurs towards the base of the Merensky Reef unit, however, within the reef PGE grade is commonly higher at the top (Cawthorn et al., 2006). Although the UG2 chromitite layer has a significantly low sulphide content, its PGE grades are similar to those of the Merensky Reef (Cawthorn et al., 2006). Both the LG and MG carry a higher chromite content of between 50% and 85% in comparison to both the UG2 and the Merensky Reef (Cawthorn et al., 2006).

1.3.5 Main Zone

Based on the nature of low-calcium pyroxene, von Gruenewaldt (1973) subdivided the Eastern Bushveld Main Zone into three Subzones (A, B & C), with Subzone A being the lower subzone and Subzone C being the upper subzone. Von Gruenewaldt (1973) further located the Pyroxenite Marker at the boundary between Subzone B and Subzone C, interpreting it as an injection of undifferentiated magma into the Main Zone. Nex et al. (1998) suggested that an inverted pigeonite-bearing Subzone B separated Subzone A and Subzone C from primary orthopyroxene-bearing gabbronorite. In the Western Bushveld, Subzone A & B are regarded as Lower Main Zone while Subzone C is regarded as the Upper Main Zone (Mitchell, 1990).

1.3.6 Upper Zone

The Upper Zone is comprised of gabbronorite, gabbro and anorthosite with variable amounts of olivine and Fe-rich pyroxenes. Its base was defined by the onset of cumulus magnetite (Molyneux, 1974). Ashwal et al. (2005) suggested that the base of the Upper Zone should be defined by a higher magnetic susceptibility. Magnetite makes up 8% by volume of the Upper Zone with ilmenite abundance exceeding magnetite towards the top (Reynolds, 1985). The zone is the most laterally extensive with all the magnetitite layers containing vanadium. Vanadium (V_2O_5) decreases from 2% at the base to 0.3% at the top of the Upper Zone (Cawthorn et al., 2006).

CHAPTER 2

GEOLOGY OF THE NORTHERN LIMB

The exposed Northern limb is separated from the Western and Eastern limbs by the 25 km wide and 500 km long-WSW-ENE striking Thabazimbi-Murchison Lineament (TML). The limb extends for a strike length of 110 km from the Zebediela Fault (a branch of the TML) all the way to the Hout River Shear Zone in the north (Figure 2.1).

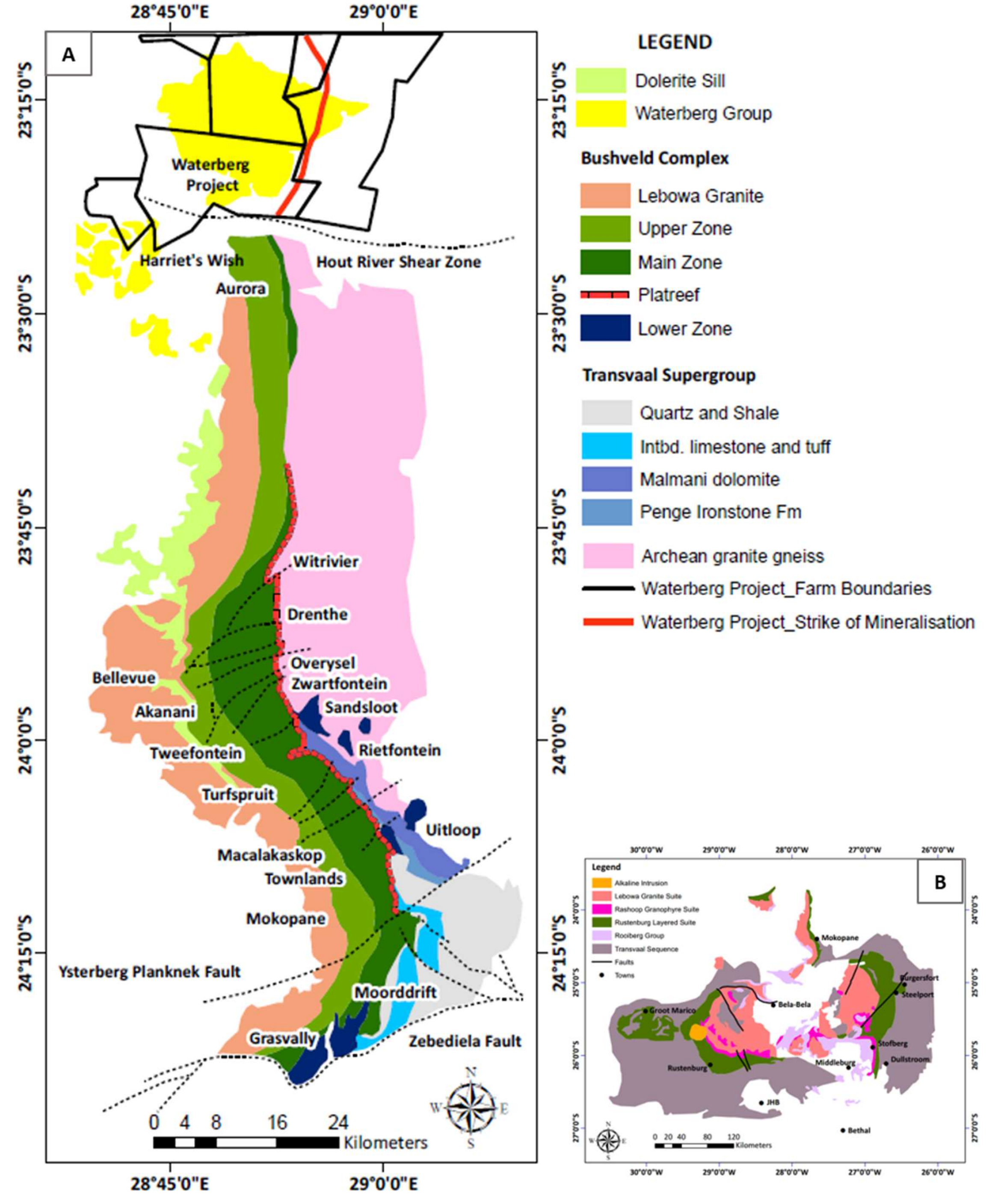

Figure 2.1. Geological map (A) of the Northern Limb showing the location and extent of the Waterberg Project. Modified after 1:250 000 geological map of the northern limb (modified after van der Merwe, 1976). (B) simplified geological map of the Bushveld Large Igneous Province (modified after Kinnaird, 2017).

The northern limb unconformably overlies older Paleoproterozoic Transvaal Supergroup metasediments from the southerly direction, progressing unconformably onto Archean granite-gneisses towards the north (van der Merwe, 1976). The “chonolithic-like” Lower Zone intruded both the Transvaal metasediments and Archean granite forming thick lenses beneath the Platreef on Turfspruit, Sandsloot and Grasvally (Yudovskaya et al., 2013). Above the Lower Zone is a PGE bearing unit equivalent to the Critical Zone known as the Platreef (van der Merwe, 1976) (Figure 2.2). The ~2 000 m thick Main Zone unconformably overlies the Platreef. An onset of disseminated magnetite marks the boundary between the Main Zone and Upper Zone (Ashwal et al., 2005).

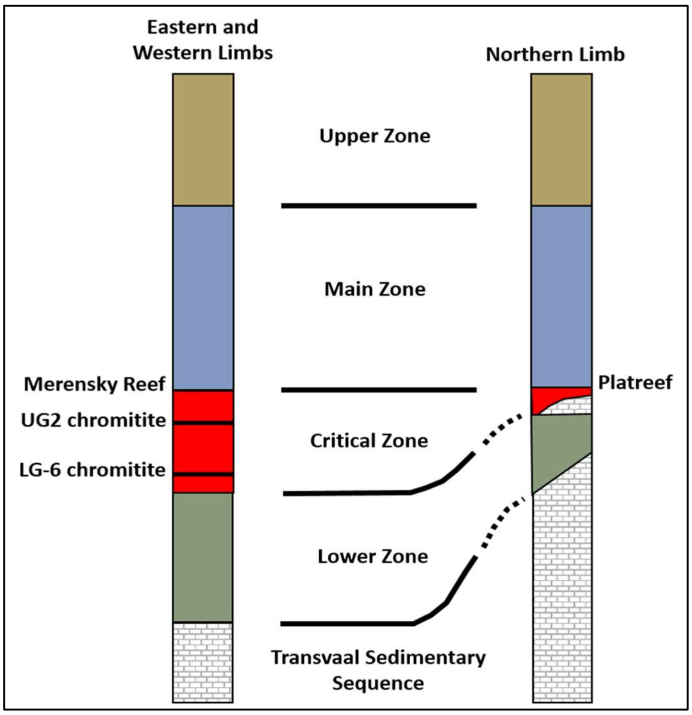

Figure 2.2 Stratigraphic position of the Platreef on the Northern Limb in relation to the conventional Western and Eastern Bushveld Complex (modified after McDonald and Holwell, 2011).

The Platreef extends from Mokopane, northwards with a strike length of 30 km and average dip of 43° to the west (Kinnaird et al., 2005). It is comprised of variably altered and texturally heterogenous harzburgite, pyroxenite, norite and occasional anorthosite. Its thickness varies from approximately 50 m in the north to about 600 m in the south (Kinnaird and Nex, 2012).

Based on variations in footwall lithology, the Platreef is further subdivided into three sectors. The southern sector, the central sector and the northern sector (Kinnaird et al., 2005). The footwall of the southern sector is comprised of Duitschland Formation shale, mudstone, calc-silicate, siltstone and banded iron formation (Gain and Mostert, 1992; Kinnaird et al., 2005). The sector extends from the farm Townlands in the south to the farm Tweefontein in the north (Figure 2.1 & Figure 2.3). The footwall of the central sector is comprised of dolomite of the Malmani Subgroup. It extends across the farms Tweefontein and Sandsloot to Zwartfontein (Figure 2.1 & Figure 2.3). The northern sector is characterised by Archean granite-gneiss footwall. It extends northwards from the farms Zwartfontein, Overysel and Drenthe to Witrivier (Figure 2.1 & Figure 2.3).

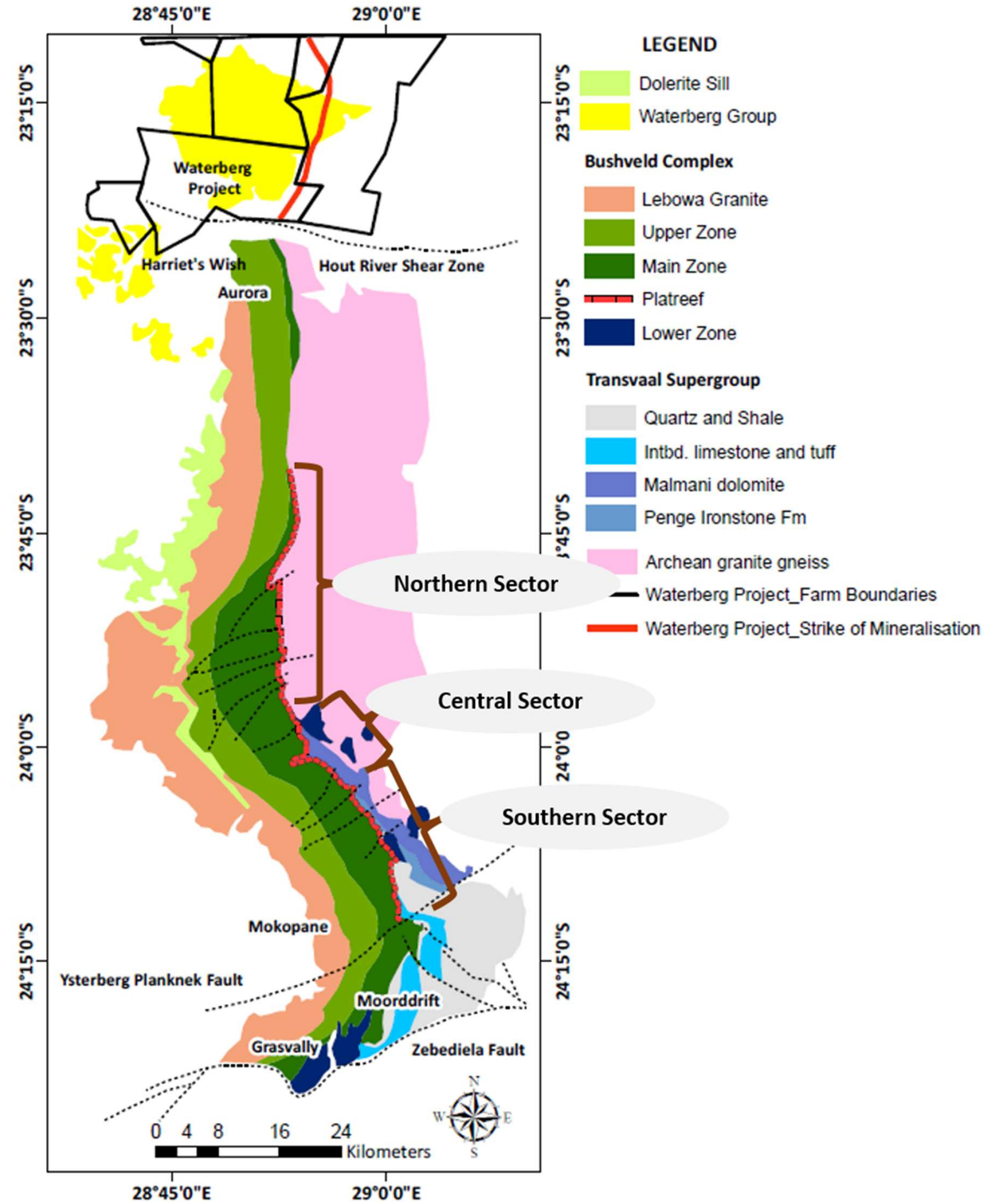

Figure 2.3. A geological map of the northern limb showing the three sectors based on variations in the footwall lithology (modified after van der Merwe, 1976).

The geology of Turfspruit, Aurora and Harriets Wish is discussed in the following subsections with a rationale of providing an overview of both the similarities and the variations in relation to the Waterberg Project.

2.1 Geology of Turfspruit

Unlike the up-dip section of the Platreef which dips at an average of 43° to the west, the reef at Turfspruit dips at 40° from surface becoming flat with depth to about 10° -15° towards the south-westerly direction (Kekana, 2014). The gently dipping part of the succession is referred to as the Flatreef (Kekana, 2014).

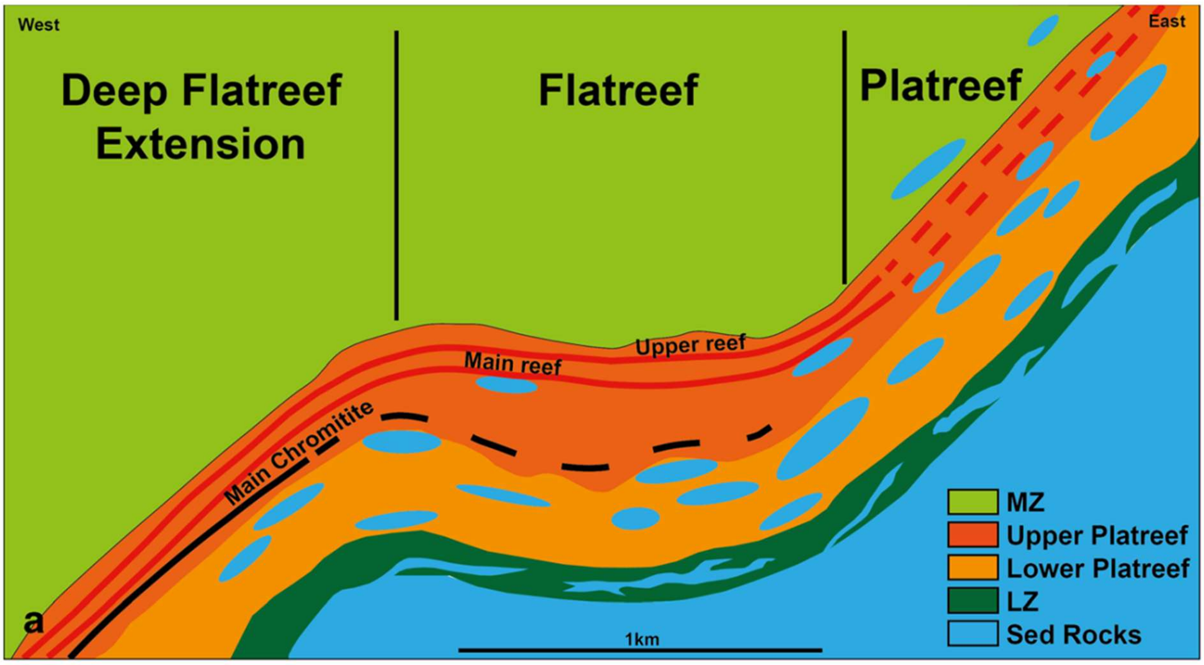

Figure 2.4. A schematic diagram showing the change in dip angle of the Turfspruit sequence from east to west. The Platreef sequence is characterised by the raft infested Lower Platreef and the highly mineralised Upper Platreef. Note the Upper reef and Main reef within the Upper Platreef (Grobler et al., 2018).

According to Kekana (2014), the Flatreef is characterised by the following distinguishable factors with respect to the steeper and shallower Platreef up-dip: -

The geological units are better defined and can be correlated along strike and dip for kilometres.

- Thicker intervals of high grade mineralisation with higher PGE tenors
- Persistent chromitites associated with the main reefs as well as separate layers and lenses.
- Less reef contamination by xenoliths.

The B-pyroxenite is the main mineralised zone within the upper section of the Platreef. Based on lithological variations, Grobler and Nielsen (2012) subdivided the B-pyroxenite into two broader zones which are T1 and T2 Upper. The harzburgite below the T2 Upper has been reclassified as T2 Lower (Grobler and Nielsen, 2012). The well mineralised zones within T2 are associated with the pegmatoidal texture (Kekana, 2014). Within the T1, the mineralised portion has been reclassified as T1m.

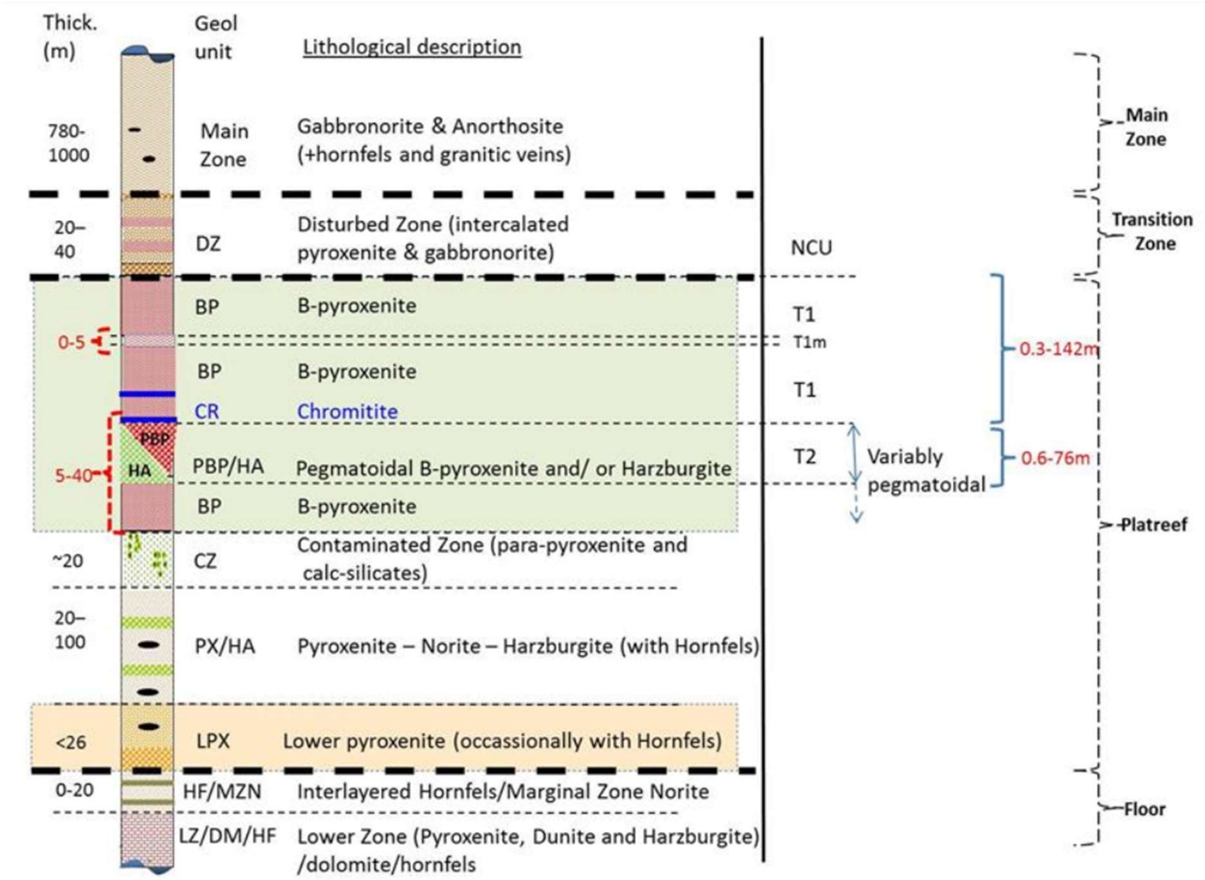

Figure 2.5. Generalised stratigraphy of Turfspruit with detailed lithological description (Kekana, 2014).

Unlike the T2 which becomes more pegmatoidal downwards, the T1 is a fairly homogenous feldspathic pyroxenite with rare chromitite stringers (Kekana, 2014). Chromitite stringers, seams and blobs of variable thickness (30 cm to 1 m) are common at the contact between pegmatoidal pyroxenite (T2 Upper) and feldspathic pyroxenite (T1). Where the chromitite is absent, the contact is still conspicuous due to textural variations (Kekana, 2014).

Unlike the central and northern sectors where chromitite can be identified 17 – 20 m below the top contact of the Platreef (Yudovskaya and Kinnaird, 2010), this does not seem to be the case with Turfspruit where the distance is quite variable from centimetres to several tens of metres (Kekana, 2014).

Below the T2 is parapyroxenite of a variable thickness and calc-silicates known as the Contaminated Zone (CZ). The CZ is not to be confused with the Critical Zone. The base of the Flatreef is distinguished by fine-grained pyroxenite which is fairly homogenous and continuous (Kekana, 2014).

2.2 Geology of the Aurora Project

The Aurora Project is located in the far north of the exposed northern limb (Figure 2.1). The project represents the far northern facies of the Platreef along the basal margin of the complex (Naldrett, 2005; Maier et al., 2008; McFall et al., 2019). McDonald et al. (2017) has shown that the Aurora project does not represent a strike extension of the Platreef on the basis of lithological association, lithophile, PGE geochemistry and host mineralogy.

The stratigraphy of Aurora has been simplified into three major units (Figure 2.6). Unit 1 rests unconformably on the basement granite. It comprises melagabbronorite and pyroxenite (Manyeruke, 2007). Rafts/xenoliths of calc-silicates are common within this unit.

Above Unit 1 lies Unit 2. This unit comprises gabbronorites and leucogabbronorites (Manyeruke, 2007), that are characterised by coarse-grained plagioclase. The middle of the unit is characterised by thin troctolite and olivine gabbronorite. Interstitial base metals sulphides are common within this unit. Zones of pegmatoidal gabbros within this unit occasionally carry pervasive cumulus magnetite with base metal sulphides (McDonald et al., 2017).

Unit 3 represents the upper portion of the Aurora stratigraphy. The unit is characterised by dark, coarse grained gabbronorites with conspicuous inverted pigeonite (McDonald et al., 2017).

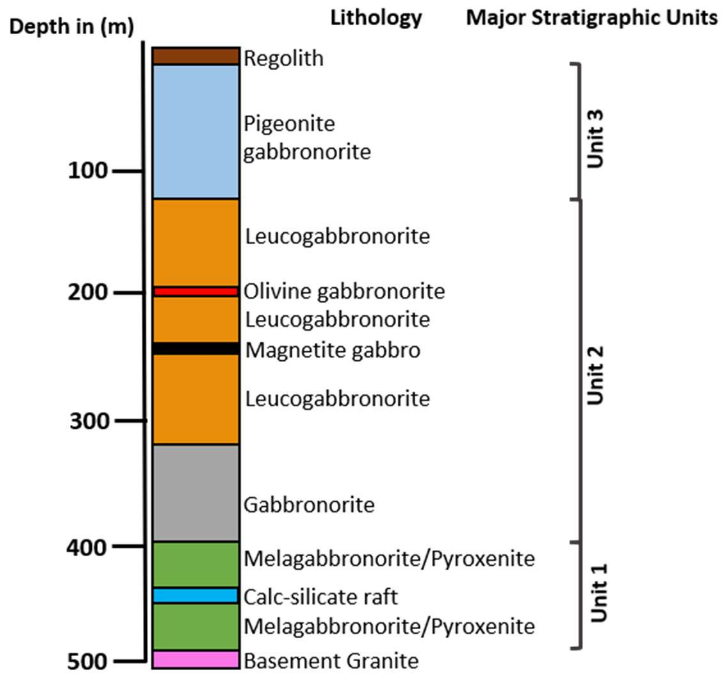

Figure 2.6. Simplified Stratigraphy of the Aurora Project showing major stratigraphic units and their relative lithological description (Simplified after McDonald et al., 2017).

2.2 Geology of Harriet's Wish

The farm Harriet's Wish is located between the Aurora and Waterberg Project with the E - W striking Hout River Shear Zone (HRSZ) transecting the farm mid-section (Figure 3.10), page 13. The geological characteristics from drillcore obtained from this farm were initially defined by Kinnaird et al. (2017) and further discussed by van Scheltema (2019). Most of the interpretations were based on the four holes drilled north of the HRSZ adjacent to Harriet's Wish and Waterberg (Ketting 368 LR & Goedetrouw 366 LR) boundary.

The magmatic sequence on the farm Harriet's Wish has been subdivided into lower and upper lithological units (Figure 2.7). The lower lithologic unit is composed of leucogabbronorite, gabbronorite, melagabbronorite, pegmatoidal gabbronorite, gabbro, pyroxenite, olivine bearing gabbronorite, olivine norite, troctolite, anorthosite and some calcsilicate xenoliths (van Scheltema, 2019). Although the lower lithologic unit is > 200 m in thickness, the extent of this unit is not well defined as the holes were not drilled into the basement. The 220 m thick upper lithologic unit is distinguished from the lower lithologic unit by the presence of cumulus magnetite crystals (van Scheltema, 2019). The unit is characterised by gabbronorite, olivine bearing gabbronorite, gabbro, magnetitite and magnetite-rich gabbro and some minor anorthosites. The contact between the magmatic sequence and the overlying Waterberg Group sediments is considered to be an erosional unconformity (van Scheltema, 2019). Mineralisation occurs in the form of conspicuous base metal sulphide such as pentlandite, chalcopyrite, pyrrhotite and pyrite. The 50 m thick lower mineralised zone occurs within the lower lithologic unit with the host rocks being feldspathic pyroxenite, gabbronorite and troctolite. The 20 m thick upper mineralised zone occurs at the interface between the lower and upper lithologic units. The host rocks for mineralisation are gabbronorite, gabbro and anorthosite (van Scheltema, 2019).

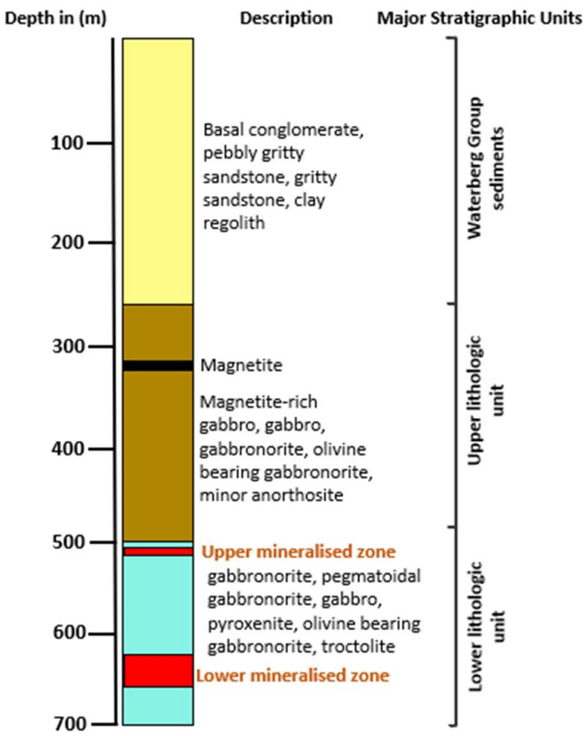

Figure 2.7. Simplified Stratigraphy of Harriet's Wish showing major stratigraphic units and their relative lithological description (simplified after van Scheltema, 2019)

CHAPTER 3

THE WATERBERG PROJECT

The Waterberg Project is separated from the Northern Limb by the Hout River Shear Zone (HRSZ) (Figure 2.1). Unlike the exposed Northern Limb which unconformably overlies the Transvaal and Archean rocks of the Kaapvaal craton, the Waterberg Project, located to the north of the HRSZ rests unconformably on granite-gneiss of the Southern Marginal Zone (SMZ) of the Limpopo Mobile Belt (Kinnaird, 2017). The 1100 m - 1 200 m thick succession strikes SW - NE and dips at 34 - 38° NW (Kinnaird, 2017).

From the inception of the project, it was obvious that there were some significant stratigraphic differences between the conventional Northern limb and the mafic-ultramafic succession of the Waterberg Project. These differences impelled the exploration team to collate a stratigraphic nomenclature specific to the project (Figure 3.1).

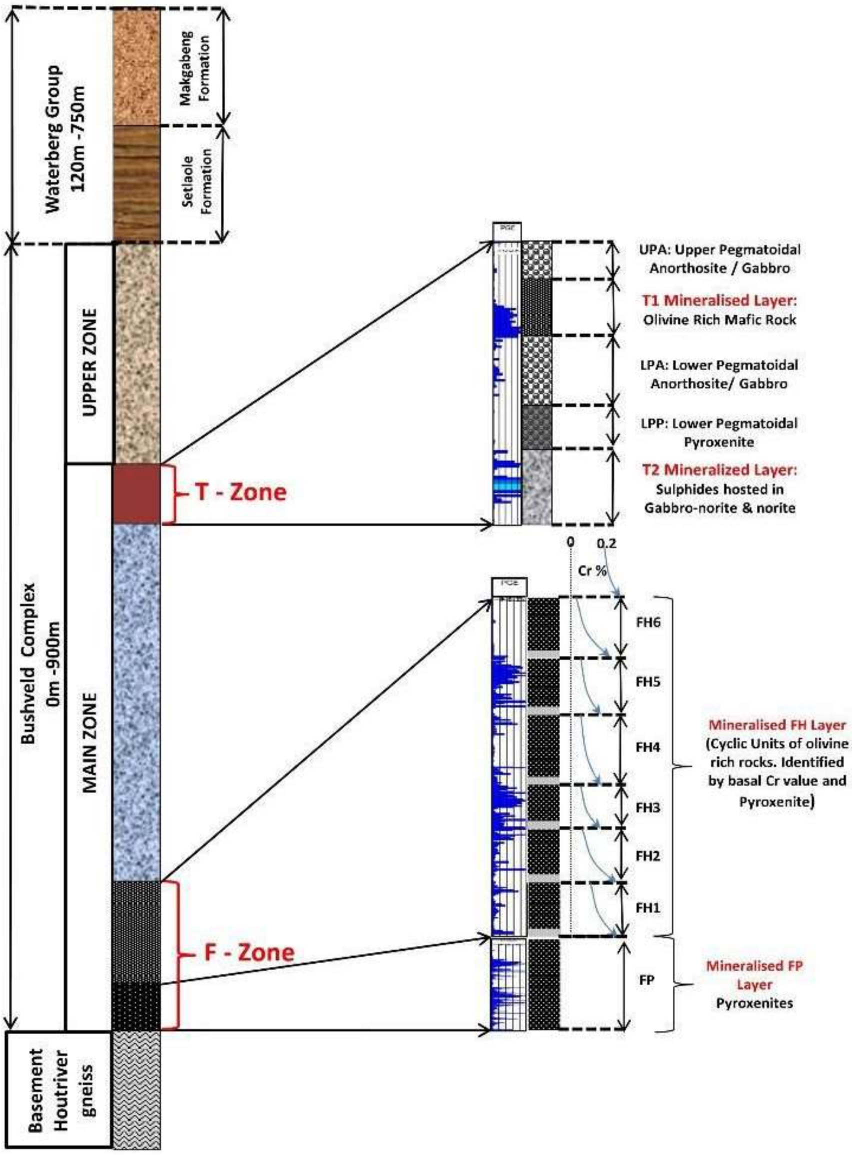

Figure 3.1. Initial stratigraphy of the Waterberg Project (Lomberg and Goldschmidt, 2014).

The lowermost lithologies of the mafic-ultramafic Waterberg succession are characterised by granofels, marginal pyroxenite, marginal norite and serpentinised pyroxenite. Since these lowermost lithologies represent the first Bushveld magma influxes which intermingled with the granite basement rocks, the unit was classified as the Transitional Zone (TRNZ).

Above the TRNZ is the Ultramafic Sequence which hosts the lower mineralised F Zone. This mineralised F Zone is characterised by the lower FP (F Zone Pyroxenite) and the upper FH (F Zone Harzburgite). An attempt to subdivide the FH into six cyclic units based on spikes in chromium content was made (Lomberg and Goldschmidt, 2014). Although the units were observed in some drill logs, they seemed to be highly variable and difficult to observe in drillcore.

The contact between the F Zone and the Main Zone is defined by the lower troctolite which grades from melanocratic troctolite at the bottom to leucocratic troctolite at the top. The leucocratic troctolite grades upwards into olivine bearing gabbronorite, gabbronorite and anorthosite. The anorthosite represents the uppermost Main Zone lithology.

The interface between the Main Zone and the Upper Zone (UZ) is defined by the upper mineralised T Zone. Based on lithological and textural variations, the T Zone was divided into five distinctive subzones with the lowermost subzone being the well mineralised T2 gabbronorite and feldspathic pyroxenite. There is no conspicuous contact between the T Zone and the Main Zone. The transition was therefore defined by the disappearance of sulphides in down into the Main Zone. The top of the T2 subzone is characterised by an occasional pegmatitic pyroxenite referred to as the LPP subzone. Above the LPP is a distinctive pegmatitic anorthosite. The olivine-rich mafic layer referred to as T1 mineralised subzone splits the pegmatitic anorthosite into the well mineralised Lower Pegmatoidal Anorthosite (LPA) and the sporadically mineralised Upper Pegmatoidal Anorthosite (UPA). It is important to note that the T2 and T1 of the Waterberg succession do not equate to the T2 and T1 of Turfspruit.

The uppermost lithologies of the mafic-ultramafic Waterberg succession are characterised by gabbro, gabbronorite, pyroxenite and some sporadic pegmatitic anorthosite. Due to the high magnetite content similar to those observed in the Upper Zone of the rest of the Bushveld Complex, this upper unit was correlated with the rest of the known Bushveld Complex and classified as the Upper Zone. Although the Main Zone beneath the Upper Zone has similar rock assemblages to the Upper Zone, the two are distinguished by the lack of primary magnetite within the Main Zone.

A U-Pb radiometric geochronological study was conducted by Huthmann et al. (2016) on zircon extracted from the mafic-ultramafic succession. Detrital zircons from basal conglomerate of the overlying sediments were also analysed. The analysis showed that the 3.5 km x 24 km mafic-ultramafic succession is 2053 ± 5 to 2059 ± 3 million years old; the age of which is coeval to that of the Bushveld Complex. The analysis of the detrital zircons from the basal conglomerate indicated a maximum sedimentary deposition of ~2045 Ma. With the baddeleyite age of 1125 Ma, Huthmann et al. (2016) was also able to confirm that the sill within the sedimentary succession is part of the Umkondo Igneous Province.

The initial stratigraphy as prescribed by the exploration team has since then been reviewed and amended by Huthmann et al. (2017 & 2018) and McCreesh et al. (2018). Although this is a progressive academic initiative in understanding and appreciating the unique nature of the geology of the project, the initial stratigraphy remained unchanged at the exploration site for consistency purposes.

Figure 3.2 is a slightly modified stratigraphy of the Waterberg Project as published by Huthmann et al. (2017). Since, Huthmann et al. (2017) bundled the T Zone into the TGA, this stratigraphy has been modified to unbundle this significant mineralised zone for several reasons. Namely, the distinctive and continuous nature of the different lithologies within the T Zone serve as crucial markers and therefore need to remain distinctive. By unbundling the T Zone, explaining mineralisation controls and PGE tenors becomes easier and much more informative. The contentious nature of whether the T Zone is part of the lower Upper Zone (McCreesh et al. 2018) or upper Main Zone (Huthmann et al. 2017) has warranted this unit to be an independent zone in the interim for the purpose of this study.

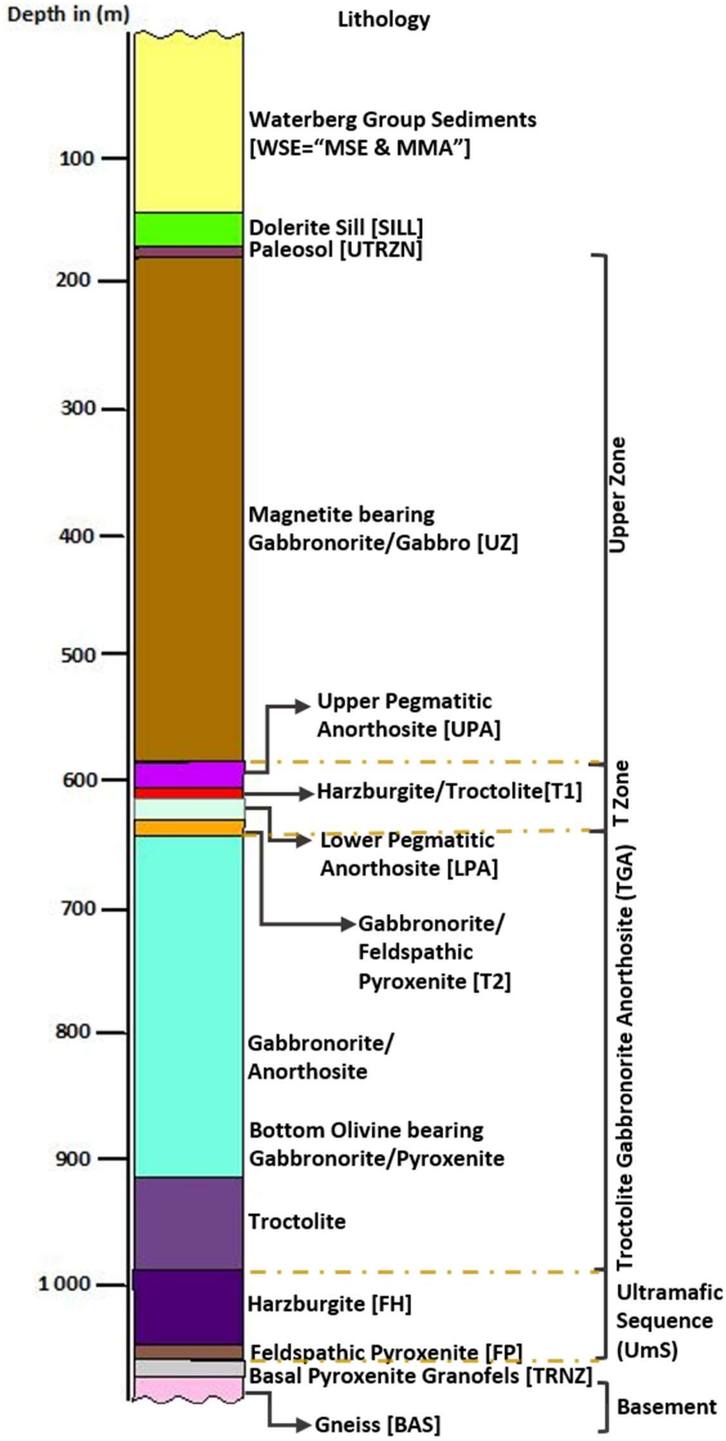

Figure 3.2. Stratigraphic column for the Waterberg Project with descriptive T Zone subzones/units (modified after Huthmann et al., 2017).

3.1 The lithostratigraphy of the Waterberg Project

Intensive work on the lithostratigraphy of the project has been done by McCreesh (2013); Huthmann et al. (2016); Huthmann et al. (2017), Huthmann et al. (2018); Kinnaird et al. (2017) and McCreesh et al. (2018). This subsection is a simplified overview of the rock types that constitute the lithostratigraphy of the Waterberg Project. For the locality of the rock samples displayed below, refer to Appendix 2.

3.1.1 Basement granite-gneiss

Granite-gneiss of the Southern Marginal Zone of the Limpopo Mobile Belt (SMZ) forms the base of the Waterberg lithostratigraphic sequence. These granite-gneisses are variable from plagioclase-bearing (Figure 3.3A) in the south proximal to the HRSZ to more orthoclase-bearing (Figure 3.3B) towards the north, further away from the HRSZ.

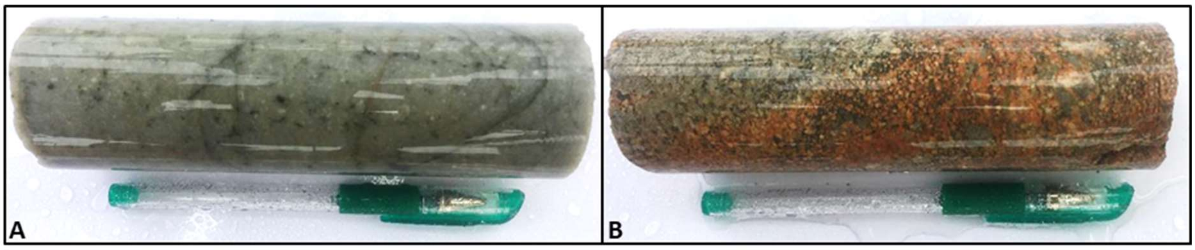

Figure 3.3. Basement rocks of the Waterberg Project. (A)Tonalitic granite gneiss proximal to the HRSZ (B) orthoclase bearing granite gneiss further north of the HRSZ.

3.1.2 Transitional Zone (TRNZ)

Intermingling between the first influxes of Bushveld magma with the basement granite-gneiss resulted in the formation of granofels (Kinnaird et al., 2017). Distinctive layering of alternating pyroxenite with felsic basement defines granofels in closer proximity to basement (Figure 3.4D). Within such intercalation, the contacts between the felsic and mafic layers show a distinctive angle of Bushveld magma emplacement. In places, the granofels is characterised by magmatic breccia texture (Figure 3.4C). The granofels grades up into fine grained homogenous basal pyroxenite (Figure 3.4B). Massive and blebby sulphides (pyrrhotite, chalcopyrite and pentlandite) are sometimes present in the pyroxenite. However, these sulphides are PGE-barren. In several instances where volatiles from the overlying UmS interacted with the basal pyroxenite, a serpentine lineation fabric defined by serpentine becomes conspicuous within the pyroxenite (Figure 3.4A).

Calc-silicates xenoliths similar to those of the Northern Sector of the Platreef have been reported by Kinnaird et al. (2017) on the Waterberg Project. These xenoliths were observed at the base of the Bushveld intrusion and sporadically throughout the rest of the succession. Kinnaird et al. (2017) further suggested a possible local dolomitite on top of the basement granite.

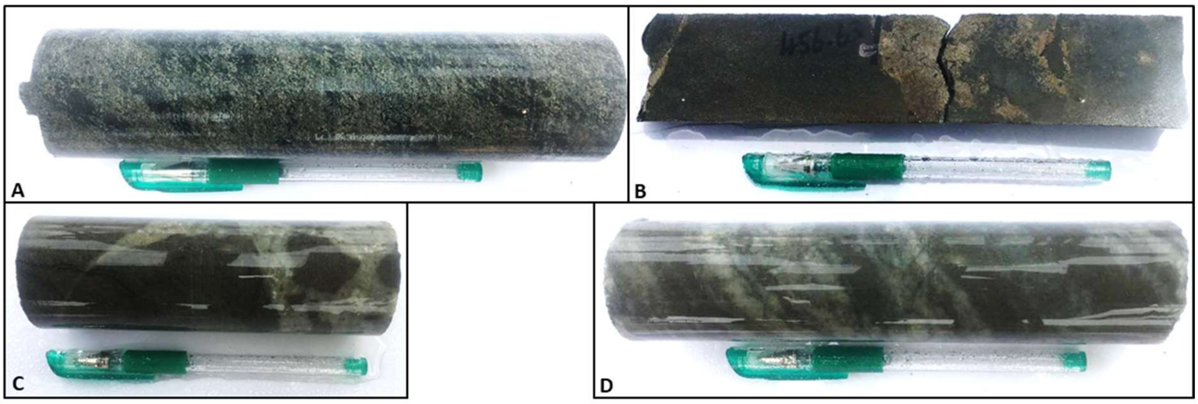

Figure 3.4. Transitional Zone rocks of the Waterberg Project. (A) serpentinised pyroxenite, (B) homogenous basal pyroxenite, (C) granofels with pyroxenite remnant, (D) granofels with alternating bands of pyroxenite and basement felsics.

3.1.3 The Ultramafic Sequence (UmS)

The Transitional Zone is overlain by a 2.5 – 137 m thick Ultramafic Sequence (McCreesh et al., 2016; Kinnaird et al., 2017 and Huthmann et al., 2017). This well mineralised sequence is characterised by mineralised basal feldspathic pyroxenite locally referred to as the FP (Figure 3.5C), the mineralised feldspathic harzburgite locally referred to as the FH (Figure 3.5B) and some poikilitic melanocratic troctolites which also form part of the FH subzone (Figure 3.5D). The poikilitic melanocratic troctolite becomes less mineralised towards the top of the sequence.

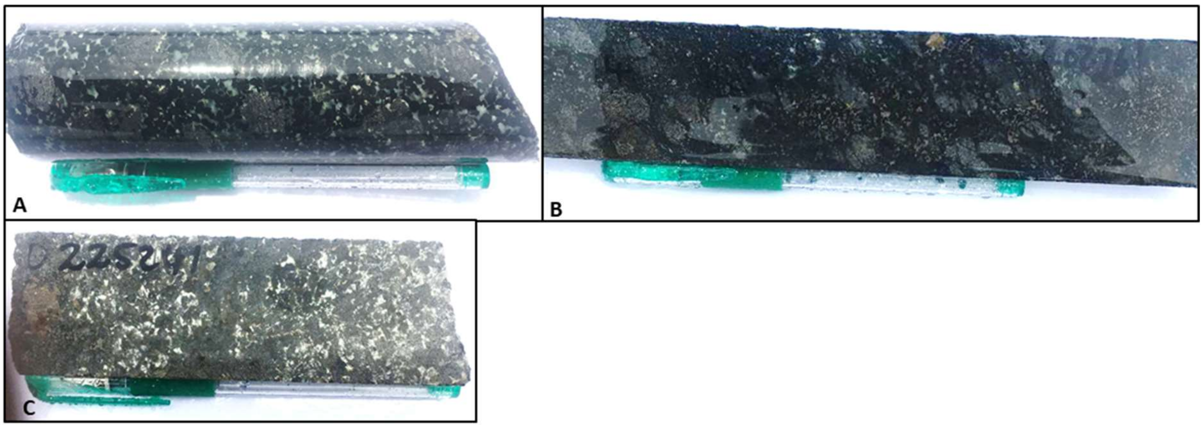

Figure 3.5. Ultramafic Sequence of the Waterberg Project. (A) poikilitic melanocratic troctolite, (B) feldspathic harzburgite with disseminated and blebby sulphides and (C) feldspathic pyroxenite with blebby and disseminated sulphides.

Olivine gabbronorite and minor serpentinite bands are common towards the base of the sequence. The harzburgite has <65% olivine with orthopyroxene, minor plagioclase and minor clinopyroxene. A higher degree of alteration of olivine is shown by the presence of serpentine and secondary magnetite (McCreesh, 2016; Kinnaird et al., 2017). The FH subzone becomes less pegmatoidal from the base upwards with xenoliths of feldspathic pyroxenite in places.

Chromitite stringers have been observed in some drillholes. However, these are extremely rare (McCreesh, 2016; Kinnaird et al., 2017).

3.1.4 Troctolite – Gabbronorite – Anorthosite Sequence (TGA)

The TGA varies in lithology throughout the sequence from troctolite at the base to feldspathic pyroxenite, gabbronorite and anorthosite (McCreesh, 2016; Kinnaird et al., 2017). The troctolite is melanocratic to mesocratic at the base grading upwards into leucotroctolite (Figure 3.6F). The leucocratic troctolite grades upwards into olivine bearing feldspathic pyroxenite (Figure 3.6E) and occasional olivine bearing gabbronorite. Further up the sequence, the lithologies are characterised by olivine depleted feldspathic pyroxenite (Figure 3.6D), melanocratic gabbronorite (Figure 3.6C), mesocratic gabbronorite (Figure 3.6B) and leucocratic gabbronorite (Figure 3.6A).

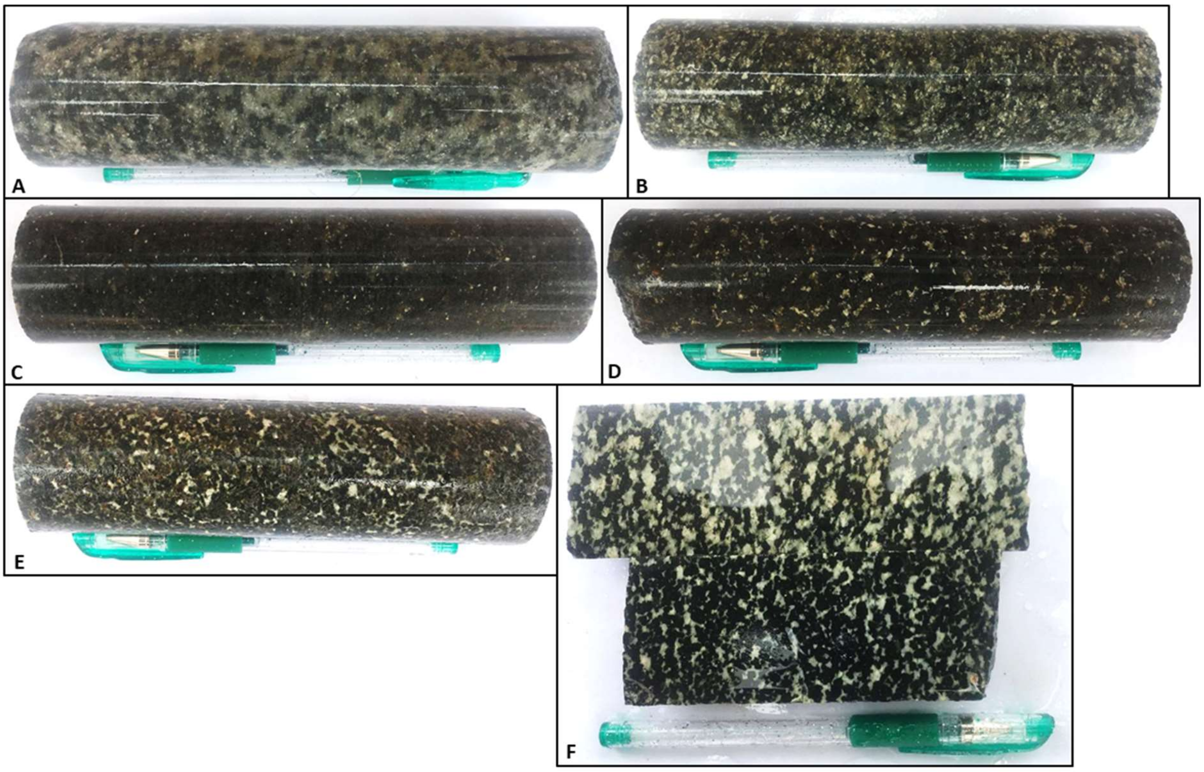

Figure 3.6. TGA rocks from the Waterberg Project. (A) leucocratic gabbronorite, (B) mesocratic gabbronorite, (C) melanocratic gabbronorite, (D) feldspathic pyroxenite, (E) olivine-bearing feldspathic pyroxenite, (F) leucocratic troctolite and mesocratic troctolite.

Anorthosites with varying textures are common within the TGA sequence (Figure 3.7). Alteration seems to be pervasive with intense veins and veinlets in the anorthosite as compared to other rock types.

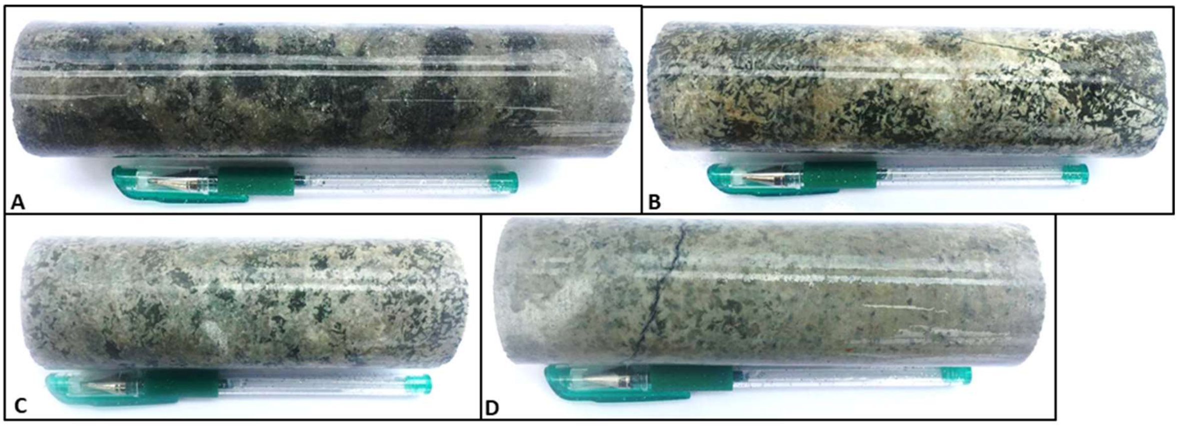

Figure 3.7. Anorthosites of the Waterberg Project. (A) varied textured unaltered poikilitic anorthosite, (B) altered anorthosite with chloritised clinopyroxene oikocrysts, (C) altered varied textured anorthosite, (D) altered pyroxenitic anorthosite [PYXAN]

3.1.5 The T Zone

Within the T Zone, the T2 subzone constitutes the most prominent and continuous mineralised subzone within the T Zone. This subzone is hosted by feldspathic pyroxenite (Figure 3.8E), mesocratic gabbronorite and leucocratic gabbronorite. The Pegmatitic Pyroxenite (LPP) immediately above the T2 subzone (Figure 3.8D) is very rare and occurs sporadically throughout the T Zone. The Lower Pegmatoidal Anorthosite (LPA) is characterised by anorthosite which is distinctively pegmatitic in texture (Figure 3.8C). The T2, the LPP and the LPA are endowed with PGEs. The sporadically mineralised Upper Pegmatoidal Anorthosite (UPA) (Figure 3.8A) is separated from the LPA by the T1 subzone which is characterised by olivine bearing rocks such as olivine bearing pyroxenite and harzburgite (Figure 3.8B). The UPA defines the uppermost subzone of the T Zone. It is important to note that the T2 and T1 of the Waterberg succession do not equate to the T2 and T1 of Turfspruit.

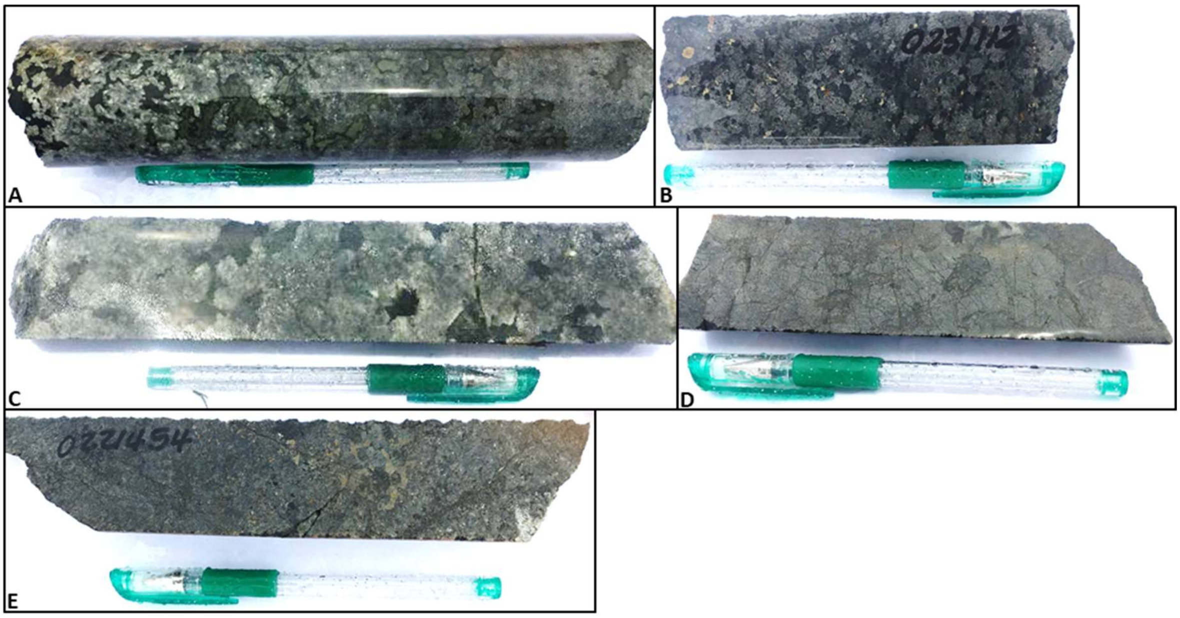

Figure 3.8. Core samples from the Waterberg T Zone. (A) Upper pegmatitic anorthosite, (B) T1 olivine bearing pyroxenite with blebby and disseminated sulphides, (C) Lower pegmatitic anorthosite, (D) Lower pegmatitic pyroxenite, (E) T2 feldspathic pyroxenite with blebby and net-textured sulphides.

3.1.6 The Upper Zone

This zone comprises mainly magnetite bearing gabbronorite (Figure 3.9B) with no ferro-gabbro (McCreesh, 2013). According to McCreesh, (2016), magnetitite seams as seen in the rest of the northern limb are not present north of the HRSZ. The magnetitite observed in WB001 (Figure 3.9A) seems to be anomalous. Some magnetitites have also been reported in three additional drillholes in the vicinity of WB001. Although the HRSZ generally traverses the farm Harriet's Wish and lower portion of the farm Cracouw with an E-W strike (Figure 3.10), the HRSZ might not be a single linear feature but a more complex zone with multiple splays stretching into the Waterberg Project.

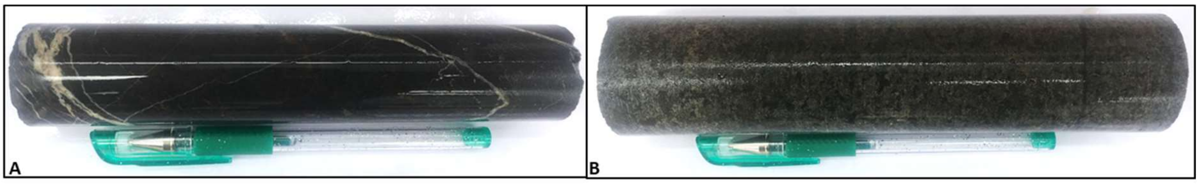

Figure 3.9. Core samples of the Upper Zone magnetite seams (A) and ferro-gabbronorite (B) as observed on the Waterberg Project

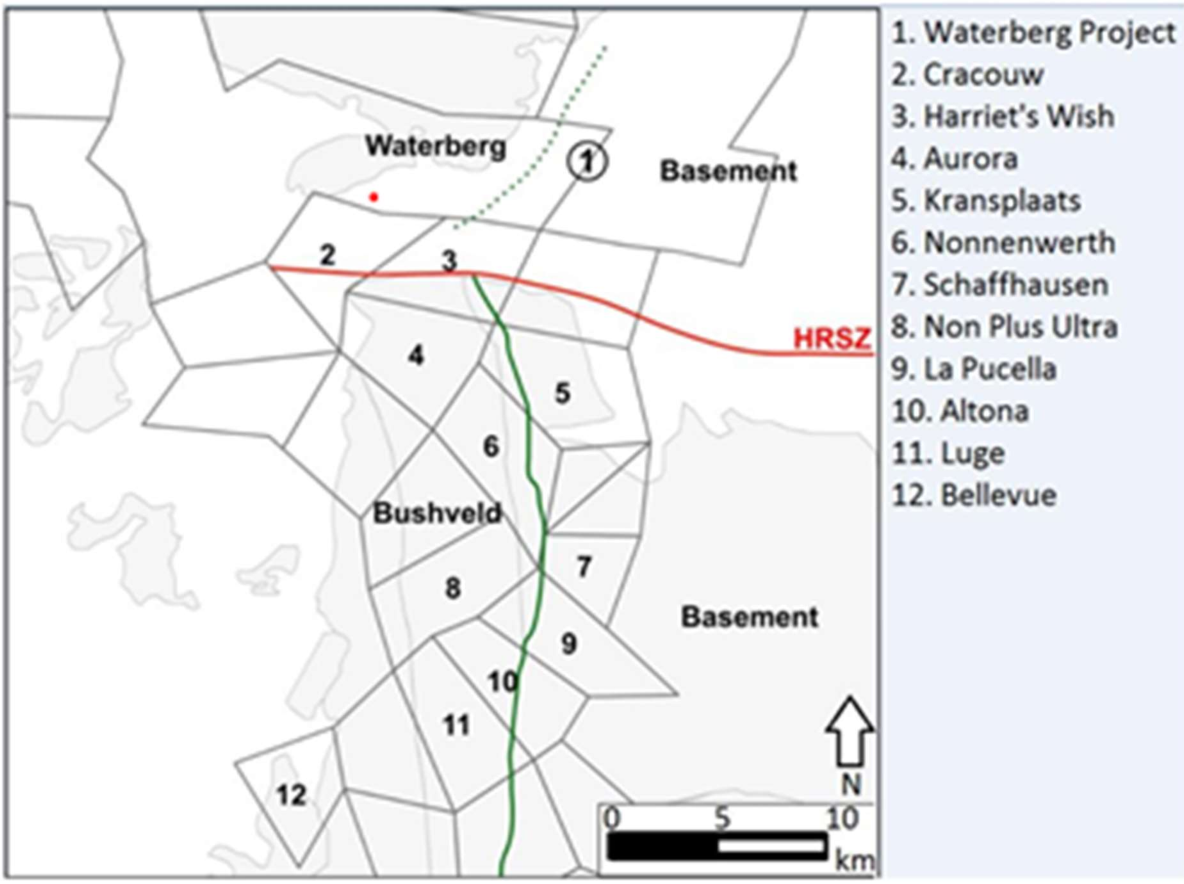

Figure 3.10. Map showing the location of WB001 (red dot) relative to the HRSZ. The red line represents the strike of the HRSZ. The labels 1 - 12 represent the farm names. The green line represents mineralised lithologies on the Aurora Project. The doted red line represents the extent of the Waterberg Project (unpublished from Huthmann, 2018).

3.1.7 The Upper Transitional Zone (UTRZN)

The contact between the Bushveld Complex igneous rocks and the overlying Waterberg Group sedimentary rocks is characterised by a Paleoproterozoic paleosol (Figure 3.11) (McCreesh, 2016). These red, sometimes shaly looking rocks are fine grained with white to grey tuffaceous layers in places. Epidotisation, hematitisation and chloritisation also defines the zone.

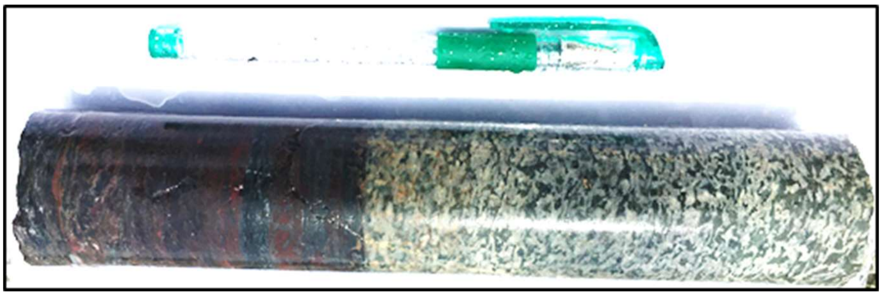

Figure 3.11. TRZN paleosol and Bushveld leucogabbronorite contact.

3.1.8 Waterberg Group Sediments

The conglomerate (Figure 3.12C) of the Setlaole Formation marks the base of the sedimentary succession at the Waterberg Project (McCreesh, 2013; Kinnaird et al., 2017). These conglomerates are characterised by sub-rounded quartz pebbles which decrease in size up the sequence into gritty siliciclastic sandstone (Figure 3.12B) (Jansen, 1982). The arkose of the Makgabeng formation (Figure 3.12A) is characterised by grey sandy nodules. Alternating layers of arkose and shale with trough cross bedding are also common within the Makgabeng succession (Jansen, 1982; Dorland, 2006).

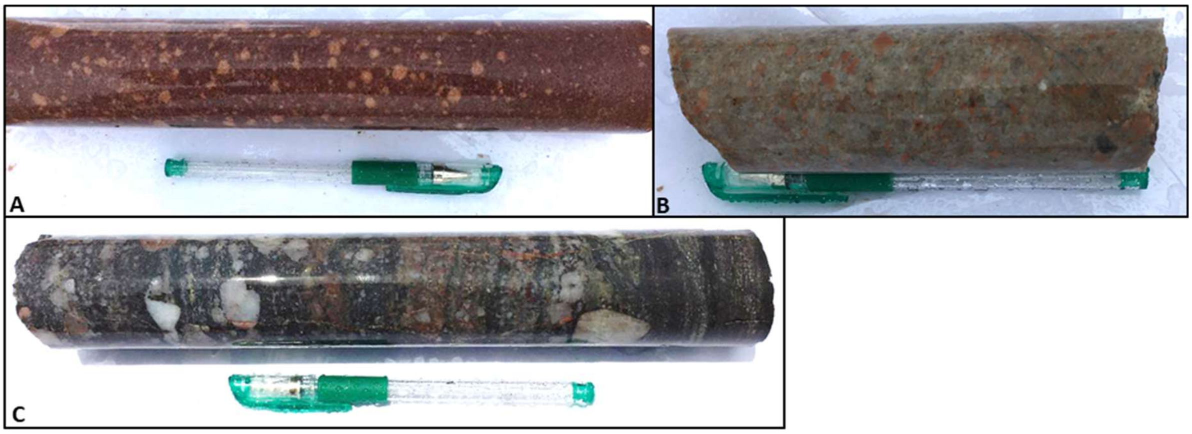

Figure 3.12. Waterberg Group sedimentary rocks at the Waterberg Project. (A) Nodular sandstone, (B) Gritty sandstone with sporadic quartz pebbles, (C) Basal conglomerate in contact with paleosol (note the loadcasting pebble on the paleosol).

3.1.9 Younger sills and dykes

The younger 1 125 Ma intrusive rocks of the Waterberg Project are Umkondo dolerite sills (Huthmann et al., 2016) (Figure 3.13A) and Karoo dolerite dykes (Figure 3.13B). The Umkondo dolerite sills are generally confined to the Waterberg Group sedimentary rocks slightly transgressing down into the top of the TGA towards the NE. To the south of the project, in the T Zone area, the top sill is closer to the surface. The fine crystalline Karoo dolerite dykes are ubiquitous within the stratigraphic succession, cutting across the Ultamafic Sequence in places, especially to the north of the project.

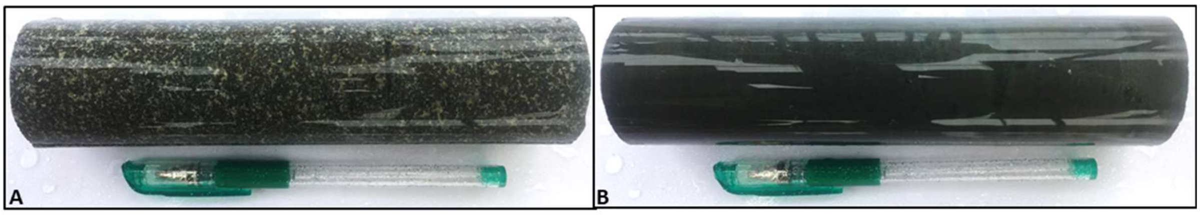

Figure 3.13. Younger intrusive rocks within the Waterberg Project. (A) Medium crystalline Umkondo dolerite sill, (B) Fine crystalline Karoo dolerite dyke.

CHAPTER 4

3D MODEL OF THE WATERBERG PROJECT

A total of roughly 380 drillholes were used to generate a simplified 3D geological model of the Waterberg Project (Figure 4.1). The designed model only covers the extent of the study area and therefore does not include the far north of the project. The model was designed using data from the project's database and therefore published stratigraphy by Huthmann et al. (2017) could not be re-assigned due to time constraints. The T Zone (TZN as on the model) is bundled and therefore does not show the subzones. The Waterberg sediments have not been differentiated into the upper Makgabeng and the Lower Setlaole Formations.

The collar data, downhole survey data and stratigraphic data was extracted from the Waterberg Project database and loaded onto Leapfrog Geo 5.1 where the stratigraphic units were modelled. Different colours were annotated to each stratigraphic unit for better visualisation. Note that some features such as dykes displayed on the stratigraphic legend might not be visible as they are thin. Also note that the stratigraphic legend is programme auto-generated and does not follow any geological chronology. The surface topography was created using surface point (X,Y,Z) data of the project area. A WGS84 LO29 coordinate format was used for the model. An aerial image of the Project Area was extracted from Google Earth Pro, georeferenced and draped onto the surface topography for better visualisation.

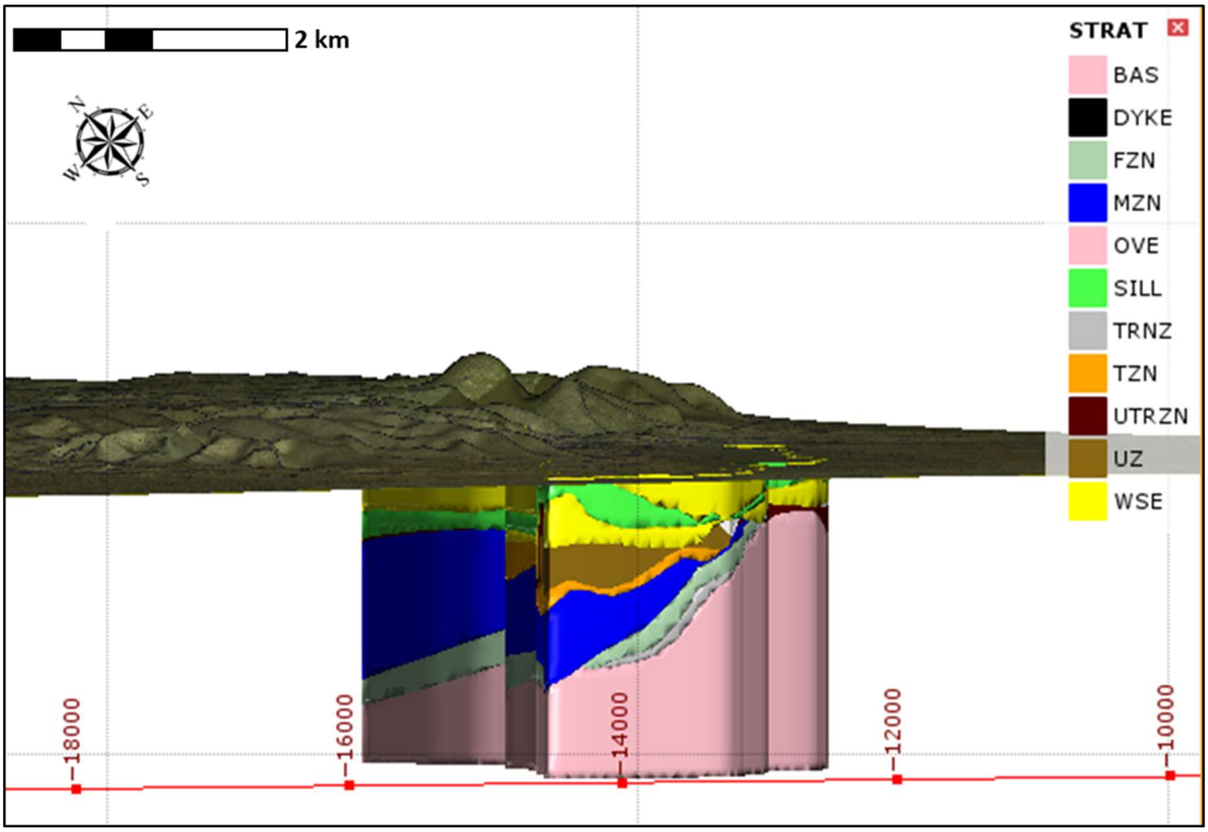

Figure 4.1. A simplified 3D Geological model of the Waterberg Project showing both the Bushveld Complex succession, overlying Waterberg Group sedimentary rocks and the younger Umkondo dolerite sill. Abbreviations: Basement granite gneiss (BAS), dolerite dyke (DYKE), the F Zone (FZN), the Main Zone (MZN), overburden (OVE), Umkondo dolerite sill (SILL), Transitional Zone (TRNZ), the T Zone (TZN), the Upper Transitional Zone (UTRZN), the Upper Zone (UZ) and the Waterberg sedimentary rocks (WSE).

Unlike the north striking Bushveld Complex south of the HRSZ, the Bushveld Complex succession across the Waterberg Project strikes NE with the sequence sub-outcropping towards the east.

The contoured basement model (Figure 4.2) shows two embayments on the granite basement.

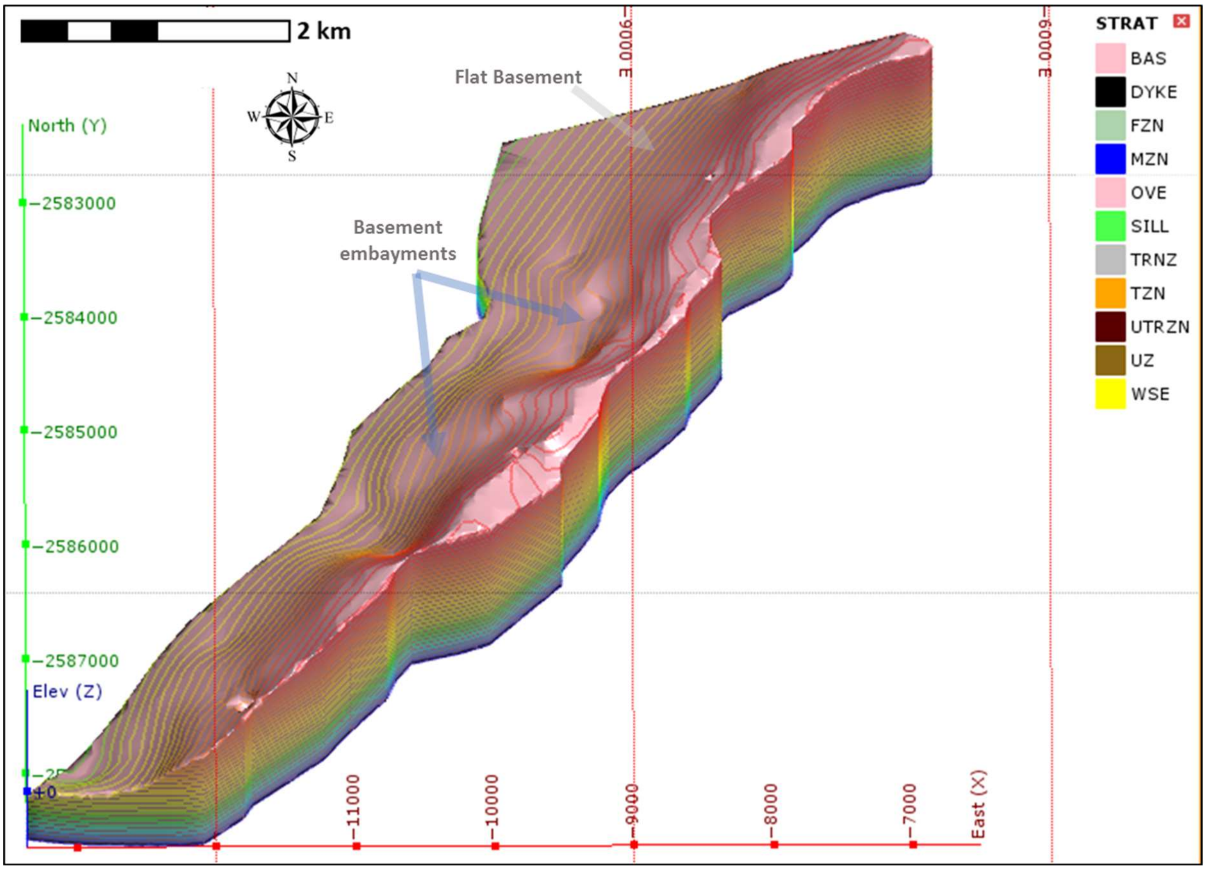

Figure 4.2. A 3D geological model of the Waterberg Project's basement. Note the embayments within the basement. Abbreviations: Basement granite gneiss (BAS), dolerite dyke (DYKE), the F Zone (FZN), the Main Zone (MZN), overburden (OVE), Umkondo dolerite sill (SILL), Transitional Zone (TRNZ), the T Zone (TZN), the Upper Transitional Zone (UTRZN), the Upper Zone (UZ) and the Waterberg sedimentary rocks (WSE)

The emplacement of both the marginal pyroxenite and the UmS which hosts the F Zone seem to have not completely filled-up the embayments (Figure 4.3).

At the stratigraphic level of the gabbronorite of the Main Zone (MZN) which significantly thickens towards the west (Figure 4.4), the morphology of the Bushveld sequence seems to be characterised by less embayments.

It should be noted that the models do not consider geological structures and therefore some areas of the model might pose a challenge in the interpretations.

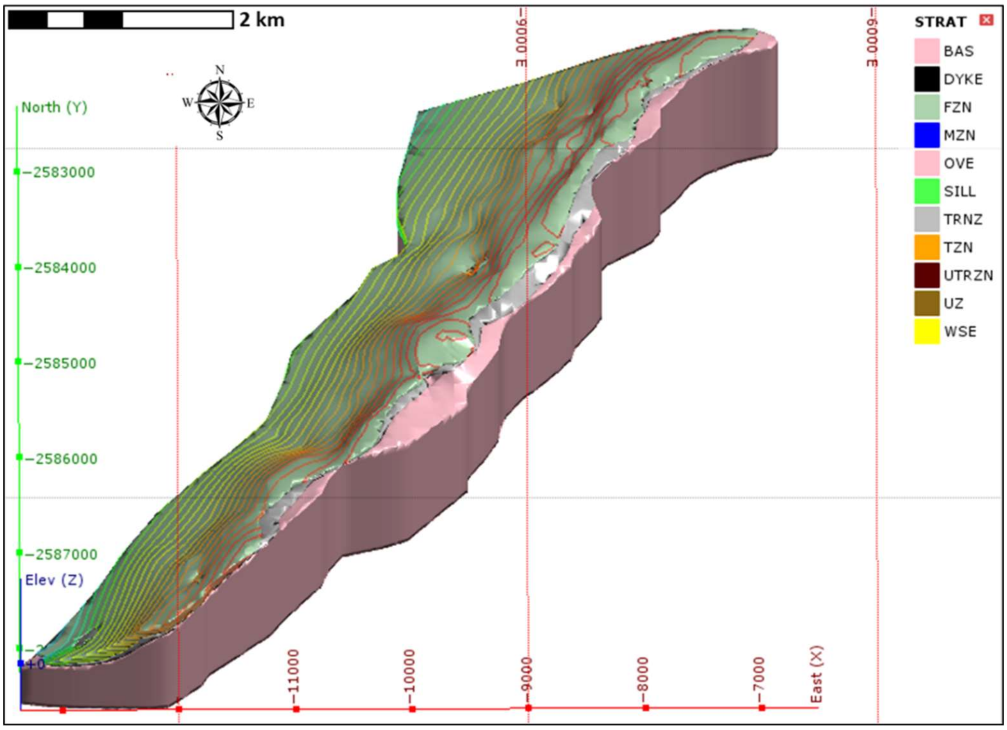

Figure 4.3. A 3D geological model of the F Zone (Ultramafic Sequence and bottom TGA troctolite) of the Waterberg Project. Abbreviations: Basement granite gneiss (BAS), dolerite dyke (DYKE), the F Zone (FZN), the Main Zone (MZN), overburden (OVE), Umkondo dolerite sill (SILL), Transitional Zone (TRNZ), the T Zone (TZN), the Upper Transitional Zone (UTRZN), the Upper Zone (UZ) and the Waterberg sedimentary rocks (WSE)

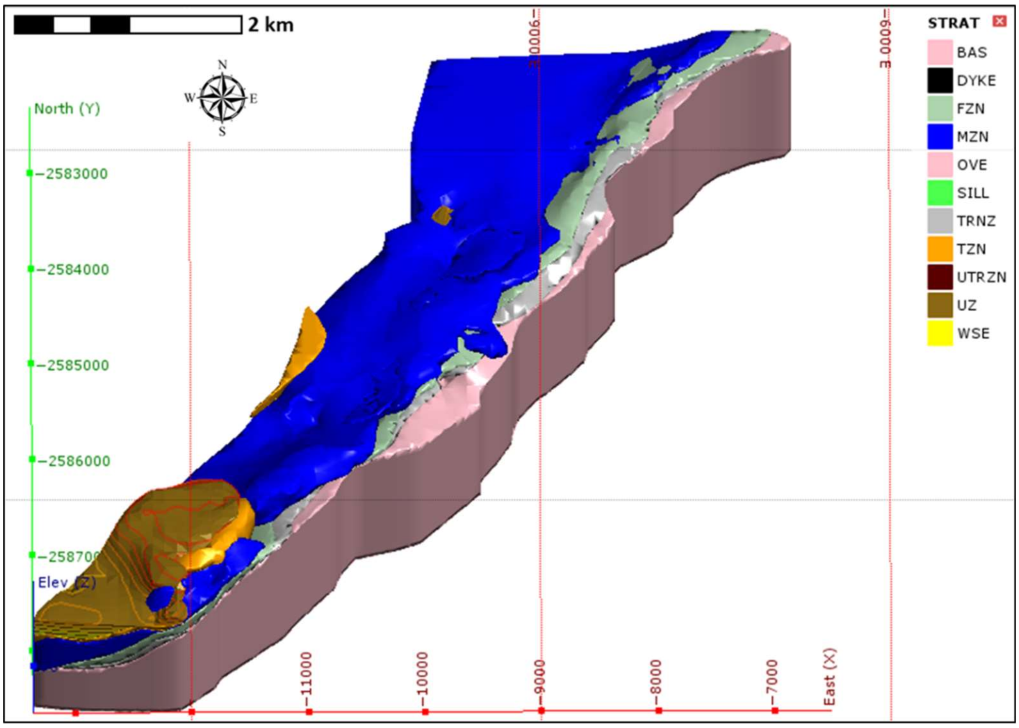

Figure 4.4. A 3D geological model of the Waterberg Project showing the top surface of the Main Zone gabbronorite. Abbreviations: Basement granite gneiss (BAS), dolerite dyke (DYKE), the F Zone (FZN), the Main Zone (MZN), overburden (OVE), Umkondo dolerite sill (SILL), Transitional Zone (TRNZ), the T Zone (TZN), the Upper Transitional Zone (UTRZN), the Upper Zone (UZ) and the Waterberg sedimentary y rocks (WSE)

Although the T Zone and the Upper Zone seem to be confined to the south of the project (Figure 4.4), drilling on top of the mountain north of the section has confirmed continuity of the T Zone and its mineralisation to the west.

Figure 4.5 is a 3D model of the Waterberg Group sedimentary succession intruded by the Umkondo Dolerite sill. The slightly elevated portion of the sedimentary succession to the west is the foot of the Makgabeng plateau. Where the sill outcrops, the surface is predominantly characterised by black clay which is at times mixed with calcrete.

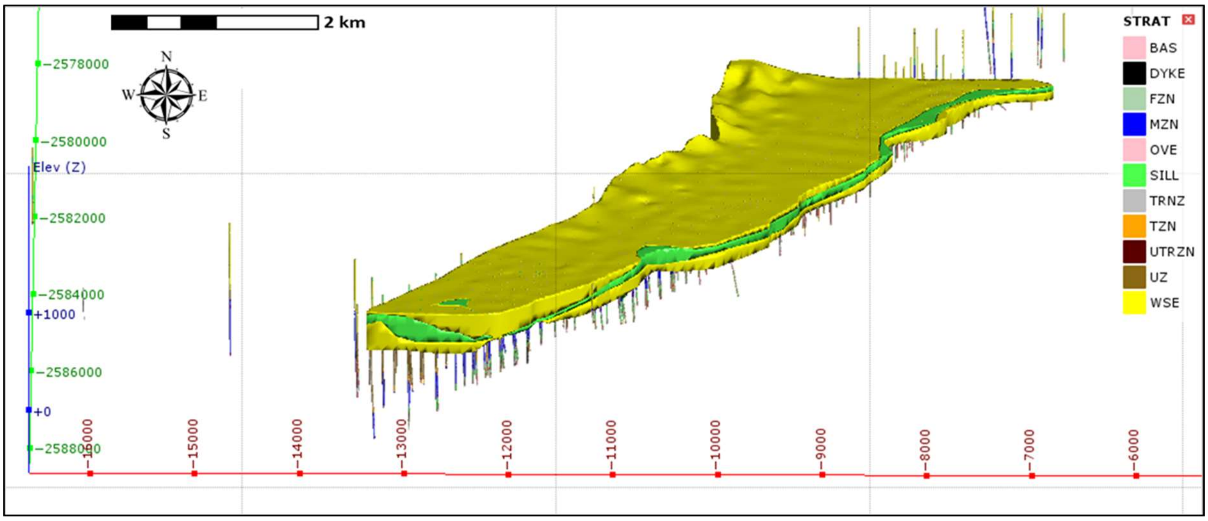

Figure 4.5. A 3D geological model of the Waterberg Project's upper sedimentary succession. The sedimentary succession is intruded by an Umkondo dolerite sill which outcrops in the far NE of the study area. Abbreviations: Basement granite gneiss (BAS), dolerite dyke (DYKE), the F Zone (FZN), the Main Zone (MZN), overburden (OVE), Umkondo dolerite sill (SILL), Transitional Zone (TRNZ), the T Zone (TZN), the Upper Transitional Zone (UTRZN), the Upper Zone (UZ) and the Waterberg sedimentary rocks (WSE)

As illustrated by the cross-sections (Figure 4.6), the sill splits into two or more smaller sills in places.

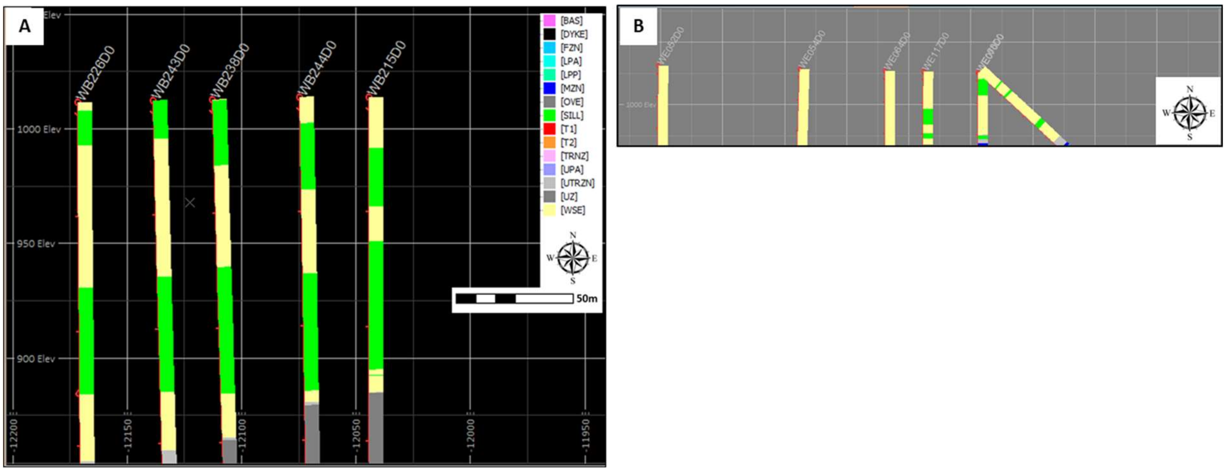

Figure 4.6. Cross sections showing partitioning of the sill into two or more sills. (A) two sills south of the study area, (B) two or more sills north of the study area. Abbreviations: Basement granite gneiss (BAS), dolerite dyke (DYKE), the F Zone (FZN), the Main Zone (MZN), overburden (OVE), Umkondo dolerite sill (SILL), Transitional Zone (TRNZ), the T Zone (TZN), the Upper Transitional Zone (UTRZN), the Upper Zone (UZ) and the Waterberg sedimentary rocks (WSE)

CHAPTER 5

BOREHOLE LOCALITIES, CORE LOGGING AND CORE SAMPLING

The mafic-ultramafic succession of the Waterberg Project extends from SW to NE with a strike extension of approximately 21 km. An intense step-out drilling on the properties has demonstrated continuity of mineralisation along this strike. Although mineralisation stretches along this strike length, thicker and higher grade mineralisation has been proven to be confined to the first 7.5- km from the SW to the farm Early Dawn in the NE (Figure 5.1).

With more information becoming available as a result of more infill drilling and sample analysis, the well mineralised portions of the mafic-ultramafic succession of the Waterberg Project was divided into six feasible districts based primarily on grade thickness and the depth of the economic mineralisation favours the mechanised mining method (Murphy et al., 2019). As illustrated on Figure 5.1, these districts are: -

- T Zone in the south
- F – South below the T Zone
- F - Central
- F - Boundary South
- F - Boundary North
- F - North

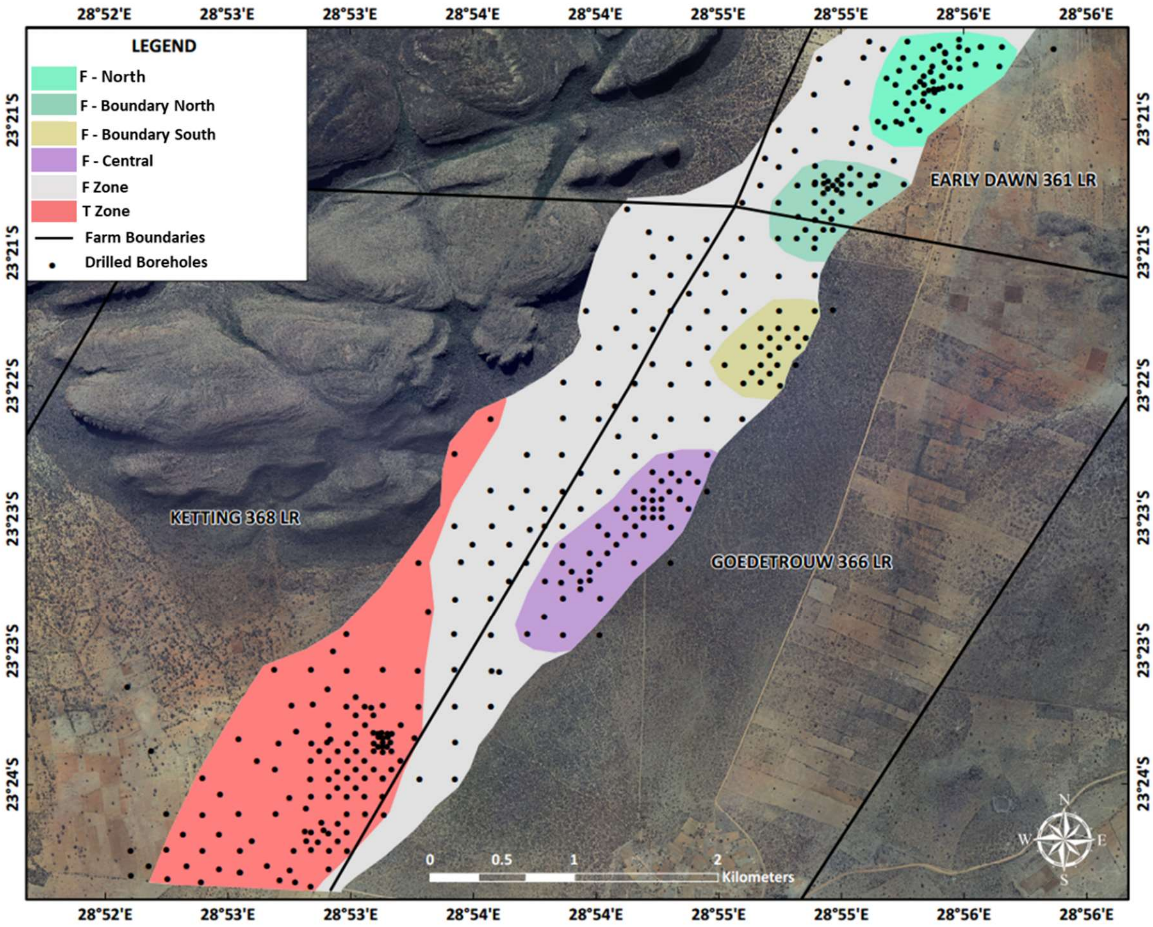

Figure 5.1. A layout plan of the Waterberg Project showing zones of current economic interest.

5.1 Borehole localities

As part of the study, an overall total of 23 drillholes were selected from these five thicker and well mineralised districts (excluding F-South). The study entailed comprehensive logging, sampling, analysing of polished ore thin sections, geochemical analysis and tenor calculations.

Seven of the overall twenty-three drillholes were selected from the T Zone (Figure 5.2). Drillholes WB222, WB221, WB213, WB237 & WB215 are on strike while WB228 & WB230 are on a dip section. WB213 is a denominator intersection point between the strike and dip section.

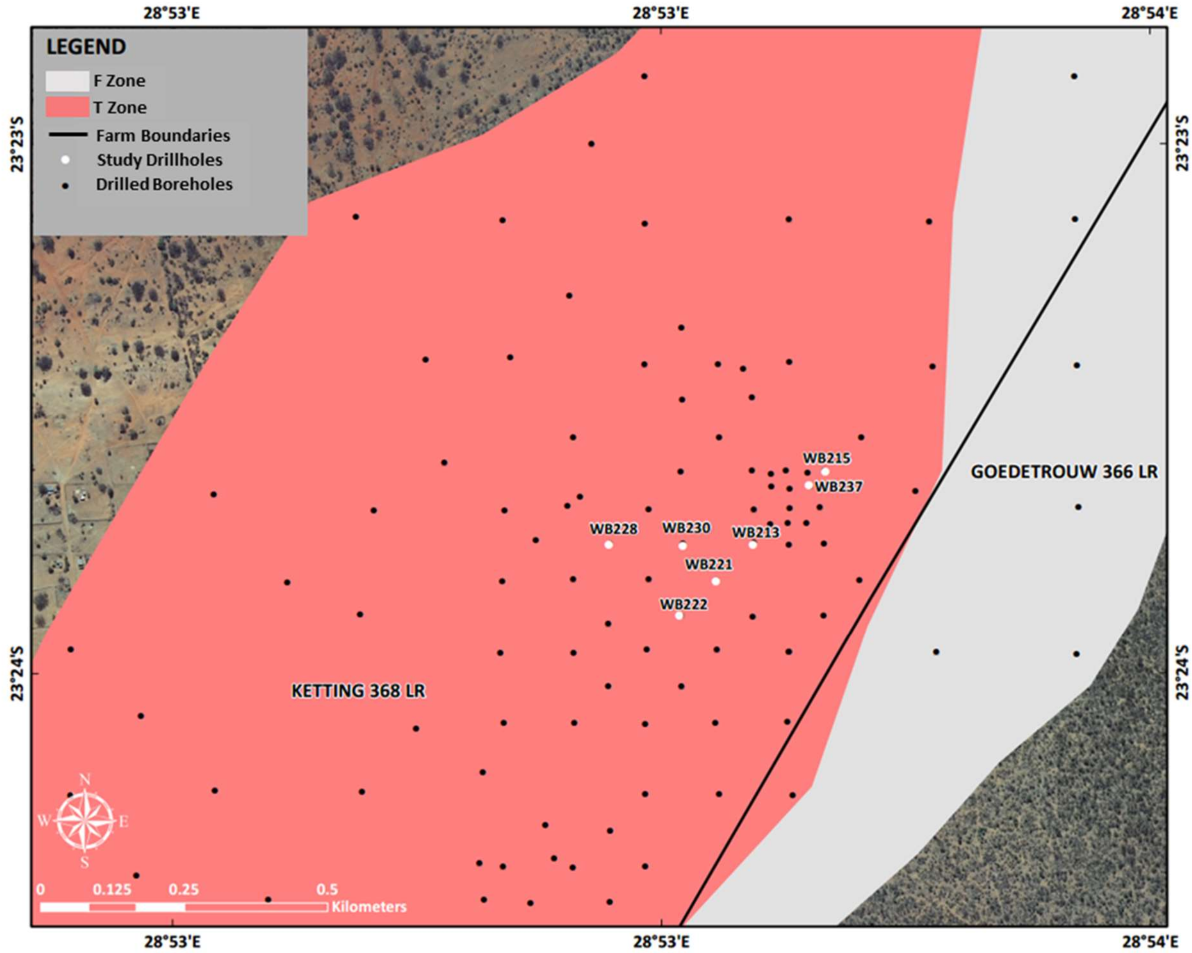

Figure 5.2. A layout plan of the T Zone showing the localities of the study holes.

Six drillholes were selected from F - Central. Three of the drillholes (WB276, WB264 & WB261) are along strike while the other three are on the dip section (WB280, WB259 & WB257). WB264 is an intersection point between the strike and dip section (Figure 5.3).

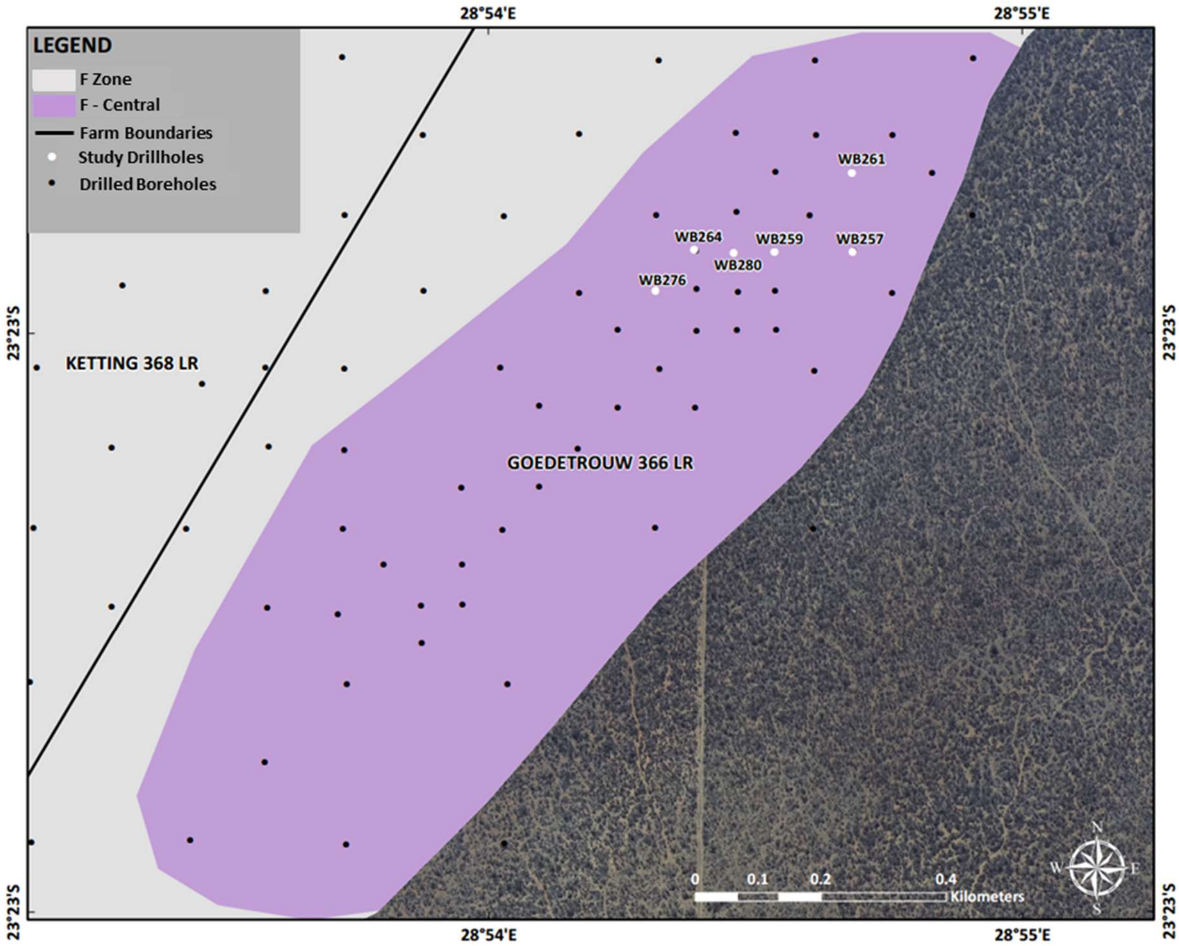

Figure 5.3. A layout plan of the F - Central district showing localities of the study holes.

Two drillholes were selected from F - Boundary South (WB254 & WB255) with three holes from F - Boundary North (WE061, WE144 & WE 145). The two drillholes from F -Boundary South are on a dip section while those on the F - Boundary North are not on any particular section (Figure 5.4).

From F - North (Figure 5.5), four dip section drillholes were selected (WE052, WE054, WE064 & WE117). An additional drillhole (WE120) south of the above-mentioned dip section was also selected for the study.

The F - North district is confined to the farm Early Dawn 361LR while F - Boundary North transgresses the Early Dawn 361LR and Goedetrouw 366LR boundary. Both F - Boundary South and F - Central districts are confined to the farm Goedetrouw 366LR. The T Zone is predominantly located to the south within the farm Ketting 368LR.

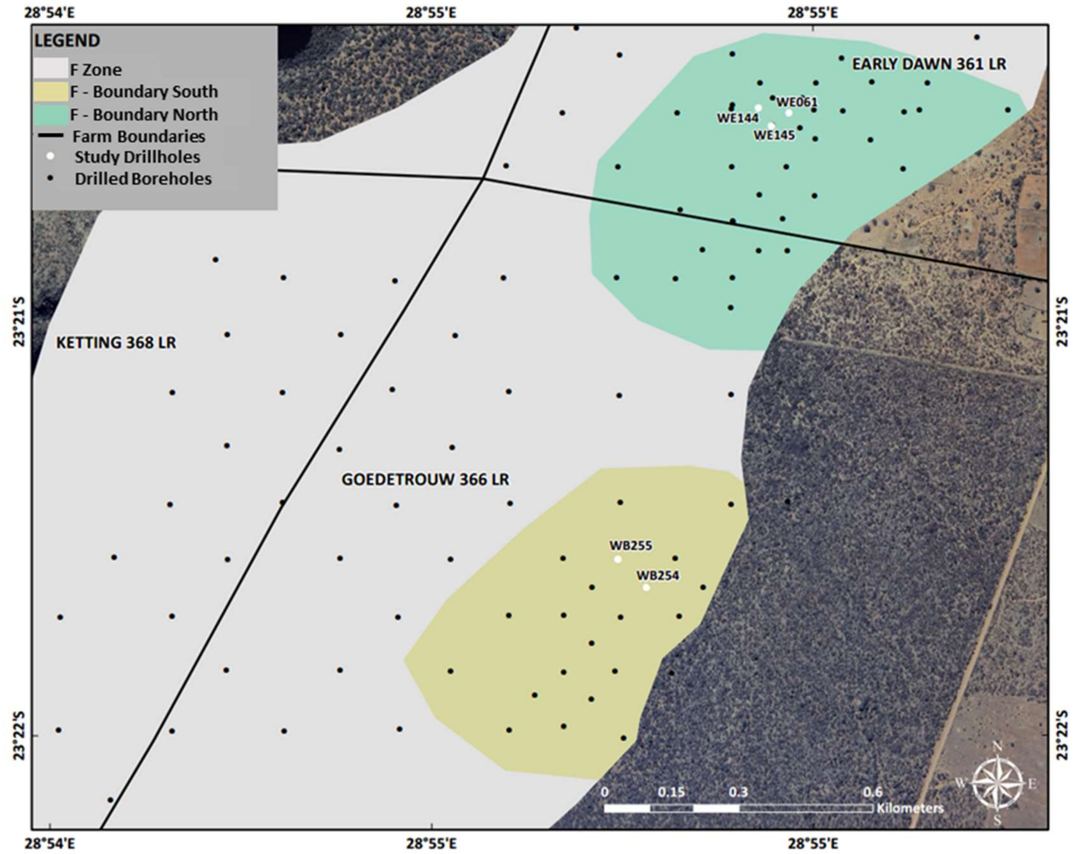

Figure 5.4. A layout plan of both F - Boundary South and F - Boundary North showing localities of the study holes.

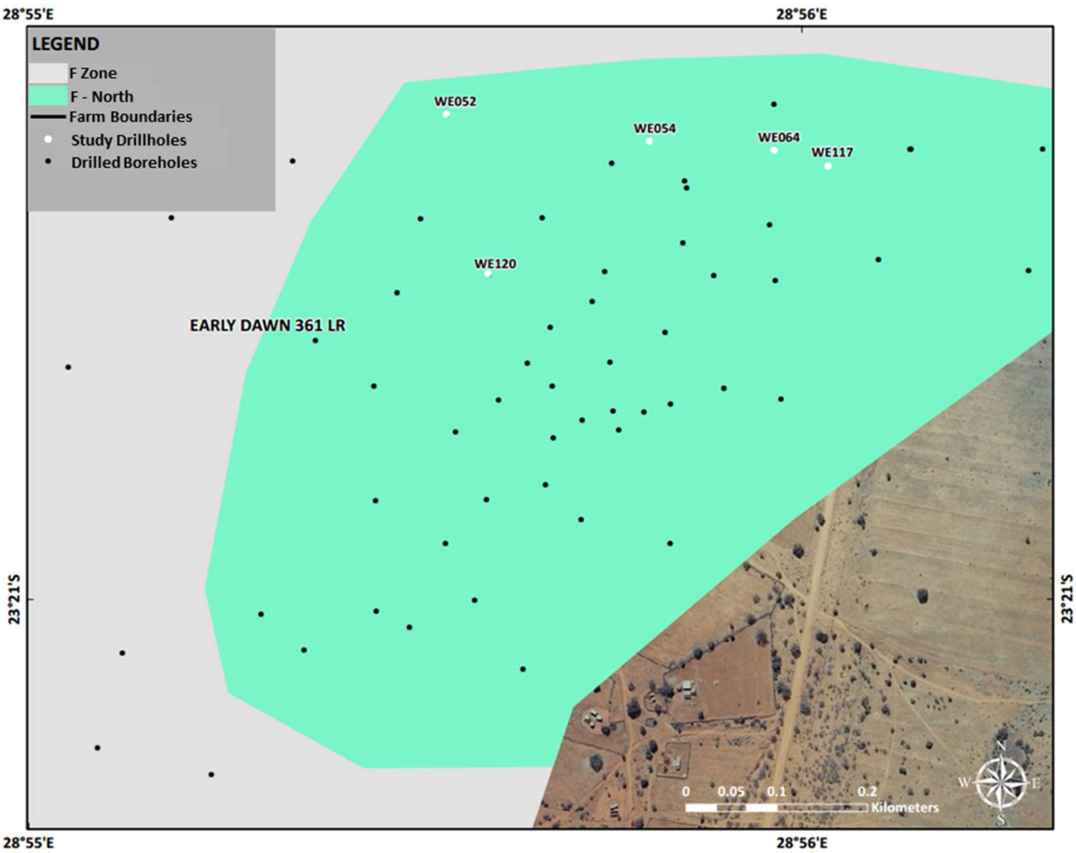

Figure 5.5. A layout plan of F - North district showing localities of the study holes.

5.2 Core logging

Prior to geological logging, the drillcore was meticulously examined to affirm suitability for logging. The core-boxes layout sequence, core recoveries, metre markings and drillcore cleanliness were confirmed for better and accurate geological interpretations. Lithostratigraphic interpretations were conducted in accordance with the SAMREC code of practice (SAMREC, 2007). While logging, the localities of the drillholes as shown in subsection 5.1 were taken into account in order to conceptualise, understand and appreciate lithostratigraphic variations from borehole to borehole, both along dip and strike sections.

All the study drillcore are HQ size (63.5 mm diameter) from collars to ∼ 60 m into the sedimentary succession. This was to enable installation of casings to support the upper unconsolidated portion of the sedimentary rocks. Where the drillcore proved to be fairly competent, an NQ drillcore size (47.6 mm) was drilled until end of hole.

5.3 Core sampling

5.3.1 <u>Core sampling for petrographic examination</u>

During the core logging process, mineralised intervals of both the lower F Zone and upper T Zone were identified. These intervals were identified by the presence of conspicuous blebby sulphides, disseminated sulphides, net-textured sulphides and occasional massive sulphides.

In order to understand the detailed mineralisation, texture and intergrowth of both the F Zone and the T Zone, a total of 29 NQ ¼ core samples were obtained from some of the study holes (Appendix 1). These samples were polished and cut into thin sections at the University of the Witwatersrand in preparation for detailed petrographic examination.

5.3.2 <u>Core sampling for geochemical analysis</u>

Core sampling for geochemical analysis was carried out subsequent to lithostratigraphic logging. Then ¼ core samples were obtained from both the T-Zone and the UmS (FH & FP). A maximum sample length of 100 cm was obtained extending for a few metres above and below a mineralised zone, with 50 cm samples taken within mineralised zones where sulphides are clearly visible. Variable samples with minimum widths of 25 cm were taken to accommodate changes in lithology.

To ensure that the field samples from the drillcore are to be analysed in a reliable and trustworthy manner, three Certified Reference Materials (CRMs) were inserted in the sampling stream as part of Quality Control and Quality Assurance procedure. Three types of PGE+Au CRMs with variable grades were used. The high-grade CRM, the low-grade CRM and the average grade CRM. Two types of blank material were also used, one being a granite aggregate blank and the other being a CRM blank (pulp) which is in the same explorer pack as the PGE+Au CRMs. All the CRMs were obtained from African Mineral Standards (AMIS).

For every 10 field samples, both a CRM and a blank were inserted.

The samples were dispatched to Set Point preparatory laboratory in Mokopane. At the preparatory lab, the samples were checked for moisture, dried if necessary and weighed. The samples were then crushed to less than 10 mm using a jaw crusher and split using a riffle splitter. Subsequent to splitting, the samples were pulverised to 90% less than 106 µm. The 106 µm is the minimum requirement for accuracy and precision during analysis (Murphy et al., 2019).

The pulverised samples were dispatched to Set Point analytical lab in Johannesburg where they were analysed for Pd (g/t), Pt (g/t) and Au (g/t) by 25g Pb fire-assay using Ag as a collector to enable easier handling of prills as well as to minimise losses during cupellation process. The resulting prills were dissolved with aqua-regia for inductively coupled plasma mass-spectrometric analysis (ICP-MS).

Subsequent to pre-concentration by fire assay and microwave dissolution, the resulting solutions were analysed for Au and PGEs by the Inductively Coupled Plasma/Optical Emission Spectrometry technique (ICP/OES).

The base metals (Cu, Ni, Cr, Co and S) were analysed using ICP/OES after a multi-acid digestion.

Upon reporting of the assay results from the laboratory, the assays were matched to the lithostratigraphy of their respective boreholes.

The following chapter (Chapter 6) deals with the petrography and mineralogy of both the F Zone and the T Zone.

CHAPTER 6

THE PETROGRAPHY AND MINERALOGY OF THE F ZONE AND THE T ZONE

6.1 Introduction

This chapter is aimed at confirming the classification of rock types and identification of the minerals. The modal mineralogical abundances, textures, mineral association and alteration intensities are described in detail as observed under a petrographic microscope at the University of the Witwatersrand. The mineralised intervals from the 29 polished samples were best observed and described under reflected light.

6.2 The rock types and mineralogy of the F Zone

The F Zone of the UmS is divided into two subzones. The lower feldspathic pyroxenite (FP) and the upper feldspathic harzburgite (FH) (Figure 6.1). The FH is typically medium grained with up to 90% orthopyroxene, up to 15% clinopyroxene and some interstitial plagioclase (Kinnaird et al., 2017).

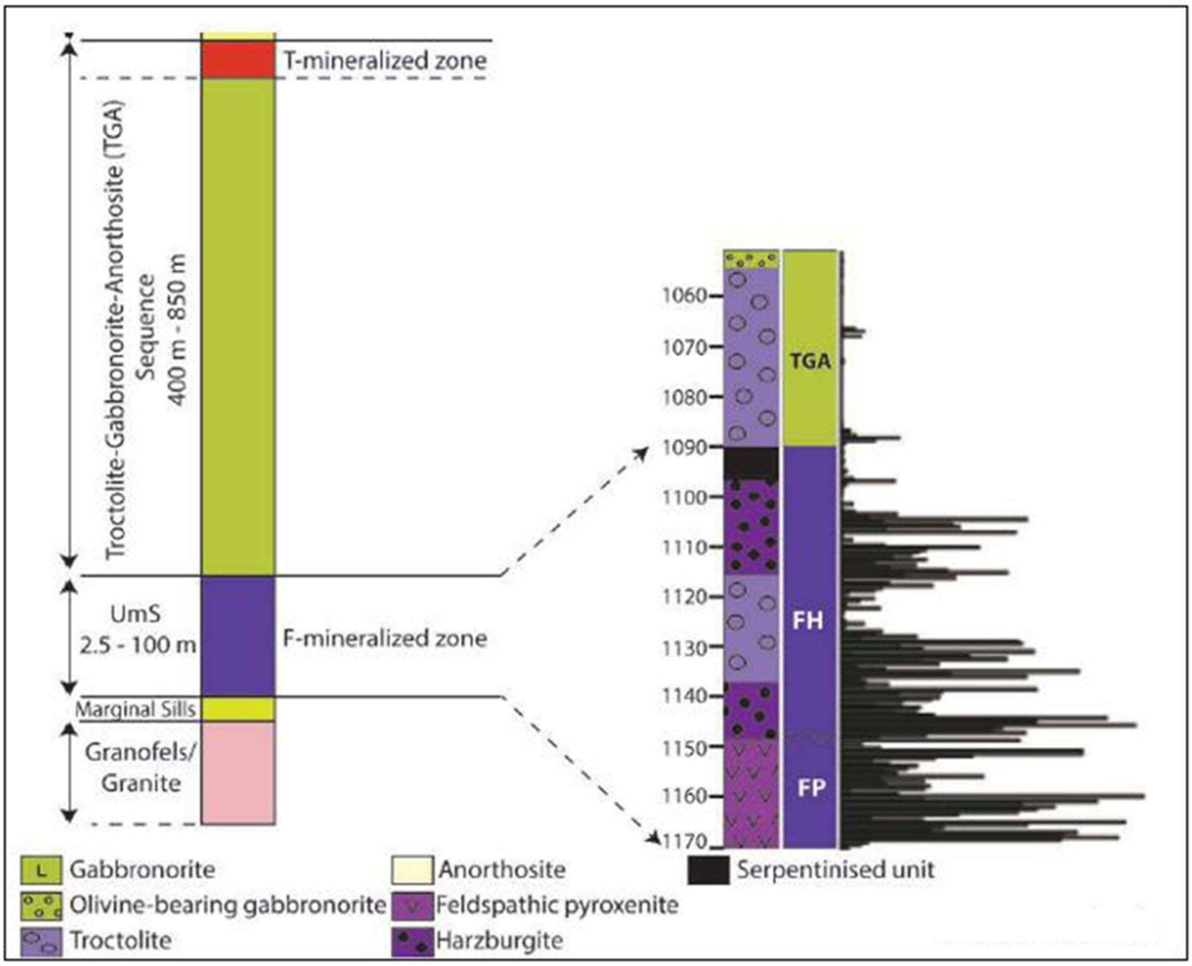

Figure 6.1. Schematic section of the Waterberg Project showing the stratigraphic position of the mineralised F Zone. The variability in Pd + Pt + Au grade is shown in the form of histograms (modified after Kinnaird et al., 2017)

The Sulphides constitute 2% - 5% of the rock composition and are widely associated with PGE mineralisation (Kinnaird et al., 2017). Rare chromitite stringers have been identified in some drillholes (Kinnaird et al., 2017).

The FH is made up of <65% olivine, 25% orthopyroxene, some interstitial plagioclase and minor clinopyroxene (Kinnaird et al., 2017). The orthopyroxenes generally occur as oikocrysts while clinopyroxene occurs as minor interstitial grains. The FH subzone is also pegmatoidal at the base and widely characterised by intense serpentinisation and chloritisation. Serpentinisation also resulted in the formation of secondary magnetite (Kinnaird et al., 2017). The 2-5% sulphides are generally associated with PGE mineralisation (Kinnaird et al., 2017).

6.3 The rock types and mineralogy of the T Zone

The T Zone at the interface between the TGA and the Upper Zone is characterised by bottom feldspathic pyroxenite which sometimes grades into gabbronorite (the T2 subzone). The T2 gabbronorites and feldspathic pyroxenite are characterised by conspicuous and distinctive elongated milky-white feldspars (Figure 6.2). Above the T2 lies an occasional pegmatitic pyroxenite (LPP). Directly above the LPP lies a medium to coarse-grained anorthosite which is in most cases pegmatitic in texture (LPA). Above the LPA lies the T1 mineralised subzone which hosts olivine-rich rock types such as troctolite, feldspathic harzburgite and some olivine-bearing feldspathic pyroxenite. Although the olivine-bearing T1 is occasionally characterised by some degree of serpentinisation and choritisation, the degree of such alteration is not as intense as that of the F Zone. As illustrated by McCreesh et al. (2018), both the LPP and the LPA which are the units between the T2 and the T1 are not always present (Figure 6.2). The medium to coarse-grained pegmatitic anorthosite (UPA) above the T1 mineralisation represents the uppermost subzone of the T Zone.

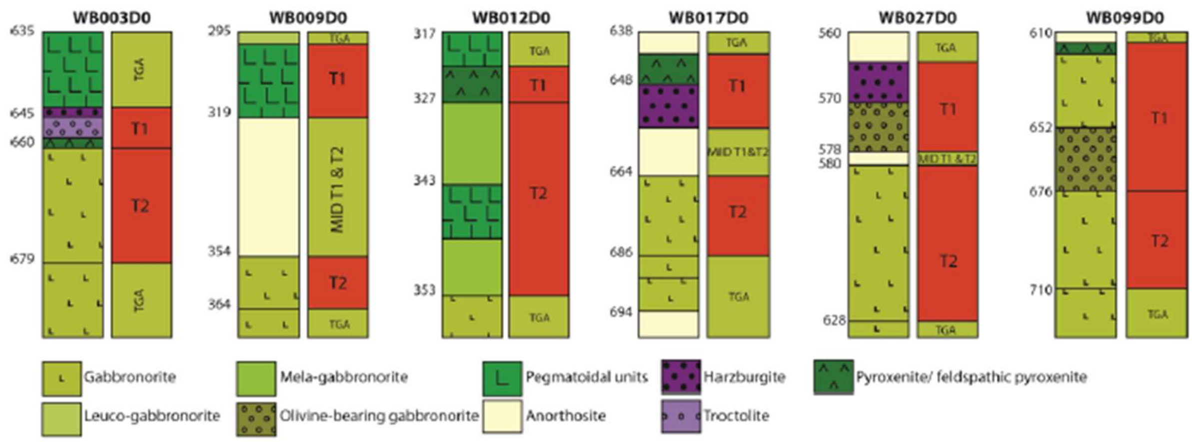

Figure 6.2. Schematic section showing host rocks of mineralisation and variability of rock types through the T Zone unit. The left column shows lithology while the right column shows the stratigraphy. It is important to note that the unit between the T2 and the T1 is synonymous to the LPP and LPA in the context of the study (McCreesh et al., 2018).

The sulphides (2-6%) within the T Zone are disseminated, blebby, net-textured and at times semi-massive. These sulphides are also associated with PGE mineralisation (McCreesh et al., 2018).

It is important to note that the T2 and T1 of the Waterberg succession do not equate to the T2 and T1 of Turfspruit.

6.4 Mineralisation in the UmS (the F Zone)

According to the study by McCreesh et al (2018), PGEs of the UmS are found to be intimately associated with magmatic base metal sulphides (pentlandite, chalcopyrite and pyrrhotite), which were altered during serpentinisation. Formation of a secondary sulphide assemblage is associated with this alteration. The study found sperrylite to be the main dominant PGE mineral within the UmS with Au-Ag alloys, Pd-Ni arsenides, Rh-Pt sulpharsenides, minor Pt-Pd bismuthotellurides and rare Pt-Fe alloys.

Within the UmS, sulphides constitute 1 - 5 vol.% within the upper part of the UmS, at times occurring as semi-massive sulphides with up to 25 vol.%. Sulphides occur as both blebby and disseminated magmatic sulphides with pyrrhotite being the dominant sulphide at 45%, followed by chalcopyrite at 30% and pentlandite at 20% (McCreesh et al., 2018). The blebby sulphides occur as an assemblage with a pyrrhotite core while both chalcopyrite and pentlandite occupies the margins of the core (Figure 6.3). At the margins of these blebs, pentlandite occur as brecciated or fractured grains and as minor exsolution blebs within pyrrhotite (Figure 6.3A). These blebs are accompanied by minor covellite.

Within the FH, disseminated chalcopyrite is progressively penetrated into the host rock forming aureoles of disseminated micrograins around sulphide blebs (Figure 6.3A). Covellite occurs as vein-like inclusions particularly within the pyrrhotite core of the sulphide blebs (Figure 6.3B). In places, the blebby sulphides are associated with both altered olivine and secondary magnetite (Figure 6.3B).

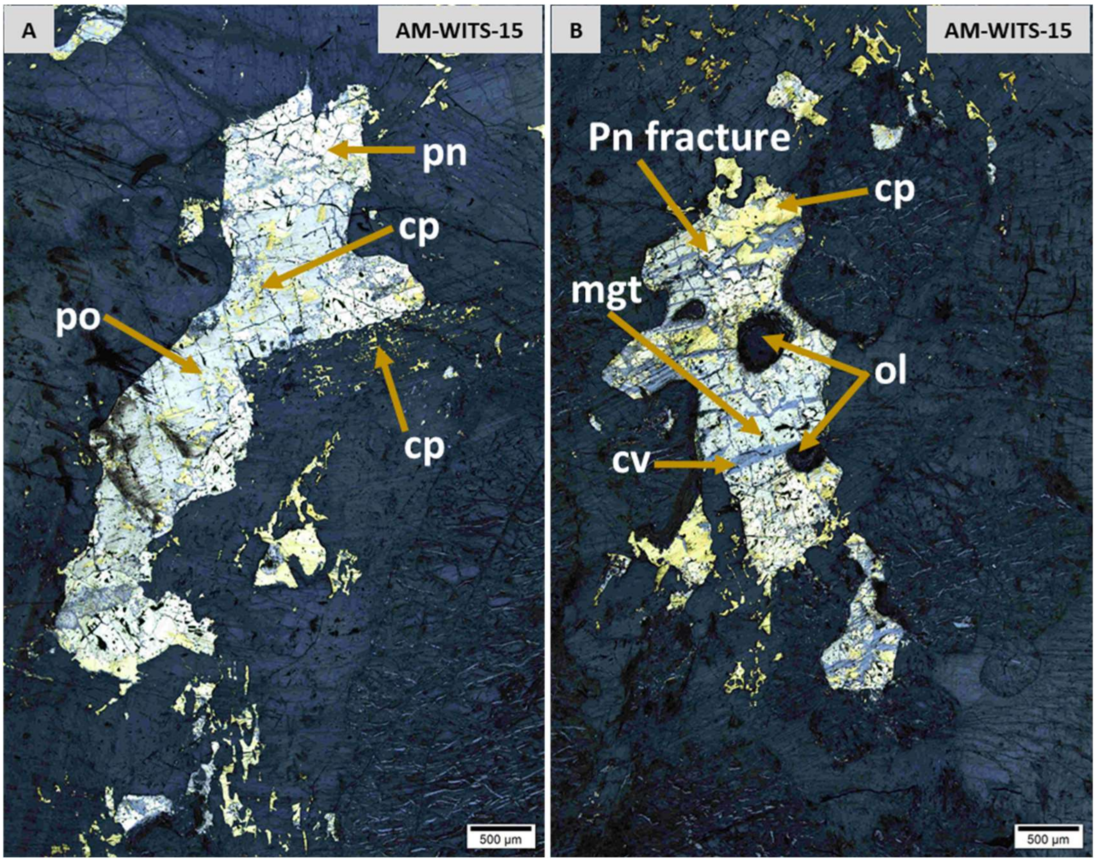

*Figure 6.3. Blebby irregular sulphides of the UmS (FH). **A (AM-WITS-15)**: sulphide bleb with pyrrhotite core and both chalcopyrite and pentlandite at the margins of the pyrrhotite core. Pentlandite occurs as fractured/brecciated grains. Note the progressive assimilation of disseminated chalcopyrite into the host rock. **B (AM-WITS-15)**: sulphide bleb with covellite and altered olivine inclusions and disseminated magnetite. The margins of the pyrrhotite core are surrounded by both pentlandite and chalcopyrite. Abbreviations: chalcopyrite (cp), covellite (cv), magnetite (mgt) olivine (ol), pentlandite (pn) and pyrrhotite (po).*

Although the FH is further characterised by remobilised disseminated chalcopyrite specks and veinlets within the olivine rich host rock (Figure 6.4A), these remobilised chalcopyrite are not prevalent within the FP orthopyroxenite host rocks. These remobilised disseminated chalcopyrite specks are identified by their elongated and at times curly morphology away from the main sulphide bleb (Figure 6.4A). Covellite also seems to be extremely rare if not absent within the sulphide blebs of the FP subzone (Figure 6.4B).

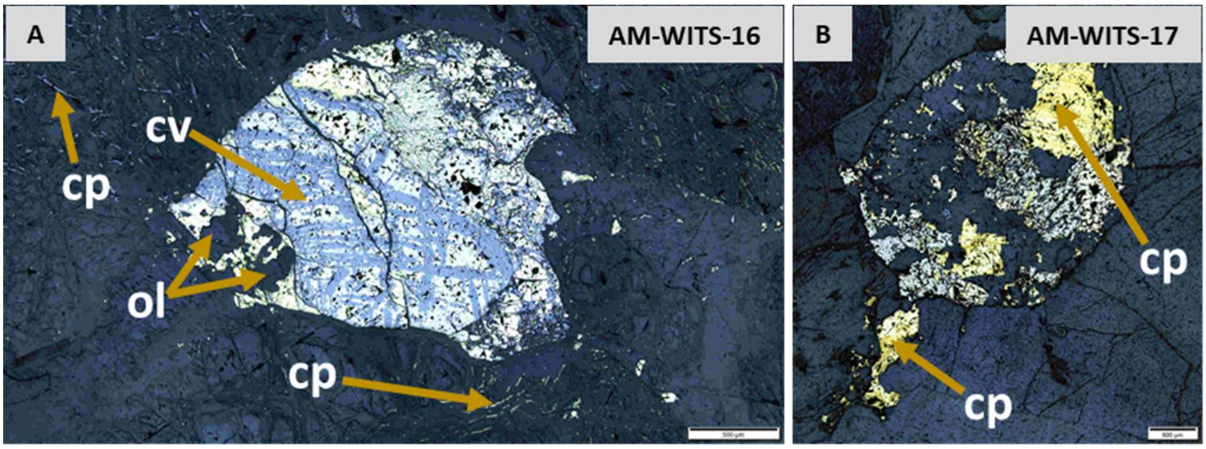

*Figure 6.4. Sulphide assemblage of both the FH and FP of the UmS (WB264D1). **A (AM-WITS-16)**: blebby sulphide assemblage of the FH characterised by vein-like covellite and some olivine inclusions. Remobilised chalcopyrite specks and veinlets are prevalent within the olivine rich host rock. **B (AM-WITS-17)**: blebby sulphide assemblage of the FP. Note the lack of chalcopyrite specks and veinlets within the orthopyroxene rich host rock. Abbreviations: chalcopyrite (cp), covellite (cv) and olivine (ol). The scale bar for both images is 500 µm.*

The F - North area is characterised by mainly pyrrhotite, exsolved chalcopyrite and pentlandite with notable quantities of orthopyroxene inclusions and an insignificant amount of disseminated chalcopyrite specks within orthopyroxenite host rock (Figure 6.5). However, there is a lack of sulphide veinlets, which attests to little or no sulphide remobilisation within the subzone.

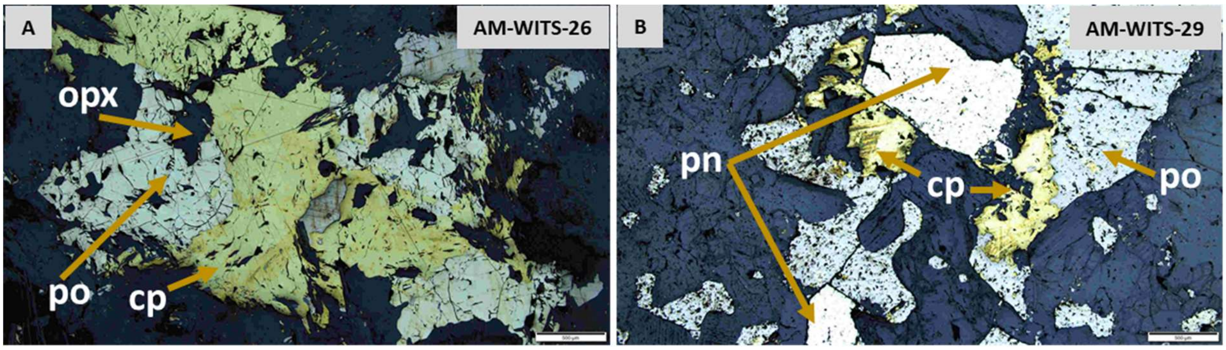

*Figure 6.5. Primary magmatic sulphide assemblage of the FP (WE120D0). **A (AM-WITS-26)**: chalcopyrite core with exsolved chalcopyrite. Note the orthopyroxene inclusion within both chalcopyrite and pyrrhotite. **B (AM-WITS-29)**: exsolved chalcopyrite and pentlandite. Note the lack of both remobilised chalcopyrite and covellite as observed within the FH. Abbreviatio*ns: chalcopyrite (cp), orthopyroxene (opx), pentlandite (pn) and pyrrhotite (po). The scale bar for both images is 500 µm.

6.5 Mineralisation in the T Zone

The T Zone is also associated with magmatic base metal sulphides and is further characterised by a chalcopyrite-millerite-pyrite assemblage associated with hydrothermal hydrous silicates and quartz (McCreesh et al., 2018). Pt-Pd bismuthotellurides are the dominant PGE minerals accompanied by Au-

Ag alloys, Pd tellurides with rare sperrylite, antimonides, braggite and Pd stannides (McCreesh et al., 2018). The higher Au/PGE, higher native Au content and the fluid induced style of mineral remobilisation are atypical of the Bushveld Complex but normal to the T Zone (McCreesh et al., 2018).

Within the T Zone, sulphides account for 3 – 10 vol.% in both the T2 and LPA subzones while T1 and the UPA account for 1 – 2 vol.%. Both the T2 and the LPA are consistently mineralised while T1 and UPA mineralisation is to some extent sporadic. Sulphides include pyrrhotite, chalcopyrite, pentlandite, pyrite, bornite and millerite. Some sphalerite, arsenopyrite and galena have been reported by McCreesh et al. (2018).

Two main sulphide assemblages have been identified within the T Zone. The primary magmatic assemblage is characterised by pyrrhotite as the dominant sulphide while the secondary assemblage is characterised by millerite as the dominant sulphide. Both assemblages are characterised by chalcopyrite as the second most abundant sulphide followed by pentlandite within the primary magmatic assemblage while pyrite is the third dominant mineral within the secondary assemblage.

Primary magmatic sulphides occur as discrete blebs and finely disseminated interstitial inclusions (Figure 6.6A).They also tend to occur as subrounded or irregular inclusions inside titanomagnetite (Figure 6.6B). Chalcopyrite is predominantly found at the margins of aggregates with pyrrhotite and pentlandite (Figure 6.6A). In places, chalcopyrite also occurs in micro-veinlets (Figure 6.6B) while some pyrrhotite is converted into pyrite (Figure 6.6C). Pyrite is a major mineral within the T Zone, predominant within the UPA and the LPA. Secondary disseminated sulphides and minor sulphide blebs are also common within the new amphibole crusts (Figure 6.6D).

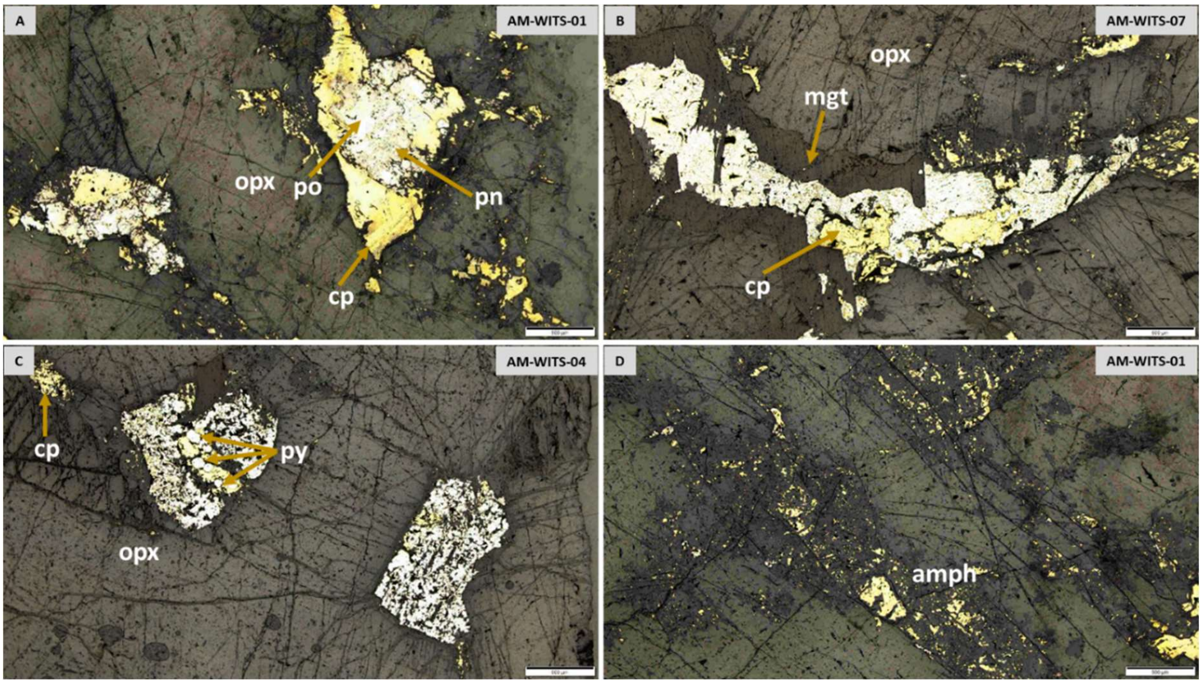

Figure 6.6. Sulphides of the mineralised T Zone under reflected light. ***A (AM-WITS-01)****: immiscible sulphides of the primary magmatic assemblage (WB222D1) attributed to segregation and migration of immiscible sulphide melts.* ***B (AM-WITS-07)****: coarse irregular sulphide aggregate of the T Zone partly surrounded by titanomagnetite (WB230D0). Note the chalcopyrite stringers.* ***C (AM-WITS-04)****: pyrite associated with pyrrhotite (WB213D0).* ***D (AM-WITS-01)****: new amphibole crust associated with a disseminated and blebby secondary sulphide assemblage. Abbreviations: amphibole (amph), chalcopyrite (cp), magnetite (mgt), orthopyroxene (opx), pentlandite (pn), pyrrhotite (po) and pyrite (py). Scale: 500 µm for all four images.*

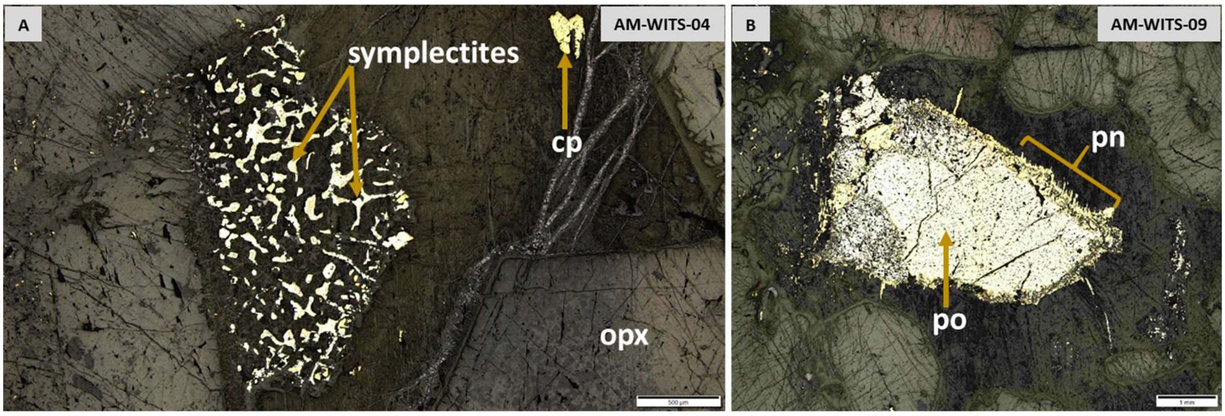

Figure 6.7. Rock textures and sulphides of the mineralised T Zone under reflected light. ***A (AM-WITS-04)****: symplectic intergrowth of millerite, chalcopyrite and magnetite with an altered amphibole rim. Olivine shows some degree of serpentinisation.* ***B (AM-WITS-09)****: larger T2 sulphide bleb with flame-like pentlandite. Both pentlandite and chalcopyrite form a rim around the pyrrhotite. Abbreviations: chalcopyrite (cp), orthopyroxene (opx), pentlandite (pn) and pyrrhotite (po). Scale* ***A****: (500 µm)* ***B****: (1mm).*

Within the anorthositic units, a symplectic intergrowths with millerite, chalcopyrite and titanomagnetite are prevalent locally with an amphibole rim (Figure 6.7A). Blebby sulphides as large as 4 mm are common within a well mineralised T2. These sulphides are predominantly pyrrhotite rimmed by chalcopyrite and pentlandite, with pentlandite showing a flame-like exsolution texture (Figure 6.7B).

6.6 Conclusion

The F Zone of the Ultramafic Sequence is divided into two subzones. The lower feldspathic pyroxenite (FP) and the upper feldspathic harzburgite. The two subzones are characterised by magmatic base metal sulphides occurring as disseminated, blebby, net-textured and at times semi-massive sulphides. The texture of the sulphides is primarily attributed to immiscible sulphide melt crystallisation.

The sulphide veinlets and the remobilised disseminated chalcopyrite specks are prevalent within the olivine-rich host rock of the FH and less prevalent within the FP. The vein-like covellite inclusions within the pyrrhotite core of the FH sulphide blebs are not common within the FP.

The upper T Zone is also associated with magmatic base metal sulphides. The primary magmatic assemblage is characterised by pyrrhotite while the secondary assemblage is characterised by millerite. The primary magmatic sulphides occur as discrete blebs and finely disseminated interstitial inclusions as attributed to the segregation and migration of sulphide immiscible sulphide melts. These sulphides also occur subrounded or irregular inclusions inside titanomagnetite.

The following chapter (Chapter 7) deals with geochemical aspects of the mineralisation associated with the base metal sulphides.

CHAPTER 7

DISTRIBUTION OF MINERALISATION - GEOCHEMICAL ASPECTS

7.1 Introduction

The mafic-ultramafic succession of the Waterberg Project is characterised by two main mineralised zones which are the lower F Zone and the upper T Zone. The F Zone is further characterised by two well-mineralised subzones which are the lower feldspathic pyroxenite (FP) and the upper feldspathic harzburgite (FH). The upper mineralised T Zone is located at the interface between the Troctolite-Gabbronorite-Anorthosite Sequence (The TGA). This mineralised zone (The T Zone) is subdivided into five distinctive subzones with the lowermost subzone being the T2 subzone and the uppermost subzone being the Upper Pegmatoidal Anorthosite (UPA). The Lower Pegmatoidal Anorthosite (LPA) is separated from the UPA by olivine-bearing T1 subzone. It is important to note that the T2 and T1 of the Waterberg succession do not equate to the T2 and T1 of Turfspruit.

The entire mafic-ultramafic succession of the Waterberg Project dips at 38° to the NW with a NE trend. The sub-outcrop of the entire mafic-ultramafic succession unconformably abuts the base of the Waterberg Group sedimentary rocks.

In this chapter, the lithostratigraphic logs and the geochemical samples results are used to evaluate the distribution of mineralisation in each drillhole. In order to understand the continuity and mineralisation control in both the F Zone and the T Zone, the mineralisation was studied in both dip and strike sections. Cross sections for the T Zone, F - Central, F - Boundary South, F - Boundary North and F - North were plotted and thoroughly evaluated.

Subsequent to the evaluation of grade distribution within the F Zone and the T Zone, the calculated sulphide tenor variations within both mineralised zones are presented. The tenors are for the selected drillcores calculated using the methodology outlined by Naldrett (2004). Both vertical and lateral variations in tenors were evaluated. The vertical variations in tenors were evaluated to determine whether the sulphides segregated from the magma in-situ or whether the sulphides were deposited in a mush without undergoing any segregation. Both the lateral tenor variations and the lateral Cu/Pd ratios were evaluated to determine the direction of the feeder zone(s) for the magma influxes.

Barnes et al. (1992) demonstrated that the Cu/Pd ratios of silicate rocks in the Munni Munni Complex of Australia show a distinctive increase in the vicinity of a PGE-endowed horizon. This was interpreted to be as a result of sulphide segregation. In the segregating sulphide melt, the Cu/Pd ratio is significantly lower compared to the silicate magma (Maier et al., 1998). This is as a result of the partition coefficient ($D_{sulph/sil}$) of Pd far exceeding that of Cu (Barnes and Picard, 1993). In comparison with the segregating sulphide melt, the residual silicate melt will have higher Cu/Pd ratios, hence rocks, which crystallised from such residual silicate magma, have higher Cu/Pd ratios. Since primary mantle magmas have Cu/Pd ratios of ~6500, rocks with Cu/Pd ratios below this value should contain Pd endowed sulphides while those with ratios higher than this value crystallised from magma which experienced sulphide segregation and thus are depleted in PGEs (Barnes et al., 1988). This method was tested in the Bushveld Complex by Maier et al. (1996b). Similar patterns as in the Munni Munni Complex (Barnes et al. 1992) were observed in the Bushveld Complex where the main shift in Cu/Pd occurred in the vicinity of the economically viable Merensky Reef and UG2 chromitite (Naldrett et al., 2009; 2011).

Cu/Pd ratios also highlight evolution of sulphides in the conduit-type deposits. In the Uitkomst Complex, harzburgite in the central portion of the intrusion have low Cu/Pd ratios (Maier et al., 2004) implying that it crystallised from un-depleted magma that streamed through the conduit (Maier et al., 1998).

Although vertical Cu/Pd ratio variations were studied on the drill cores, attempts to determine whether this method can show lateral variations were also made. This approach might shed some light in showing the direction of the magmatic feeder zone.

7.2 The Assay results

In this section, the assay results for each drillhole are evaluated, in particular the 2PGE + Au (Pd, Pt and Au) and the base metals (Cu, Ni and Cr).

The drillhole assay results were evaluated on both dip and strike sections as per district (Figure 5.1), starting from the south with the T Zone and ending in the north with the F - North.

In all stratigraphic logs of assay chemical data, the following abbreviations are used: -

Basement granite gneiss (BAS), dolerite dyke (DYKE), the Feldspathic Pyroxenite (FP), the Feldspathic Harzburgite (FH), the Troctolite-Gabbronorite-Anorthosite Sequence (TGA), the Upper Pegmatoidal Anorthosite (UPA), the Lower Pegmatoidal Anorthosite (LPA), the Lower Pegmatoidal Pyroxenite (LPP), The T í mineralised subzone (T——————————í), the T——————————î mineralised subzone (T——————————î), the Umkondo dolerite sill (SILL), Transitional Zone (TRNZ), the Upper Transitional Zone (UTRZN), the Upper Zone (UZ) and the Waterberg sedimentary rocks (WSE).

7.2.1 <u>The T Zone</u>

For localities of the T Zone boreholes on the strike and dip sections, refer to Figure 5.2

7.2.1.1 <u>The T Zone dip section</u>

The base metal content of the T2 mineralised interval of WB228D0 is 0.10% Cu, 0.08 % Ni and 0.005% Cr; with a Cu/Pd ratio of 100 (Figure 7.1). The Cu/Pd ratio of 693 in the mineralised portion of the Upper Zone (T0) is significantly higher compared to that of T2. However, the Cu and Ni content is lower at 0.03% and 0.02%, respectively. The T0 interception is characterised by slightly elevated Cr content of 0.007%, which is slightly higher than that of the T2 mineralised interval.

The base metal content of the T2 mineralised interval in WB230D0 is 0.12% Cu, 0.09% Ni and 0.003% Cr; with a Cu/Pd ratio of 297 (Figure 7.1). The Cu/Pd of 104 in the T0 is higher compared to that of T2. The Cu content of 0.2%, Ni of content 0.1% and Cr content of 0.006 in the are also higher in comparison to those of the T2.

The base metal content of the T2 mineralised interval in WB213D0 is 0.27% Cu, 0.15% Ni and 0.006% Cr; with a Cu/Pd ratio of 311 (Figure 7.1). The Cu/Pd of 732 in the T0 is significantly higher compared to that of T2. However, the Cu and Ni content is lower at 0.06% and 0.04%, respectively. The Cr content of 0.009% Cr is slightly higher than that of the T2 mineralised interval.

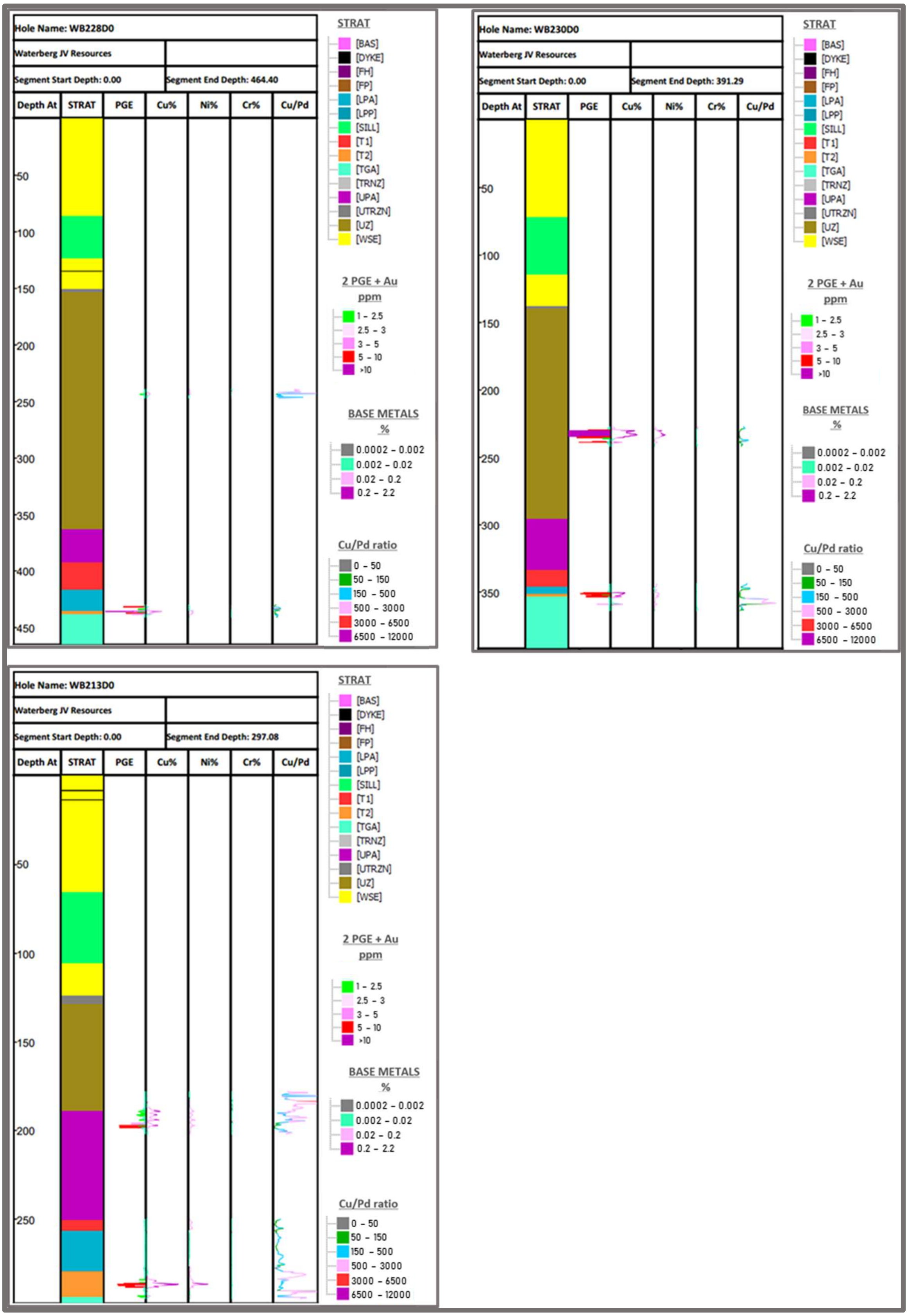

Figure 7.1. T Zone (dip section) stratigraphic logs with matched assay results.

7.2.1.2 <u>The T Zone strike section</u>

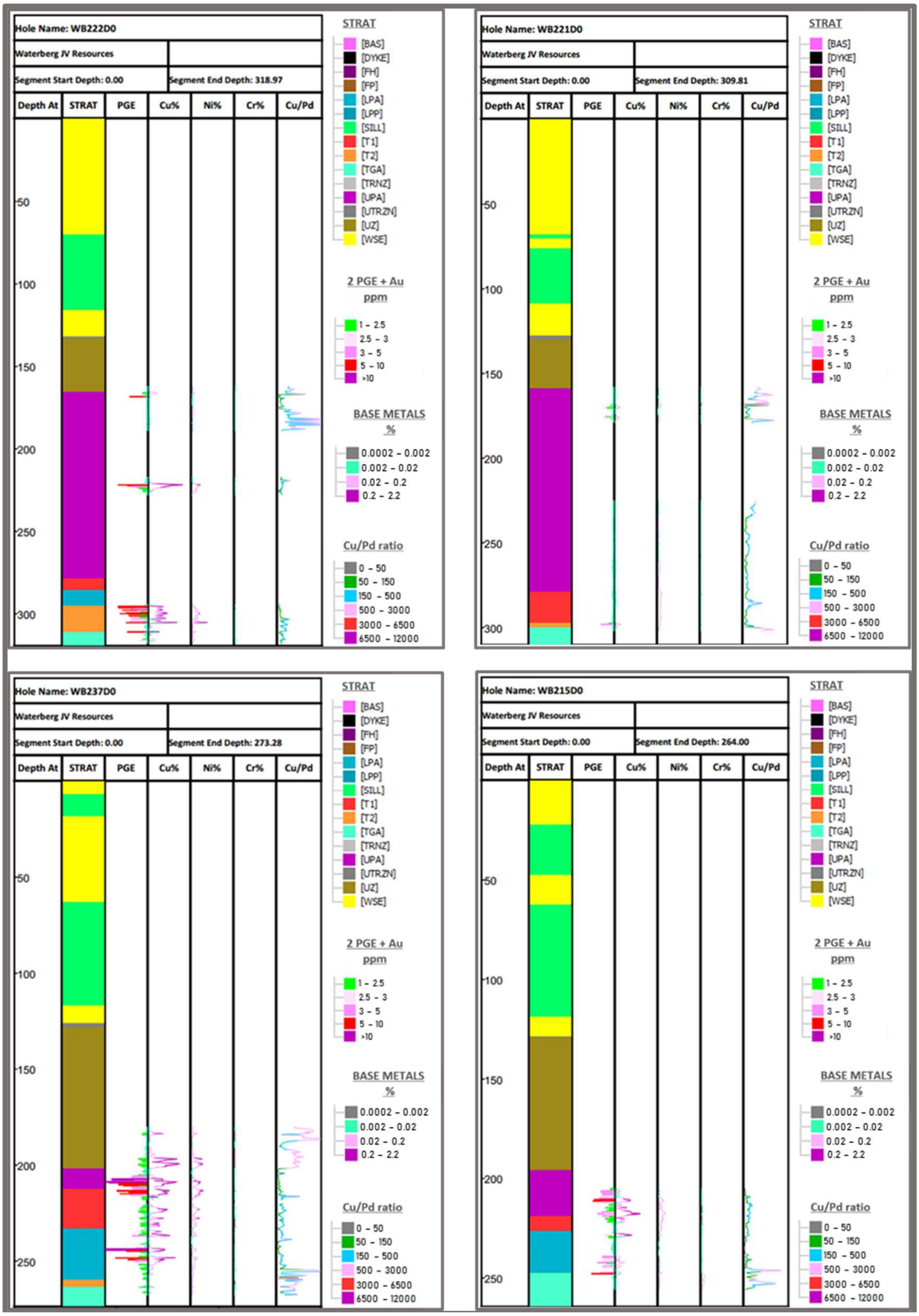

Figure 7.2. T Zone (strike section) stratigraphic logs with matched assay results.

The base metal content of the T2 mineralised interval of WB222D0 is 0.38% Cu, 0.20% Ni and 0.004% Cr; with a Cu/Pd ratio of 95 (Figure 7.2). The Cu/Pd of 520 in the T0 is significantly higher compared to that of T2. However, Cu and Ni content is lower at 0.01% and 0.02%, respectively. The 0.005% Cr content within the T0 is slightly higher than that of the T2 mineralised interval.

In WB221D0, the base metal content of the T2 mineralised interval is 0.05% Cu, 0.05% Ni and 0.004% Cr; with Cu/Pd ratio of 176 (Figure 7.2). The 476 Cu/Pd in T0 is higher compared to that of T2. However, Cu and Ni content is lower at 0.01% and 0.02% respectively. The 0.007% Cr content within the T0 is slightly higher than that of the T2 mineralised interval.

The base metal content of the LPA mineralised interval of WB237D0 is 0.015% Cu, 0.07% Ni and 0.04% Cr; with a Cu/Pd ratio of 235 (Figure 7.2). The Cu/Pd of 79 in T0 is lower compared to that of the LPA. However, Cu and Ni content is slightly higher at 0.17% and 0.08%, respectively. The Cr content of 0.003% within the T0 is slightly lower compared to that of the LPA mineralised interval.

In WB215D0, the base metal content of the LPA mineralised interval is 0.05% Cu, 0.03% Ni and 0.015% Cr; with a Cu/Pd ratio of 255 (Figure 7.2). The Cu/Pd of 161 in T0 is lower compared to that of the LPA. However, Cu and Ni content is higher at 0.14% and 0.07%, respectively. The 0.011% Cr content within the T0 is slightly higher compared to that of the LPA mineralised interval.

7.2.1.3 Discussion (The T Zone)

On dip section, particularly within the T2 mineralised subzone, the three drillholes show an increase in both base metal content (Cu and Ni) and Cu/Pd from west to east. The Cr content of about 0.007% within the T0 is slightly higher than that of the T2 mineralised subzone. However, the Ni content seem to be slightly variable. On strike section, all the base metal distributions are highly variable.

Generally, the Cu/Pd ratios of the T0 are higher that of the T2 subzone. The Cu/Pd ratios within both the T2 mineralised subzone and the T0 are significantly lower than the ∼6500 of the primary mantle magmas. These lower ratios suggest that the magma contained Pd endowed sulphides. If the ratios were to be higher than ∼6500, this would have implied that the magma experienced sulphide segregation and would have been depleted in PGEs (Barnes et al., 1988)

7.2.2 The F - Central

The modified stratigraphic nomenclature after Huthmann et al. (2016) is used in this section (Figure 3.2). Vertical variations in metal content were noted and are discussed here in detail for both the lower FP and the upper FH of the F Zone. The variations are studied along both strike and dip sections. For localities of the F Zone boreholes on strike and dip section, refer to Figure 5.2.

7.2.2.1 The F - Central strike section

As shown on Figure 7.3, only WB264D0 has both FH and FP. Both WB276D0 and WB261D0 drillholes are characterised by FH only.

Figure 7.3. F - Central (strike section) stratigraphic logs with matched assay results.

The base metal content of the PGE bearing FH of WB276D0 is 0.06% Cu, 0.18% Ni and 0.08% Cr; with a Cu/Pd ratio of 87 (Figure 7.3).

In WB264D0, the base metal content of the F Zone (FH & FP) mineralised interval is 0.09% Cu, 0.22% Ni and 0.06% Cr; with a Cu/Pd ratio of 45 (Figure 7.3). The Cu/Pd ratio of FP is 52 while that of FH is slightly lower at 45. The FH has slightly elevated Ni content of 0.22% compared to the 0.18% in the FP. The Cu content in FH is 0.09% while that in the FP is 0.10%. Both FH and FP have a Cr content of 0.06%.

The base metal content of the PGE bearing FH of WB261D0 is 0.04% Cu, 0.15% Ni and 0.04% Cr; with a Cu/Pd ratio of 69 (Figure 7.3).

Mineralisation within WB264D0 is consistent throughout the FH. In both WB276D0 and WB261D0, the mineralised interval of the F Zone is top and bottom loaded with grades higher than 2.5 ppm. The middle of the mineralised intervals are characterised by grades lower than 2.5 ppm. These areas of lower PGE mineralisation seem to be associated with elevated Cu/Pd ratios.

7.2.2.2 <u>The F - Central dip section</u>

As shown on Figure 7.4, both WB259D0 and WB257D0 are characterised by FP and FH mineralised subzones. WB280 is characterised by FH and a very thin FP that is disregarded.

The base metal content of the PGE bearing FH of WB280D0 is 0.05% Cu, 0.18% Ni and 0.09% Cr; with Cu/Pd ratio of 62 (Figure 7.4).

In WB259D0, the base metal content of the F Zone (FH and FP) mineralised interval is 0.037% Cu, 0.16% Ni and 0.07% Cr; with a Cu/Pd ratio of 159 (Figure 7.4). The Cu/Pd ratio of FP is 30 while that of FH is higher at 166. The FH has slightly elevated Ni content of 0.16% compared to the 0.15% in the FP. The Cu content in FH is 0.03% and than in the FP is 0.05%. The Cr content in FP is 0.04% while that of FH is higher at 0.08%.

The base metal content of the PGE bearing F Zone (FH & FP) and the lower mineralised portion of the TGA of WB257D0 is 0.03% Cu, 0.16% Ni and 0.08% Cr; with a Cu/Pd ratio of 58 (Figure 8.4). The Cu/Pd ratio of FP is 59 while that of FH is slightly higher at 65. The FH has elevated Ni content of 0.16% compared to the 0.11% in the FP. The Cu content in FH is 0.03% while that in the FP is 0.02%. The Cr content in FP is 0.05% while that of FH is higher at 0.08%. The uncommonly mineralised lower portion of the TGA is characterised by a Cu/Pd ratio of 36 with an elevated Cu and Ni content of 0.047% and 0.2%, respectively. The Cr content is slightly lower than that of the FH at 0.07% but higher than that of the FP.

The F Zone mineralisation in WB280D0 is top and bottom loaded with grades above 2.5 ppm. The mineralised interval is further characterised by thinner intervals of grades less than 2.5 ppm. In WB259D0, the best grade thickness is in the middle of the F Zone. The top and the bottom portion of the mineralised F Zone is generally characterised by lower grades with sporadic higher grades.

WB257D0, which is far up-dip on the section (Figure 5.3) is characterised by good grades in the lower portion of the TGA. The F Zone is not so well mineralised compared to the rest of the drillholes on the dip section. Areas of lower PGE mineralisation seem to be associated with elevated Cu/Pd ratios.

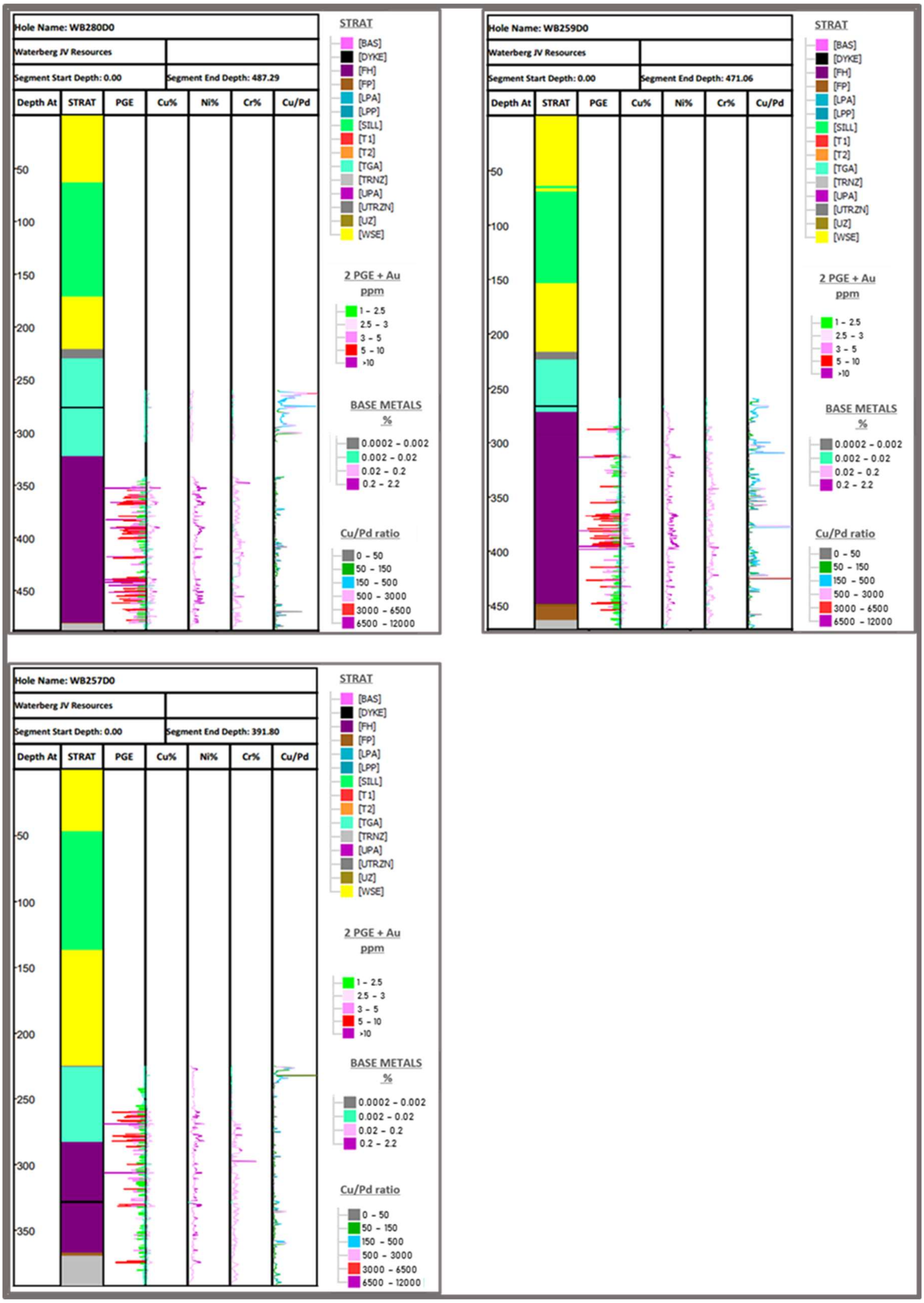

Figure 7.4. F - Central (dip section) stratigraphic logs with matched assay results.

7.2.3 The F - Boundary South

As shown on Figure 7.5, both WB255D0 and WB254D0 are characterised by FH and FP.

The base metal content of the PGE bearing F Zone (FH & FP) is 0.06% Cu, 0.16% Ni and 0.05% Cr; with a Cu/Pd ratio of 100 (Figure 7.5). The Cu/Pd ratio of the FP is 94 while that of the FH is higher at 107. The FH has an elevated Ni content of 0.20% compared to the 0.13% in the FP. The Cu content in FH is 0.07% while that in the FP is 0.05%. The Cr content in the FP is 0.03% while that of FH is higher at 0.07%.

In WB254D0, the base metal content of the (FH & FP) mineralised interval is 0.04% Cu, 0.11% Ni and 0.03% Cr; with a Cu/Pd ratio of 183 (Figure 7.5). The Cu/Pd ratio of the FP is 123 while that of FH is higher at 182. The FH has slightly elevated Ni content of 0.11% compared to the 0.10% in the FP. The Cu content in both the FP and the FH is 0.04%. The Cr content in the FP is 0.03% while that of the FH is slightly higher at 0.03%.

In both WB255D0 and WB254D0, the mineralised interval of the FH is top loaded. However, in WB255D0, the top loaded mineralisation is thinner compared to that on the up-dip WB254D0.

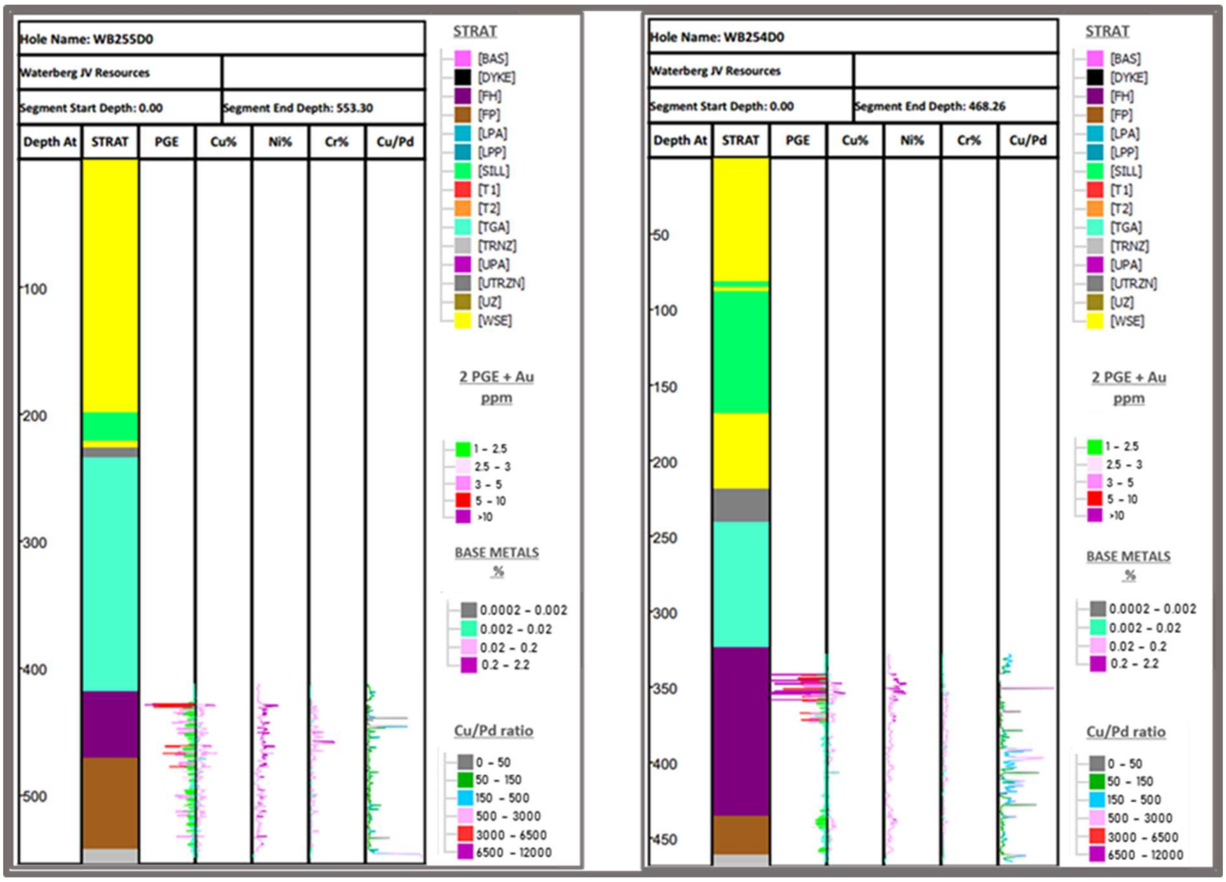

Figure 7.5. F - Boundary South stratigraphic logs with matched assay results.

7.2.4 The F -Boundary North

As shown on Figure 7.6, both WE144D0 and WE061D0 intersected FH only with an exception of WE045D0 which has both FH and FP (Figure 7.6).

The base metal content of the PGE bearing FH of WE061D0 is 0.010% Cu, 0.21% Ni and 0.09% Cr; with a Cu/Pd a ratio of 73 (Figure 7.6).

Within WE144D0, the base metal content of the FH mineralised interval is 0.08% Cu, 0.19% Ni and 0.09% Cr; with a Cu/Pd ratio of 120 (Figure 7.6).

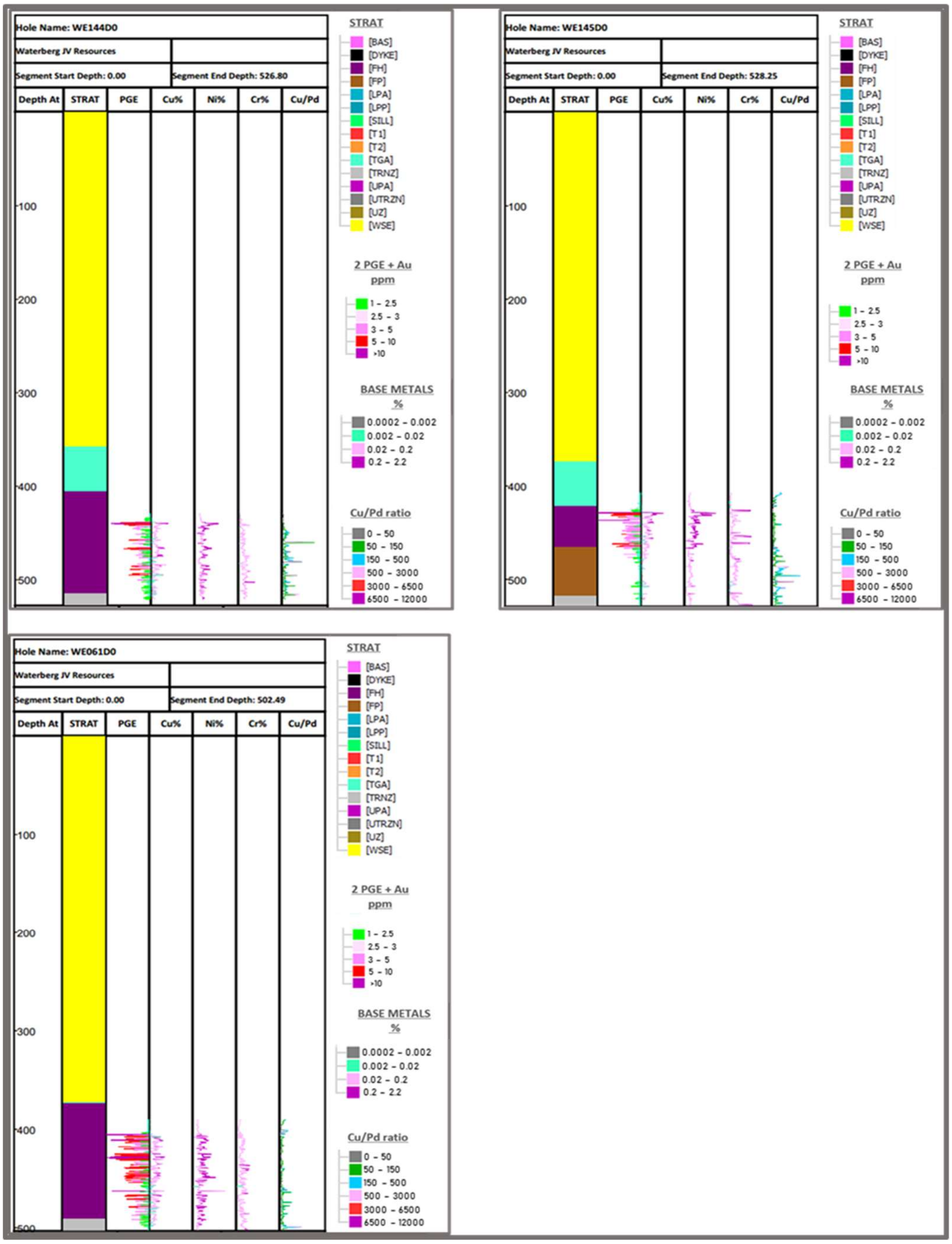

Figure 7.6. F - Boundary North stratigraphic logs with matched assay results.

The base metal content of the PGE bearing F Zone (FH & FP) of WE145D0 is 0.07% Cu, 0.17% Ni and 0.09% Cr; with a Cu/Pd ratio of 126 (Figure 7.6). The Cu/Pd ratio of the FP is 177 while that of the FH is lower at 61. The FH has slightly elevated Ni content of 0.24% compared to the 0.12% in the FP. The Cu content in FP is 0.04% while that of the FH is higher at 0.11%. The Cr content in the FP is 0.08% while that of the FH is slightly higher at 0.08%.

In WE061D0, the FH interval is very well mineralised without PGE poor middlings. The FP in WE145D0 is poorly mineralised with grades below 2.5 ppm while the FH is well mineralised with grades well above 2.5 ppm. The overall mineralised interval of the FH in WE145D0 is also without poorly mineralised middlings. The FH interval in WE144D0 is characterised by thin top loaded mineralisation. The overall FH mineralisation is not as desirable as those of WE061D0 and WE0145D0.

The FP of the F - Boundary North is characterised by higher Cu/Pd ratios in comparison to those of F - Boundary South and F - Central.

7.2.5 The F - North

As illustrated on Figure 7.7, all four boreholes (WE052D0, WE054D0, WE064D0 and WE117D0) are characterised by both FP and FH. From the westerly WE052D0 to the easterly WE117D0, the FH is gradually thinning while the FH is thickening.

The base metal content of the PGE bearing F Zone (FH & FP) of WE052D0 is 0.09% Cu, 0.19% Ni and 0.08% Cr; with a Cu/Pd ratio of 54. (Figure 7.7). The Cu/Pd ratios of the FP is 53 while that of the FH is slightly higher at 65. The FH has slightly elevated Ni content of 0.22% compared to the 0.19% in the FP. The Cu content in the FH is 0.10% while that in the FP is 0.09%. The Cr content in FP is 0.08% while that of the FH is slightly higher at 0.09%.

In WE054D0, the base metal content of the PGE bearing F Zone (FH & FP) are 0.06% Cu, 0.15% Ni and 0.04% Cr; with a Cu/Pd ratio of 95 (Figure 7.7). The Cu/Pd ratio of the FP is 130 while that of the FH is lower at 50. The FP has slightly elevated Ni content of 0.16% compared to the 0.14% in the FH. The Cu content in the FH is 0.03% while that in the FP is 0.08%. The Cr content in the FP is 0.05% while that of FH is slightly lower at 0.04%.

The base metal content of the PGE bearing F Zone (FH &FP) of WE064D0 is 0.08% Cu, 0.14% Ni and 0.06% Cr; with a Cu/Pd ratio of 81 (Figure 7.7). The Cu/Pd ratio of the FP is 100 while that of the FH is lower at 75. The FH has slightly elevated Ni contents of 0.15% compared to the 0.12% in the FH. The Cu content in the FH is 0.03% while that in the FP is 0.08%. The Cr content in the FP is 0.10% while that of the FH is slightly lower at 0.04%.

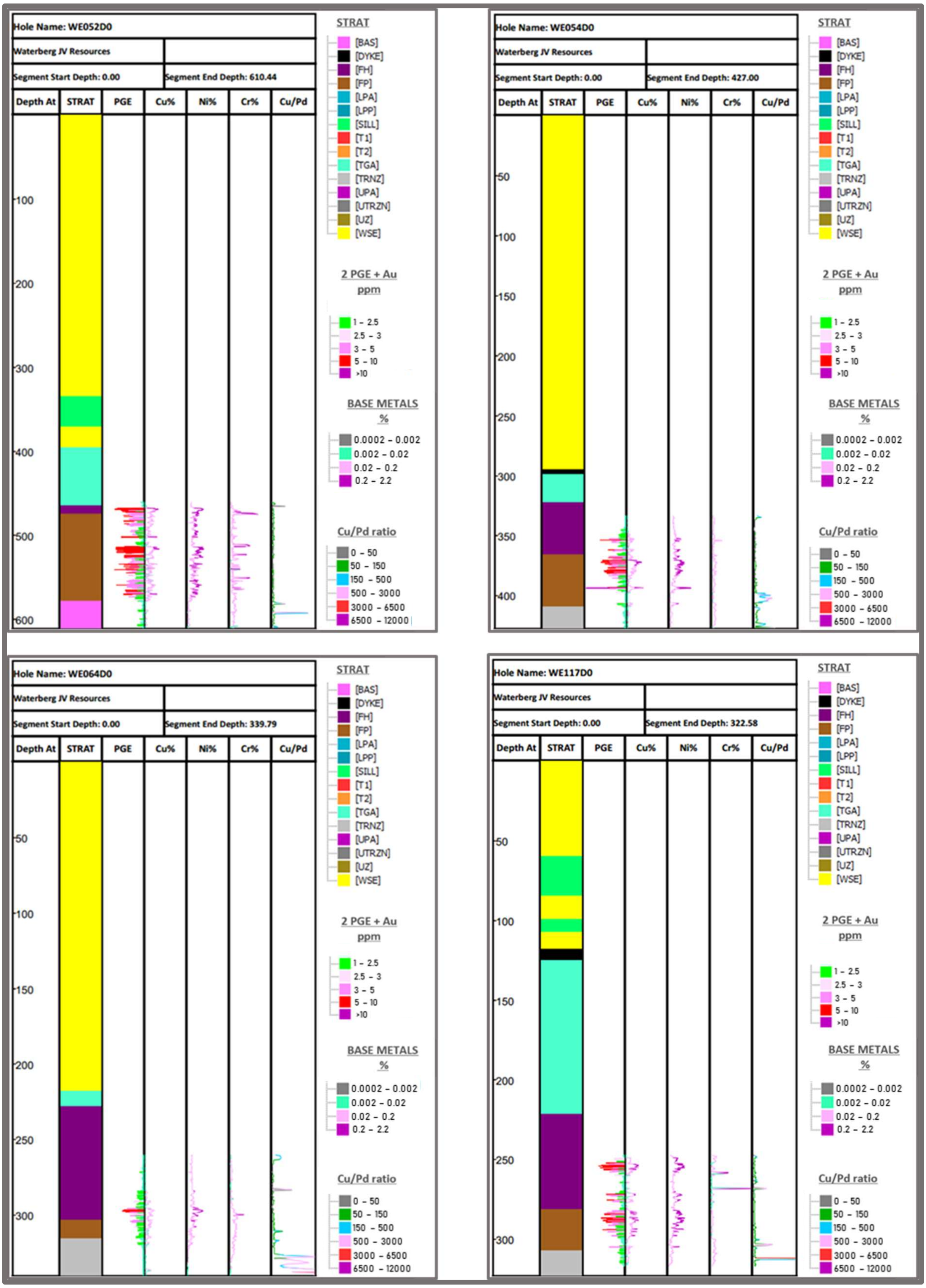

Figure 7.7. F - North stratigraphic logs (dip section) with matched assay results.

In WE0117D0, the base metal content of the PGE bearing F Zone (FH & FP) is 0.09% Cu, 0.20% Ni and 0.05% Cr; with a Cu/Pd ratio of 88 (Figure 7.7). The Cu/Pd ratio of the FP is 105 while that of the FH is lower at 75. The Ni content in both the FP and the FH is 0.20%. The Cu content in the FH is 0.08% while that in the FP is 0.12%. The Cr content in the FP is 0.4% while that of the FH is slightly lower at 0.05%.

As shown on the drillholes layout (Figure 7.8), WE120D0 is not on section with the above discussed drillholes. The drillhole is located SE of WE052D0 and SW of WE054D0. Similar to the dip section drillholes, this WE120D0 intersected both FH and FP (Figure 7.8). The base metal content of the F Zone (FH & FP) mineralised interval is 0.17% Cu, 0.26% Ni and 0.06% Cr; with a Cu/Pd ratio of 64. The Cu/Pd ratio of the FP is 66 while that of the FH is slightly lower at 50. The FH has slightly elevated Ni content of 0.34% compared to the 0.2% in the FP. Cu content in both the FH and the FP is 0.17%. The Cr content in the FP is 0.06% while that in the FH is slightly higher at 0.08%.

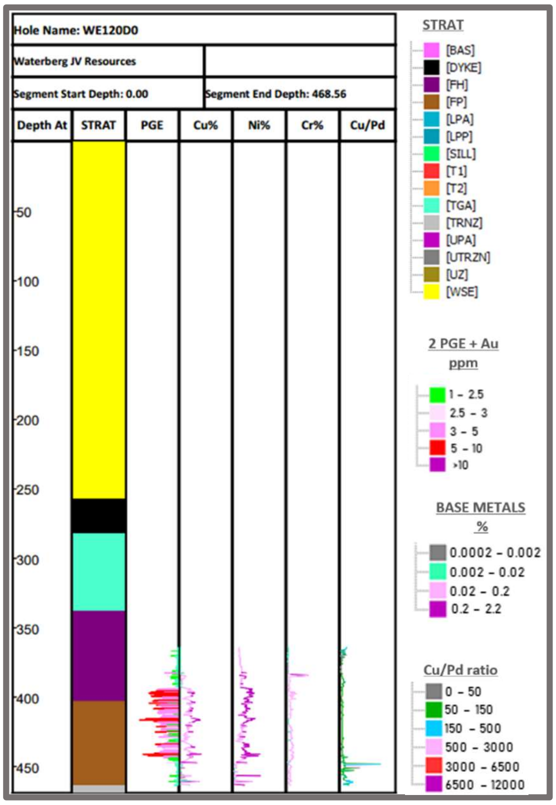

Figure 7.8. F - North stratigraphic log of WE120D0 with matched assay results.

In comparison to the F - Boundary North, F - Boundary South and F - Central; the FP of the F - North is highly mineralised. Within WE052D0, WE064D0 and WE120D0; the FH bottom contacts are characterised by thinner high grade while the rest of the subzone is poorly mineralised. The FH of WE117D0 is characterised by relatively high but thinner PGE mineralisation towards the middle portion.

Overall, areas of good PGE mineralisation are characterised by very low Cu/Pd ratios of 50-80. Elevated Cu/Pd ratios of over 100 towards the bottom of the F Zone and top of the Transitional Zone are attributed to the observed massive and blebby sulphides (Figure 3.4B) which have proven to be PGE barren. These sulphides are predominantly found within the basal pyroxenite.

7.2.6 Discussion (The F Zone)

The F Zone is characterised by well a mineralised FP and a well mineralised upper FH. In general, the thickness of the F Zone is > 50 m at times reaching a thickness of ~100 m. Although several drillholes have shown consistent high grade mineralisation throughout the mineralised interval, most of the mineralised intervals are characterised by top and bottom loaded mineralisation with patches of low grade mineralisation. Areas of higher grade are associated with higher base metal content (Cu and Ni) and very low Cu/Pd ratios. Patched areas of low grade are associated with slightly elevated Cu/Pd ratios and very low base metal content (Cu and Ni). The overall Cr content of the F Zone is low with slightly elevated content of 0.02 – 0.2% within the F - Central. In comparison to the FP, the FH is characterised by slightly elevated Ni content of ~0.2%. Within the FH, ~0.004% of the Ni is in silicates (Yudovskaya, unpublished - personal communication).

The significantly lower Cu/Pd ratios imply that the F Zone magma did not experience sulphide segregation and was therefore enriched with PGEs.

7.3 Mineral (PGE + Au) distribution and continuity

Based on the lithostratigraphic logs and geochemical sample results, PGE + Au mineralisation control and continuity were studied in both dip and strike sections. Cross sections for the T Zone, the F-Central, the F - Boundary South, the F - Boundary North and the F - North were plotted and thoroughly evaluated.

The PGE + Au grade thicknesses were evaluated on both dip and strike sections per district (Figure 5.1), starting from the south with the T Zone and ending in the north with the F - North.

7.3.1 The T Zone

7.3.1.1 The T Zone dip section

On the dip section, from west to east, PGE mineralisation within the T2 subzone can be traced up-dip from WB228D0 to WB213D0. This mineralisation subsequently migrates from T2 into LPA further east from WB241D0 to WB212D0 (Figure 7.9).

In WB228D0, the T2 subzone is well mineralised (2PGE + Au) with grade thickness of 3m @ 3.89g/t. The T2 in both WB230D0 & WB212D0 is also well mineralised with grade thicknesses of 3m @ 6.20g/t and 4.69m @ 4.27g/t, respectively. WB241D0 has no T2 subzone. However, low grade mineralisation of 1m @ 1.02g/t is present towards the bottom of the LPA. Although WB212 has no T2, the LPA is well mineralised with a grade thickness of 2m @ 4.64g/t. Overall, the T1 is poorly mineralised throughout the section.

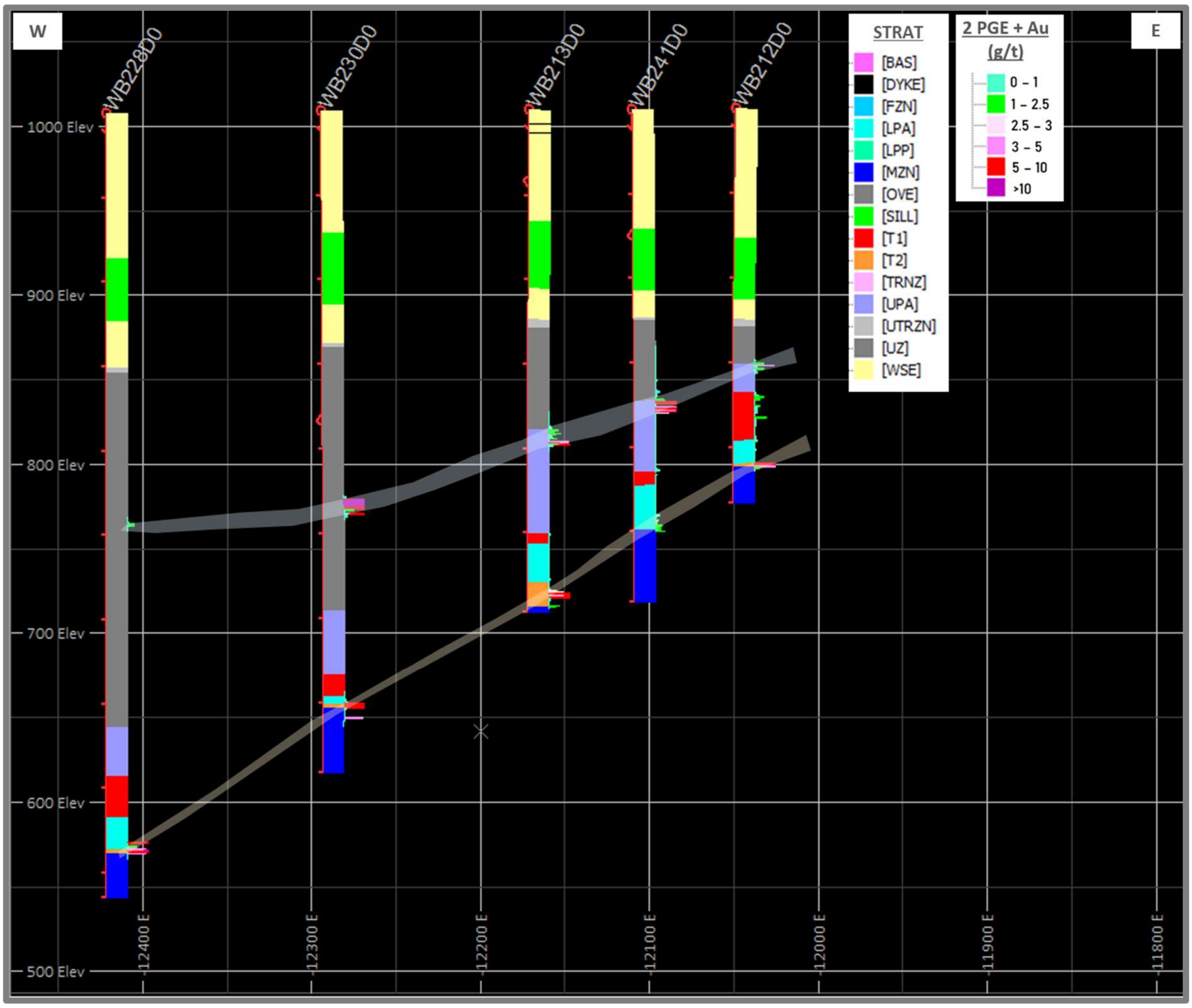

Figure 7.9. A T Zone dip-section showing PGE + Au mineralisation. The lower grey shaded area shows continuity of mineralisation within the subzones of the T Zone while the upper grey shaded area shows continuity of mineralisation within the T0. The shaded areas demonstrate the continuity of mineralisation on the cross section.

Above the T Zone, a fairly continuous mineralised zone (2PGE +Au) can be traced up-dip from west to east (the T0). To the west, the T0 mineralisation is in the Upper Zone from WB228D0 to WB230D0. From WB213D0 to WB212D0, this mineralisation migrates from the Upper Zone into the UPA. WBB228D0 is poorly mineralised with grade thickness of 1m @ 1.19g/t while the rest of the other holes are well mineralised. WB230D0 is well mineralised with grade thickness of 5.45m @ 15g/t (the highest grade on this section). Mineralisation from WB213D0 to WB212D0 seem to be confined to upper portion of the UPA at the contact between the UPA and the Upper Zone. Within WB213D0, the grade thickness is 2.76m @ 3.94g/t with 6.75m @ 4.89g/t in WB241D0. Although mineralisation in WB212D0 is thinner with a thickness of 0.89m, the PGE + Au grade is 2.12g/t.

Both the T Zone mineralisation (T2 & LPA) and the upper T0 mineralisation (*Sensu lato*) converges from west to east. The T0 mineralisation is the mineralisation located within the Upper Zone, at times migrating progressively into the upper part of the UPA.

7.3.1.2 The T Zone strike section

On the strike section, from SW to NE (Figure 7.10), PGE mineralisation in the T2 subzone can be traced from WB222D0 to WB235D0. This mineralisation subsequently transgresses from T2 into LPA further NE from WB025D0 to WB215D0 (Figure 7.10).

T2 in WB222D0 is well mineralised (2PGE + Au) with grade thickness of 9m @ 5.92g/t. Mineralisation within WB221D0 is significantly thinner with grade thickness of 1.5m @ 2.27g/t. WB213D0 is well mineralised with grade thickness of 4.69m @ 4.27g/t. From WB025D0 further NE, mineralisation transgresses from T2 into the LPA. The LPA in both WB237D0 and WB215D0 is well mineralised with grade thickness of 7.35m @ 4.26g/t and 6.00m @ 4.52g/t respectively. T1 is poorly mineralised throughout the section.

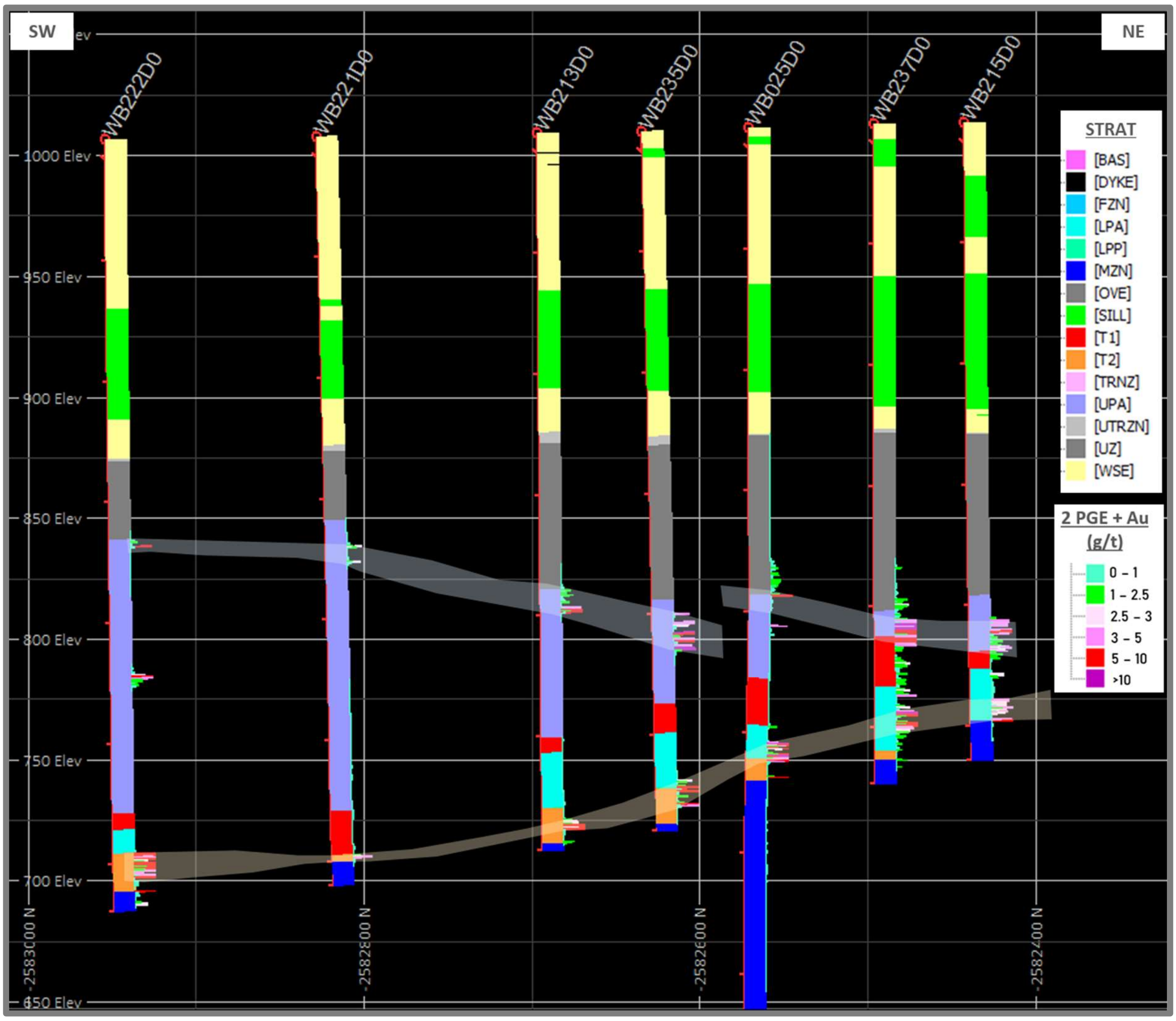

Figure 7.10. A T Zone strike-section showing PGE + Au mineralisation. The lower grey shaded area shows continuity of mineralisation within the subzones of the T Zone while the upper grey shaded area shows continuity of mineralisation within the T0.The shaded areas demonstrate the continuity of mineralisation on section.

A fairly continuous mineralised zone in the upper portion of the UPA (near the UPA/Upper Zone boundary) is also traced on the strike section from SW to NE. Within WB222D0, mineralisation is thinner with grade thickness of 1.38 m @ 2.01 g/t. The adjacent borehole to WB222D0 (WB221D0) is poorly mineralised with a grade thickness of 2.85 m @ 1.15 g/t. WB213D0, WB237D0 and WB215D0 are well mineralised with a grade thickness of 2.76 m @ 3.94 g/t, 11.63 m @ 5.8 g/t and 6m @ 3.02 g/t, respectively.

Both the T Zone mineralisation (T2 & LPA) and the upper T0 mineralisation (*Sensu lato*) converges from SW to NE.

It should be noted that the T Zone study holes do not cover the entire lithostratigraphic sequence as they were not drilled deeper into the lower mineralised UmS (the F - South). The holes were only targeting T Zone mineralisation.

7.3.2 The F - Central

The F - Central is the most mineralised district within the entire Waterberg Project with mineralisation reaching a maximum thickness of 137 m. The mineralisation is confined to ultramafic rocks, which are predominantly harzburgite and feldspathic pyroxenites. Some well mineralised gabbronorites and leucocratic gabbronorites have been observed within the F Zone of the Ultramafic Sequence (UmS).

This subsection evaluates the F Zone mineralisation on both dip and strike sections.

7.3.2.1 The F - Central dip section

All the four drillholes on the dip section are well mineralised (Figure 7.11). WB264D0 to the west is the most mineralised drillhole with a grade thickness of 116m @ 4.09g/t. WB280D0 is also very well mineralised with a grade thickness of 111m @ 3.11g/t. In WB259D0, the best mineralisation is in the middle of the UmS with a grade thickness of 44.84 m @ 3.37 g/t. In WB257D0, which is closer to the subcrop, the best mineralisation is towards the top of the F Zone with a grade thickness of 50 m @ 2.6 g/t.

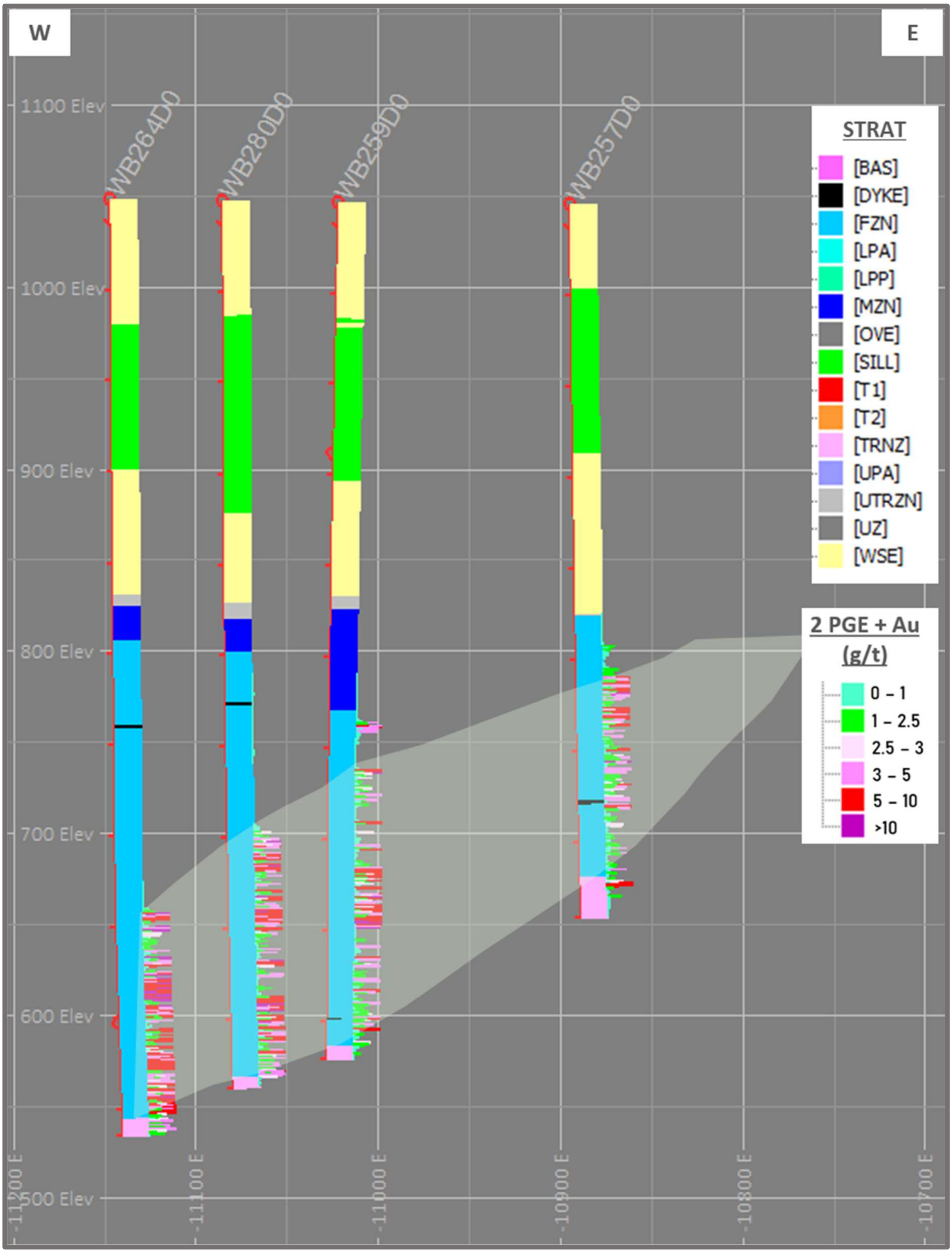

Figure 7.11. F - Central dip-section showing PGE + Au mineralisation. The grey shaded area shows continuity of mineralisation within the F Zone.

7.3.2.2 The F - Central strike section

All three drillholes on the strike section are also well mineralised (Figure 7.12). WB276D0 to the SW is well mineralised with a grade thickness of 100 m @ 2.52 g/t with the adjacent WB264D0 at 116 m @ 4.09 g/t. WB261D0 which is the furthest to the NE is also well mineralised with a grade thickness of 137 m @ 2.5 g/t.

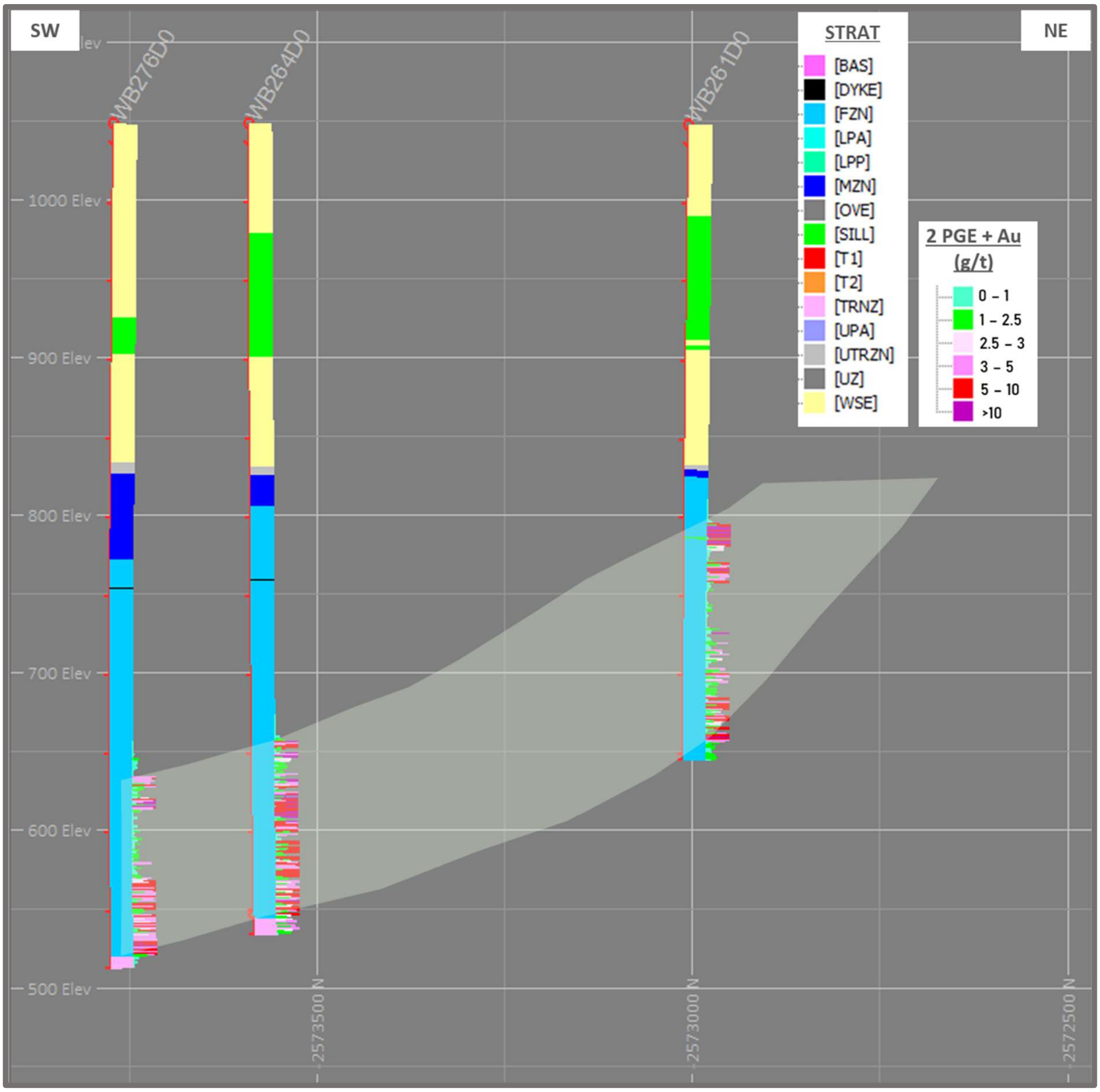

Figure 7.12. F - Central strike section showing PGE + Au mineralisation. The grey shaded area shows continuity of mineralisation within the F Zone.

7.3.3 The F - Boundary South

Within the F - Boundary South district, the mineralisation is thinner in comparison to that of the F - Central district and more biased to the upper portion of the F Zone (Figure 7.13). WB255D0 is not so well mineralised with a grade thickness of 40 m @ 2.05 g/t. WB254D0 which is up-dip of WB255D0 is well mineralised with a grade thickness of 33 m @ 3.9 g/t. Although WB202D0 is not part of the study, it is also well mineralised at both the top and middle portions of the UmS, showing continuity of mineralisation up-dip from NW to SE.

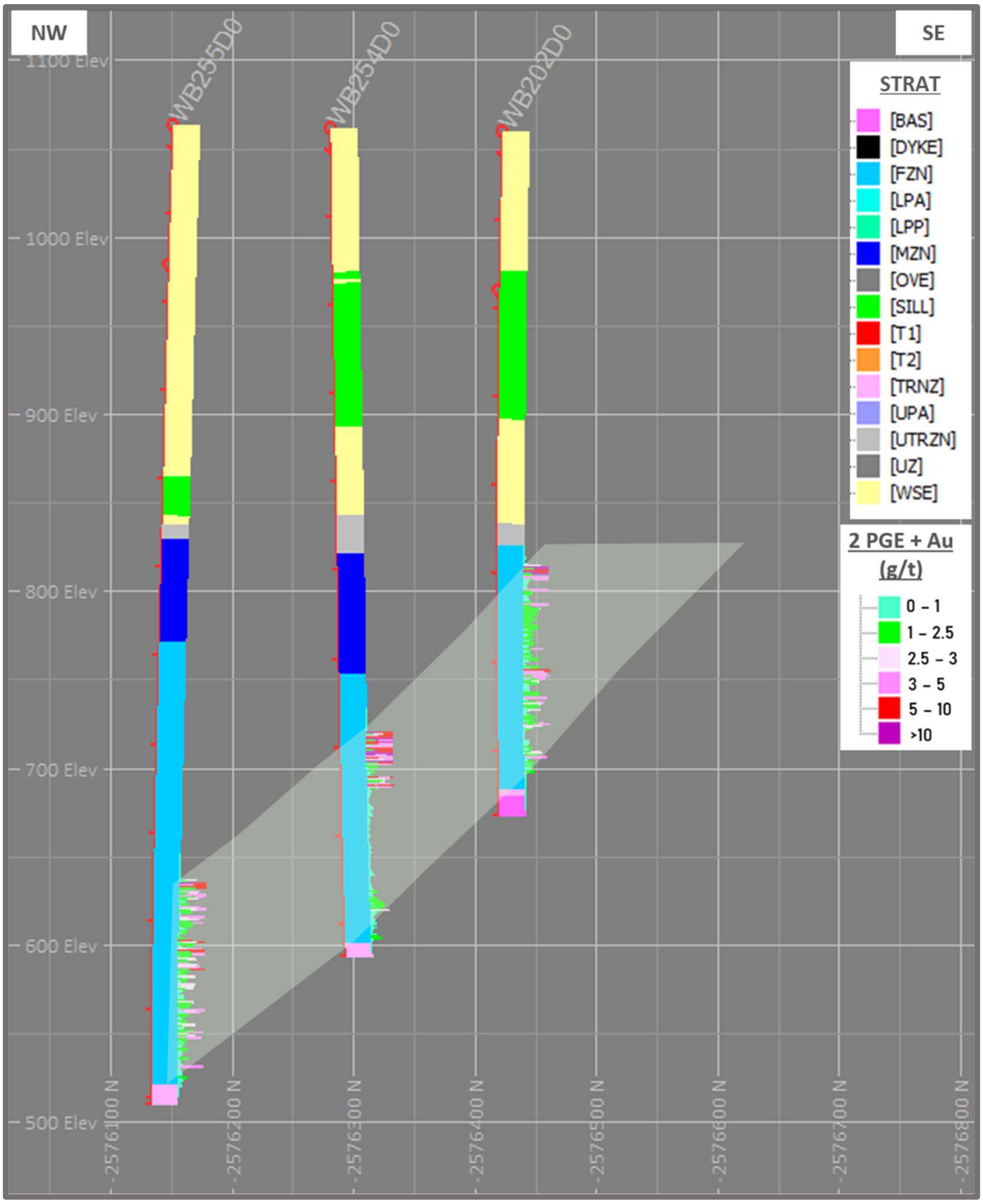

Figure 7.13. F - Boundary South dip section showing PGE + Au mineralisation. The grey shaded area shows continuity of mineralisation within the F Zone.

7.3.4 The F - Boundary North

Although not on section, WE061D0, WE144D0 and WE145D0 from F - Boundary North are well mineralised with grade thicknesses of 85 m @ 3.5 g/t, 56 m @ 2.5 g/t and 38 m @ 3.5 g/t respectively (detailed discussion in Chapter 8).

7.3.5 The F - North

The F - North is the far northern mineralised portion of the Waterberg Project. From the west, the mineralised zone is thicker with a grade thickness of 107 m @ 3.06 g/t in WE052D0. The mineralisation seems to be thinning from WE054D0 to WE064D0 with a grade thickness of 41 m @ 3.00 g/t within WE054D0 and 8.7 m @ 2.6 g/t within WE064D0. In WE117D0, mineralisation is partitioned into top and middle mineralised portions. The top mineralised portion is characterised by a grade thickness of 14.5 m @ 3.52 g/t while the middle portion is 6.9 m @ 4.05 g/t. This partitioning becomes wider towards the east.

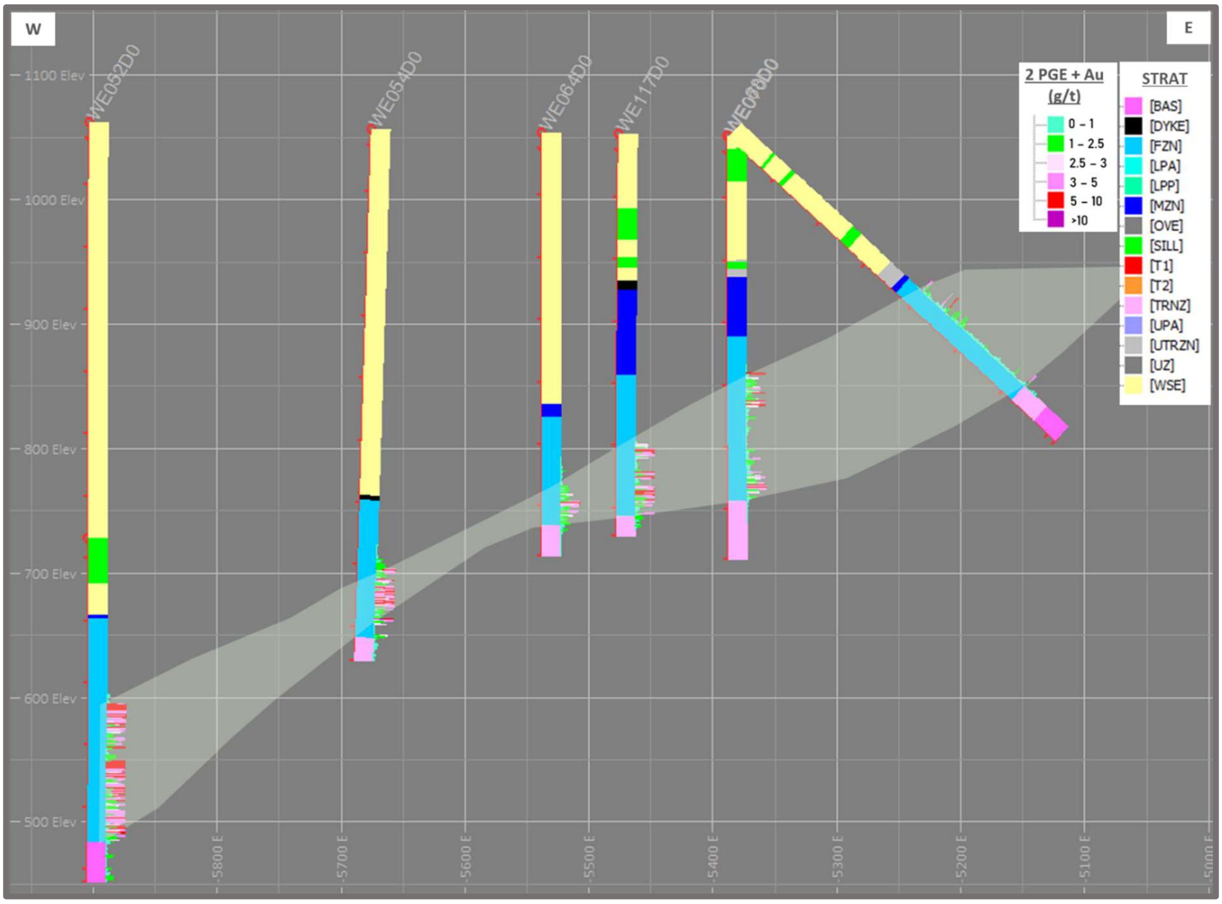

Figure 7.14. F - North dip section showing PGE + Au mineralisation.

7.3.6 Discussion

The F Zone and the T Zone of the mafic-ultramafic succession of the Waterberg Project are enriched with PGE + Au associated with base metal sulphides. The mineralisation of desirable grade (> 2.5g/t) has shown to be continuous both on the dip and along strike. In comparison to the T Zone, the F Zone is thicker at times reaching a thickness of ~100 m.

The T Zone mineralisation is thinner (1 - 10m) compared to the F Zone mineralisation. This mineralisation migrates from the T2 subzone on dip from W - E and along strike from SW - NE into the LPA.

The T0 mineralisation is thinner (1 - 5 m) and not so well developed compared to the T Zone mineralisation. This mineralisation is located in the Upper Zone migrating into the upper portion of the UPA on dip section and along strike section converging with the T Zone.

The following section presents calculated sulphide tenors for the mineralised sections of the mafic-ultramafic succession of the Waterberg Project.

7.4 The distribution of tenors in the F Zone and the T Zone

This section presents the calculated sulphide tenor variations within both the F Zone and the T Zone for the selected drillcore using the methodology outlined by Naldrett (2004).

According to Naldrett et al. (2011), PGE tenor is the concentration of metals in 100 % sulphide. It is interpreted as a representative concentration of a particular metal (Pt, Pd, Rh, Ru, Ir and Os) in the original sulphide droplet after the sulphide droplet has segregated from its host magma assuming no later sulphide loss due to any superimposed process.

The method of Naldrett et al. (2011) is based on the following assumptions: -

- The present sulphur content in the sample is equal to the original sulphur content in the magma.
- All Cu and Ni are present in the sulphides
- All PGEs were dissolved in sulphide liquid and not in other phases.

It has been asserted that the present amount of sulphide in the F Zone and T Zone of the Waterberg Project is very close to the original sulphide content; with the primary sulphides being pyrrhotite, pentlandite and chalcopyrite (McCreesh et al. 2018). As such, tenor values were calculated by taking the sulphur content of the sample, calculating all the copper in the sample as chalcopyrite and subtracting the sulphur involved from the total sulphur. This was followed by taking the nickel in the sample as pentlandite and similarly subtracting the sulphur from the total. The remaining sulphur was calculated as pyrrhotite (Naldett et al., 2011). Assuming that other present sulphide minerals are negligible, the amount of sulphide present in a sample was determined by adding chalcopyrite, pentlandite and pyrrhotite together. Where the amount of sulphides was low, much of the Ni was not in the pentlandite but in the silicate. If the Ni was calculated as pentlandite, the value was to be high. Since the pyrrhotite content is calculated by subtracting pentlandite and chalcopyrite sulphur from the total sulphur of the sample, a negative pyrrhotite was obtained for a few samples. In such samples, the 2.65 x sulphur method by Naldrett et al., (2000) was used. Due to the negligible Ni content in T Zone silicates (Yudovskaya, unpublished - personal communication), all the Ni from T Zone samples was used to determine the pentlandite content. This was different in the F Zone which is characterised by significantly higher Ni in silicates. The average silicate Ni content is 0.004% in harzburgite and

0.002% in olivine bearing pyroxenite (Yudovskaya, unpublished – personal communication). These amounts were subtracted from the overall Ni content of the respective samples prior to conducting tenor calculations.

Variations in tenors were described based on the tenor population/patterns and the proportion of Pd vs. Pt vs. Au in each lithostratigraphic unit. On each logarithmic tenor plot, a line has been drawn on the 100 000 ppb (100 ppm) vertical gridline to address the metal grades. This reference line is based on the indication that the Merensky Reef tenors are generally above 100 ppm total PGE (Naldrett et al., 2009).

The vertical grey shaded area on the tenor diagrams indicates the sulphide contents within which between 10% and 40% of trapped interstitial sulphide-saturated magma could plot (Naldrett et al., 2009). Sulphide contents plotting within or to the left of the shaded area indicate samples with little or no excess sulphide while those plotting to the right of the shaded area are interpreted as containing sulphide in excess that could be dissolved in the intercumulus liquid.

The calculated tenors were evaluated based on the mining districts starting with the T Zone in the south and ending with the F - North in the north.

Appendix 3 is tenor data for the T Zone and the F Zone.

7.4.1 The T Zone

Vertical tenor variations are studied on both dip and strike cross sections for the drillholes discussed in the previous sections. For localities of the T Zone boreholes on strike and dip sections, refer to Figure 5.2

7.4.1.1 The T Zone dip section

WB228D0

The T Zone is characterised by higher PGE tenors with palladium being the highest and platinum the second highest (Figure 7.15). The gold tenors are generally lower than PGE tenors. There is an upward increase in PGE tenors in the T2 from 51 ppm. This increase continues up the stratigraphic sequence into the LPP, reaching a maximum of 141 ppm towards the base of the LPA. At 431 m depth, the PGE tenors in the LPA decrease drastically upwards to 5 ppm. The low Au tenors follow a trend similar to that of the PGEs with the lowest tenor of 14 ppm in T2. The tenor (Au) reaches a maximum of 142 ppm in T2 and decreases upwards into the LPA.

In the T0, both PGE and Au tenors are below 100 ppm with both PGE and Au reaching a maximum of 85 ppm.

WB230D0

The PGE tenors in both the T Zone and the T0 are generally higher in comparison to gold tenors within the same units. The palladium tenors are the highest followed by the Pt tenors (Figure 7.15). The PGE tenors are generally lower in the TGA. From the base of the T2 at the contact between the T2 and TGA, the tenors drastically increase. Within the T2 subzone, the PGE tenors peak at 414 ppm and drastically decreases at the T2/LPA contact. The Au tenors follow a trend similar to that of PGEs with a maximum tenor of 88 ppm in the T2. The T2 subzone is generally characterised by Pt and Pd tenors higher than 100 ppm and Au tenors below 100 ppm.

In T0 which is located in the Upper Zone (UZ), the PGE tenors are also higher than Au tenor peaking at 434 ppm while Au tenors peak at 73 ppm. The T0 is also generally characterised by Pt and Pd tenors higher than 100 ppm and Au tenors below 100 ppm.

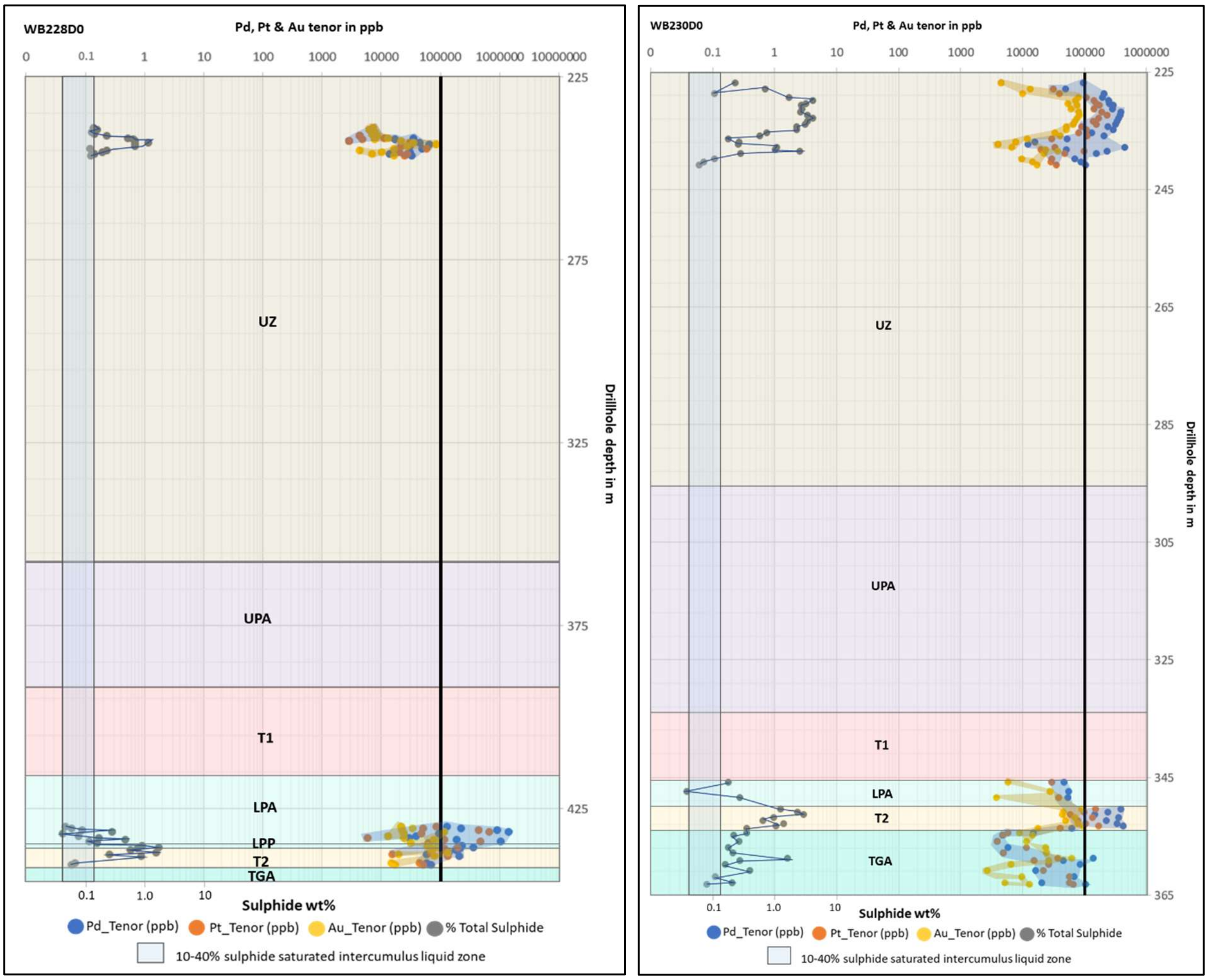

Figure 7.15. Tenor plots of WB228D0 and WB230D0 showing Pt, Pd and Au tenors along with sulphide content (wt %). The different colour units represent the lithostratigraphic units. The light blue and orange shaded areas show PGE and Au trends respectively. Abbreviations: the Upper Zone (UZ), the Upper Pegmatoidal Anorthosite (UPA), the Lower Pegmatoidal Anorthosite (LPA), the Lower Pegmatoidal Pyroxenite (LPP), The T1 mineralised subzone (T1) and the T2 mineralised subzone (T2)

<u>*WB213D0*</u>

As shown on Figure 7.16, this borehole has the lowest tenors in comparison to WB228D and WB230D0 with minor tenor peaks at the bottom of both T2 (219 ppm) and T1 (431 ppm). Within the T2 subzone, Au tenors are higher with levels similar to that of the PGEs, reaching a maximum of 149 ppm. Both Au and PGE tenors slightly regress upwards into the LPA. Towards the top of the LPA, both PGE and Au tenors increase gradually into the T1 subzone. Unlike WB228D0 and WB230D0, Au tenors in T2 are above 100 ppm.

Within the T0, PGE attain the maximum tenor of 283 ppm, gradually decreasing upwards into the Upper Zone. The Au tenors peak at 71 ppm and gradually decrease into the Upper Zone. Only PGE tenors are above 100 ppm.

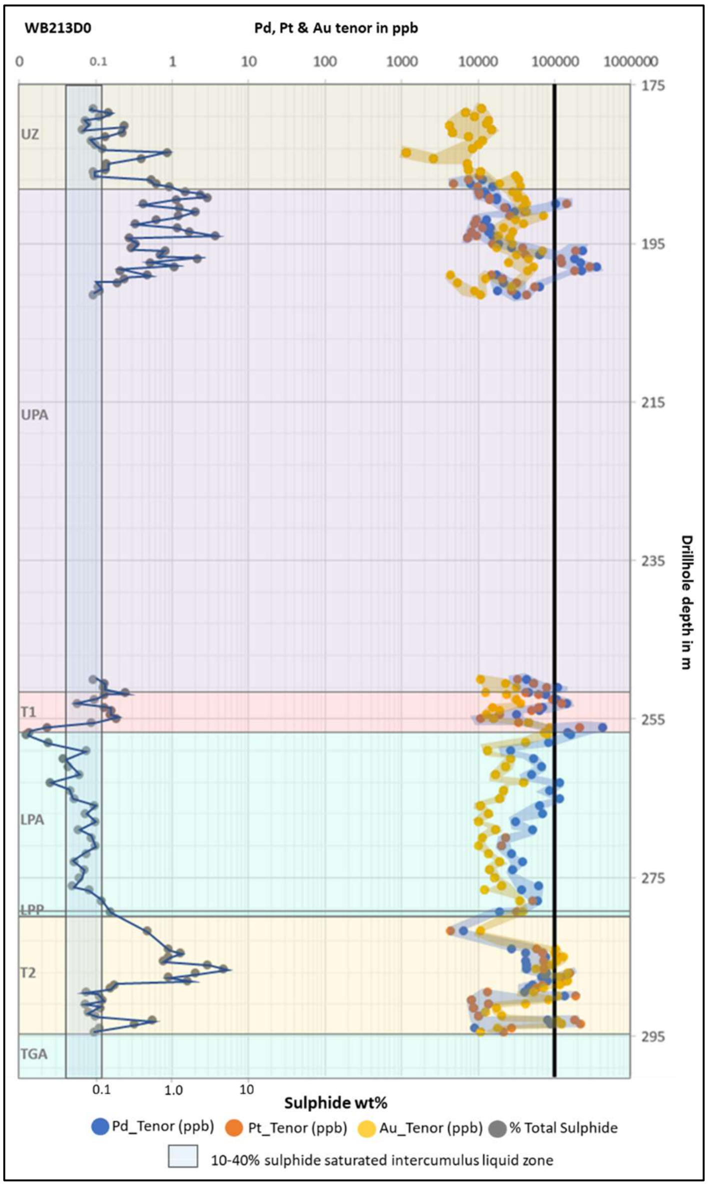

Figure 7.16. Tenor plot of WB213D0 showing Pt, Pd and Au tenors along with sulphide content (wt %). The different colour units represent the lithostratigraphic units. The light blue and orange shaded areas show PGE and Au trends respectively.

7.4.1.2 The T Zone strike section

WB222D1

The T Zone is characterised by higher PGE tenors. The palladium tenors are the highest followed by the Pt tenors (Figure 7.17). The PGE tenors are generally lower in the TGA and slightly higher towards the TGA/T2 contact. These tenors increase gradually in the T2 from the bottom upwards with general Pd tenors of more than 100 ppm and general Pt tenors lower than 100 ppm. The PGE attain a maximum tenor of 659 ppm at the contact between the T2 and the LPA. The Au tenors also follow the same trend with a maximum tenor of 279 ppm in the middle of T2. At the T2/LPA contact, the Au attains a peak tenor of 105 ppm.

Within the T0, PGE and Au tenors peak at 127 ppm and 16 ppm respectively, decreasing further upwards into the UPA.

WB221D0

The PGE tenors increase from the bottom of T2 upwards, reaching a maximum of 352 ppm (Figure 7.17). The tenors then regress towards the T2 and T1 contact (no LPA). Within the T1 subzone, the PGE tenors are well below 100 ppm (17 ppm), increasing gradually into the UPA. The Au tenors follow the same trend attaining a maximum tenor of 136 ppm in T2 but well below 100 ppm in both T1 and UPA subzones (7 ppm).

The PGE in the T0 attain a maximum tenor of 183 ppm, gradually decreasing towards the UPA/UZ contact. Au tenors follow a similar trend; however, the tenors are below 100 ppm peaking at 57 ppm and gradually decreasing towards the UPA/UZ contact.

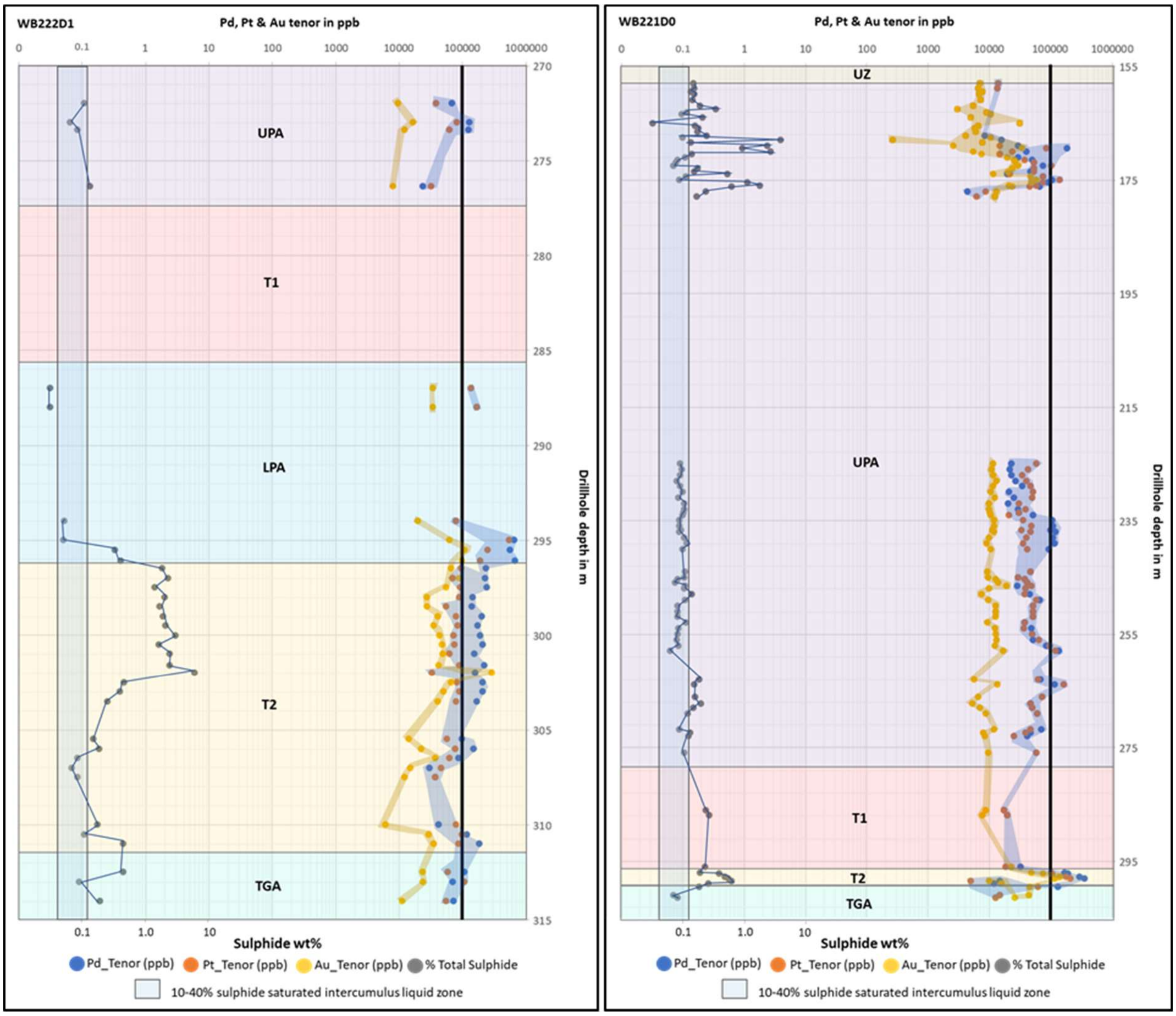

Figure 7.17. Tenor plots of WB222D1 and WB221D0 showing Pt, Pd and Au tenors together with sulphide wt%. The different colour units represent the lithostratigraphic units. The light blue and orange shaded areas show PGE and Au trends respectively. Abbreviations: the Upper Zone (UZ), the Upper Pegmatoidal Anorthosite (UPA), the Lower Pegmatoidal Anorthosite (LPA), The T1 mineralised subzone (T1) and the T2 mineralised subzone (T2)

WB237D0

In the T Zone, the PGE tenors are 99 ppm at the bottom of the T2, increasing gradually to the bottom portion of the LPA (1 045 ppm). The PGE in both the LPA and the UPA have an upward increasing trend attaining maximum tenors of 1 013 ppm and 639, respectively (Figure 7.18). PGE tenors in both T2 and T1 are significantly lower than those in the LPA and the UPA. However, the tenor in T1 increases gradually upwards to over 100 ppm into the UPA. At the UPA/UZ contact, the PGE tenors decrease gradually into the UZ. The Au tenors follow a trend similar to that of the PGEs with a maximum tenor of 212 ppm towards the base of the LPA. Towards the top of the LPA, the Au reaches a maximum tenor of 151 ppm while the UPA attains a maximum Au tenor of 127 ppm.

WB215D0

The PGE tenor increases gradually from the TGA/LPA contact (no T2) upwards into the LPA, peaking at 744 ppm (Figure 7.18). However, the Au tenors do not follow the PGE trend. The highest Au tenor is at the contact between the TGA and the LPA (1 164 ppm). There seems to be a slight anti-correlation between Au and PGE tenors from the base to the top of the LPA.

The PGE tenors increase gradually from 109 ppm at the top portion of T1, peaking at 434 ppm in the upper portion of the UPA. Au tenors follow the same trend peaking at 217 ppm.

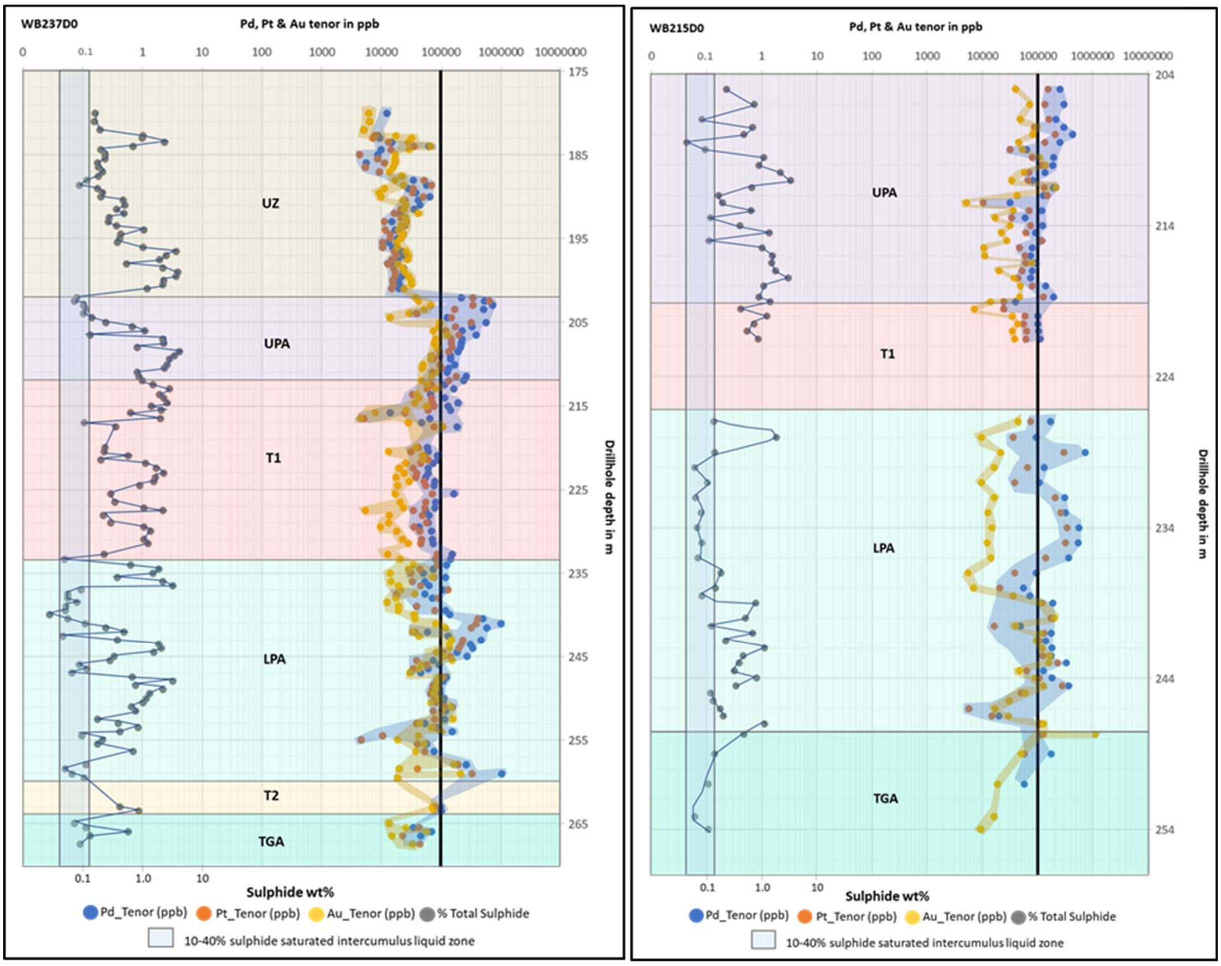

Figure 7.18. Tenor plots of WB237D0 and WB215D0 showing Pt, Pd and Au tenors along with sulphide content (wt %). The different colour units represent the lithostratigraphic units. The light blue and orange shaded areas show PGE and Au trends respectively. Abbreviations: the Upper Zone (UZ), the Upper Pegmatoidal Anorthosite (UPA), the Lower Pegmatoidal Anorthosite (LPA), The T1 mineralised subzone (T1) and the T2 mineralised subzone (T2)

7.4.2 The F - Central

Lateral and vertical tenor variations for the drillholes are evaluated in both dip and strike sections.

7.4.2.1 The F - Central dip Section

WB280D0

The lower Feldspathic Pyroxenite (FP) and the upper Feldspathic Harzburgite (FH) of the F Zone are characterised by higher PGE tenors (Figure 7.19). The palladium tenors are generally higher, followed by the platinum tenors. These PGE tenors (Pd and Pt) increase upwards from 11 ppm in the Transitional Zone (TRNZ) to a maximum tenor of 1 050 ppm in the mid-section of the FH. Generally, both Pd and Pt have higher average tenor of more than 100 ppm (340 ppm Pd and 138 ppm Pt) throughout the F Zone. The gold tenors follow a trend similar to that of the PGE, attaining a maximum tenor of 71 ppm. In comparison to the PGE tenors, Au has a significantly lower average tenor compared to that of the PGE (21 ppm).

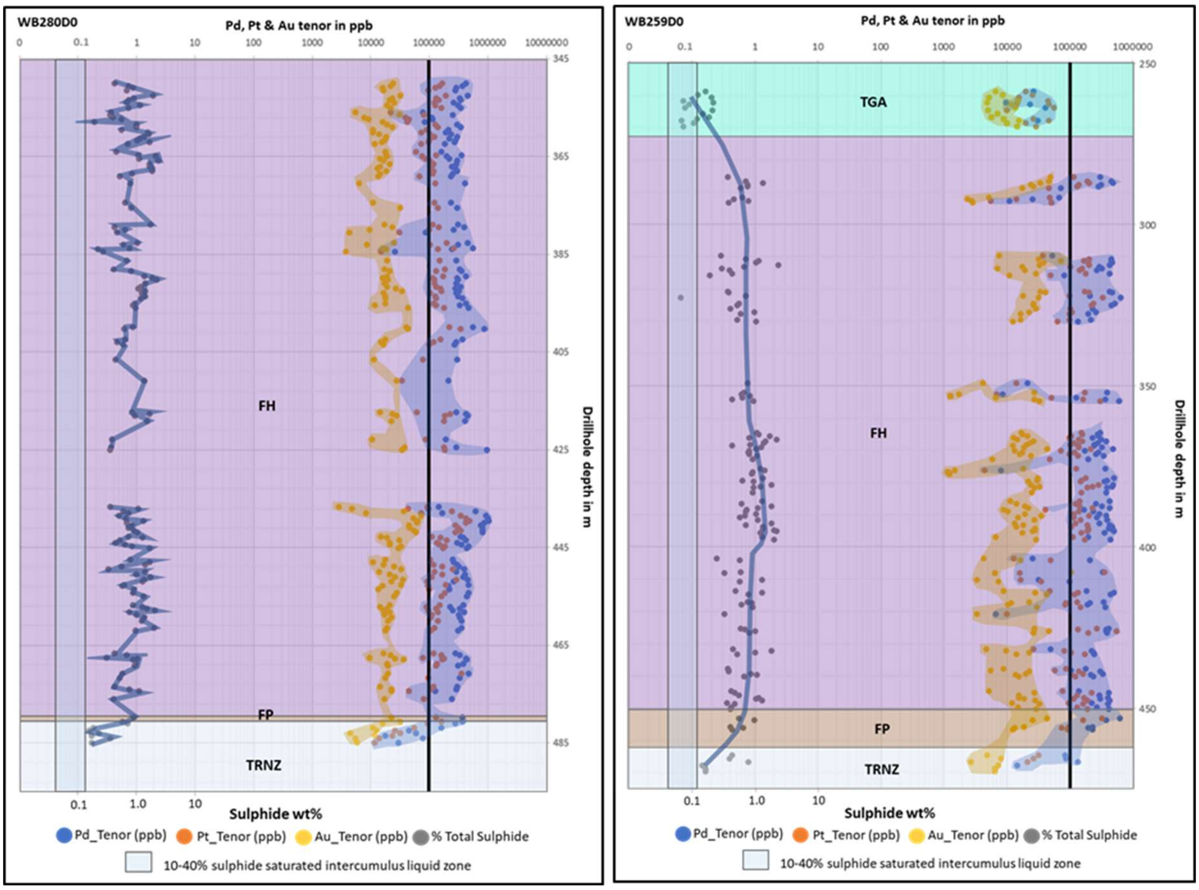

Figure 7.19. Tenor plots of WB280D0 and WB259D0 showing Pt, Pd and Au tenors along with sulphide content (wt %). The different colour units represent the lithostratigraphic units. The light blue and orange shaded areas show PGE and Au trends respectively. Abbreviations: the Feldspathic Pyroxenite (FP), the Feldspathic Harzburgite (FH), the Troctolite-Gabbronorite-Anorthosite Sequence (TGA) and the Transitional Zone (TRNZ).

WB259D0

In this drillcore, the lower FP and the upper FH of the F Zone are also characterised by higher PGE tenors (Figure 7.19). The Pd tenors are higher than the Pt tenors. These PGE tenors (Pd and Pt) increase upwards from 14 ppm in the TRNZ to a higher tenor of 617 ppm in the FP. The highest PGE tenor of

629 ppm is in the upper section of the FH (Figure 7.19). Generally, both Pd and Pt have an elevated average tenor of more than 100 ppm (250 ppm Pd and 115 ppm Pt) throughout the F Zone. The gold tenors follow a trend similar to that of the PGE, reaching a maximum of 101 ppm. Although the highest Au tenor is 101 ppm, the average is significantly lower at 18 ppm.

WB257D0

There is an upward increase in PGE (Pd and Pt) tenor from 3 ppm in the Transitional Zone (TRNZ) to a higher tenor of 455 ppm in the Troctolite-Gabbronorite-Anorthosite Sequence (TGA) (Figure 7.20). From 455 ppm, the tenors in the TRNZ decrease towards the TRNZ/FP contact. There is an upward increase in tenors from bottom (56 ppm) to top (262 ppm) in the FH. Within the FH subzone, there is a gradual upward increase in PGE tenors with a high tenor of 541 ppm. Generally, Pd tenors are above 100 ppm throughout the FH while Pt tenors are slightly below 100 ppm from the base upwards to a depth of 332m. From 332m upward, the Pt tenors gradually increase to over 100 ppm. The maximum tenor in the study borehole is 722 ppm in the TGA. This highest tenor attained by the TGA is uncommon as the bottom portion of this sequence is usually not associated with mineralisation. The gold tenors follow a trend similar to that of the PGE; however, the 40 ppm peak tenor is in the FH rather than in the TGA. Although the highest Au tenor is 101 ppm, the average is significantly lower at 18 ppm.

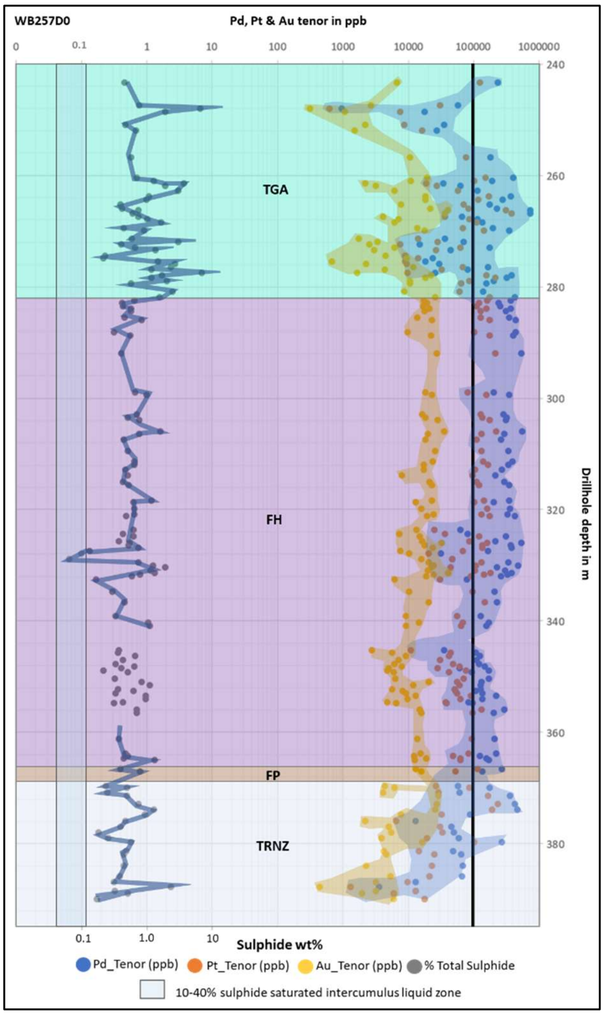

Figure 7.20. Tenor plot of WB257D0 showing Pt, Pd and Au .tenors along with sulphide content (wt %). The light blue and orange shaded areas show PGE and Au trends respectively.

WB276D0

In this drillcore, the lower FP is not present. The upper FH is characterised by higher PGE tenors (Figure 7.21). The palladium tenors are higher than platinum tenors. These PGE tenors (Pd and Pt) increase upwards from 15 ppm in the TRNZ to a higher tenor of 375 ppm at the TRNZ/FH contact. The highest PGE tenor of 612 ppm is in the upper section of the FH (Figure 7.21). Generally, both Pd and Pt have a higher average tenor of more than 100 ppm (275 ppm Pd and 111 ppm Pt) throughout the F Zone. The gold tenors follow a trend similar to that of the PGE, peaking at 42 ppm with an average of 18 ppm.

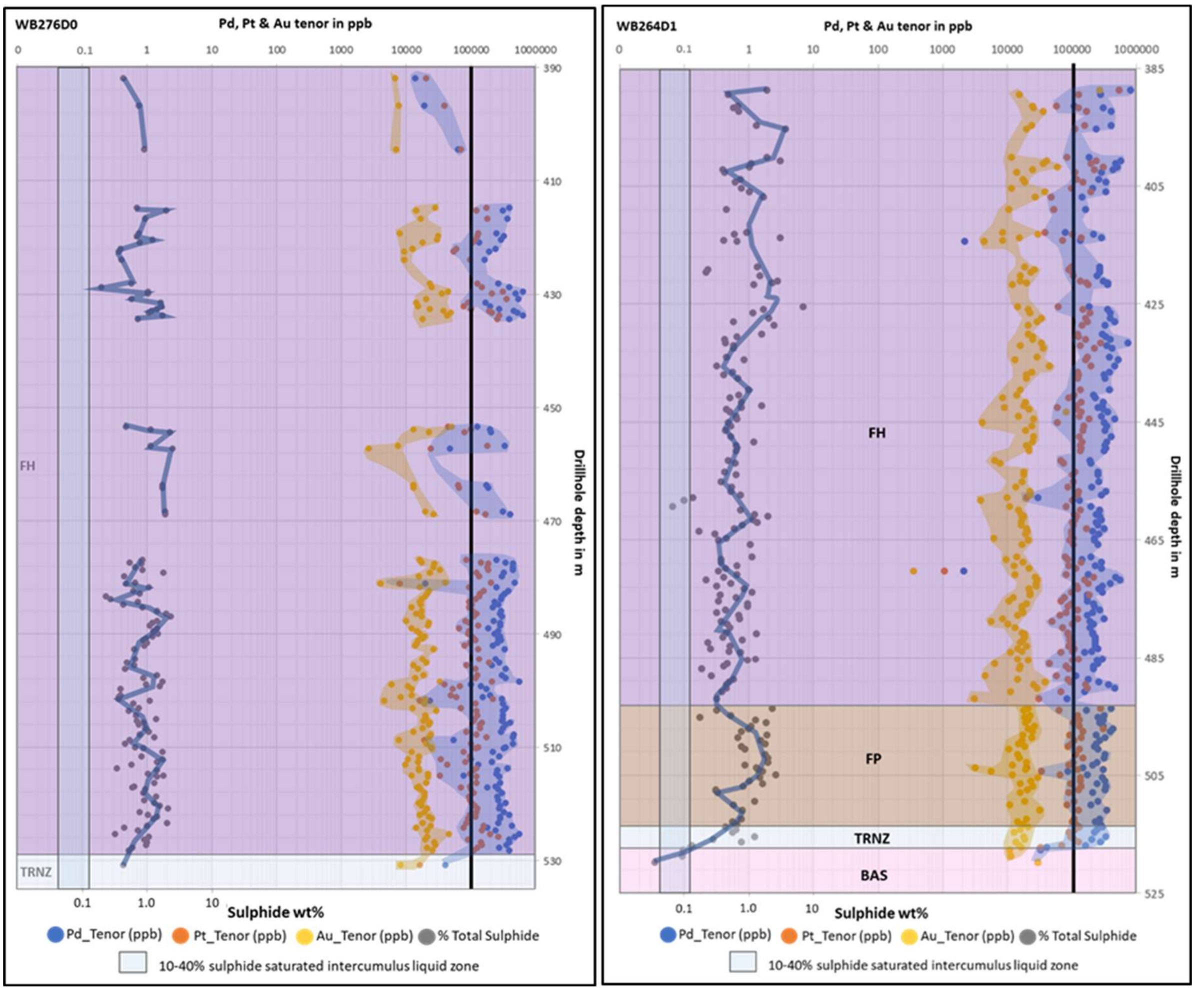

Figure 7.21. Tenor plot of WB276D0 and WB264D1 showing Pt, Pd and Au tenors along with sulphide content (wt %). The different colour units represent the lithostratigraphic units. The light blue and orange shaded areas show PGE and Au trends respectively. Abbreviations: the Feldspathic Pyroxenite (FP), the Feldspathic Harzburgite (FH), the Transitional Zone (TRNZ) and the Basement granite gneiss (BAS).

WB264D1

The lower FP and the upper FH of the F Zone are characterised by higher PGE tenors (Figure 7.21). The palladium tenors are higher than the platinum tenors. These PGE tenors (Pd and Pt) increase upwards from 32 ppm in the Basement (BAS) to 334 ppm in the TRNZ (Figure 7.21). The PGE tenors in the FH show a slight upward increase with high tenor of 449 ppm and an average tenor of more than 100 ppm (248ppm Pd and 105 ppm Pt). The gold tenors follow a trend similar to that of the PGE, with an average tenor of 17 ppm and a maximum tenor of 31 ppm. Within the FH, there is a gradual upward increase in PGE tenors with the highest tenor of 791 ppm towards the top of the FH. The average PGE tenor is more than 100 ppm (275 ppm Pd and 117 Pt).The Au tenors follow a trend similar to that of PGE, peaking at 263 ppm towards the upper section of FH; with an average tenor of 20 ppm.

WB261D0

In this drillcore, both the TRZN and the FP are not present (Figure 7.22). The upper FH is characterised by higher PGE tenors with higher palladium tenors than platinum tenors. These PGE tenors (Pd and Pt) generally increase upward from the base (128 ppm) of the FH upwards. The highest PGE tenor of 889 ppm is in the mid-section of this FH. Generally, both Pd and Pt have a higher average tenor of more than 100 ppm (343 ppm Pd and 149 ppm Pt) throughout the FH. The gold tenors follow a trend similar to that of the PGE, attaining a maximum of 147 ppm in the upper section of the FH. The average gold tenor throughout the FH is 23 ppm.

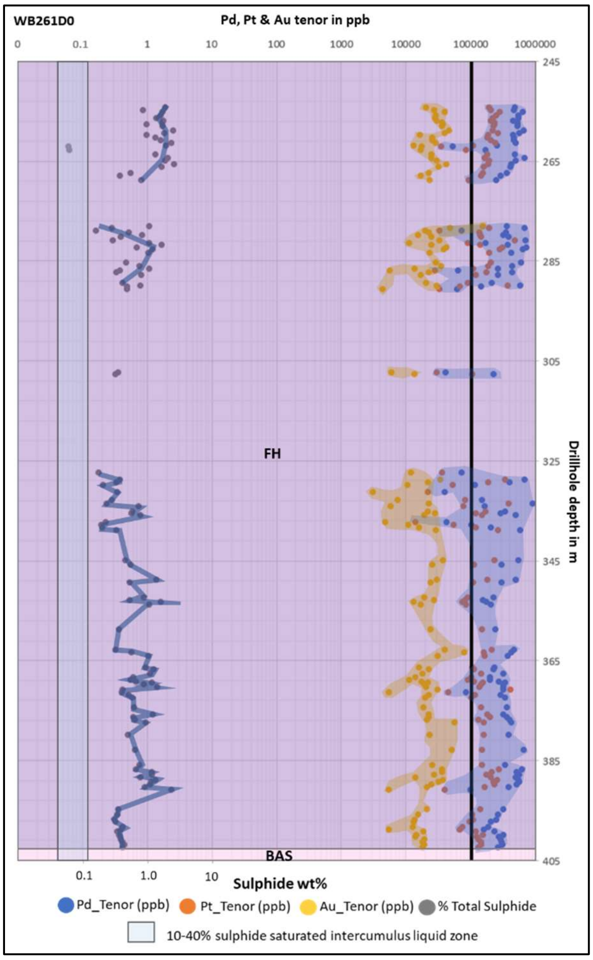

Figure 7.22. Tenor plot of WB261D0 showing Pt, Pd and Au tenors along with sulphide content (wt %). The light blue and orange shaded areas show PGE and Au trends respectively.

7.4.3 The F - Boundary South

WB255D0

The lower FP and the upper FH of the F Zone are characterised by higher PGE tenors with palladium tenors higher than platinum tenors (Figure 7.23). These PGE tenors (Pd and Pt) increase upward from 4 ppm in the TRNZ to 73 ppm at the contact between the TRZN and the FP (Figure 7.15). Within the FP, the highest tenor is 474 ppm in the mid-section; however, there is no obvious upward increase in tenors. Generally, the Pd tenors are above 100 ppm (135 ppm) while the Pt tenors are below 100 ppm (55 ppm). The FH shows an upward increase in PGE tenors with a highest tenor of 610 ppm at the very top of the unit. The Pd tenors are above 100 ppm (172 ppm) while Pt tenors are slightly below 100 ppm (73 ppm). The gold tenors follow trends similar to those of PGEs in both FP and FH, attaining a maximum tenor of 180 ppm at the top of the FH. Generally, the gold tenors are 11 ppm and 18 ppm in FP and FH, respectively.

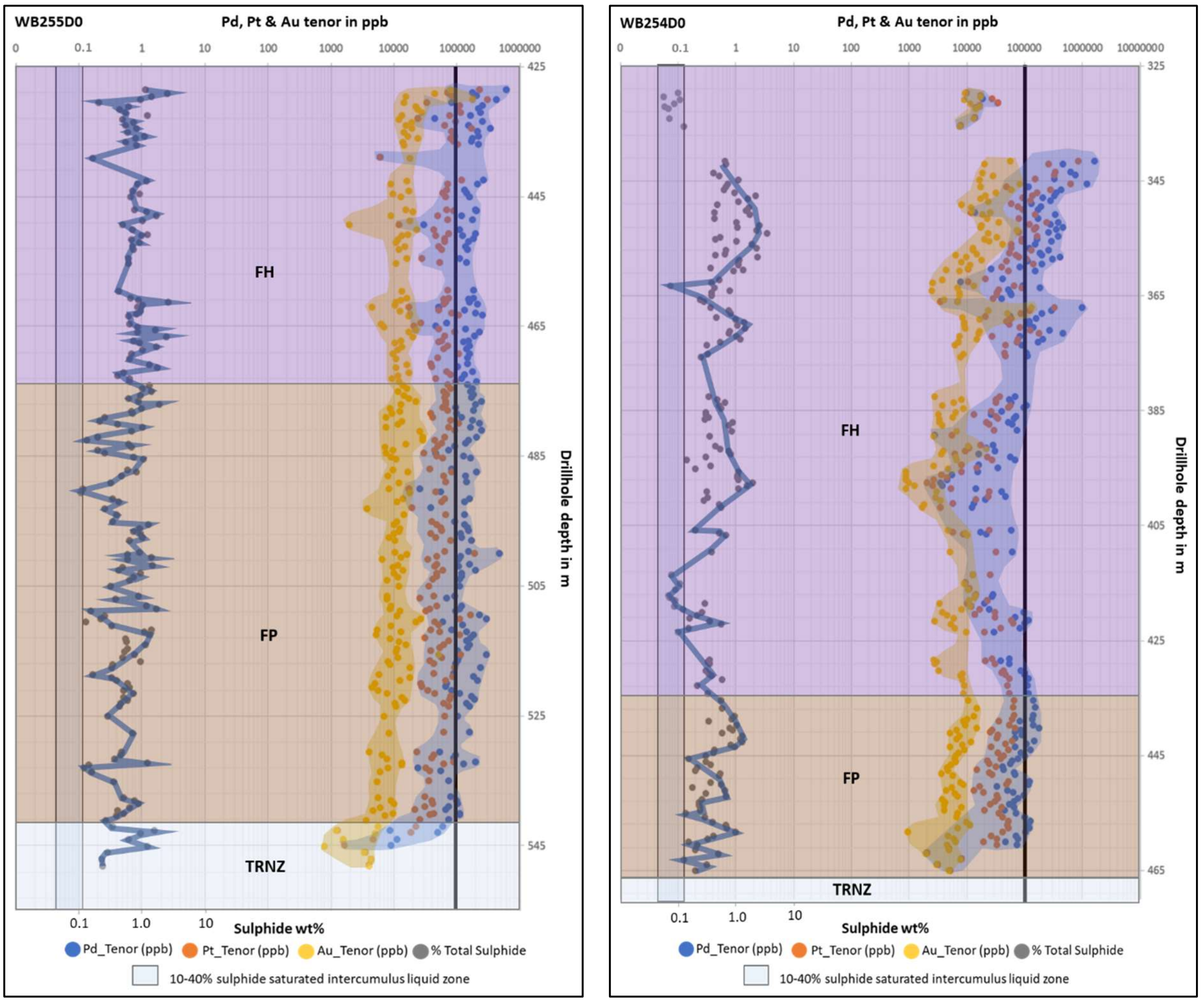

Figure 7.23. Tenor plots of WB255D0 and WB254D0 showing Pt, Pd and Au tenors along with sulphide content (wt %). The light blue and orange shaded areas show PGE and Au trends respectively. The different colour units represent the lithostratigraphic units. Abbreviations: the Feldspathic Pyroxenite (FP), the Feldspathic Harzburgite (FH) and the Transitional Zone (TRNZ).

WB254D0

In this drillcore, the lower FP and the upper FH are characterised by higher PGE tenors with palladium tenors higher than platinum tenors (Figure 7.23). These PGE tenors (Pd and Pt) increase upward from 5 ppm at the bottom of the FP to 175 ppm towards the top of the FP (Figure 7.23). A slight PGE tenor reduction occurs towards the contact between the FP and the FH. Although there is an upward increase in PGE tenors in the FP, the average tenor is below 100 ppm (90 ppm for Pd and 38 ppm for Pt). In the FH, the PGE significantly reduces upwards to below 100 ppm from the base to a depth of 497 m. From this depth, the PGE tenors gradually increase upward peaking at 1 593 ppm at the top of the FH. The average Pd tenors in the FH are above 100 ppm (146 ppm) while the Pt tenors are lower (68 ppm). The gold tenors follow trends similar to those of the PGEs in both the FP and the FH, attaining a maximum of 130 ppm towards the top of the FH. Generally, the Au tenors are 7 ppm and 13 ppm in the FP and the FH, respectively.

7.4.4 The F - Boundary North

WE144D0

In this drillcore, the lower FP is not present (Figure 7.24). The upper FH is characterised by higher PGE tenors with higher palladium tenors than platinum tenors. These PGE tenors (Pd and Pt) decrease upward from 125 ppm in the TRNZ to 18 ppm at the TRZN/FH boundary (Figure 7.24). There is generally an increase in the PGE tenors from the bottom of the FH upwards. The tenors drastically decrease from 482 m to 480 m, then gradually increase upwards towards the upper portion of the FH. A maximum tenor of 575 ppm is attained towards the top of the FH. Generally, the Pd tenors are above 100 ppm (113 ppm) while the Pt tenors are lower (56 ppm). The gold tenors follow a trend similar to that of the PGE reaching a maximum of 127 ppm with an average tenor of 10 ppm.

WE145D0

The lower FP and the upper FH of the F Zone are characterised by higher PGE tenors with palladium tenors higher than platinum tenors (Figure 7.24). These PGE tenors (Pd and Pt) generally decrease upward from 68 ppm in the TRNZ to 3 ppm in the mid-section of the FP (Figure 7.24). From a depth of 485 m, the PGE tenors generally increase towards the FP and FH contact. Within the FH, the tenors gradually increase upwards, attaining a maximum of 495 ppm. Generally, the Pd tenors are above 100 ppm (124 ppm) while the Pt tenors are lower (64 ppm). The gold tenors follow a trend similar to that of the PGE, reaching a maximum of 36 ppm with an average trend of 10 ppm.

WE061D0

In this drillcore, the lower FP is not present (Figure 7.25). The upper FH is characterised by higher PGE tenors with higher palladium tenors than platinum tenors. These PGE tenors (Pd and Pt) slightly increase upwards from the TRNZ to the TRZN/FH contact (Figure 7.25). There is a slight increase in PGE tenors from the base towards the upper portion of the FH with an elevated tenor of 781 ppm. Generally, both Pd and Pt tenors are above 100 ppm (237 ppm Pd & 116 ppm Pt). A minor tenor reduction from 442 m to 440 m depth is apparent within the FH. The gold tenors follow a trend similar to that of the PGE. However, the maximum tenor of 684 ppm is attained at the bottom portion of the FH. The average gold tenor within the FH is 20 ppm.

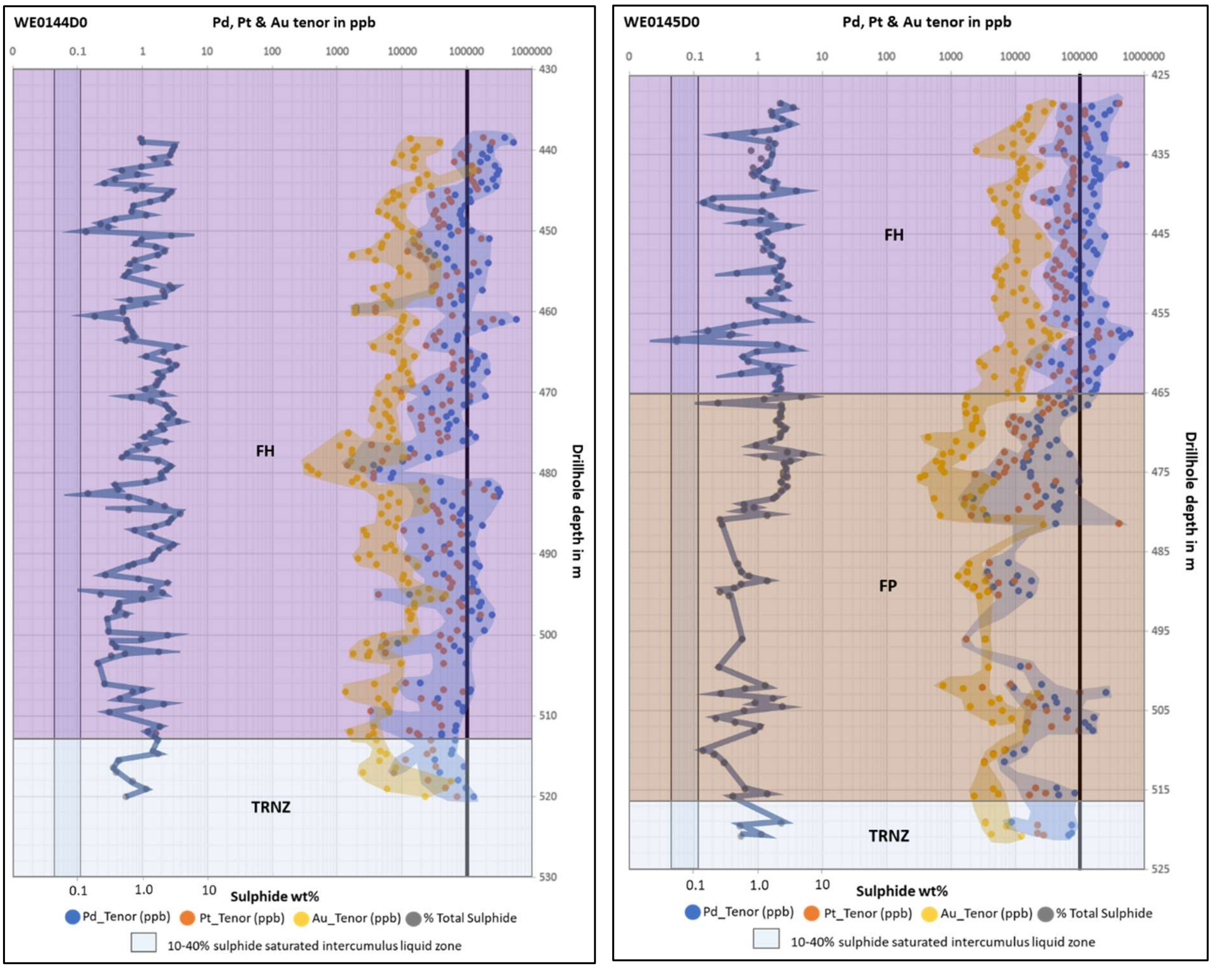

Figure 7.24. Tenor plots of WE144D0 and WE145D0 showing Pt, Pd and Au tenors along with sulphide content (wt %). The light blue and orange shaded areas show PGE and Au trends respectively. The different colour blocks represent the lithostratigraphic units. Abbreviations: the Feldspathic Pyroxenite (FP), the Feldspathic Harzburgite (FH) and the Transitional Zone (TRNZ).

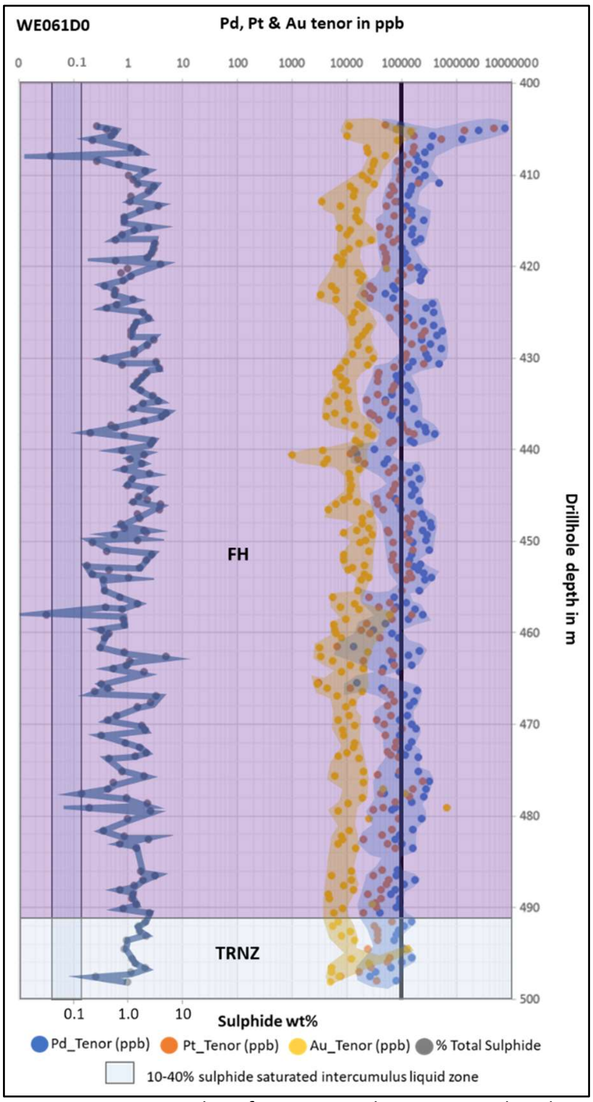

Figure 7.25. Tenor plot of WE061D0 showing Pt, Pd and Au tenors along with sulphide content (wt %). The light blue and orange shaded areas show PGE and Au trends respectively.

7.4.5 <u>The F - North</u>

7.4.5.1 <u>The F - North dip section</u>

<u>WE052D0</u>

There is an upward decrease in tenor from the Basement granite gneiss (BAS) to the BAS/FP boundary (Figure 7.26). There seems to be no significant upward increase in tenors in the FP with tenors attaining a maximum of 465 ppm. However, at a depth of 512 m, the tenors slightly decrease followed by a minor upward increase. Within the FP, the Pd tenors are generally above 100 ppm (189 ppm) while the Pt tenors are lower (73 ppm). There is an upward increase in tenors within the FH with the higher tenor of 390 ppm. The Pd tenors in the FH (186 ppm) are slightly lower than the FP tenors while Pt tenors are equal at 73 ppm. The gold tenors follow trends similar to those of PGEs in both the FP and the FH, reaching a maximum of 51 ppm towards the upper portion of the FP. Generally, the gold tenors are 14 ppm and 15 ppm in the FP and the FH, respectively.

WE054D0

In this drillhole, the lower FP and the upper FH are characterised by higher PGE tenors with higher palladium tenors than platinum tenors (Figure 7.26). These PGE tenors (Pd and Pt) increase upwards from the TRNZ to the TRNZ/FP boundary (Figure 7.26). From the TRNZ/FP boundary, there is a slight upward decrease in tenor up to a depth of 401 m. The PGE tenors subsequently increase gradually towards the FP/FH boundary. Within the FP, the Pd tenors are generally above 100 ppm (173 ppm) while the Pt tenors are lower (70 ppm). There is an upward increase in tenors within the FH with an elevated tenor of 355 ppm. The Pd and Pt tenors in the FH are higher than those of the FP (208 ppm Pd and 90 ppm Pt). The gold tenors follow trends similar to those in both the FP and the FH, attaining a maximum of 31 ppm at the bottom of the FH. Generally, the gold tenors are 13 ppm and 16 ppm in the FP and the FH, respectively.

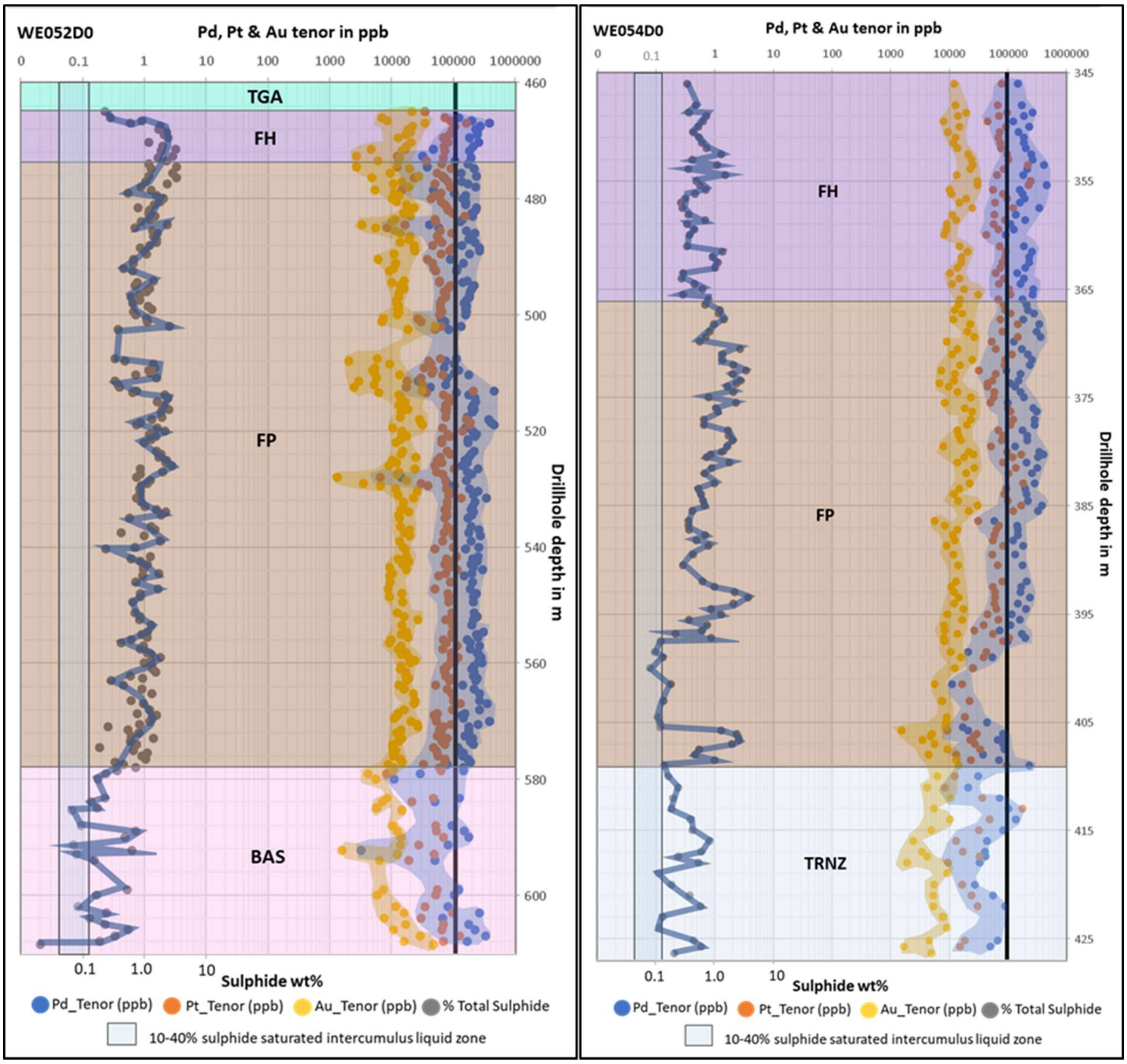

Figure 7.26. Tenor plots for WE052D0 and WE054D0 showing Pt, Pd and Au tenors along with sulphide content (wt %). The light blue and orange shaded areas show PGE and Au trends respectively. The different colour blocks represent the lithostratigraphic units. Abbreviations: the Troctolite-Gabbronorite-Anorthosite Sequence (TGA), the Feldspathic Pyroxenite (FP), the Feldspathic Harzburgite (FH), the Transitional Zone (TRNZ) and the Basement granite gneiss (BAS).

WE064D0

The lower FP and the upper FH of the F Zone are characterised by high PGE tenors with palladium tenors higher than platinum tenors (Figure 7.27). These PGE tenors (Pd and Pt) increase from the TRNZ to the TRNZ/FP boundary (Figure 7.27). From the TRNZ/FP boundary, the PGE tenors increase upwards from the bottom to the upper portion of the FP attaining a high tenor of 282 ppm. There seems to be a slight reduction in PGE tenors from the bottom of the FH upwards to a depth of 288 m. The tenors then drastically increase upward, reaching a maximum of 636 ppm and then drastically decrease. Within the FP, the Pd tenors are generally above 100 ppm (147 ppm) while the Pt tenors are lower (61 ppm). The Pd and the Pt tenors in the FH are higher than those of the FP (194 ppm Pd and 91 ppm Pt). The gold tenors follow a trends similar to those of the PGEs in both the FP and the FH, attaining a maximum tenor of 46 ppm in the FH. Generally, the gold tenors are 12 ppm and 14 ppm in the FP and the FH, respectively.

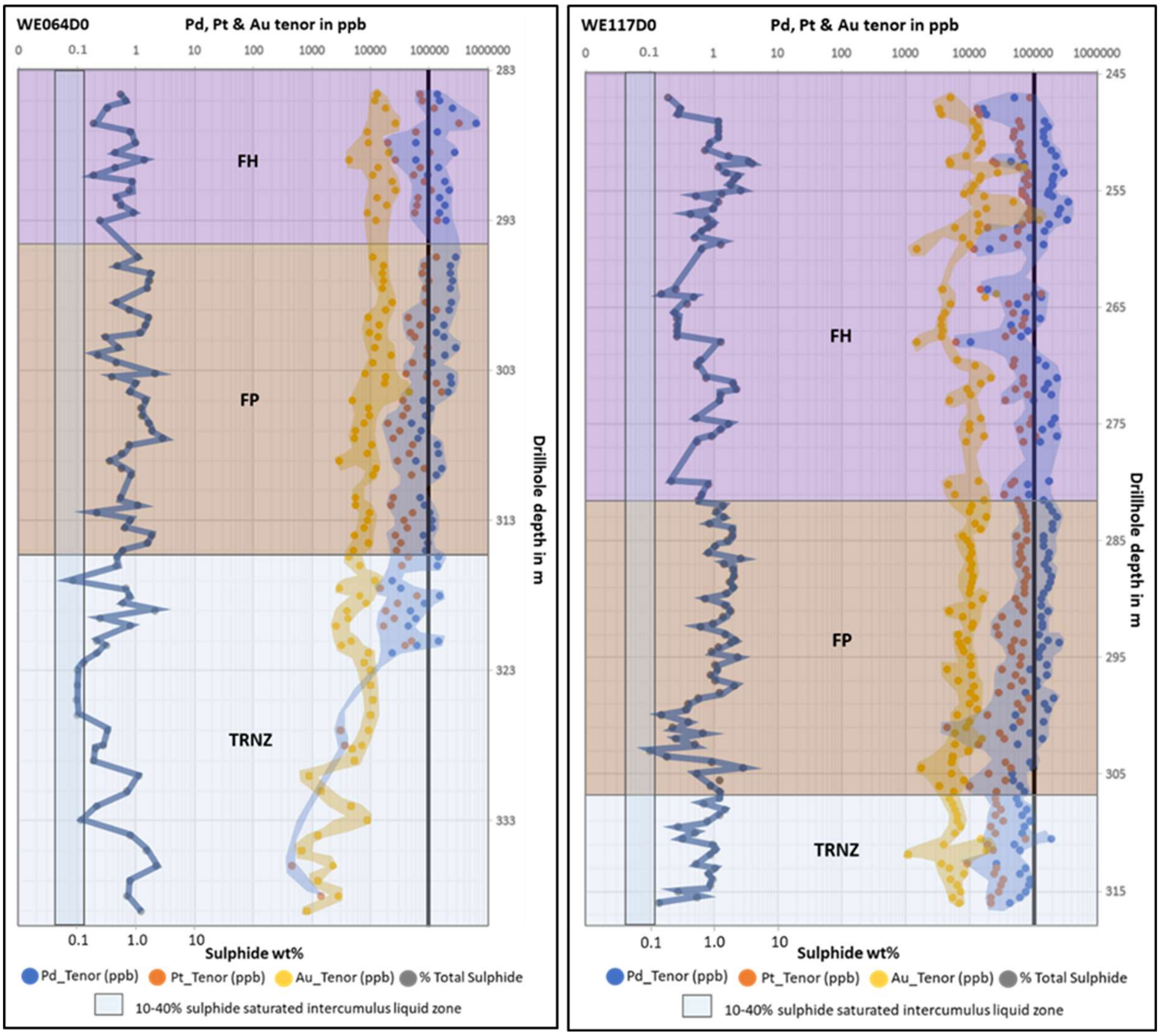

Figure 7.27. Tenor plots from WE064D0 and WE117D0 showing Pt, Pd and Au tenors along with sulphide content (wt %). The light blue and orange shaded areas show PGE and Au trends respectively. The different colour blocks represent the lithostratigraphic units. Abbreviations: the Feldspathic Pyroxenite (FP), the Feldspathic Harzburgite (FH) and the Transitional Zone (TRNZ).

WE117D0

In this drillhole, the lower FP and the upper FH of the F Zone are characterised by high PGE tenors with palladium tenors higher than platinum tenors (Figure 7.27). These PGE tenors (Pd and Pt) increase upwards from the TRZN to the upper section of the FP, attaining a higher tenor of 256 ppm in the mid-section (Figure 7.27). There is a slight decrease in tenor towards the FP/FH boundary. There is also an upward increase in the PGE tenor in the FH. However, there is a major reduction in tenors between 271 m and 211 m depths. Within the FP, the Pd tenors are generally above 100 ppm (131 ppm) while the Pt tenors are lower (50 ppm). The Pd and the Pt tenors in the FH are higher than those in the FP (147 ppm Pd and 60 ppm Pt). The gold tenors follow a trend similar those in both the FP and the FH, attaining a peak tenor of 124 ppm in the FH. Generally, the gold tenors are 9 ppm and 14 ppm in the FP and the FH, respectively.

<u>*WE120D0*</u>

In this drillhole, there is an upward increase in tenor in the FP from the TRZN upwards into the FP to a depth of 442m (Figure 7.28). From this depth upwards, there is a slight increase in the PGE tenors with a peak tenor of 246 ppm towards the upper portion of the FP. The PGE tenors decrease slightly in the FH from the base upwards. Within the FP, the Pd tenors are generally slightly above 100 ppm (102 ppm) while the Pt tenors are lower (37 ppm). The Pd and the Pt tenors in the FH are higher than those in the FP (178 ppm Pd and 72 ppm Pt). The gold tenors follow a trend similar to those of PGEs in both the FP and the FH, peaking at 28 ppm in the FH. Generally, the gold tenors are 8 ppm and 14 ppm in the FP and the FH, respectively.

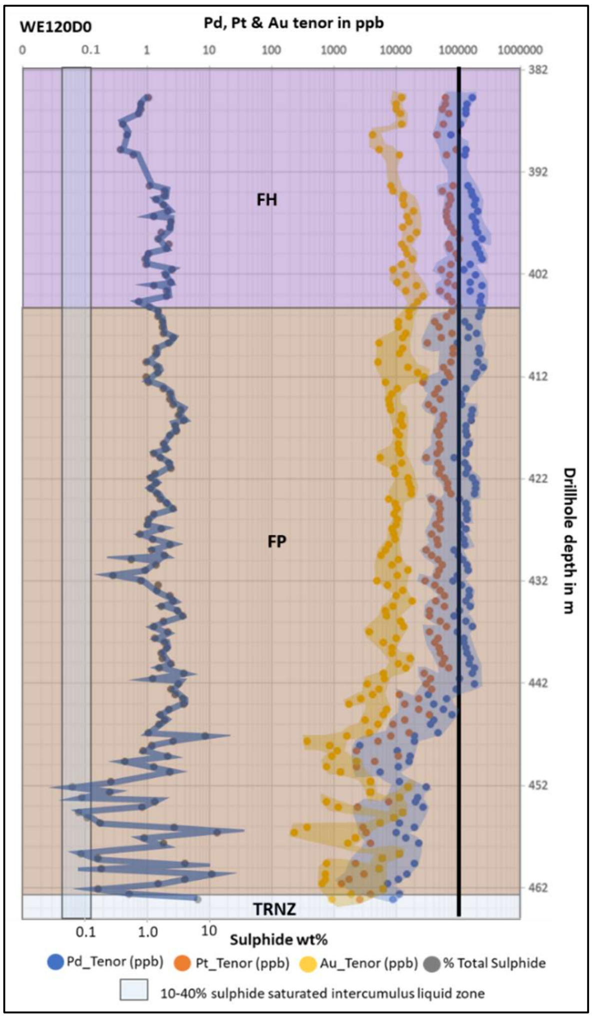

Figure 7.28. Tenor plot of WE120D0 showing Pt, Pd and Au tenors along with sulphide content (wt%). The light blue and orange shaded areas show PGE and Au trends respectively.

7.4.6 Discussion of drillhole tenors

Both the F Zone and the T Zone are characterised by high PGE (Pd and Pt) and Au tenors. The palladium tenors are higher than both the platinum and gold tenors while the platinum tenors are higher than the gold tenors. In both the F Zone and the T Zone, the gold tenors are significantly lower than the PGE tenors. The gold tenors within the T Zone are generally higher than the F Zone gold tenors ranging between 18 ppm - 84 ppm while the F Zone ranges between 7 ppm - 23 ppm. The palladium tenors in the F Zone seem to be higher than those in the T Zone.

In the F Zone, there is generally an upward increase in PGE + Au tenors from the bottom of the lower FP to the top of the upper the FH. This could imply that the F Zone magma influxes were already enriched in PGE sulphides when entering the magma chamber suggesting that rather than the sulphides gaining their tenors in situ, the tenors might have been gained elsewhere and deposited in bulk or as a mush. A gradual upward decrease in tenors would have suggested a fractional sulphide segregation from the magma influxes with PGE becoming more rapidly depleted in the magma than the base metals.

In the following section, lateral variations in tenors between the subzones of both the F Zone and the T Zone are evaluated and discussed.

7.5 Lateral variations in PGE (Pd and Pt) and Au tenors

If a body of magma is moving in a certain direction, there will be a lateral decrease in tenor towards the direction of movement from the proximal facies to the distal facies (Naldrett et al., 2009). As observed in the Merensky Reef, if the body of magma is stationary, there will be a vertical upward decrease in tenor (Naldrett, in personal communication with Kekana, 2013). However, if sulphides may exchange with flowing magma, as envisaged for the magmatic conduits, the tenor may increase upwards depending on the sulphide/silicate proportion (Campbell et al., 1983).

In this section, variations in tenors (Pd, Pt and Au) are evaluated and discussed from the T Zone in the south to the F - North in the north. The evaluations and discussions are in the following order: -

T Zone
F - Central
F - Boundary South
F - Boundary North
F - North

For the T Zone, the variations are studied in the T2, the LPA, the T1, the UPA and the T0 while in the F Zone, the variations are studied in both the FP and the FH.

7.5.1. The T Zone

The Pd tenors

As illustrated in Figure 7.29 by the bubble sizes, there is a decrease in Pd tenor from SW (WB221D1) to NE (WB237D0) in the T2 subzone. The T2 tenors on the west (WB228D0) to east (WB213D0) dip section are variable with no tenor increase/decrease towards a preferred direction. There is a Pd tenor anti-correlation on strike between T2 and LPA. Within the LPA, the Pd tenors gradually decrease from NE (WB215D0) to SW (WB213D0). On the dip section, Pd tenors in the LPA gradually decrease from west (WB228D0) to east (WB213D0).

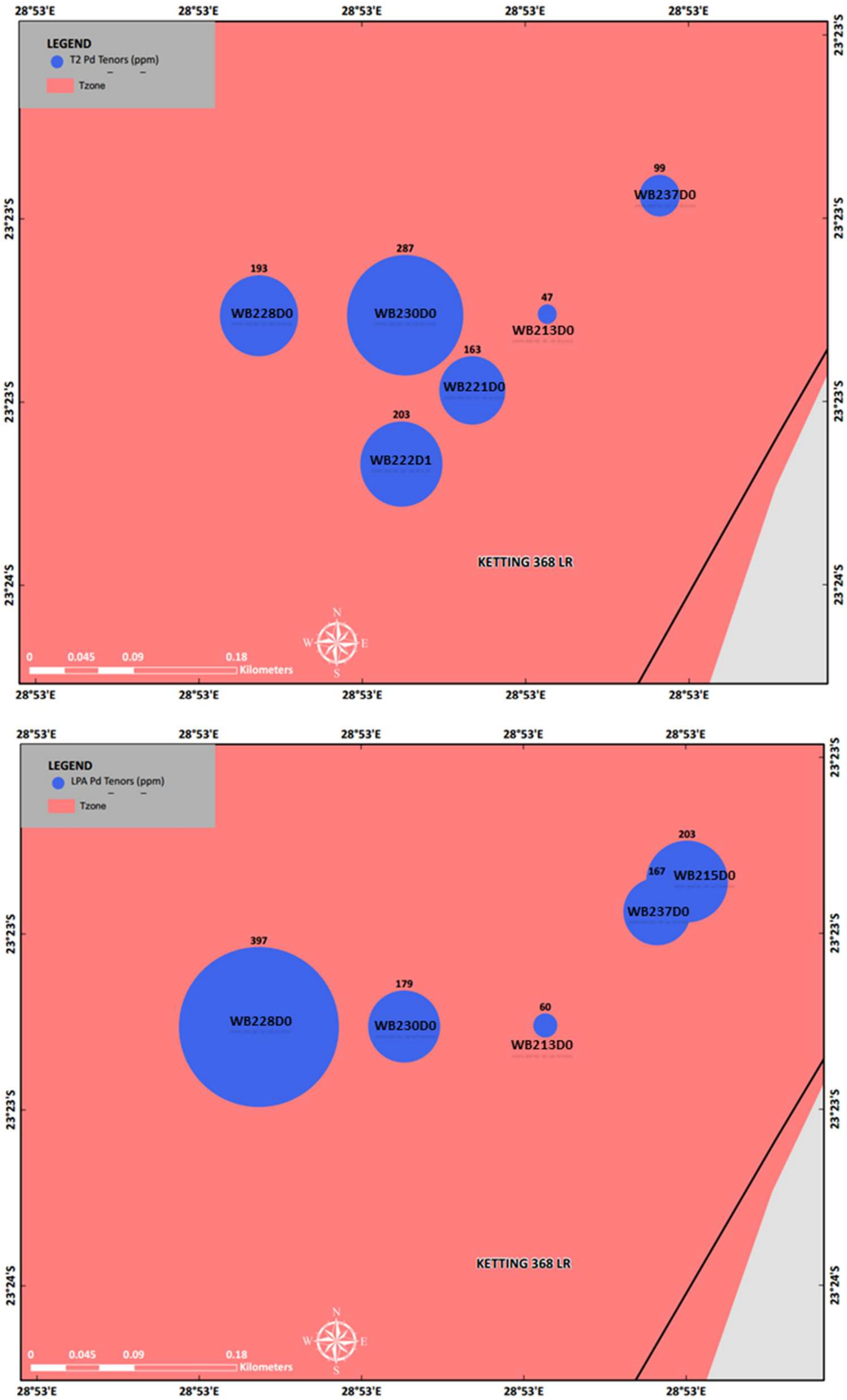

Figure 7.29. Plan sections of the T Zone showing lateral Pd tenor variations in the T1 and the UPA. The size of the bubble represents the proportional size as per the tenor value (values on top of the bubbles).

As illustrated on Figure 7.30, there is a decrease in Pd tenor from SW (WB213D0) to NE (WB215D0) in the T1. Unlike the LPA, Pd tenors in the UPA (strike section) are variable with no tenor increase/decrease towards a preferred direction

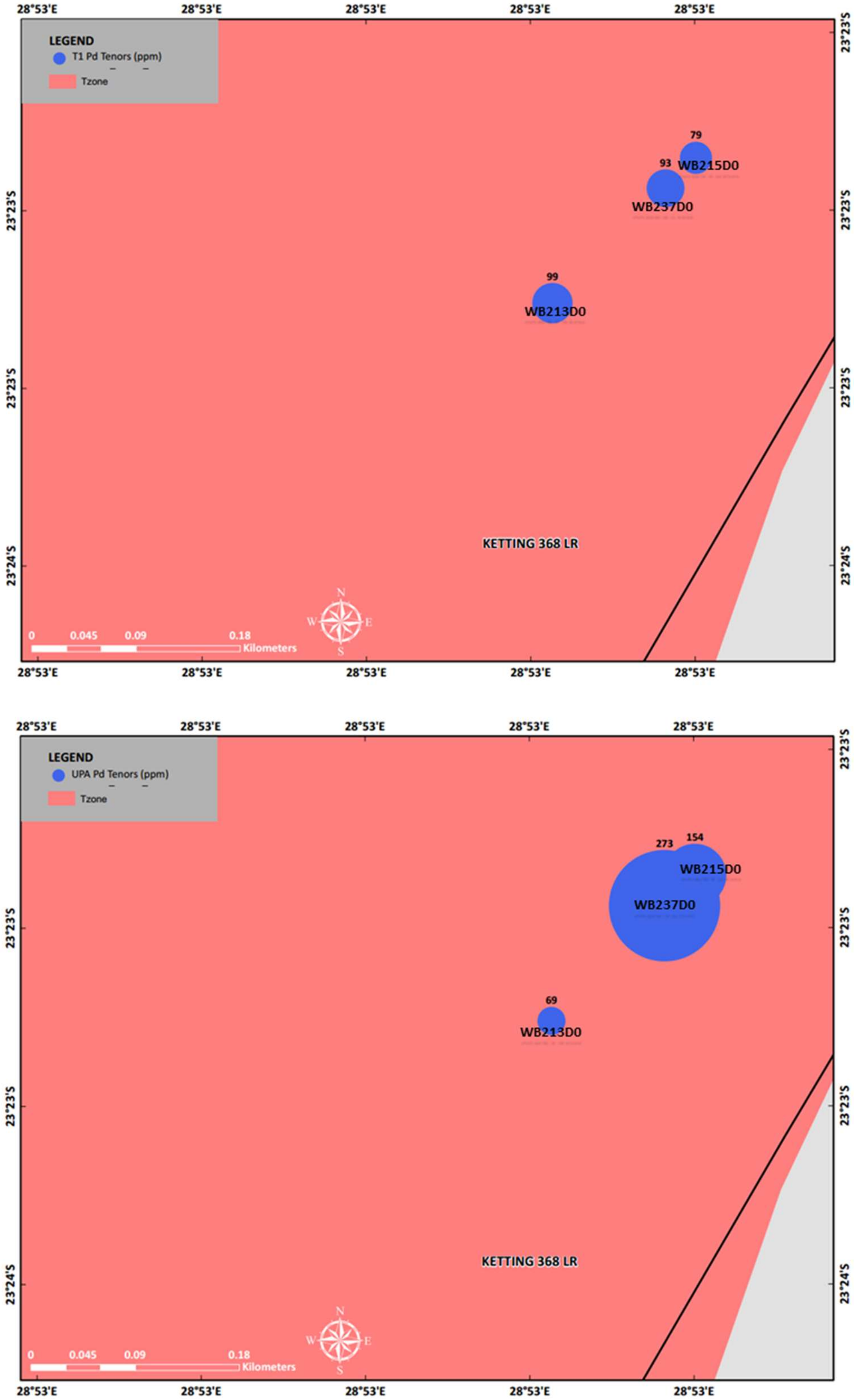

Figure 7.30. Plan sections of the T Zone showing lateral Pd tenor variations in the T1 and the UPA. The size of the bubble represents the proportional size as per the tenor valus (values on top of the bubbles).

As illustrated on Figure 7.31, there is a decrease in Pd tenors in the T0 from SW (WB222D0) to NE (WB221D0). On dip section, there is a decrease in the Pd tenors from east (WB230D0) to west (WB228D0).

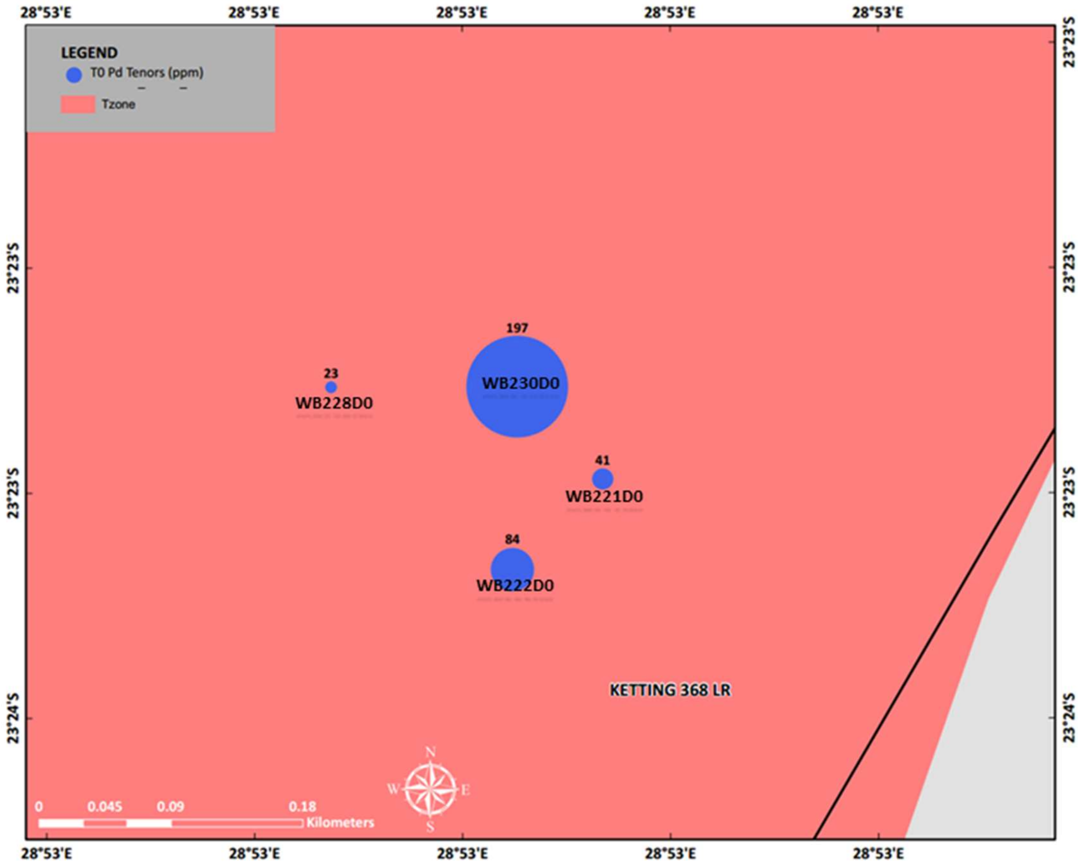

Figure 7.31. Plan section of the T Zone showing lateral Pd tenor variations in the T0. The size of the bubble represents the proportional size as per the tenor value (values on top of the bubbles).

<u>The Pt tenors</u>

As illustrated in Figure 7.32, there is a decrease in Pt tenor in the T2 from SW (WB221D1) to NE (WB237D0). On the dip section, there is a decrease in Pt tenors from west (WB228D0) to east (WB213D0). There is a Pt tenor anti-correlation on strike between the T2 and the LPA on the strike section with the LPA decreasing in Pt tenor from NE (WB215D0) to SW (WB213D0). On the dip section, Pt tenors in the LPA correlate with those of the T2 subzone with a gradual decrease from west (WB228D0) to east (WB213D0).

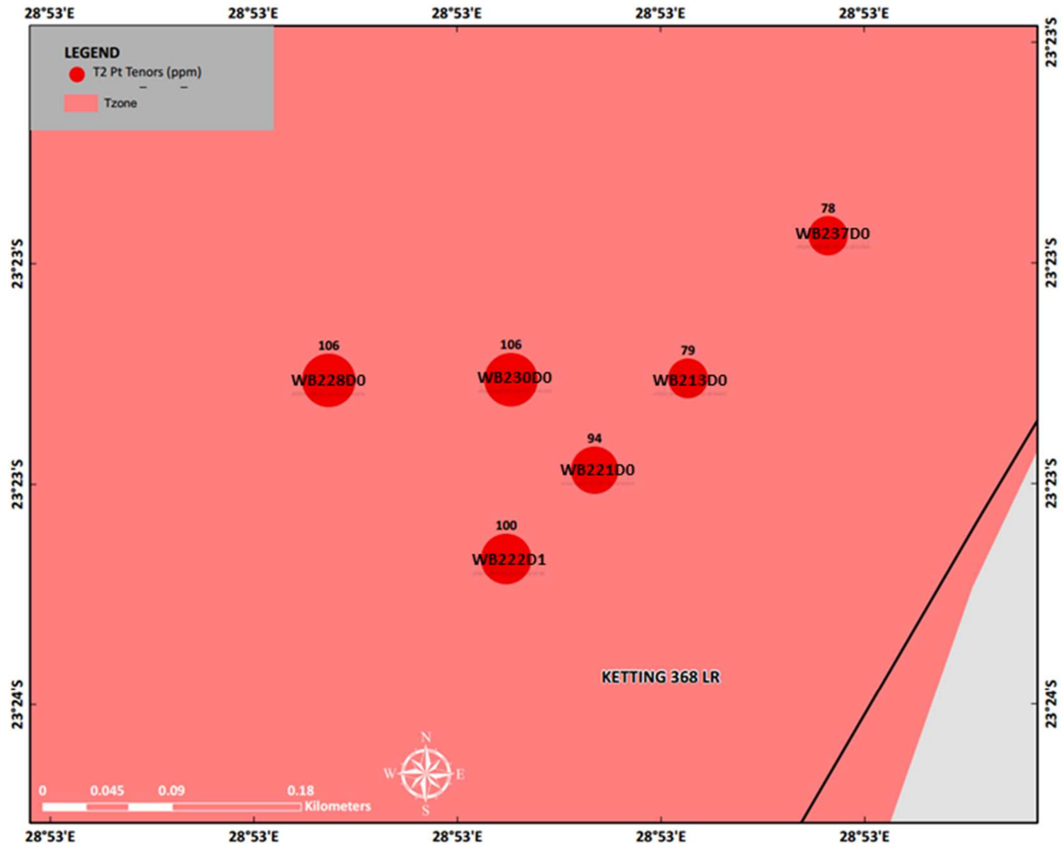

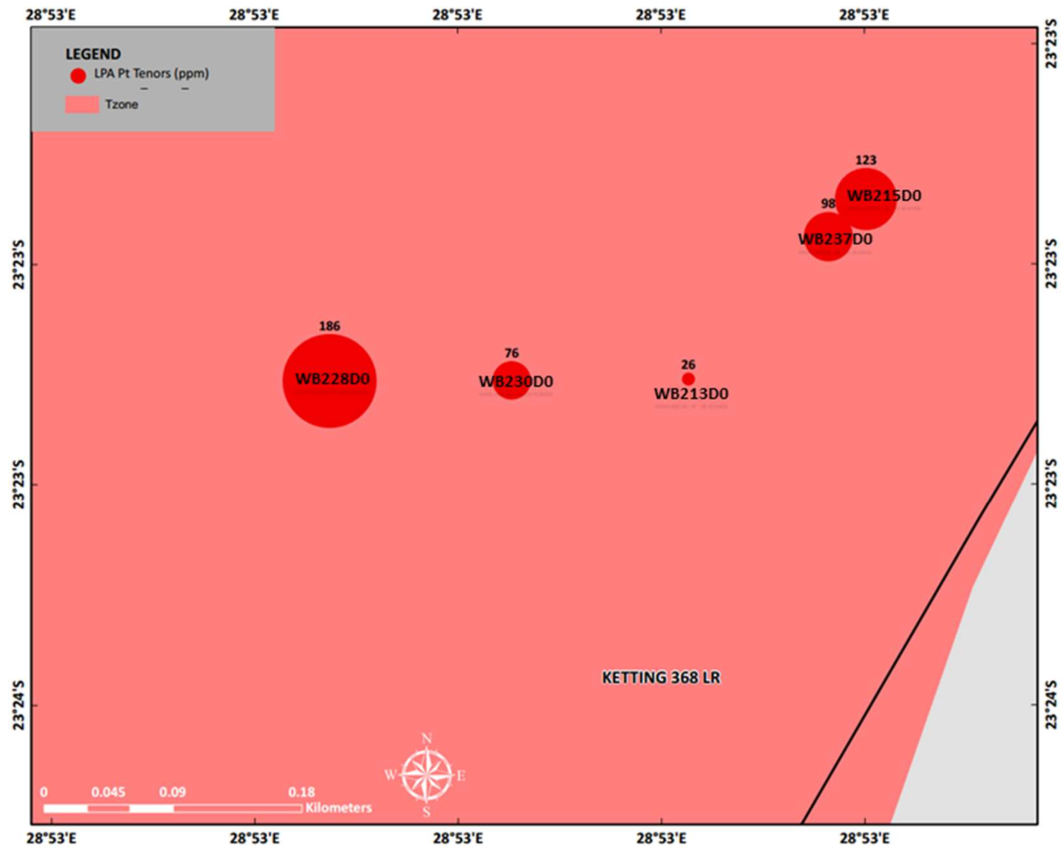

Figure 7.32. Plan sections of the T Zone showing lateral Pt tenor variations in the T2 and the LPA. The size of the bubble represents the proportional size as per the tenor value (values on top of the bubbles).

In both T1 and UPA, the Pt tenors do not show any gradual increase towards a preferred direction (Figure 7.33). However, the T1 has a minor bias towards a tenor decrease from NW to SE.

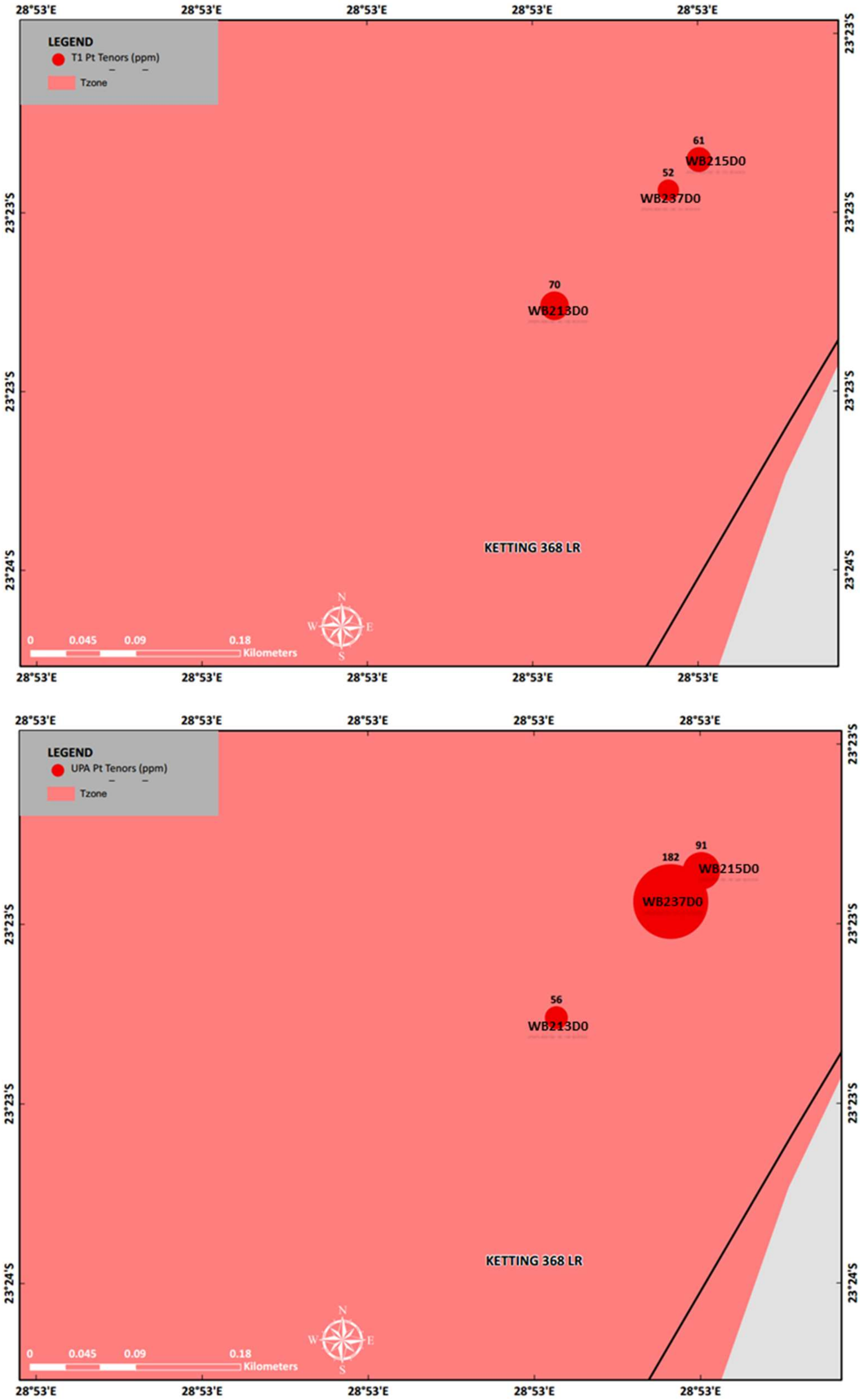

Figure 7.33. Plan sections of the T Zone showing lateral Pt variation in the T1 and the UPA. The size of the bubble represents the proportional size as per the tenor value (values on top of the bubbles).

As illustrated on Figure 7.34, there is a decrease in Pt tenors in the T0 from SW (WB222D0) to NE (WB221D0). On the dip section, there is a decrease in Pt tenors from east (WB230D0) to west (WB228D0).

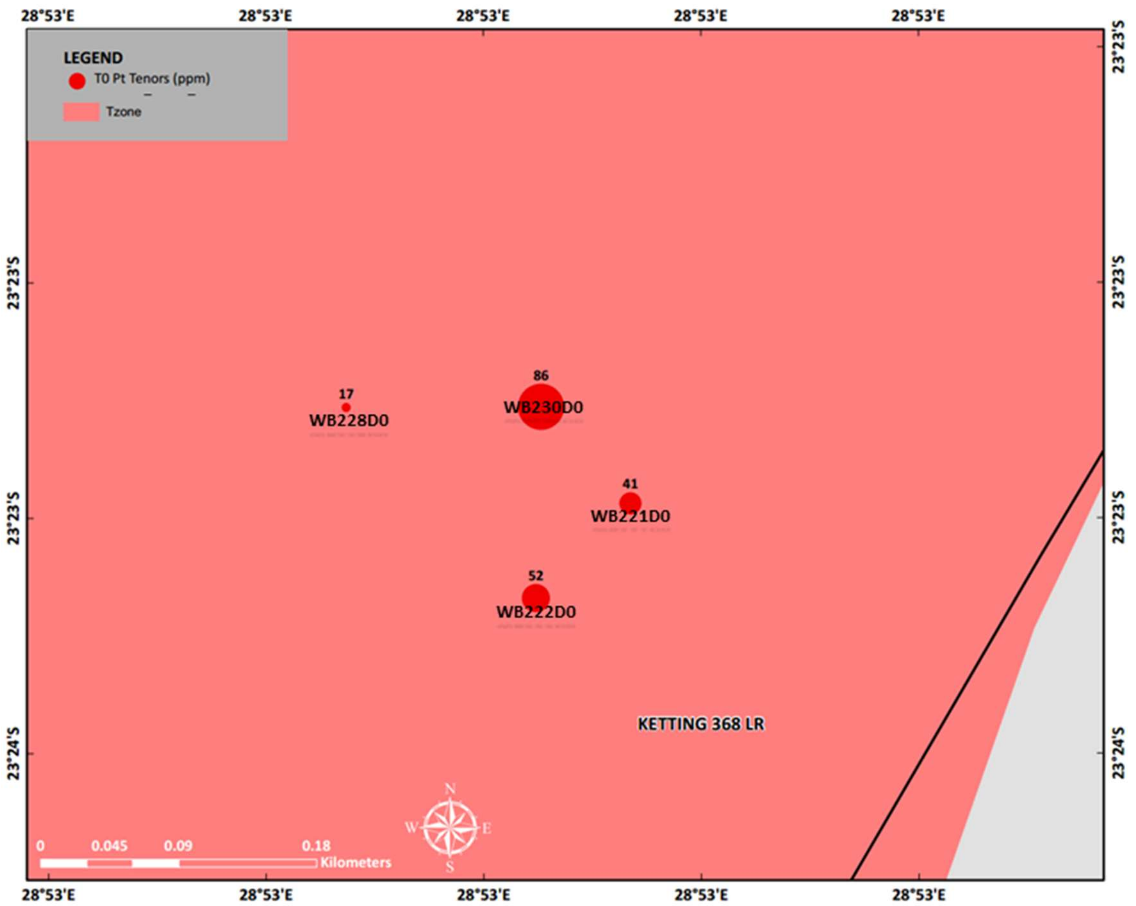

Figure 7.34. Plan section of the Zone showing lateral Pt variations in theT0. The size of the bubble represents the proportional size as per the tenor value (values on top of the bubbles).

<u>*The Au tenors*</u>

Unlike Pd and Pt tenors which decrease gradually in T2 along strike from SW to NE, Au tenors gradually decrease from NE (WB237D0) towards the SW (WB222D1). The same trend is observed in the LPA where Au tenors are also decreasing from NE to SW (Figure 7.35). On the dip section, Au tenors in T2 do not show a gradual increase or decrease towards a preferred direction; however, the tenors in the LPA gradually decrease from west (WB228D0) to east (WB213D0). PGE and Au tenors in the LPA gradually decrease towards the same direction both on dip and along strike.

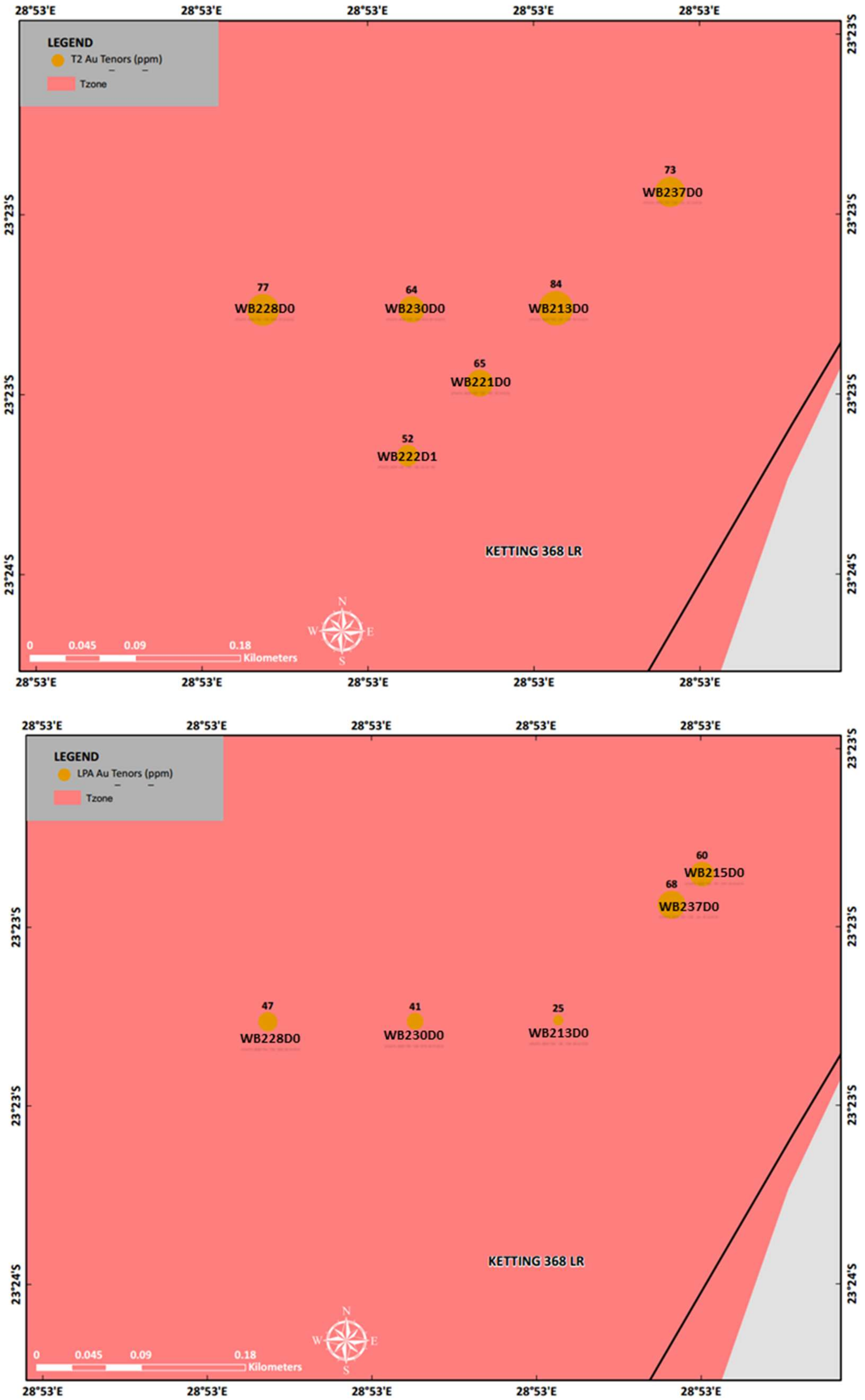

Figure 7.35. Plan sections of the T Zone showing lateral Au variations in the T2 and the LPA. The size of the bubble represents the proportional size as per the tenor value (values on top of the bubbles).

Within the T1 subzone, there is also a gradual decrease in Au tenors on strike from NE (WB215D0) to SW (WB213D0). The Au tenors in the UPA do not show any gradual increase towards a preferred direction (Figure 7.36).

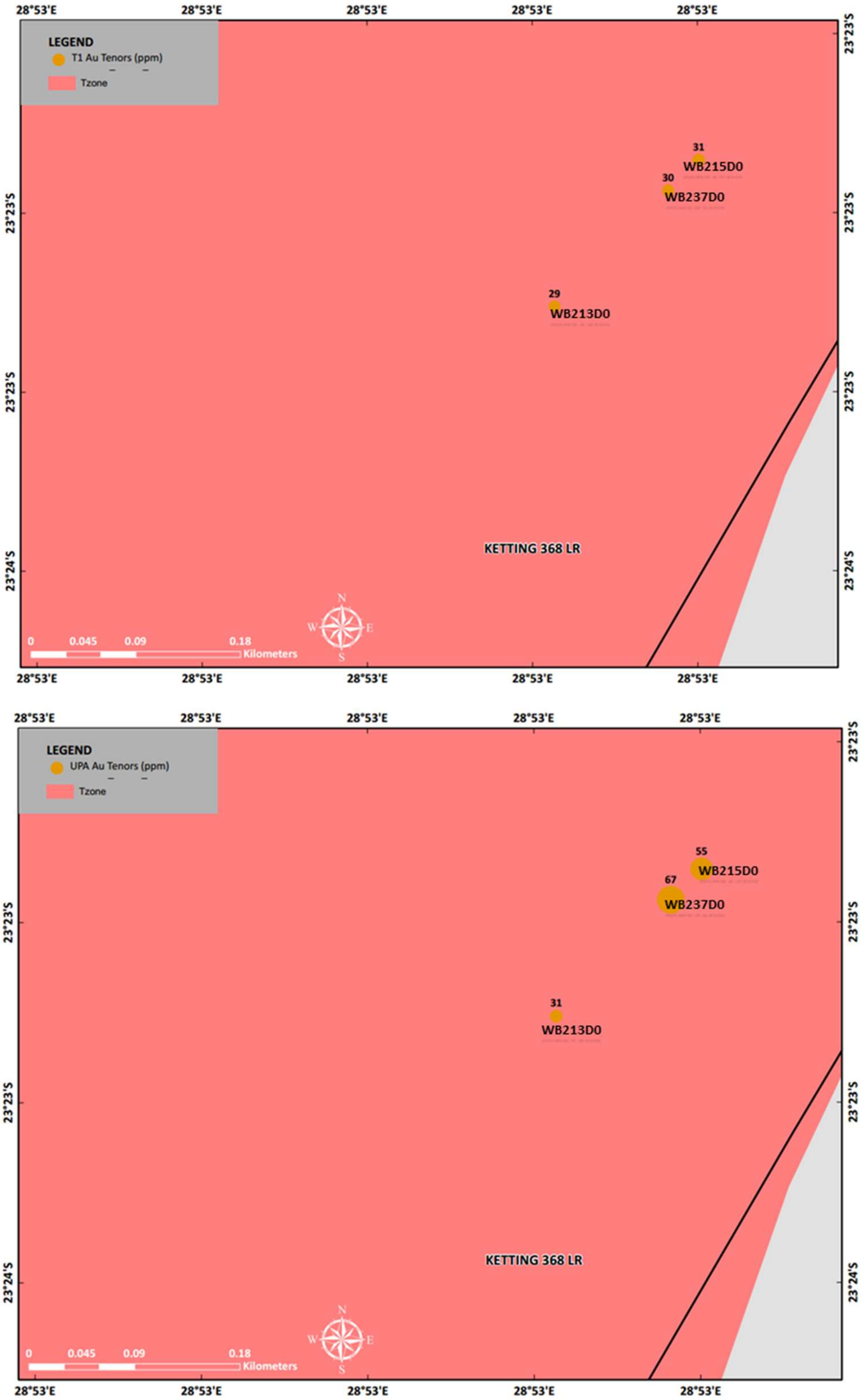

Figure 7.36. Plan sections of the T Zone showing lateral Au variations in the T1 and the UPA. The size of the bubble represents the proportional size as per the tenor value (values on top of the bubbles).

As illustrated on Figure 7.37, there is a gradual decrease in Au tenors in the T0 from NE (WB221D0) to SW (WB222D1). The Au tenors also decrease gradually on the dip section from west (WB230D0) to east (WB228D0).

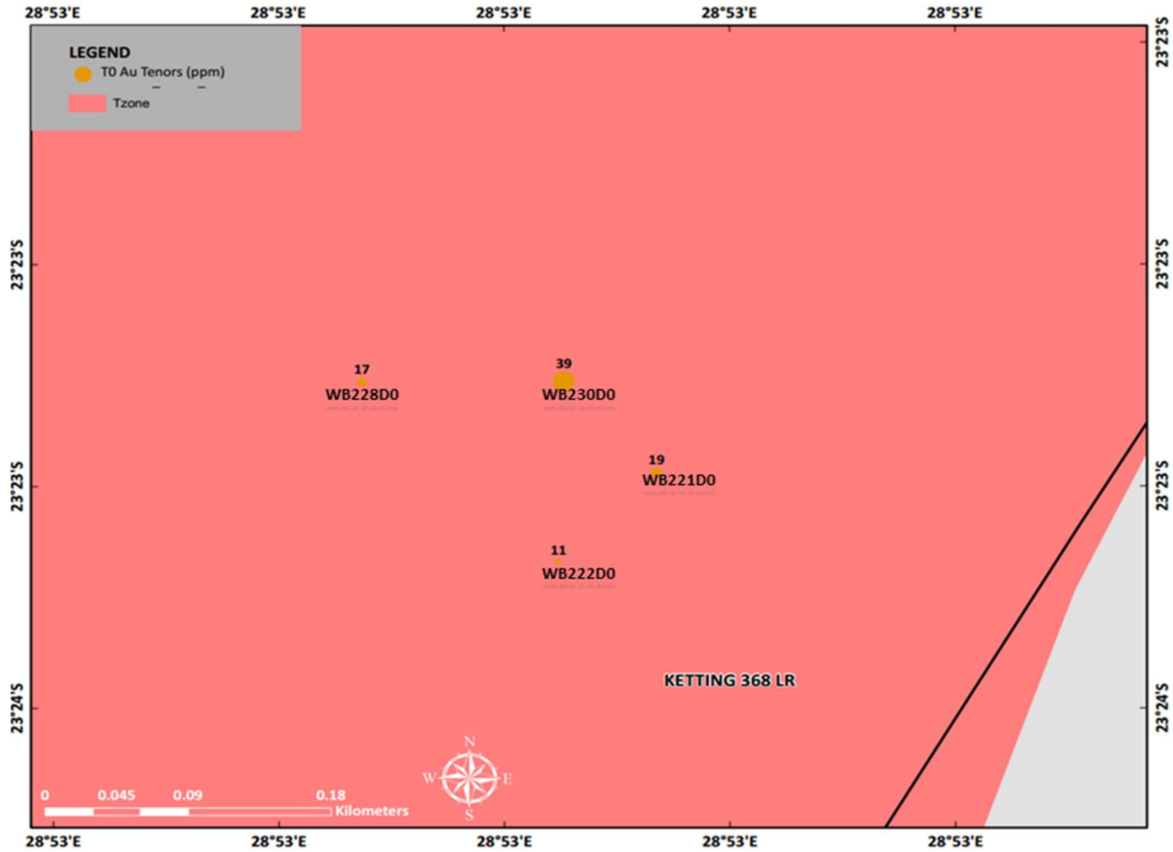

Figure 7.37. Plan section of the T Zone showing lateral Au variations in the T0. The size of the bubble represents the proportional size as per the tenor value (values on top of the bubbles).

For the T Zone lateral tenor variations data, refer to Appendix 4.

7.5.2 <u>The F - Central</u>

<u>The Pd tenors</u>

As illustrated in Figure 7.38 by the bubble sizes, there is a decrease in Pd tenor on strike from NE (WB261D0) to SW (WB276D0) in the FH. On the dip section, in the FH, the Pd tenors are higher at the centre of the dip section (WB280D0and WB259D0) with a gradual decrease to both the east and west. Within the FP, the highest Pd tenor is also at the centre of the dip section (WB259D0).

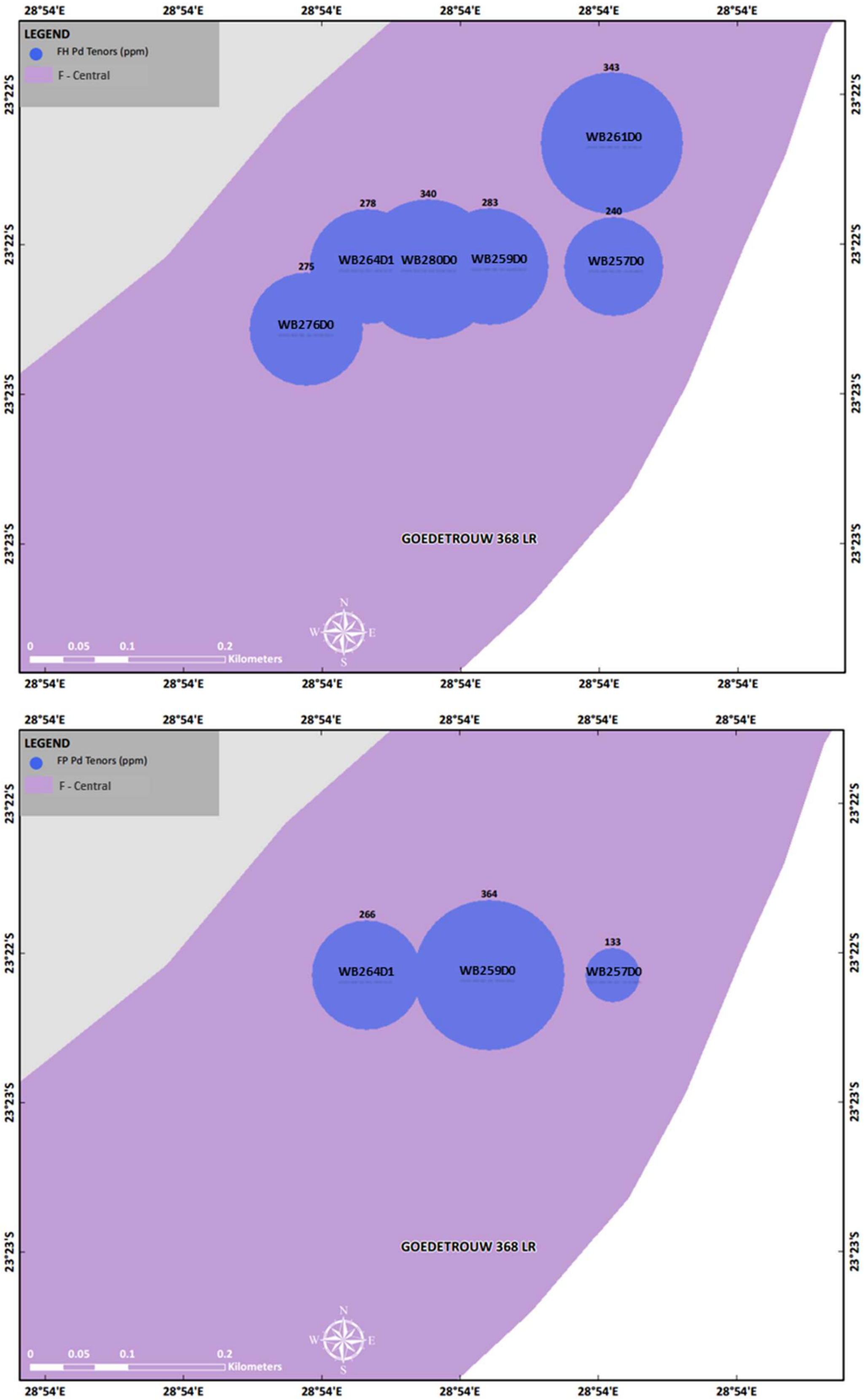

Figure 7.38. Plan sections of the F - Central showing lateral Pd variations in the FH and the FP. The size of the bubble represents the proportional size as per the tenor value (values on top of the bubbles).

The Pt tenors

As with the Pd tenors, there is a decrease in Pt tenor on strike from NE (WB261D0) to SW (WB276D0) in FH (Figure 7.39). On the dip section, the FH Pt tenors are higher at the centre of the dip section (WB280D0 & WB259D0) with a gradual decrease towards the west and east. Within the FP, the highest Pt tenor is also at the centre of the dip section (WB259D0).

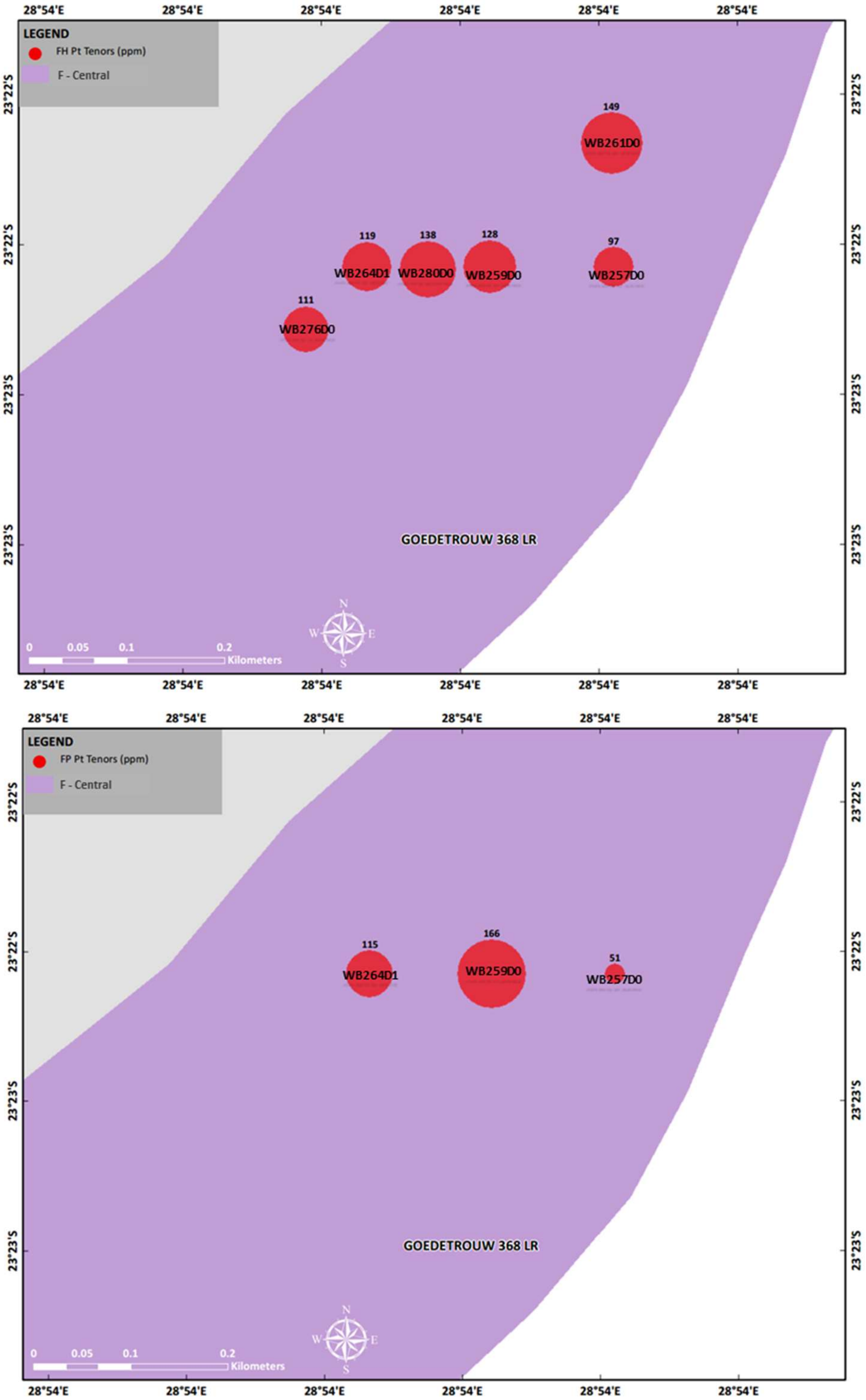

Figure 7.39. Plan sections of the F - Central showing lateral Pt variations in the FH and the FP. The size of the bubble represents the proportional size as per the tenor value (values on top of the bubbles).

The Au tenors

As illustrated in Figure 7.40, there is a decrease in Au tenor on strike from the NE (WB261D0) to SW (WB276D0) in FH. On the dip section, Au tenors in the FH decrease gradually from west (WB64D1) to east (WB257D0). Within the FP, the highest Au tenor is at the centre of the dip section (WB259D0) with a gradual decrease towards the west and to the east.

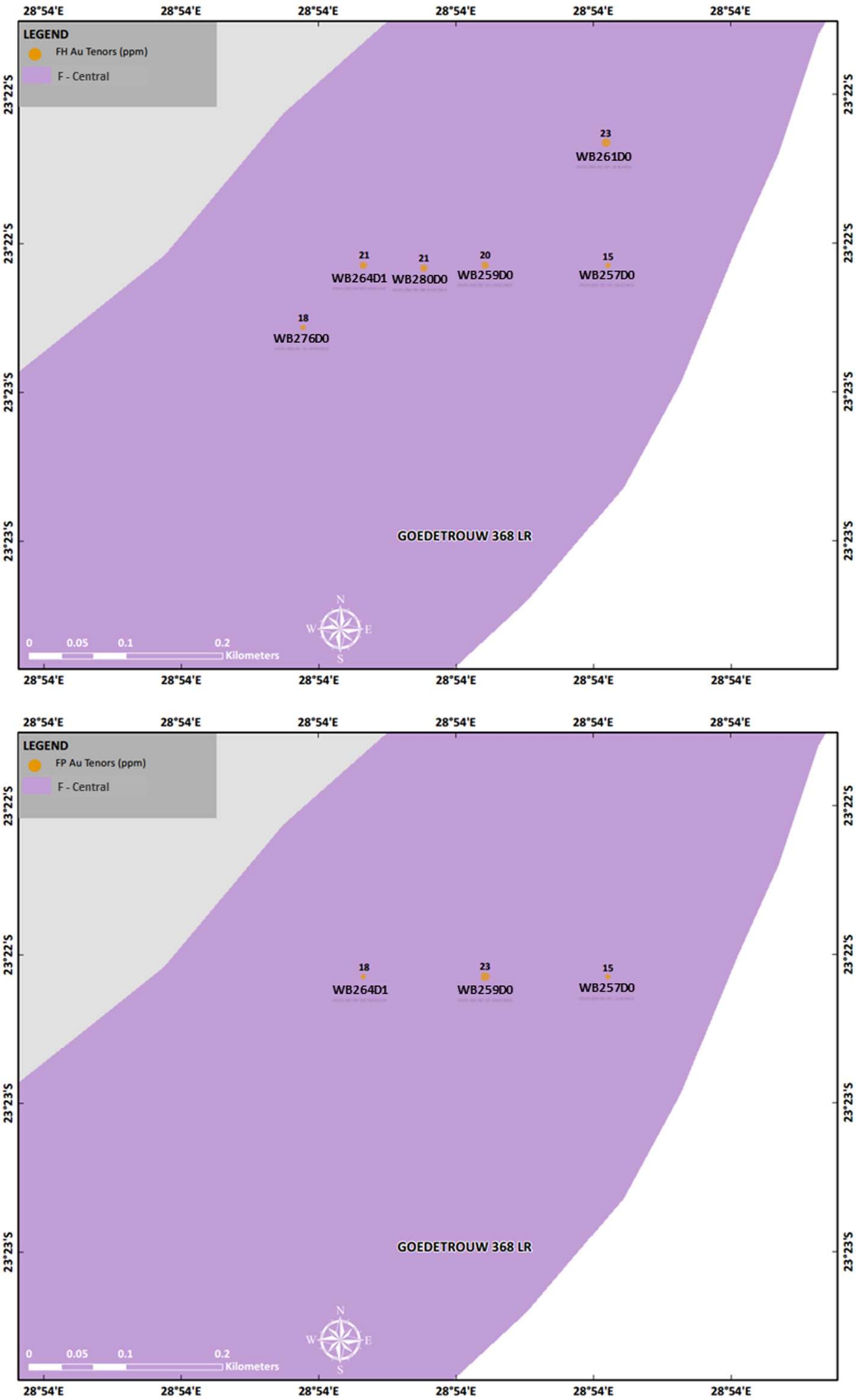

Figure 7.40. Plan sections of the F - Central showing lateral Au variations in the FH and the FP. The size of the bubble represents the proportional size as per the tenor value (values on top of the bubbles).

7.5.3 The F - Boundary South

Pd tenors

As illustrated in Figure 7.41, there is a decrease in Pd tenor on the dip section from NW (WB255D0) to SE (WB254D0) in both the FH and the FP. Pd tenors in the FH are higher than those of the FP.

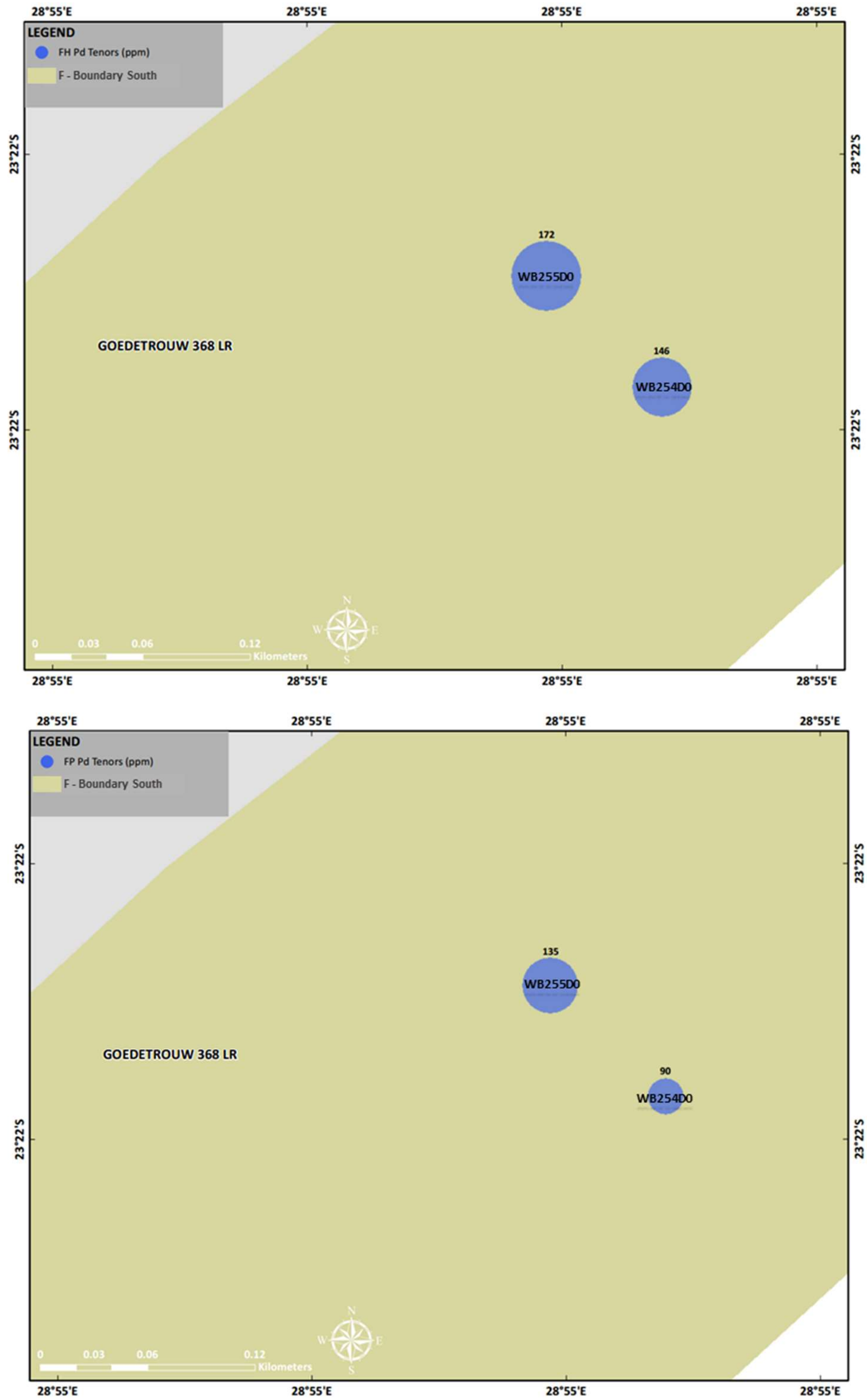

Figure 7.41. Plan sections of F - Boundary South showing lateral Pd variations in FH and FP. The size of the bubble represents the proportional size as per the tenor value (values on top of the bubbles).

As with the Pd tenors, the Pt tenors also decrease on dip section from NW (WB255D0) to SE (WB254D0) with higher tenors in the FH compared to the FP (Figure 7.42).

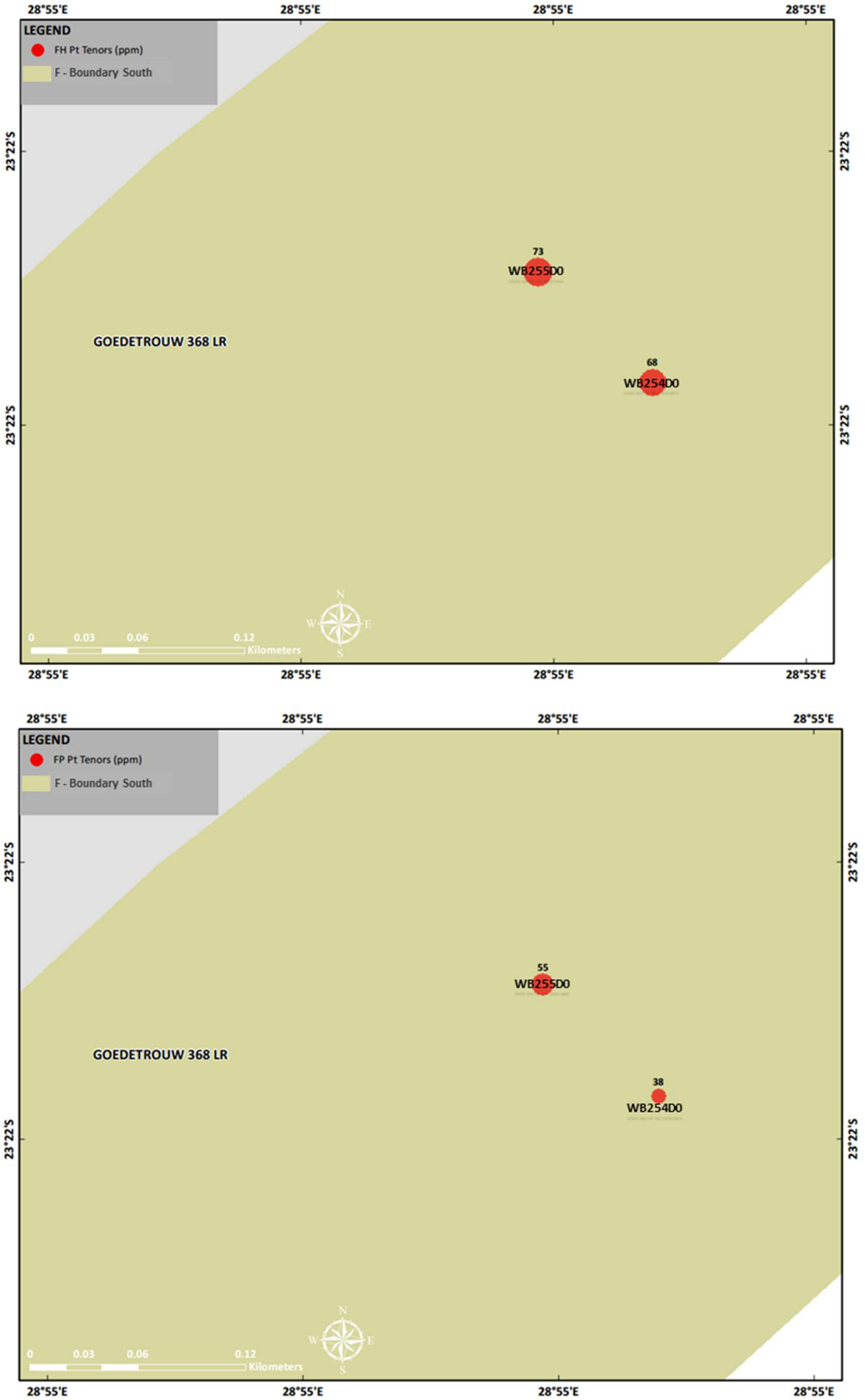

Figure 7.42. Plan sections of the F - Boundary South showing lateral Pt variations in the FH and the FP. The size of the bubble represents the proportional size as per the tenor value (values on top of the bubbles).

The gold tenors are similar to the PGE tenors as they also decrease on the dip section from NW (WB255D0) to SE (WB254D0) with higher tenors in FH in comparison to FP (Figure 7.43).

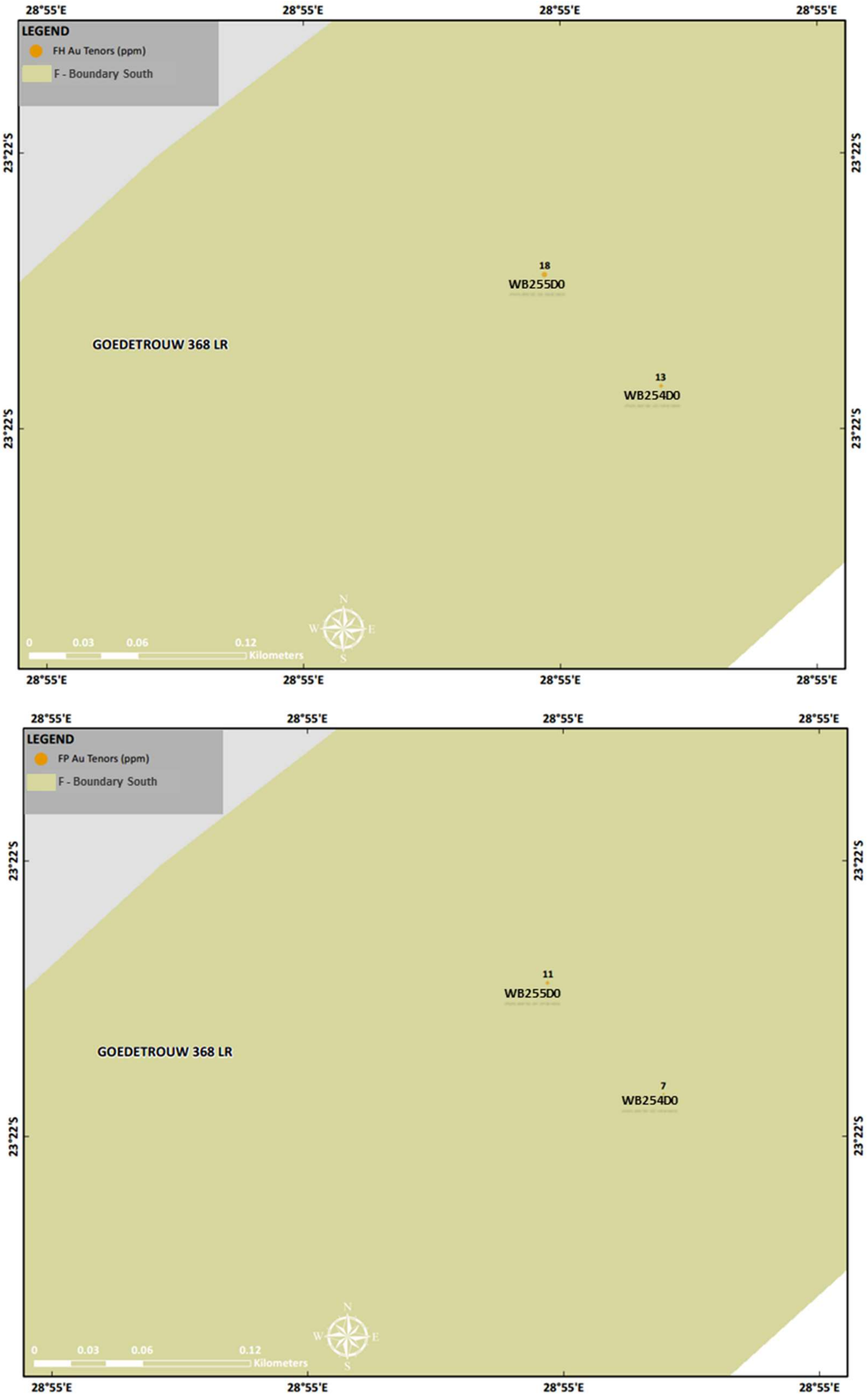

Figure 7.43. Plan section of the F - Boundary South showing lateral Au variations in the FH and FP. The size of the bubble represents the proportional size as per the tenor value (values on top of the bubbles).

7.5.4 The F - Boundary North

The Pd tenors

Unlike the areas of the F - Central and F - Boundary South, the Pd tenors in F - Boundary North (Figure 7.44) seem to be higher to the east (WE061D0) and lower to the west (WE144D0 & WE145D0).

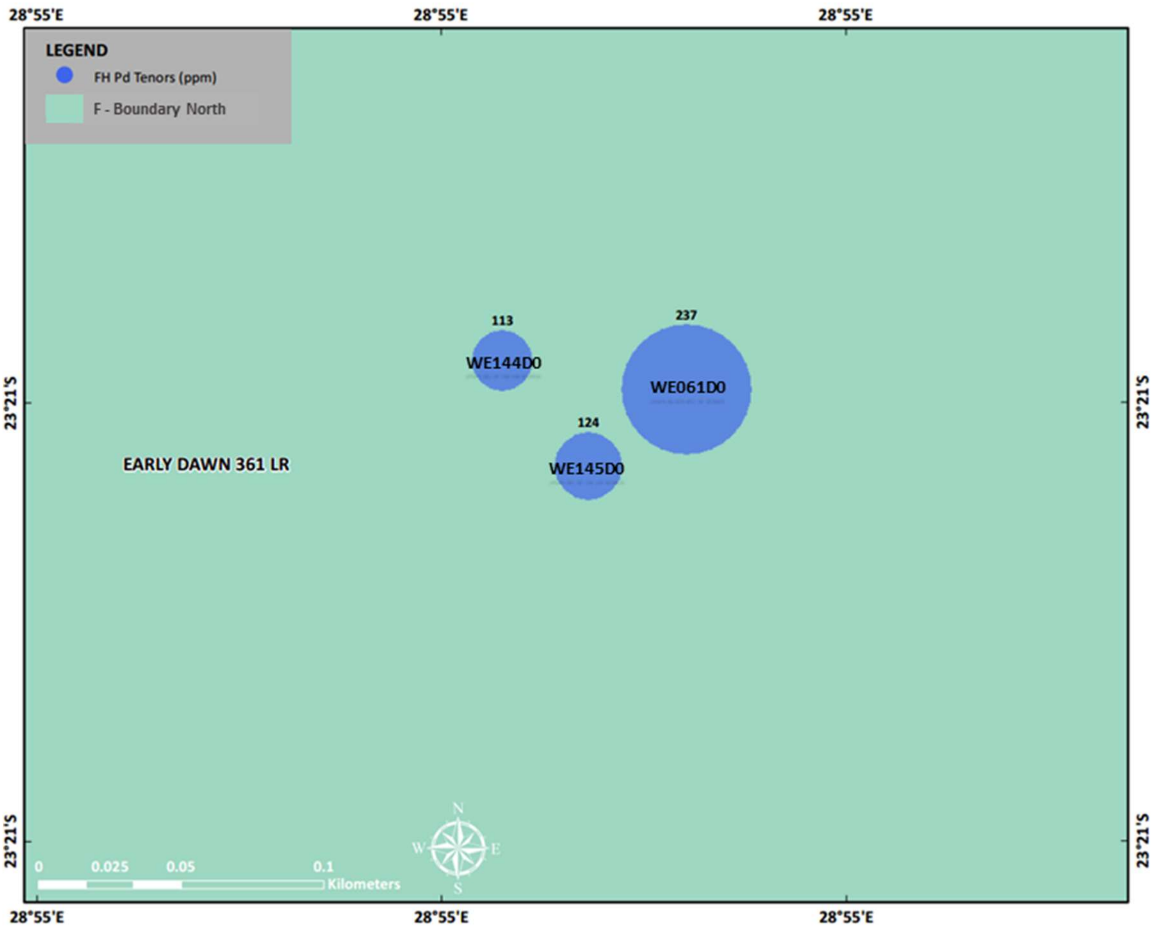

Figure 7.44. Plan section of the F - Boundary North showing lateral Pd variations in the FH. The size of the bubble represents the proportional size as per the tenor value (values on top of the bubbles).

The Pt tenors

As with the Pd tenors, the Pt tenors (Figure 7.45) seem to be higher to the east (WE061D0) and lower to the west (WE144D0 & WE145D0).

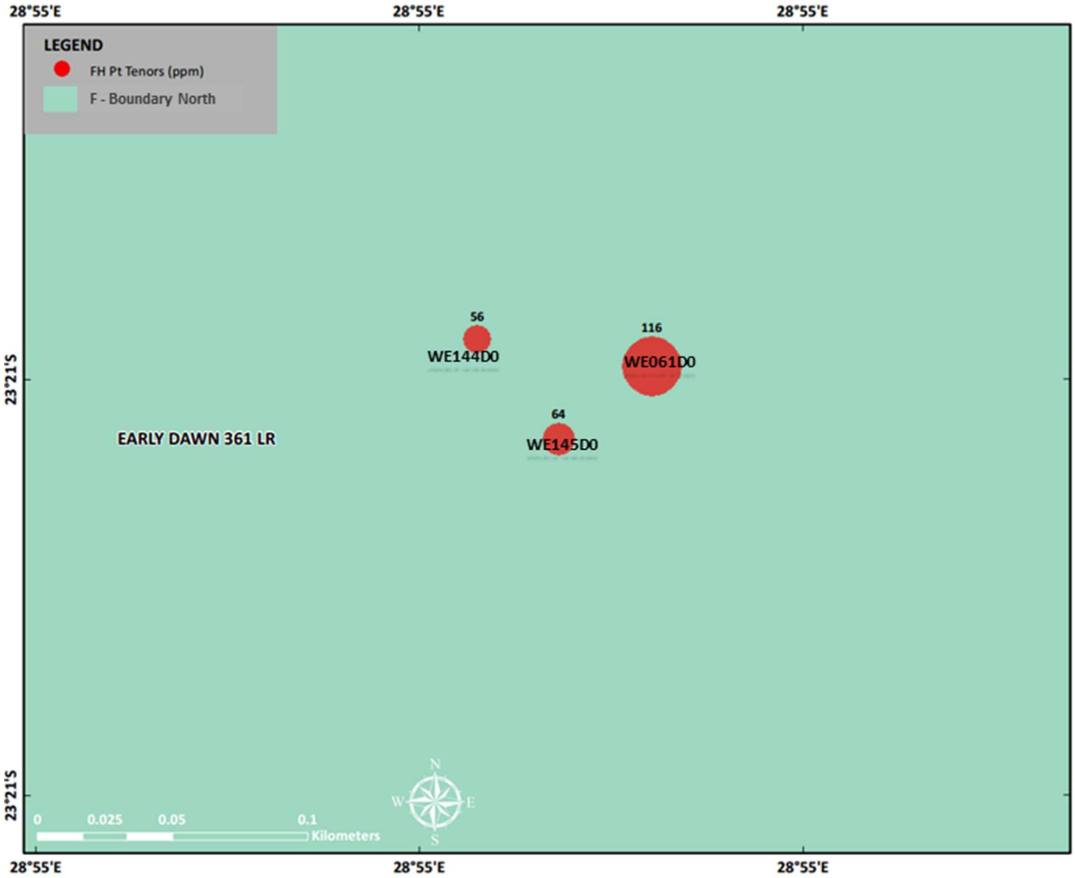

Figure 7.45. Plan section of the F - Boundary North showing lateral Pt variations in the FH. The size of the bubble represents the proportional size as per the tenor value (values on top of the bubbles).

<u>The Au tenors</u>

Au tenors follow a similar trend to that of PGE, with higher tenors to the east (Figure 7.46).

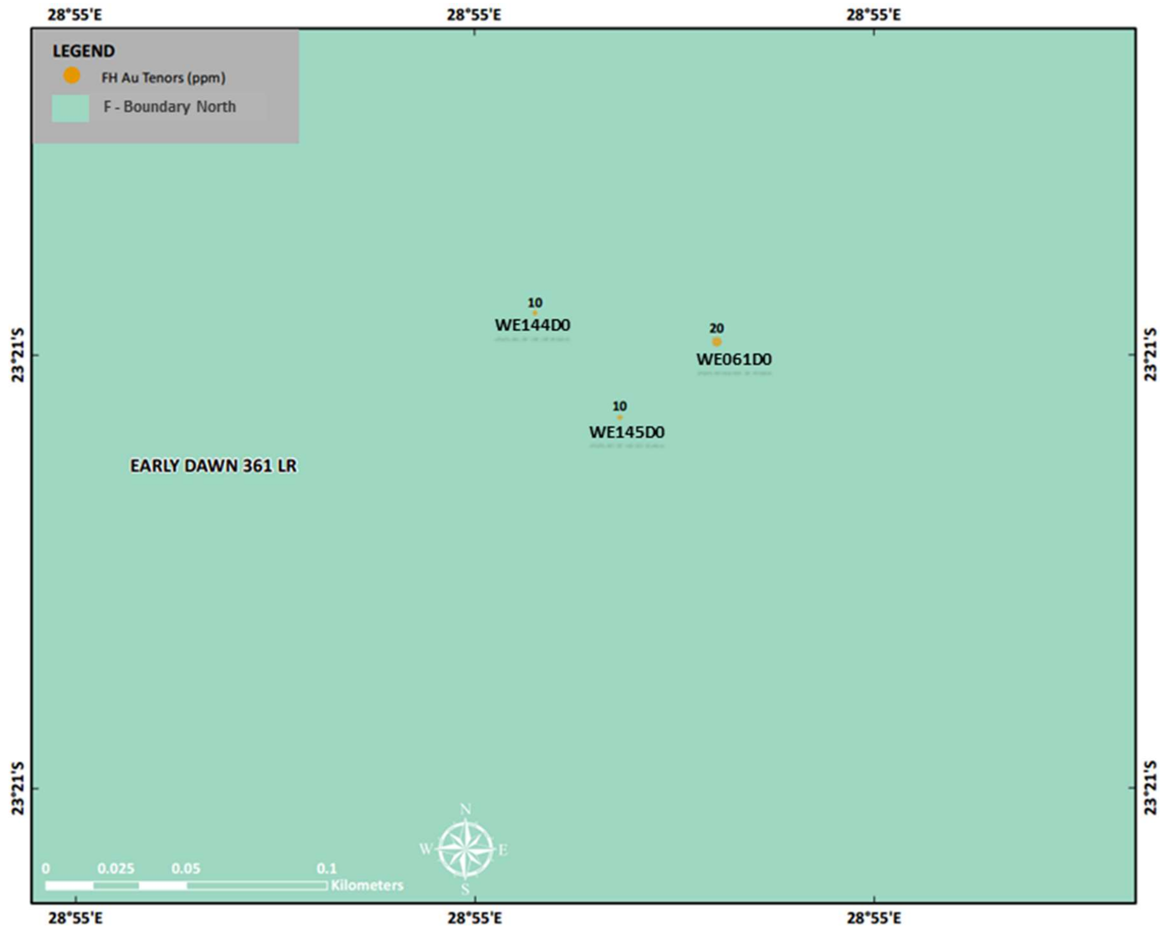

Figure 7.46. Plan section of the F - Boundary North showing lateral Au variations in the FH. The size of the bubble represents the proportional size as per the tenor value (values on top of the bubbles).

7.5.5 <u>The F - North</u>

As illustrated on Figure 7.47, there is a gradual decrease in Pd tenors from west (WE052D0) to east (WE117D0) in the FP of the area of the F-North. Although the trend is not gradual in the FH, there does seem to be a general decrease in tenors from west to east with the lowest tenor in WE117D0. On the strike section, the tenors decrease from NE to SW in both FP and FH.

Pt tenors follow trends similar to those of Pd with a gradual decrease from west to east in the FP (Figure 7.48). Although the trend is not gradual in the FH, there is a general decrease similar to that noted for the FP with the lowest tenor in WE117D0. On the strike section, the tenors decrease from NE to SW in both FP and FH.

Au tenors follow trends similar to those of PGEs with a gradual decrease from west to east in the FP (Figure 7.49). Although the trend is not gradual in the FH, there is a general decrease similar to that of PGEs with the lowest tenor in WE117D0. On the strike section, the tenors decrease from NE to SW in both the FP and FH.

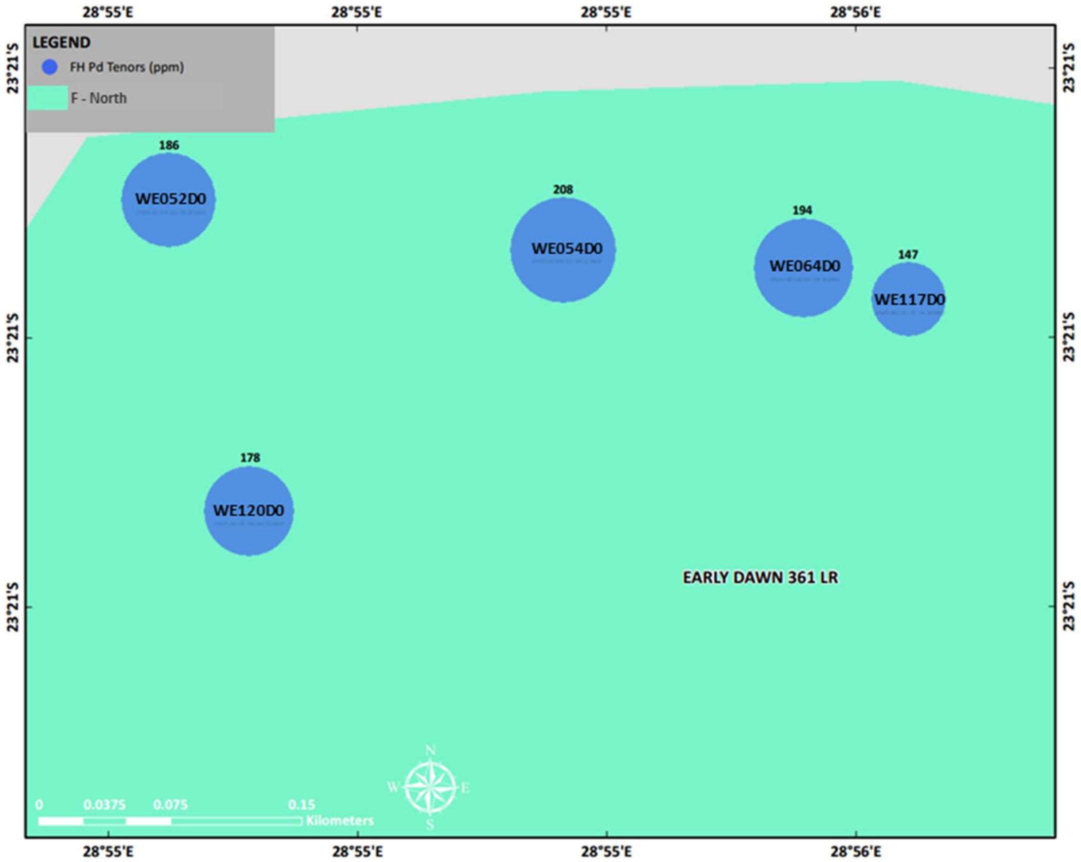

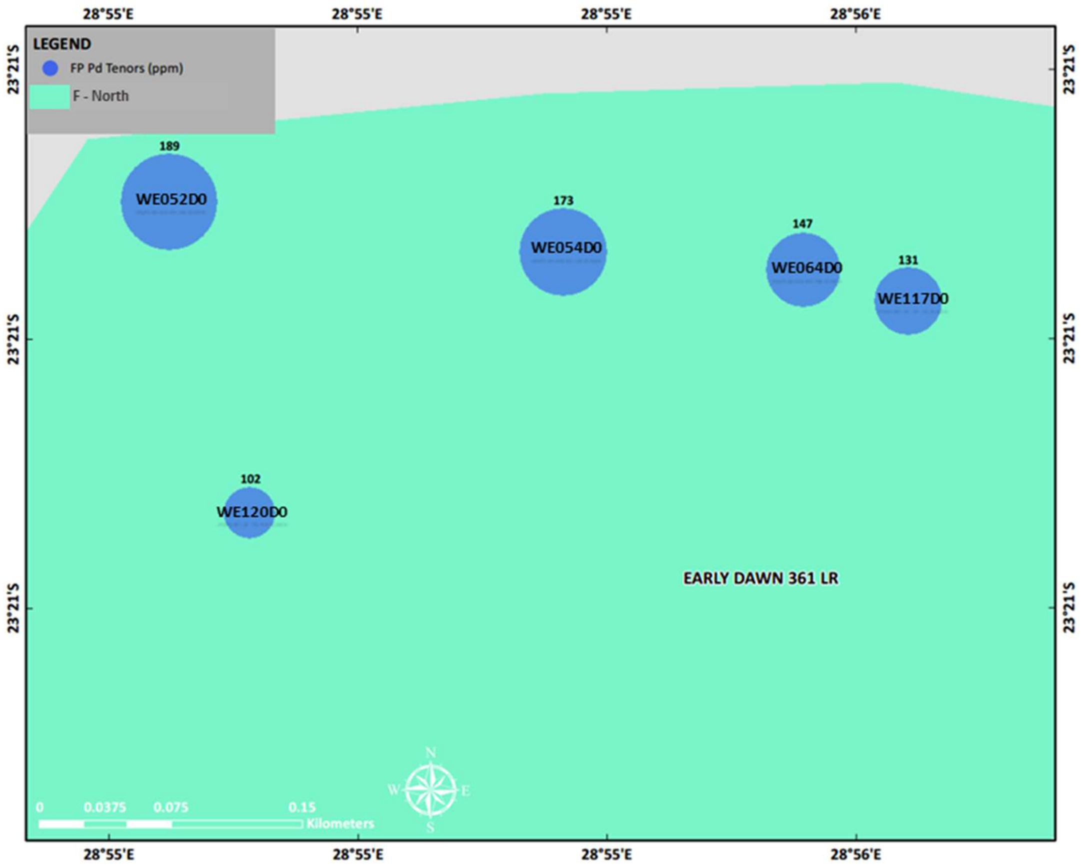

Figure 7.47. Plan section of the F - North showing lateral Pd variations in the FH and FP. The size of the bubble represents the proportional size as per the tenor value (values on top of the bubbles).

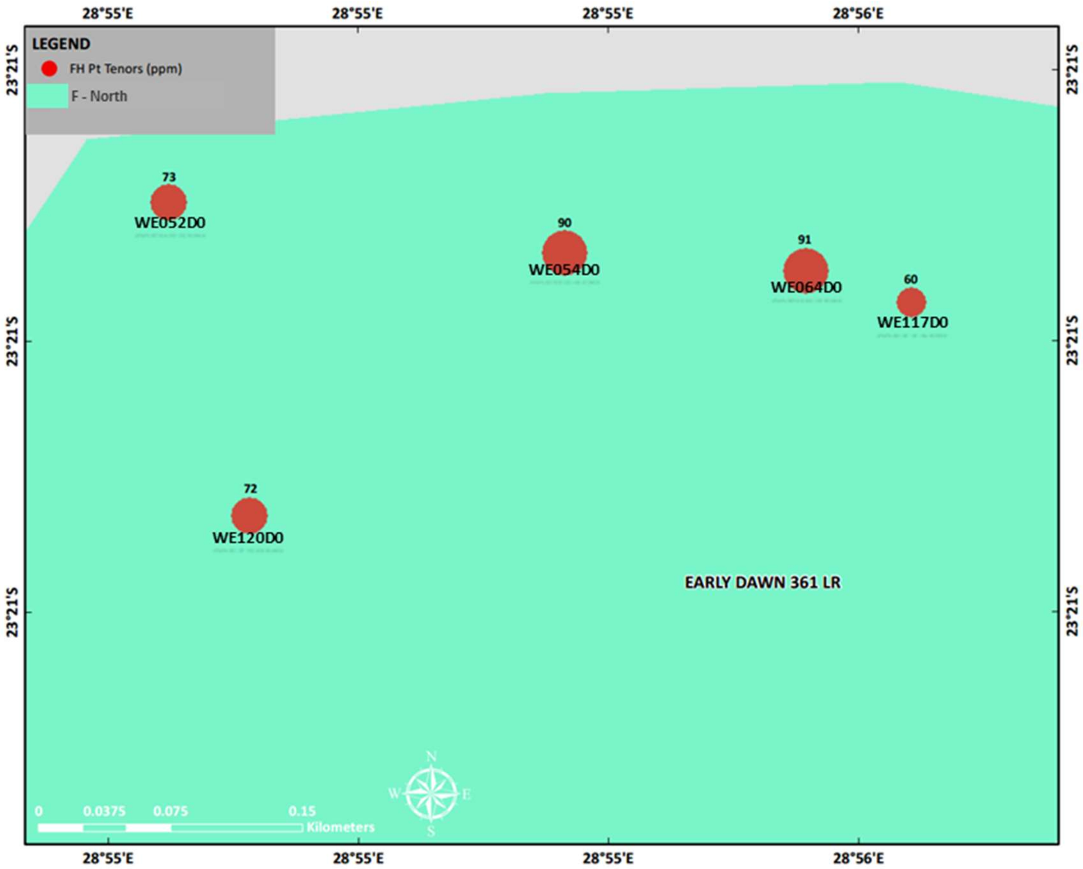

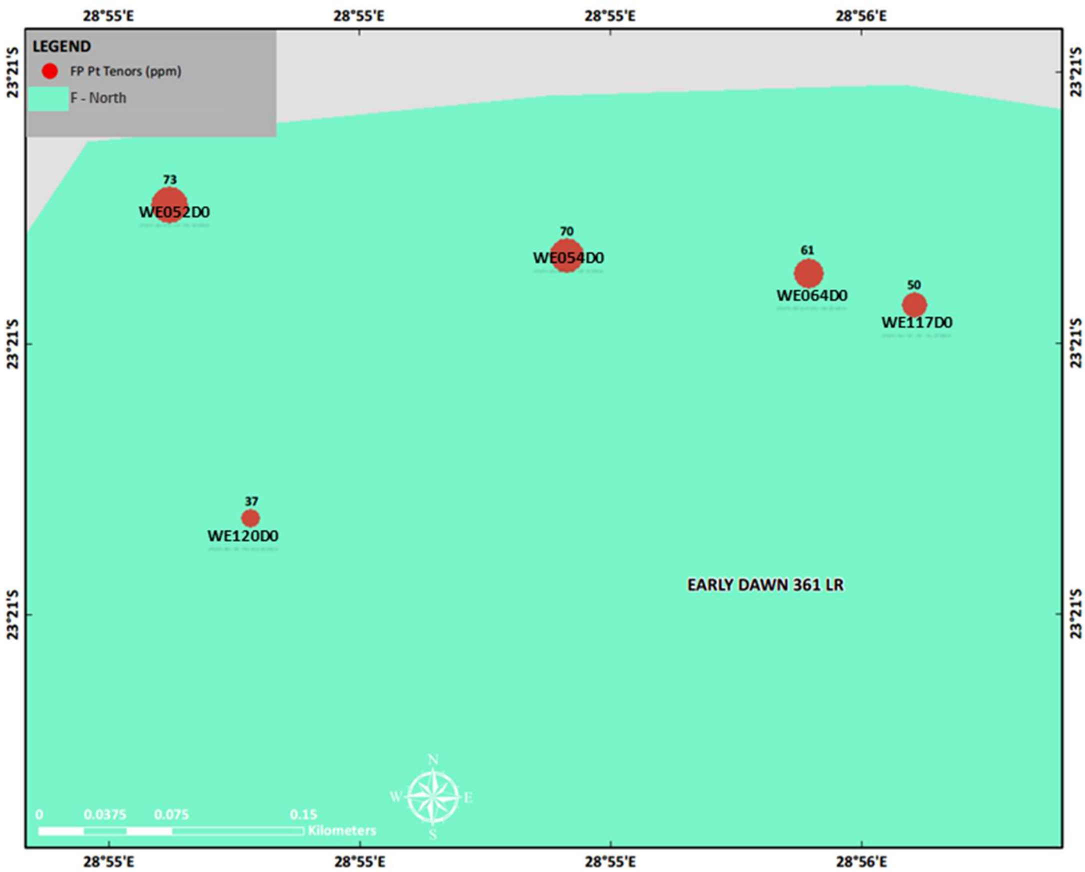

Figure 7.48. Plan section of the F - North showing lateral Pt variations in the FH and FP. The size of the bubble represents the proportional size as per the tenor value (values on top of the bubbles).

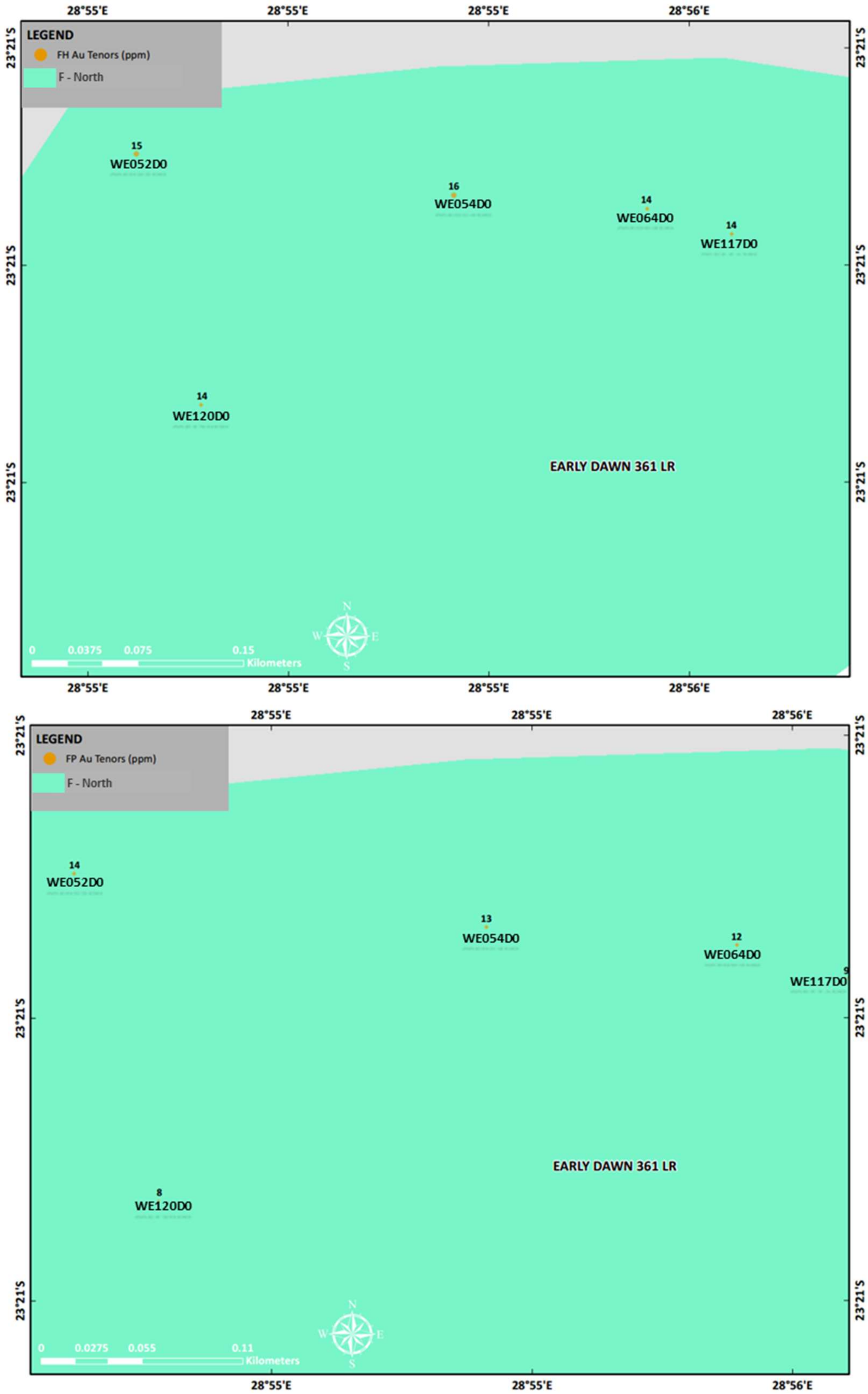

Figure 7.49. Plan section of the F - North showing lateral Au variations in the FH and FP. The size of the bubble represents the proportional size as per the tenor value (values on top of the bubbles).

7.5.6 Discussion of lateral tenor variations

Both the F Zone and the T Zone are characterised by high PGE (Pd and Pt) and Au tenors. The palladium tenors are higher than both the platinum and gold tenors while the platinum tenors are higher than the gold tenors. In both the F Zone and the T Zone, the gold tenors are significantly lower than the PGE tenors. The gold tenors within the T Zone are generally higher than the F Zone gold tenors ranging between 18 ppm - 84 ppm while the F Zone ranges between 7 ppm - 23 ppm. The palladium tenors in the F Zone seem to be higher than those in the T Zone.

In the F Zone, the highest PGE + Au tenors are found in the upper FH with the highest tenors located in the F-Central district. The F-North is also characterised by higher tenors in comparison to the F-Boundary South and F-Boundary North districts. Although the F-North tenors do not show a gradual decrease from west to east, the higher tenors are generally more biased to the west.

In the T Zone, the highest PGE +Au tenors are found in the T2 and the LPA subzones. In the T2 and the T1 subzones, the tenors are higher in the SW gradually decreasing towards the NE. Both the LPA and the UPA subzones do not show any preferential tenor increase/decrease direction. This might be attributed to the possibility that the sulphides and the PGE within these pegmatitic subzones were extensively remobilised

Both the vertical and lateral tenor variations generally suggests that the magma influxes were not stationary but moving from the west/SW towards the east/NE. The sulphides might have exchanged with the flowing magma, as envisaged for the magmatic conduits, resulting in the upward tenor increase.

For the F Zone lateral tenor variations, refer to Appendix 4.

In the following section, lateral variations in Cu/Pd ratios between the subzones of both the F Zone and the T Zone are evaluated and discussed.

7.6 Lateral variations in Cu/Pd ratios

The Cu/Pd ratios are plotted on a plan section with an attempt to evaluate and establish the probable direction of the feeder zone (s). A comparison between the lateral tenor variations and the lateral Cu/Pd variations is to be conducted with the aim of determining whether the two data sets lead to the same conclusion regarding the direction of the feeder zone (s).

The Cu/Pd ratio data for F Zone and T Zone is on Appendix 5.

Variations in Cu/Pd ratios are discussed in the following order: -

T Zone
F - Central
F - Boundary South
F - Boundary North
F - North

For the T Zone, the variations are studied in three units (T2, LPA and T0). It is important to note that the T0 is widely not part of the T Zone but a mineralised area within the Upper Zone (UZ) which migrates on dip and along strike from the UZ to the upper portion of the UPA. Due to a lack of sufficient T1 assay data across both dip and strike sections, no references will be made to this lithostratigraphic subzone during the discussions.

7.6.1 The T Zone

As illustrated in Figure 7.50 by the bubble sizes, there is an increase in Cu/Pd ratios from SW to NE in both the T2 and the LPA. In the T2 subzone, there is an increase in Cu/Pd ratio on the strike section from SW (WB222D1) to NE (WB213D0). The dip section also shows a similar trend with an increase in ratios from west (WB228D0) to east (WB213D0). Where the PGE grade increases/transgresses from the T2 to the LPA, a similar trend can be observed whereby the ratio increase from SW (WB237D0) to NE (WB215D0).

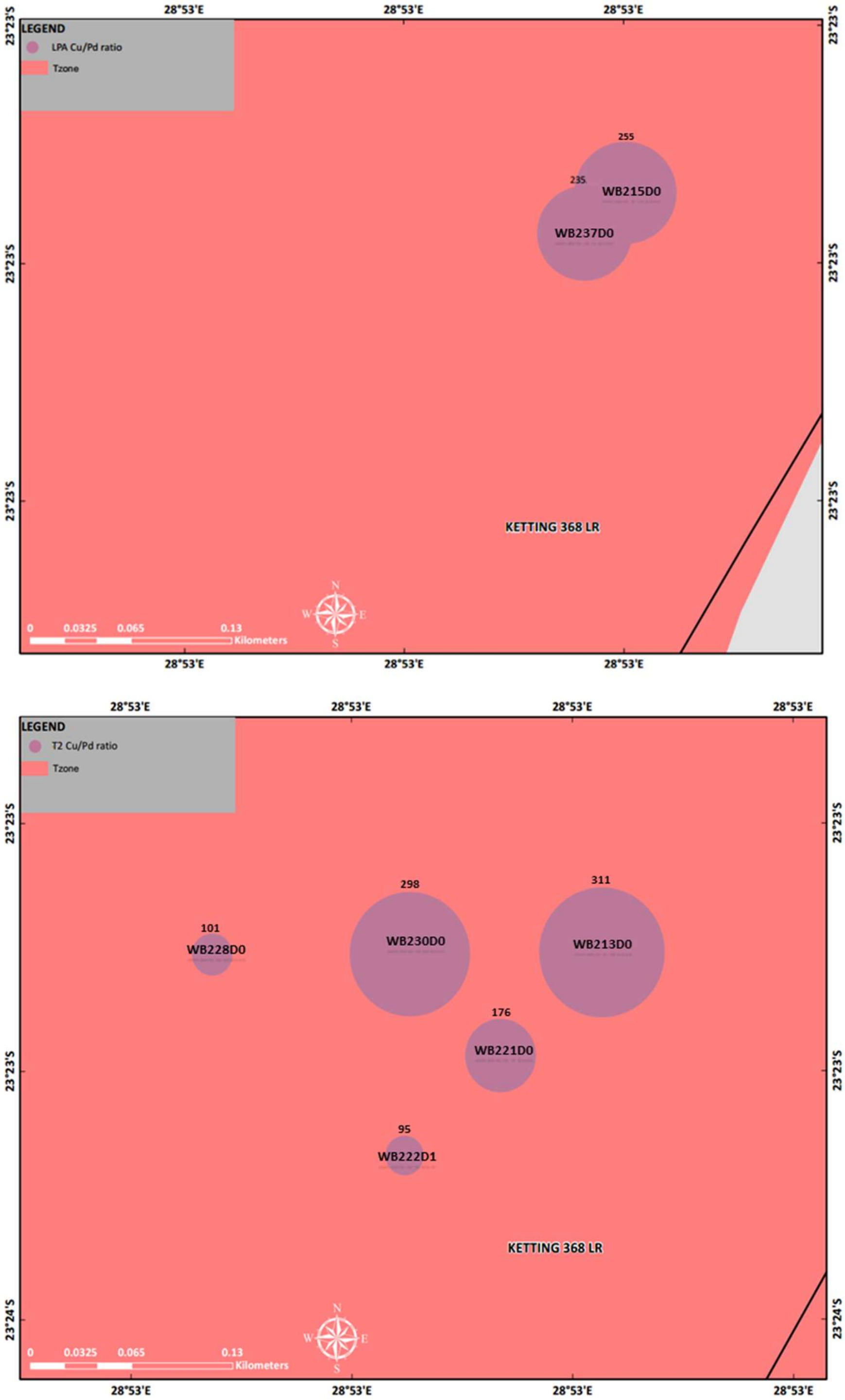

Figure 7.50. Plan sections of the T Zone showing lateral Cu/Pd variations in both the T2 and the LPA. The size of the bubble represents the proportional size as per the Cu/Pd value (values on top of the bubbles).

Generally, the Cu/Pd ratios in the T0 are extremely variable and higher than those of the T Zone (Figure 7.51).

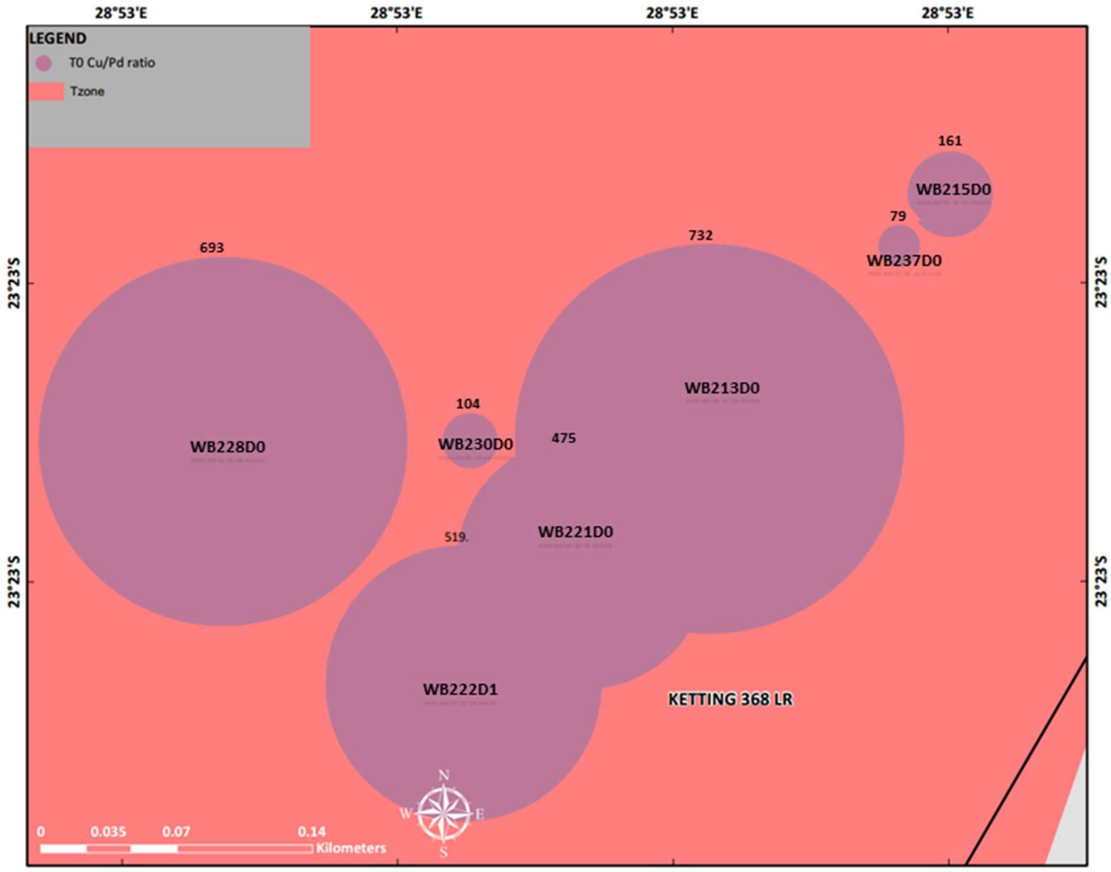

Figure 7.51. Plan section showing Cu/Pd variations in the T0. The size of the bubble represents the proportional size as per the Cu/Pd value (values on top of the bubbles).

7.6.2 <u>The F - Central</u>

In comparison to the T Zone, there is a significantly lower Cu/Pd ratio in both the FP and FH (Figure 7.52). The FP has a slightly lower ratio in comparison to the FH. The variable ratios in both FH and FP do not show any gradual increase towards a preferred direction.

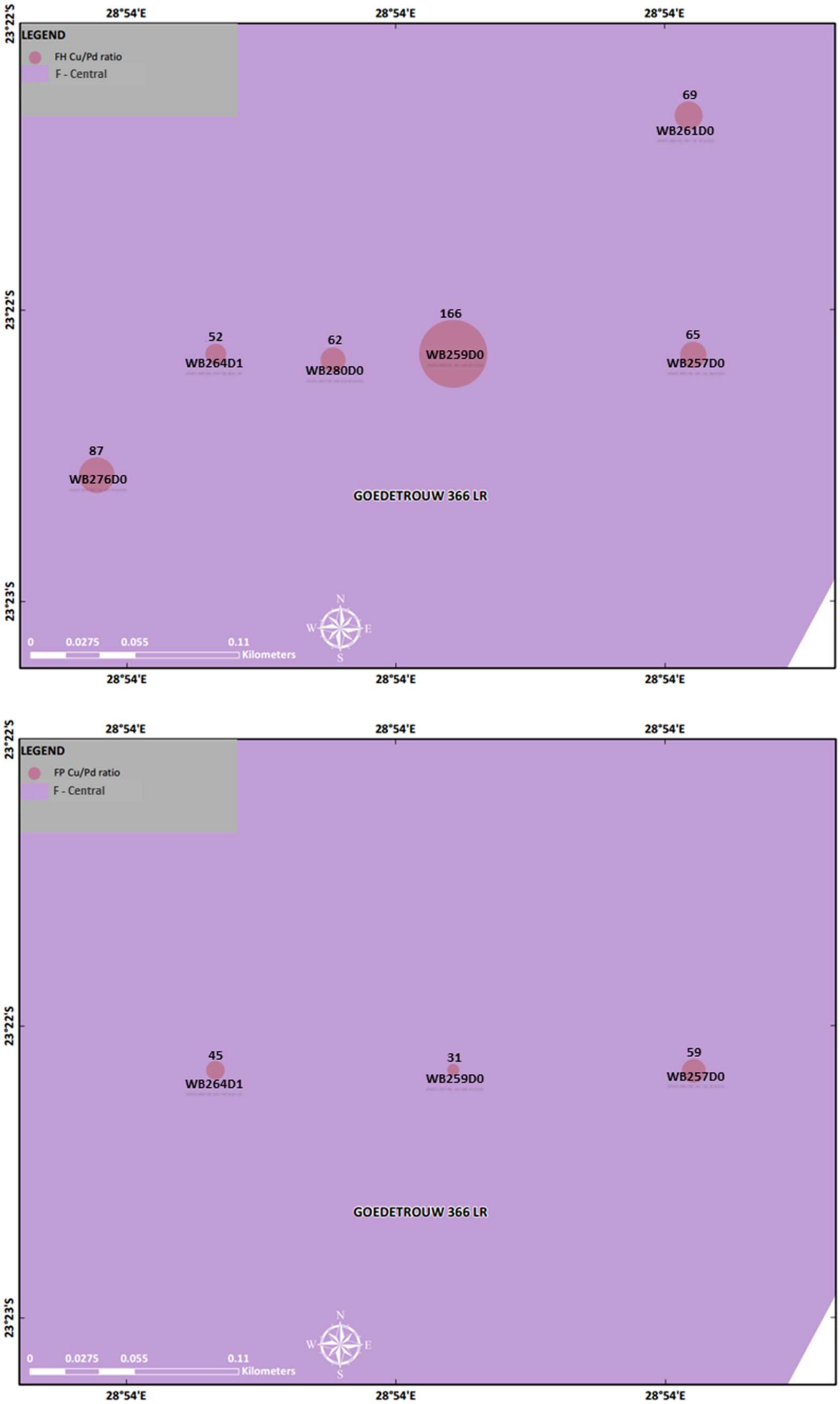

Figure 7.52 Plan sections of the F - Central showing the FP and FH lateral Cu/Pd variations. The size of the bubble represents the proportional size as per the Cu/Pd value (values on top of the bubbles).

7.6.3 The F - Boundary South

As illustrated in Figure 7.53 by the bubble sizes, there is an increase in Cu/Pd ratios from NW (WB255D0 to SE (WB254D0) in both the FP and FH. Similar to the F-Central, the Cu/Pd ratios are less in the FP in comparison to FH.

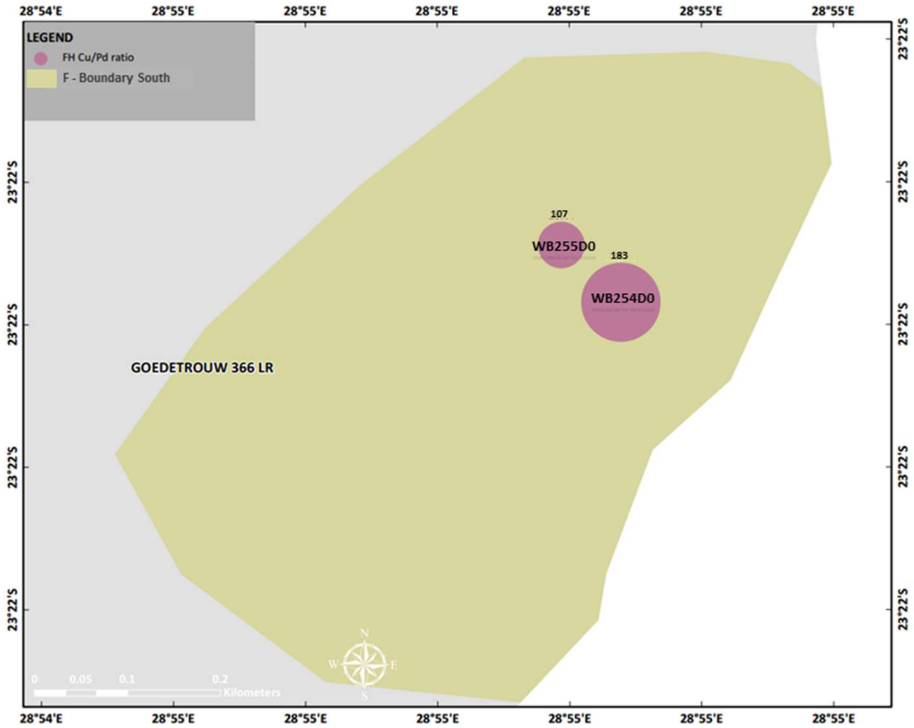

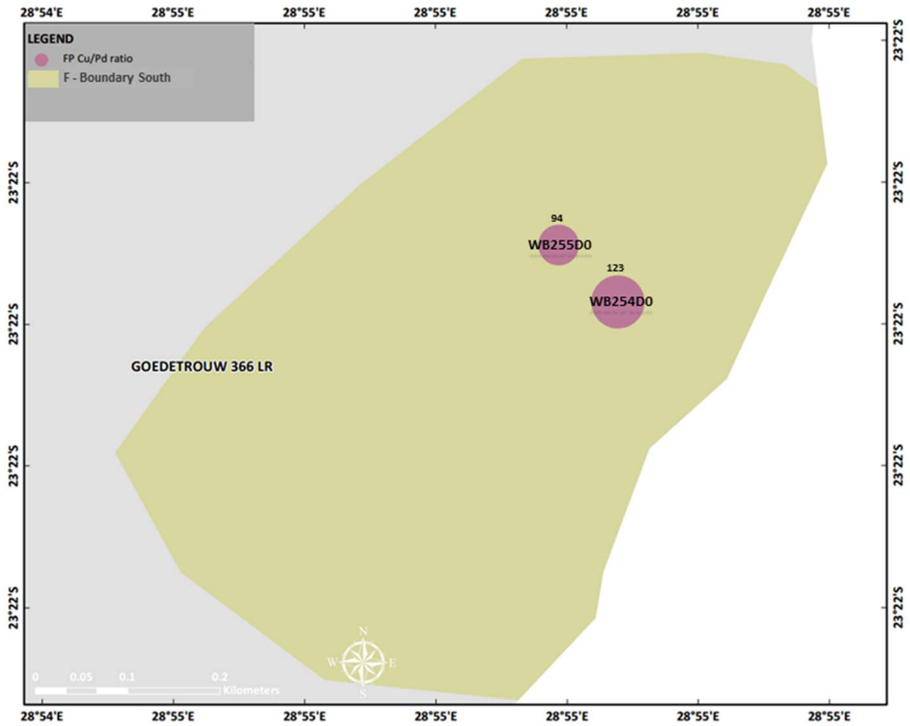

Figure 7.53. Plan sections of the F - Boundary South showing the FP and FH lateral Cu/Pd variations. The size of the bubble represents the proportional size as per the Cu/Pd value (values on top of the bubbles).

7.6.4 The F - Boundary North

Cu/Pd ratios are variable (Figure 7.54). From WE145D0, there is an increase in ratio to both the NE and NW direction. There is also an increase in the ratio from east (WE061D0) to west (WE144D0).

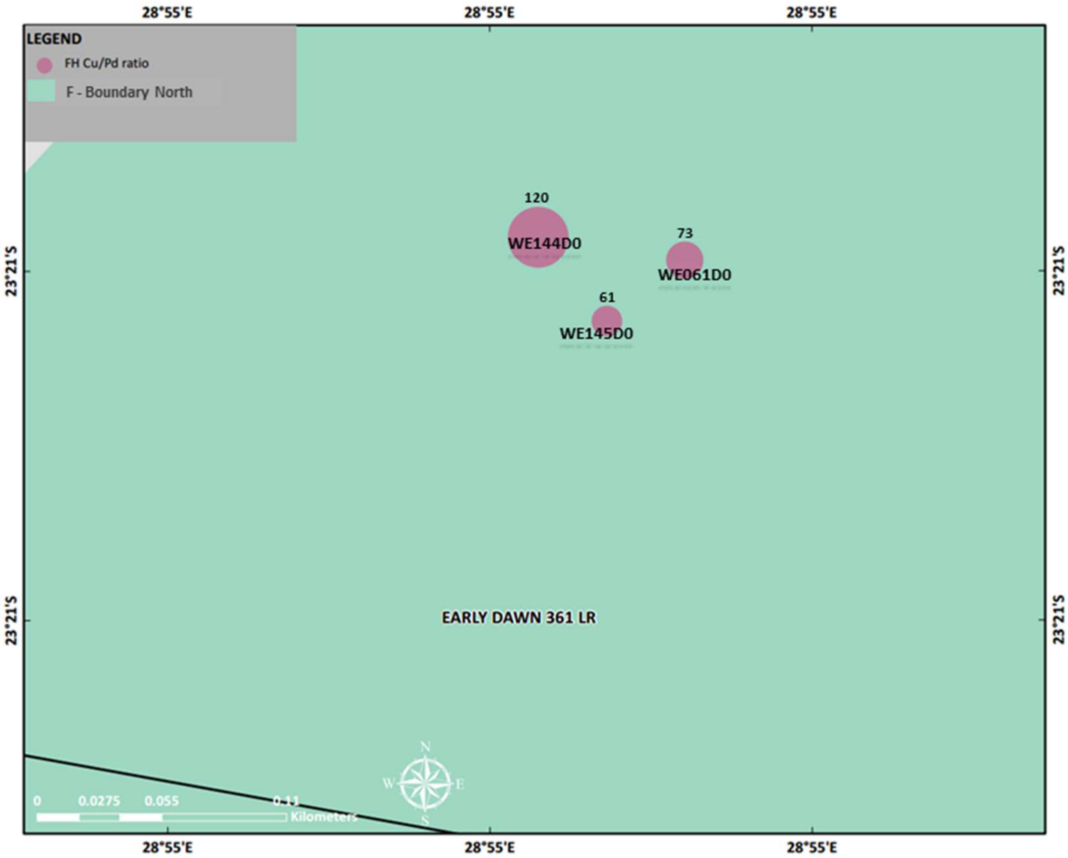

Figure 7.54. Plan section of the F - Boundary North showing the FH lateral Cu/Pd variations. The size of the bubble represents the proportional size as per the Cu/Pd value (values on top of the bubbles).

7.6.5 The F - North

Unlike all the other F Zones, the Cu/Pd ratios are higher in the FP compared to the FH (Figure 7.55). Although there is a lack of gradual increase/decrease in ratios from borehole to borehole, there seem to be higher ratios to the east (in both FH & FP) in comparison to the west.

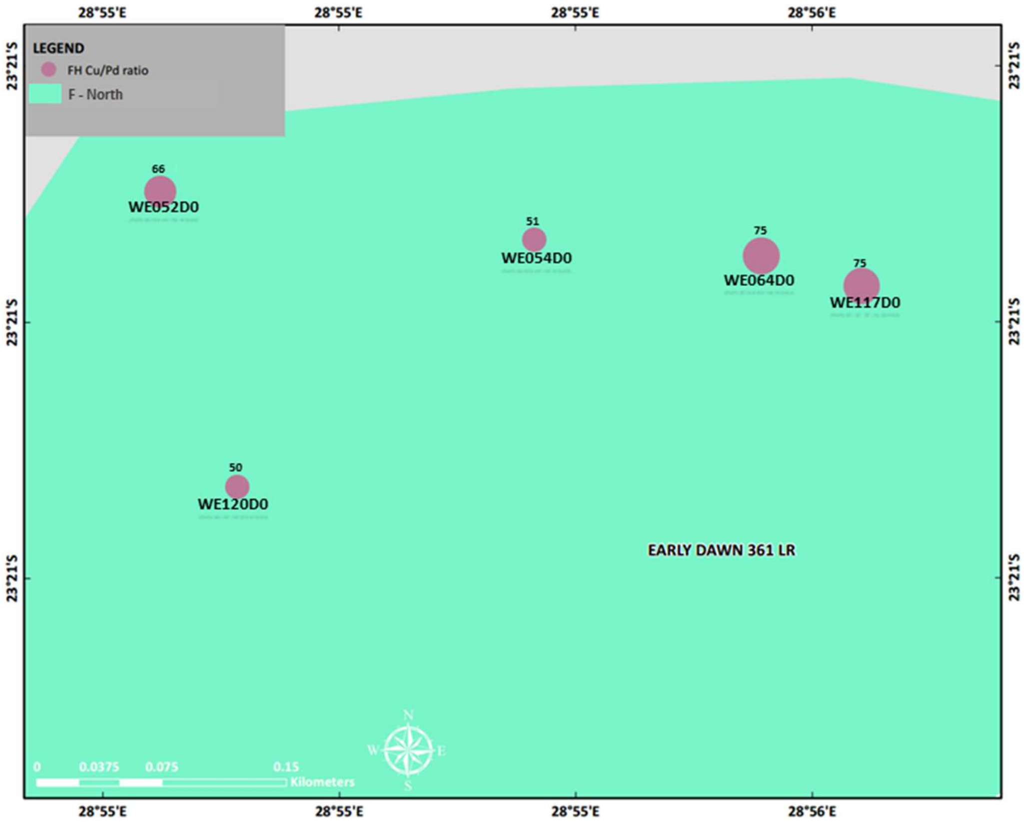

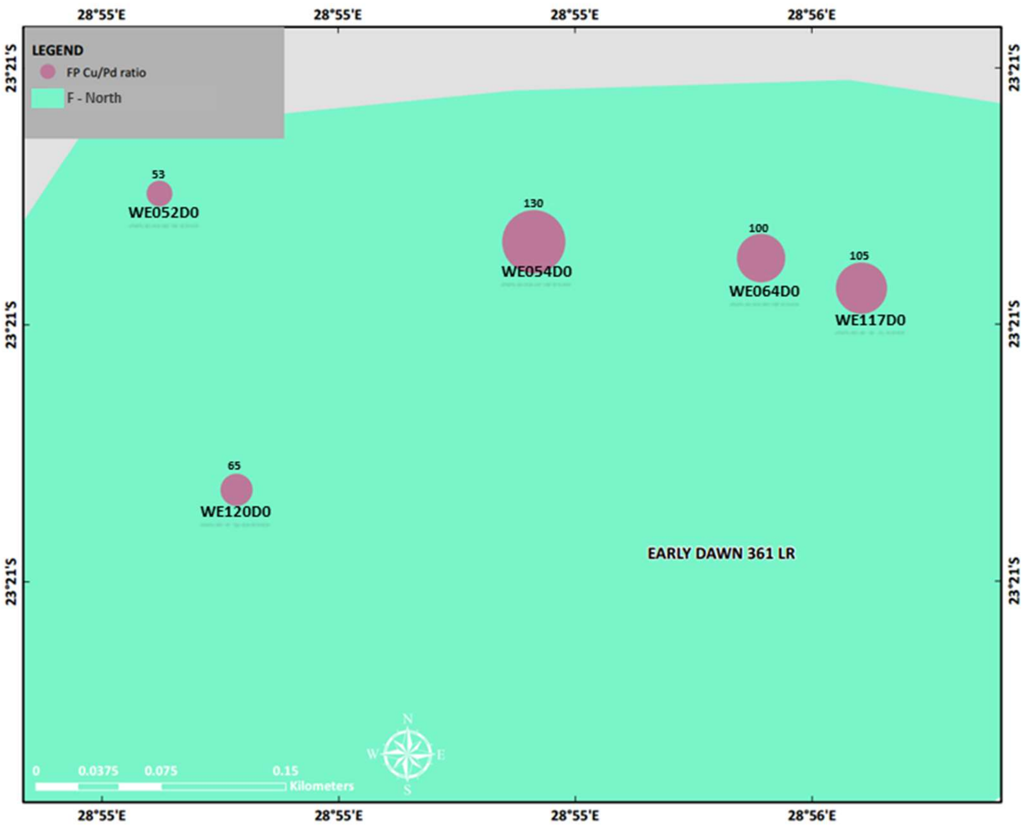

Figure 7.55. Plan sections of the F - North showing the FH and the FP lateral Cu/Pd variations. The size of the bubble represents the proportional size as per the Cu/Pd value (values on top of the bubbles).

7.6.6 Discussion of Cu/Pd ratios

The F-Central and the F-Boundary South are characterised by very low Cu/Pd ratios in the lower FP with slightly elevated ratios in the upper FH. In the F-North, the Cu/Pd ratios in the lower FP are slightly higher in comparison to those of the upper FH. In general, the F Zone is characterised by very low Cu/Pd ratios of between 31 and 166. These low ratios are associated with very good PGE mineralisation of >2.5g/t. Generally, the F Zone is further characterised by lower ratios to the west and higher ratio to the east.

The Cu/Pd ratios of the T Zone are higher than those of the F Zone ranging from 95 to 311. In the T2 and the LPA, the ratios show a gradual increase from the west/SW to the east/NE.

The highest Cu/Pd ratios ranging from 79 to 732 are associated with the sporadically mineralised and at times low grade T0. The T0 is largely not part of the T Zone but a mineralised area within the Upper Zone (UZ) which migrates on dip and along strike from the UZ to the upper portion of the UPA

Both the lower F Zone and the T Zone are characterised by very low Cu/Pd ratios implying that they crystallised from un-depleted magma that streamed through the conduit. The lower Cu/Pd ratios in the west/SW and the higher ratios in the east/NE might suggest that the magma streamed from west/SW to east/NE. This magma streaming direction suggested by the lateral variations in Cu/Pd ratios is similar to that suggested by the lateral variations in tenors.

CHAPTER 8

DISCUSSION

8.1 Introduction

In order to understand the geology and the mineralisation controls in the mafic-ultramafic sequence of the Waterberg Project, several drillholes were selected across the T Zone to the south, the F-Central, the F-Boundary South, the F-Boundary North and the F-North complexes. The drillholes were logged by identifying different rock types and their respective stratigraphic zones. The mineralised intervals defined by the presence of conspicuous disseminated, blebby, net-textured and at times semi-massive sulphides were identified (the lower F Zone, the T Zone and the T0). Samples from the F Zone and the T Zone were collected, cut and prepared into thin sections for petrographic evaluation. For geochemical analysis, samples were collected across the mineralised zones and submitted to the lab for PGE (Pd, Pt) + Au analysis. The samples were also analysed for base metal content such as Cu, Ni and Cr. The geochemical assay results were matched to their respective lithostratigraphic logs for evaluation. In order to understand and project the continuity of the mineralisation, cross sections along the dip and the strike sections were drawn for the districts (excluding F-Boundary North).

To further understand the mineralisation controls and the probable feeder zones for the magma influxes, the assay results for the respective drillholes were used to calculate PGE tenors. The PGE tenors were calculated to provide an insight as to whether the F Zone and the T Zone magma influxes were already enriched in PGE sulphides when entering the magma chamber or whether the sulphides gained their tenors in situ as a result of fractional sulphide segregation from a body of magma resulting in the PGEs becoming more rapidly depleted than the base metals. Both the lateral variations in tenors and Cu/Pd ratios were used to determine whether the magma was stationary or moving along a conduit and to further determine the direction of the possible feeder zone.

The Waterberg Project is further compared to the Harriet's Wish Project, the Aurora Project and the Platreef to establish whether the are some similarities in the lithostratigraphy and mineralisation. Both the Waterberg Project and the Harriet's Wish Project are to the north of the Hout River Shear Zone while the Platreef and the Aurora Project are located to the South of the Hout River Shear Zone.

8.2 The Waterberg Project, Harriet's Wish, Aurora and the Platreef

8.2.1 <u>Lithostratigraphic comparisons</u>

There are some slight similarities between the mineralised F Zone of the UmS on the Waterberg Project and the lower mineralised unit on Harriet's Wish and to the basal contact-style Platreef mineralisation (Figure 8.1). According to van Scheltema (2019), there is evidence in the lower lithologic unit (LLU) on Harriet's Wish indicating that some earlier ultramafic cumulates might have been digested by later gabbroic melts. The LLU shows some similarities with the mineralised Unit 1 gabbronorite of the Aurora Project that apparently eroded pyroxenite.

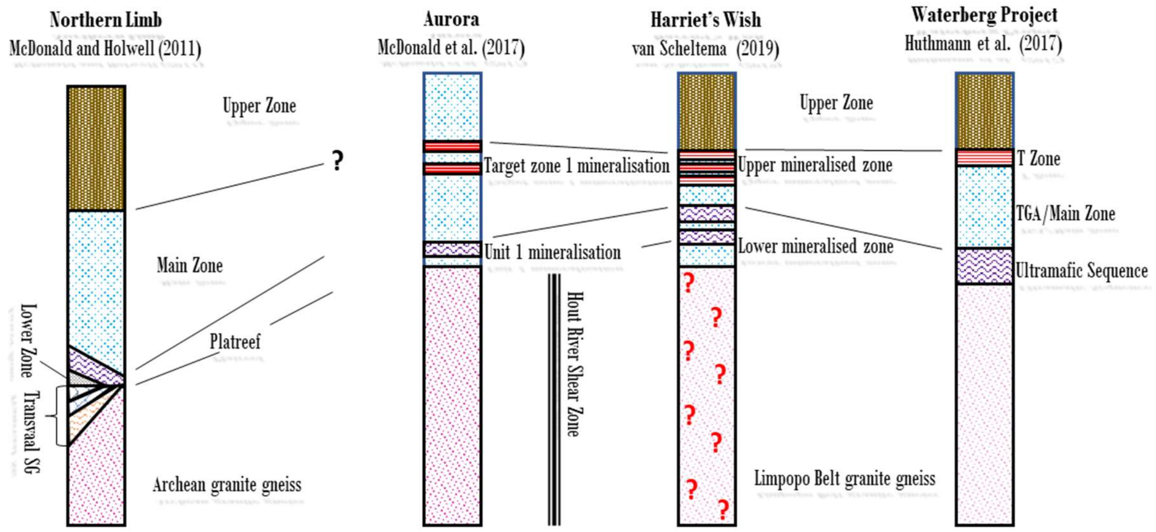

Figure 8.1. Stratigraphic comparisons between the Waterberg Project, Harriet's Wish, Aurora and the northern limb (modified after van Scheltema, 2019).

Although van Scheltema (2019) suggested that there is no strong ground for a definitive correlation of mineralisation between the Platreef, Aurora, and Harriet's Wish and the Waterberg Project, there seem to be some degree of correlation between the FP of the Waterberg Project, the LLU of the Harriet's Wish and the Unit 1 mineralisation of the Aurora Project. All these units are comprised of well mineralised feldspathic pyroxenite, gabbronorite and occasional leucogabbronorite. Although the stratigraphic position of the three units are different (basal FP, stratigraphically higher LLU and slightly higher Unit 1 mineralisation), these differences may be attributed to the basement morphology (basement highs and lows) and some pre-existing structures within the earlier gabbroic rocks (Figure 8.2).

Therefore, the basal part of the Waterberg Project sequence (that is the Ultramafic Sequence or UmS) is analogous to the lower lithologic unit of the Harriet's Wish and Aurora Project (McDonald et al., 2017; Huthmann et al., 2018; McCreesh et al., 2018; van Scheltema, 2019). The Upper Zone is analogous to the upper lithologic unit (ULU) at Harriet's Wish (van Scheltema, 2019).

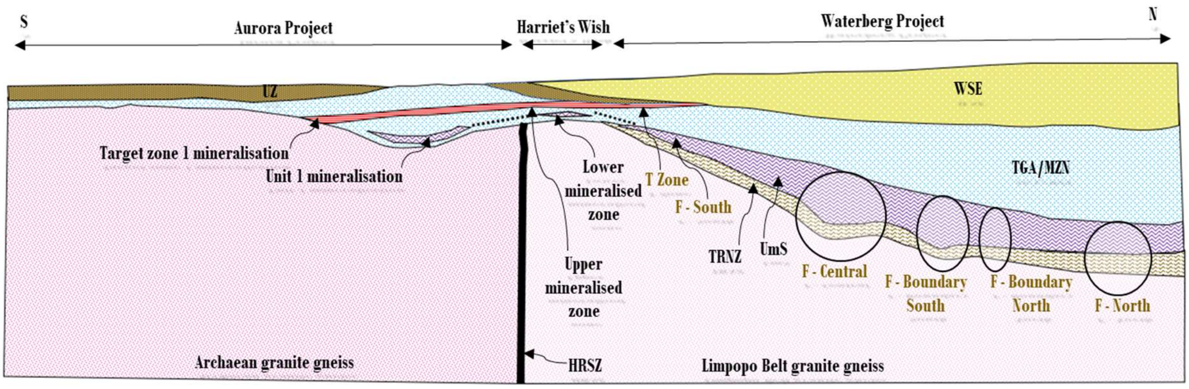

Figure 8.2. A schematic diagram showing the relationship between the Waterberg Project, Aurora and Harriet's Wish mineralisation. The dotted lines are inferred links between the bottom mineralisation (modified after McDonald et al., 2017).

The T Zone mineralisation of the Waterberg Project is geochemically analogous to the upper mineralisation at Harriet's Wish and the Target zone 1 mineralisation on the Aurora Project (McDonald et al., 2017; van Scheltema, 2019). As initially suggested by Kinnaird et al. (2017) and McDonald et al. (2017), both Harriet's Wish and Aurora are distal and far distal facies of the T Zone, respectively. Figure 8.2 demonstrates the relationship between the mineralisation of the Waterberg Project, Aurora and Harriet's Wish.

The T Zone of the Waterberg Project, the mineralisation of Harriet's Wish and the Aurora Project differ significantly to the Platreef mineralisation in both metal percentage split and stratigraphic position. Mineralisation of the T Zone, Harriet's Wish and Aurora Project corresponds to the boundary between the TGA/Main Zone and the Upper Zone while the stratigraphic position of the Platreef corresponds to the Critical Zone below the Main Zone (Grobler et al., 2018).

There are definitive differences in the lithostratigraphy, chemostratigraphy and petrology across the Hout River Shear Zone (HRSZ) supporting the idea that separate sub-chambers exist for mineralisation south and north of the HRSZ (Huthmann et al., 2016, Kinnaird et al., 2017).

Recent work by McFall et al. (2019) suggests that mineralisation of Aurora is similar to that of the T Zone and fundamentally different to that of the F Zone in both the host rock and mineralisation. McFall et al. (2019) further asserted that the T Zone and Aurora reflect the same fluid-controlled processes operating in different times, different structural basins and different parts of the Main Zone.

As illustrated on Figure 8.3, there is some variability in the morphology and the distribution of mineralisation within the four UmS districts. The F - Central is characterised by a well-defined embayment with FH dominated by FP xenoliths towards the basal contact. Higher and thicker PGE+Au mineralisation within the F - Central is predominantly in the FH. The F - Boundary South is characterised by a less-developed embayment with minor FP xenoliths. PGE+Au mineralisation predominantly enriches the FH as compared to the FP. Although the F - Boundary North is not characterised by an embayment with xenoliths, PGE+Au mineralisation is also more biased towards the FH. Within the F - North, emplacement of TRNZ (marginal pyroxenite), FP and subsequent FH seem to have taken place on a flat terrain with FH devoid of FP xenoliths. Unlike the three districts (F - Central, F - Boundary South and F - Boundary North), PGE+Au mineralisation within F - North is well developed within FP.

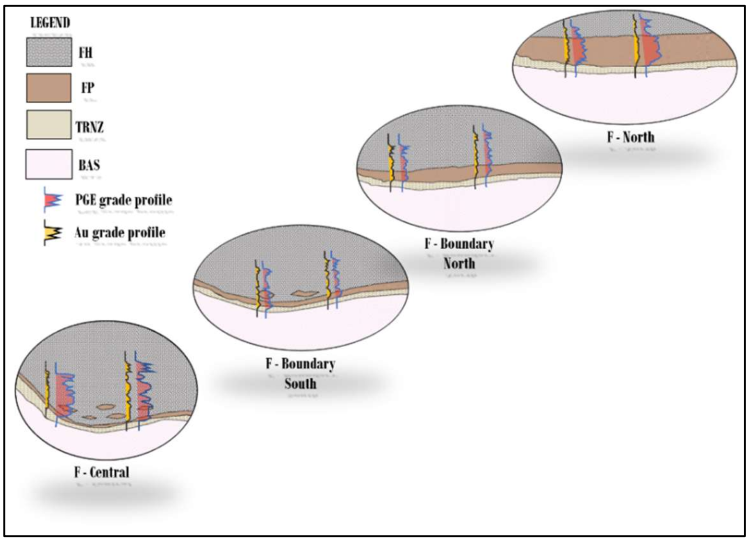

Figure 8.3. A schematic diagram showing different morphological and mineralisation attributes within the F - Central, F - Boundary South, F - Boundary North and F - North.

8.3 The genesis model for the Waterberg Project

An origin of the PGE mineralisation and the emplacement of the igneous succession was initially proposed by Kinnaird et al. (2017) and Huthmann et al. (2018). The work was further expanded by McCreesh et al. (2018).

According to the provisional genesis model (Figure 8.4) by McCreesh et al. (2018): -

The initial emplacement of the 2.05 Ga (Huthmann et al., 2016) igneous succession started with the intrusion of marginal orthopyroxenite, norite sills and gabbronorite into the basement granite gneiss. The pre-existing geological anisotropies within the basement played a pivotal role in defining the chonolithic morphology of the mafic and ultramafic bodies. Upon intrusion, the pyroxenitic magma melted and intermingled with the granite gneiss resulting in the formation of an agmatite breccia commonly known as granofels.

Continuous influxes of ultramafic magmas progressed in carving out pathway channels through thermo-mechanical erosion under lateral dilation thus forming floor embayments. The earlier influxes of ultramafic magmas crystallised a well mineralised feldspathic pyroxenite (FP) while the later influxes crystallised a well mineralised feldspathic harzburgite (FH). The presence of abundant xenoliths of mineralised feldspathic pyroxenite and orthopyroxene oikocrysts within feldspathic harzburgite is indicative of entrainment and resorption during the emplacement process. According to Naldrett (2010), an effective mechanism for sulphide-droplet concentration during magma emplacement is through continuous propagation of magma through chonoliths resulting in the formation of thicker and higher-grade ore zones. Following the emplacement of channelised ultramafic melt, continuous influxes of troctolitic magma exploited the pre-existing anisotropies to form laterally extensive sheet-like bodies.

The initial influx of the Mg-rich magma intermingled with the ultramafic melts in the floor of the basement embayments resulting in the formation of a basal melanocratic troctolite. The melanocratic troctolite grades upwards into mesocratic troctolite, leucocratic troctolite, olivine gabbronorite, gabbronorite and anorthosite of the TGA. The formation of the fractionated voluminous TGA might have been aided by floor depression and roof uplift prior to and during emplacement.

Prolonged TGA fractionation was most likely a key factor in the development of the T Zone due to incompatible elements such as S, Pd, Pt, Cu and Au becoming enriched in the residual melt and precipitated at the top of the sequence. The first appearance of cumulus magnetite within the upper part of the TGA is indicative of the first influx of Upper Zone magma. Sulphide saturation and exsolution of T2 sulphides might have been triggered by intermingling between the TGA residues and the Upper Zone melt with magnetite on the liquidus. The prominent T1 harzburgite above the LPA, which at times transgresses onto T2, is a manifestation of an influx of olivine saturated magma. The highly conspicuous pegmatitic texture above and below the T1 (UPA & LPA, respectively) is indicative of re-melting and prolonged cooling of the anorthosites. Although geochemically different, the metal percentage split in both T1 and T2 is similar. However, the T1 mineralisation is sporadic and at times barren in certain localities of the project. The T1 may have entrained and resorbed PGE-rich sulphides from both T2 gabbronorites and the anorthosites during emplacement. The voluminous Upper Zone above the T Zone was formed by new influxes of new evolved melts.

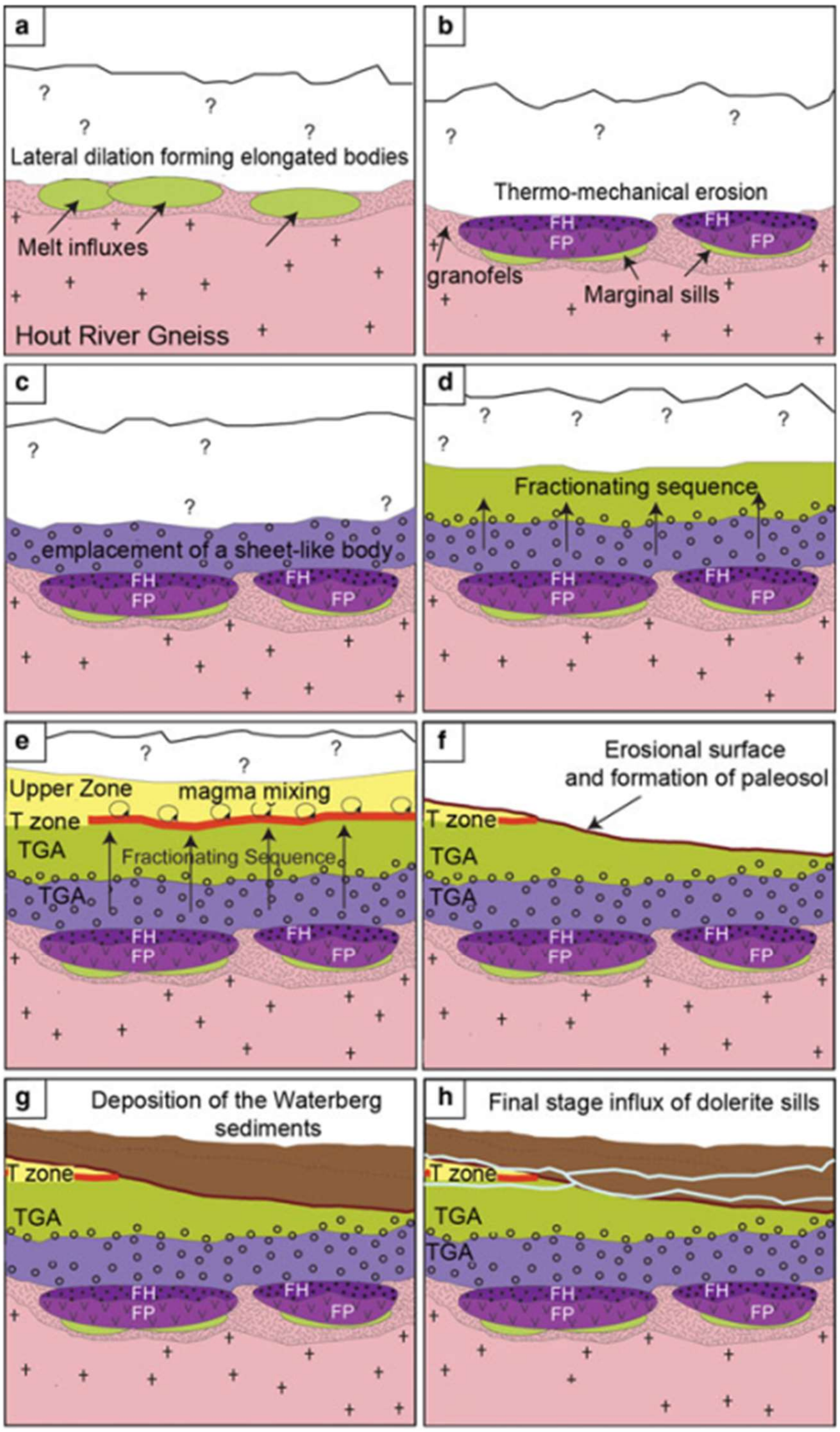

Figure 8.4. A conceptual genesis model for the magmatic mafic-ultramafic succession of the Waterberg Project including mineralisation, complete erosion of the unknown roof rocks accompanied by partial erosion of the Bushveld Complex, deposition of the Waterberg Group sedimentary succession and intrusion of younger sills and dykes (McCreesh et al., 2018).

Crystallisation of the Upper Zone was subsequently followed by an uplift, total erosion of the possible Bushveld volcanic roof rocks, partial erosion of the upper parts of the mafic-ultramafic rocks and the formation of paleosol.

Subsequent to the erosional event, Waterberg sediments were deposited onto the weathered surface by both fluvial (Setlaole Formation) and aeolian (Makgabeng Formation) processes.

According to Huthmann et al. (2016), the thick sill (> 50 m) within the Waterberg Group sedimentary succession is younger than the Bushveld Complex. In some places, especially in the F – Central, the sill transgresses from the Waterberg Group sedimentary succession into the Bushveld Complex igneous rocks. Some very thin (2 m) sub-vertical dykes have been observed within the Waterberg Group sedimentary succession and the Bushveld Complex. Although the dykes were not age dated, the assumption is that they are the youngest igneous intrusion on the Waterberg Project.

During the period of Waterberg Group sedimentation, with later emplacements of both the sill and the dykes; the F zone mineralisation underwent alteration. During the alteration process, some magmatic sulphides were replaced by secondary silicates. The olivine bearing rocks were also serpentinised. The late magmatic alteration within the T Zone involved the replacement of sulphides along the margins with secondary silicates and iron oxides to hydroxides. The late magmatic hydrothermal activities within the T Zone resulted in the replacement of magnetite, deposition of quartz, crystallisation of pyrite-millerite and remobilisation of both base metal sulphides and PGEs out of sulphide blebs into the silicate matrix.

8.4 The metal basket percentage split

In this section, a comparison in metal basket percentage split is made between mineralisation of the Waterberg Project with mineralisation of Harriet's Wish, the Aurora Project, the Platreef and the Western limb.

8.4.1 The metal basket comparisons

To the north of the HRSZ, both the Lower mineralised zone of the Harriet's Wish and the Ultramafic Sequence (UmS) of the Waterberg Project are characterised by similar metal basket with palladium being the dominant PGE with a prill split of 61 – 64 % of the Pd+Pt+Rh+Au (Figure 8.5). Platinum is the second dominant PGE with 29 – 33 % of the prill split. Both the UmS of the Waterberg Project and the Lower Mineralised Zone of the Harriet's Wish are characterised by a lower gold proportion ranging from 5 - 6 %. The rhodium proportion for Lower mineralised zone has not been reported while that of the Ultramafic Sequence is 1.6 %. Although the metal balances are similar for both the Lower mineralised zone and the Ultramafic Sequence, this does not seem to be the case with the Upper mineralised zone and the T Zone. The Upper mineralised zone of the Harriet's Wish is dominated by a significantly higher gold proportion (63 %) and lower palladium proportion (14 %) while the T Zone of the Waterberg Project is palladium dominant (50 %) with lower gold proportion (20 %). The platinum proportion in the Upper mineralised zone of the Harriet's Wish and the T Zone of the Waterberg Project is 23 % and 29 %, respectively.

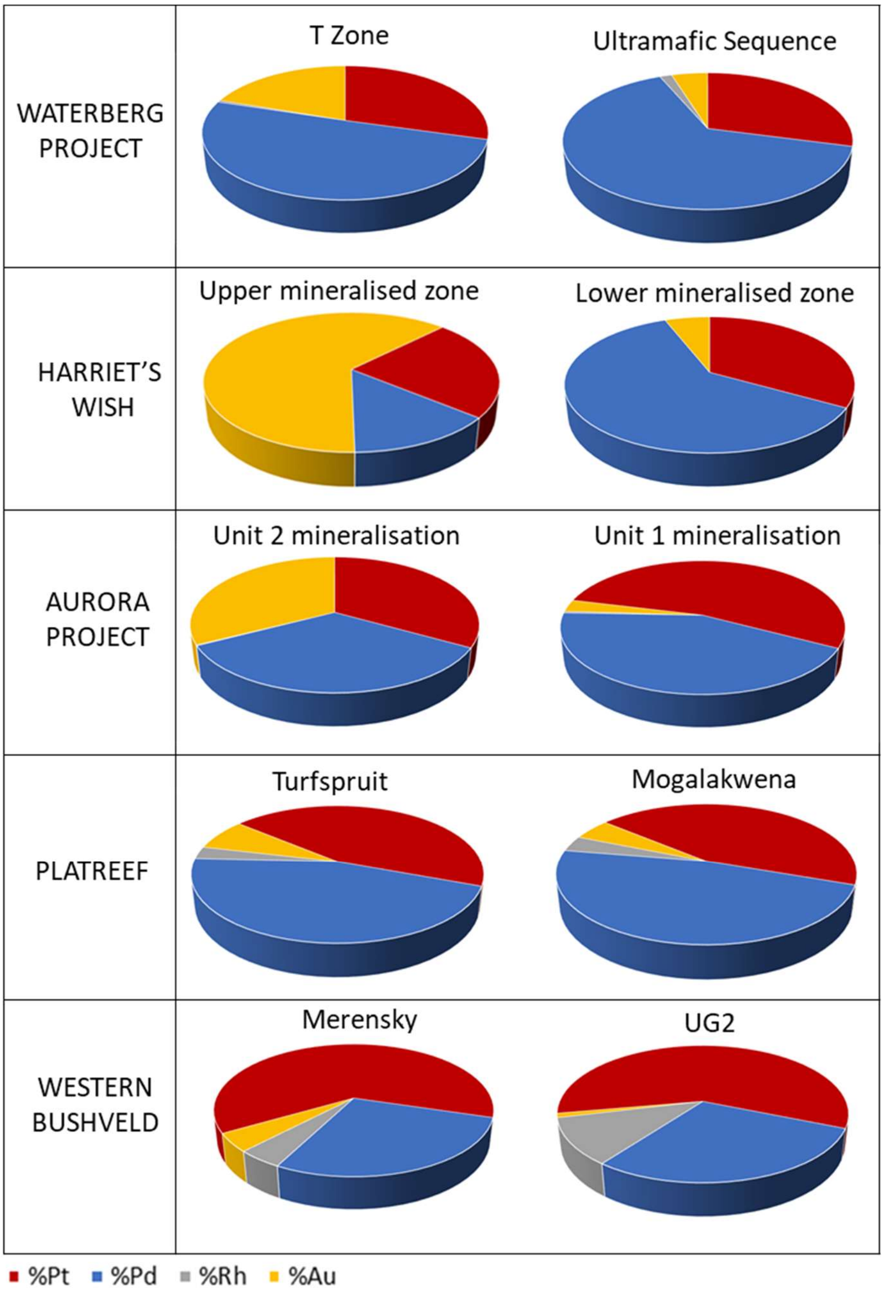

Figure 8.5. Pie charts showing Pd, Pt, Rh and Au metal baskets of the Waterberg Project (Murphy et al., 2019), Harriet's Wish (Sylvania Resource Limited, 2012), Aurora Project (McDonald et al., 2017), Turfspruit (Peters et al., 2016) and the Western Bushveld (Kinnaird, 2005).

To the south of the HRSZ, the metal content of Unit 1 mineralisation on the Aurora Project is dissimilar to that of Harriet's Wish and the Waterberg Project (Figure 8.5) with platinum being the dominant PGE (54 %). Although the metal content of the Unit 2 mineralisation is dissimilar to that of the T Zone and the Harriet's Wish Upper mineralisation, all the three zones/units are characterised by a higher gold content which has not been encountered anywhere alse within the Bushveld Complex.

Further south from the Aurora Project, the Platreef on Turspruit and Mogalakwena is dominated by equal proportions of platinum and palladium, both with 45 % in metal balances (Peters et al., 2016).

Unlike the northern limb and the far northern limb, both the Merensky Reef and the UG2 of the western Bushveld Complex are platinum dominant and characterised by a higher rhodium content (Kinnaird, 2005).

For the data used for the metal basket comparison, refer to Appendix 6.

8.5 The PGE + Au tenors of the Waterberg Project

8.5.1 The UmS (F Zone)

Regionally, tenors are higher in the FH with the highest Pd tenor of 1 593 ppm compared to the FP. There is an overall decrease in tenors along strike from F - Central; (SW) to F - Boundary South (NE). However, these tenors seem to increase from the F - Boundary North towards the F - North. On the dip section, there is a generalised decrease in tenors from west to east except for F-Boundary North, which does not show any lateral trend.

Locally, the F-Central (Figure 8.6) has the highest tenors of 240 ppm - 364 ppm Pd, 51 ppm - 149 ppm Pt and 15ppm –-23 ppm Au. A lack of gradual directional increase in tenors with higher tenors at the centre of the zone is attributed to floor embayments. There appears to be a localised gradual decrease in tenors from NE to SW. This trend is probably attributed to the dynamic emplacement of the PGE-enriched magmas as they filled-up the embayment. Mineralisation in the F-Boundary South is also significantly controlled by the floor embayment with tenors decreasing gradually from west to east. The tenor ranges within the F - Boundary South are 90 ppm -172 ppm Pd, 38 ppm - 73 ppm Pt and 11 ppm -18 ppm Au. Both the F - Boundary North and the F - North (Figure 8.6) are not characterised by significant floor embayments. Although the FP has a higher PGE grade compared to the FH within the F - North, the tenors are higher in the FH.

Regionally, the lateral variations in Cu/Pd ratios seem to complement the lateral tenor trends with the lowest ratio of 45 in the F - Central where the tenor values are high. The ratio increases along strike from the F - Central towards the F - Boundary South where the lowest ratio is 94. However, the ratio seems to be generally lower at the F-Boundary North compared to those in the F-Boundary South with the lowest ratio of 61. Cu/Pd ratios in the F - North are generally lower than those of the F - Boundary South and F - Boundary North with the lowest ratio of 50. The ratios do not show any discernible general increase on strike from the F - Central towards the F - North. However, there is a notable increase in the ratio in the dip section from the west to east across all the F Zones with the exception of the F - Boundary North, which does not show any trend.

Both the lateral variations in tenor and Cu/Pd ratios seem to favour a westerly/SW feeder zone for the UmS magma influxes as depicted by the arrows on Figure 8.6.

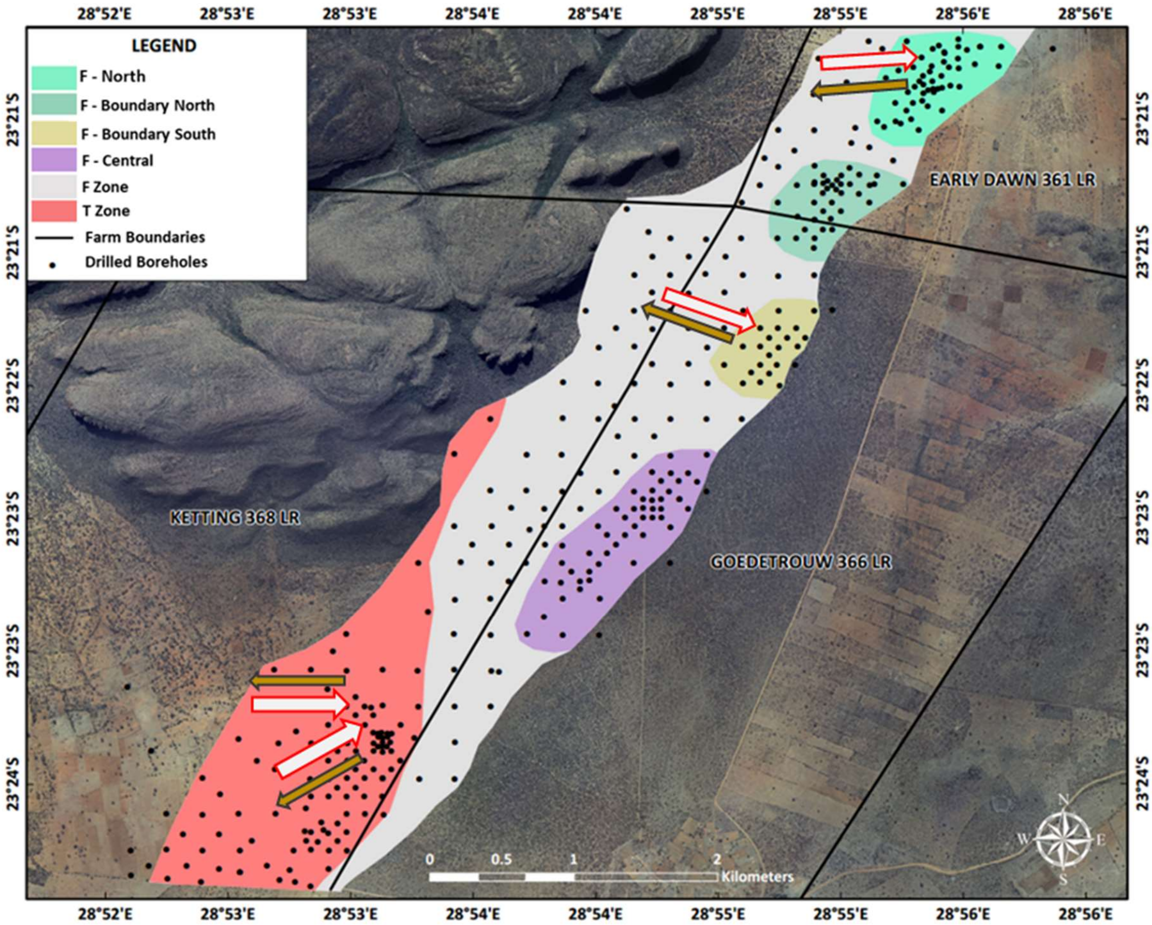

Figure 8.6. A layout plan of the Waterberg Project showing the districts of economic interest. The white arrows with red outline show the direction of the lateral tenor decrease while the gold-coloured arrow with black outline show the direction of the Cu/Pd ratio decrease. The tenors decrease away from the probable feeder zone while the Cu/Pd ratios decrease towards the probable feeder zone.

8.5.2 The T Zone

Within the T Zone, PGE and Au tenor are higher in both T2 and LPA than in the T1 and the UPA. PGE tenors in the UPA are slightly higher than those in the T1 and the T0. The LPA has the highest Pd and Pt tenor of 60 ppm - 397 ppm and 26 ppm - 186 ppm, respectively. In the T2, Pd and Pt tenor ranges are 47 ppm –-287 ppm and 79 ppm - 106 ppm, respectively. The Au tenor is higher in the T2 subzone with a range of 52 ppm – 84 ppm. In the LPA, the Au tenor ranges from 25 ppm - 68 ppm. The Pd and Pt tenor within the UPA are 69 ppm -273 ppm and 56 ppm -182 ppm, respectively, while those in the T1 and the T0 are generally below 100 ppm. There is a lateral decrease in PGE tenor in the T2, the T1 and the T0 from SW to NE. Unlike PGE tenor, Au tenor shows a lateral decrease from NE to SW in the T2, the LPA, the T1, the UPA and the T0. The PGE tenor in the LPA seems to complement a NE to SW decreasing trend. In the UPA, the PGE tenors are higher in the NE and lower in the SW.

On the dip section, PGE tenors in both T2 and LPA seem to be generally higher down-dip. The trend in the T0 is somewhat different, with the lowest tenor occurring down-dip. Within the LPA, Au tenor shows a lateral decrease from the west towards the east. Au tenor in the T2 shows no obvious trend while the T0 shows a decrease in tenor towards the west.

The Cu/Pd ratios are relatively higher in T0 (104 – 732) but with a very high degree of variability both down-dip and along the strike sections. The T2 Cu/Pd ratios range from 95 - 311 while that of the LPA range from 235 - 255. Within the T2, the Cu/Pd ratio increase gradually on strike from SW to NE. A similar trend applies in the LPA. Although the increase is not gradual, Cu/Pd seem to increase on strike section from a west to east.

Although there is some degree of variability in both the Pd and Pt tenors and Cu/Pd within the T Zone, the trends also seem to favour a feeder zone to the west or southwest (Figure 8.5).

8.5.3 Tenors in the Waterberg Project and Turfspruit

It is important to note that the T1 and the T2 of the Waterberg Project do not equate to the T1 and the T2 of the farm Turfspruit. The T1 of Turfspruit is characterised by a fairly homogenous feldspathic pyroxenite with chromitite stringers (Kekana, 2014) while the T1 of the Waterberg Project is defined by the presence of olivine with variable lithologies such as troctolite, olivine bearing feldspathic pyroxenite and harzburgite. The T2 of the Turfspruit is characterised by pegmatoidal pyroxenite and harzburgite (Kekana, 2014) while the T2 of the Waterberg Project is characterised by gabbronorite and feldspathic pyroxenite. The T1 and the T2 of Turfspruit are further classified as the Platreef below the Main Zone while the T1 and the T2 of the Waterberg Project are located at the interface between the TGA (Main Zone) and the Upper Zone (Figure 2.5; Figure 3.1 and Figure 3.2)

According to Kekana (2014), for Turfspruit, tenors decrease gradually from the NW towards the SE with the similar high tenors in both T1 and T2. The highest tenors (Pt + Pd) of 700 ppm and 1000 ppm were recorded in T1 and T2 respectively, comparable to those of the Platreef at Sandsloot and the Merensky Reef (Naldrett et al., 2009). Pt + Pd tenors of about 100 ppm dominate both the T1 and the T2 with the higher average T1 tenor of 250 ppm in both the NW and SE. The vertical tenor variations have also shown that in both T1 and T2, the highest tenors are predominantly in the topmost portions (Kekana, 2014).

Within the T Zone of the Waterberg Project, the highest Pd tenor of 659 ppm has been recorded at the contact between the LPA and T2. Au tenors have also shown to be higher compared to the rest of the Bushveld Complex with a highest recorded Pd tenor of 1013 ppm in the LPA. Tenors of Pd and Pt in both T2 and LPA are generally higher than those in all other T Zone subzones.

The highest PGE tenors of Pd are 1050 ppm in the F-Central and 1593 ppm in the F-Boundary South. Generally, Au tenor of the F zone is lower compared to that of the T Zone with a maximum tenor of 684 ppm recorded in the FH of the F-Boundary North.

Unlike the rest of the Bushveld Complex where Pt tenor is higher than Pd tenor, Pd tenor seems to be higher than Pt tenor in both the T Zone and the F zones of the Waterberg Project. The Au tenor is significantly lower than that of Pd and Pt.

CHAPTER 9

CONCLUSION

The Waterberg Project consists of two distinctively mineralised zones, namely the F Zone within the lower Ultramafic Sequence (UmS) and the upper T Zone.

The F Zone in the UmS is characterised by two subzones, namely the bottom FP and the top FH. The FP is a well mineralised subzone hosted by feldspathic pyroxenite and gabbronorite while the well mineralised FH subzone is hosted by feldspathic harzburgite, poikilitic melanocratic troctolite and olivine-bearing feldspathic pyroxenite.

Within the F-Central, F-Boundary South and F-Boundary North, mineralisation is predominantly confined to the FH; transgressing into the FP towards the northern F-North. With the exception of the F-Boundary North and the F-North, the F-Central and the F-Boundary South are characterised by floor embayments which probably played a crucial role in the development of the thicker UmS.

In general, there is a lack of an upward decrease in PGE and Au tenors (38 ppm - 1 593 ppm) within the UmS. Instead, the tenors are lower (38 ppm) at the base of the UmS (FP), increasing upwards to higher values (1 593 ppm) towards the top of the FH. The sulphide content (2 wt %) is higher than can be dissolved by intercumulus liquid, implying that the multiple influxes of the UmS magmas gained their tenors elsewhere and were already rich in PGE when entering the magma chamber (Naldrett et al., 2009). Unlike in-situ deposition of the sulphides observed in the Western Bushveld (Naldrett et al., 2009) and within the T1 of Turfspruit (Kekana, 2014), the sulphides within the UmS were probably deposited in a crystal mush without undergoing segregation. Both lateral tenor and Cu/Pd variations generally favour a westerly/SW feeder zone for the UmS magma influxes.

The T Zone is characterised by five distinctive subzones, namely the lower consistently mineralised T2, a sporadic LPP, a mineralised LPA and a variably mineralised T1 and UPA.

From west to east and along strike from SW to NE, mineralisation within the T Zone gradually transgresses downward from T2 into the LPA converging with the T0 mineralisation towards the east. The T0 mineralisation is the PGE + Au mineralisation within the UZ which transgresses the lithostratigraphy from the UZ to the UPA along strike and on dip sections. Within the T Zone, higher PGE and Au tenors occur within the LPA and the T2 respectively with a lateral PGE tenor increasing from NE to SW and lateral Au tenor increasing from SW to NE in the T2, T1 and T0. Unlike PGE tenors, the Au tenors show a lateral increase from SW to NE within these subzones. The PGE tenors in the LPA show some anti-correlation with the rest of the subzone, as they increase from SW to NE.

On the dip section, PGE tenors in both the T2 and LPA seem to be generally higher (167 ppm –203 ppm) in the west than in the east (99 ppm – 203 ppm). The trend in T0 is somewhat different, with the lowest tenor (23 ppm) in the west. Within the LPA, Au tenors show a lateral decrease from west (60 ppm) to east (47 ppm). The Au tenor in the T2 shows no conclusive trend while that of the T0 shows a decrease towards the west. Although there is some degree of variability in both tenor and Cu/Pd trends within the T Zone, the trends seem to favour a westerly/SW feeder zone.

There is evident correlation between the T Zone of the Waterberg Project with the Upper mineralised zone of Harriet's Wish and the Target zone 1 mineralisation of Aurora. There are also some signs of correlatability between the FP of the Waterberg Project with the Lower mineralised zone of the Harriet's Wish and the Unit 1 mineralisation of the Aurora Project.

Both the Harriet's Wish and Aurora projects are most likely distal and far distal southern extensions of the Waterberg Project with no direct geochemical correlation with the Platreef.

REFERENCES

Ashwal, L.D., Webb, S.J., Knoper, M.W., 2005. Magmatic stratigraphy in the Bushveld Northern Lobe: continuous geophysical and mineralogical data from the 2950m Bellevue drillcore. S.Afr.J.Geol. 108, 199-232.

Barnes, S.J., Keays, R.R., Reid, R., Hoatson, D.M., 1992. Distribution of sulfides and PGE within the porphyritic websterite zone of the Munni Munni Complex Western Astralia. Austr J Earth Sci 39, 289-302.

Barnes, S.J. and Picard, C.P., 1993. The behaviour of platinum group elements during partial melting, crystal fractionation, and sulphide segregation: An example from the Cape Smith Fold Belt, northern Quebec. Geochim. Cosmochim. Acta, 57, 79-87.

Barnes, S.J., Boyd, R., Korneliussen, A., Nilsson,L.P., Often, M., Pedersen, R.B., Robins, B., 1988. The use of mantle normalization and metal ratios in discriminating between the effects of partial melting, crystal fractionation and sulphide segregation on platinum group elements, gold, nickel and copper: examples from Norway. In: Prichard, H.M., Potts, P.J., Bowles, J.F.W., Cribb, S.J., (Eds), Geo Platinum 87. Elsevier, London, 113-143.

Barnes, J., McIntyre, J.R., Nisbet, B.W. et al. Platinum group element ,mineralisation in the Munni Munni Complex, western Australia. Mineralogy and Petrology 42, 141–164 (1990). https://doi.org/10.1007/BF01162688

Cameron, E.N., 1980. Evolution of the Lower Critical Zone, central sector, eastern Bushveld Complex. Economic Geology, 75, 845-871.

Campbell, I.H., Naldrett, A.J., and Barnes, S.J., 1983, A model for the origin of the platinum-rich sulfide horizons in the Bushveld and Stillwater Complexes: Journal of Petrology, v. 24, p. 133–165.

Cawthorn, R.G., Eales, H.V., Walraven, F., Uken, R., Watkey, M.R., 2006. The Bushveld Complex. 261-282 in: The Geology of South Africa (M.R. Johnson, C.R. Anhaeusser and R.J. Thomas, editors).

Dorland, H.C., Beukes, N.J., Evans, D.A.D., Armstrong, R.A., 2006. Precise SHRIMP U-Pb zircon age constraints on the lower Waterberg and Soutpansberg Groups, South Africa. South African Journal of Geology, 109, 139-156.

Finn, C.A., Bedrosain, P.A., Cole, J.C., Khoza, T.D., Webb, S.J., 2015. Mapping the 3D extent of the Northern Lobe of the Bushveld layered mafic intrusion from geophysical data. Precambrian Research, 268, 279-294.

Gain, S.B. and Mostert, A.B., 1982. The geological setting of the platinoid and base metal sulfide mineralization in the Platreef of the Bushveld Complex in Drenthe, north of Potgietersrus. Economic Geology. 77(6), 1395-1404.

Grobler, D.F. and Nielsen, S.A., 2012. Upper Critical Zone (Merensky Reef-UG2) correlates within the Platreef, Turfspruit, Northern Limb, Bushveld Igneous Complex. February 2012, unpublished.

Grobler, D.F., Brits, J.A.N., Maier, W.D., Crossingham, A., 2018. Litho-and chemostratigraphy of the Flatreef PGE deposit, northern Bushveld Complex, Minerallum Deposita, 1-26.

Hatton, C.J. and Schweitzer, J.K., 1995. Evidence for syn-chronous extrusive and intrusive Bushveld magmatism. J. Afr. Earth Sci., 21, 579-594.

Hulbert, L.J. & von Gruenewaldt, G. (1985). Textural and compositional features of chromite in the lower and critical zones of the Bushveld Complex south of Potgietersrus. Economic Geology 80, 872–895.

Hutchinson, D. and Kinnaird, J.A., 2005. Complex multistage genesis for the Ni-Cu-PGE mineralisation in the southern region of the Platreef, Bushveld Complex, South Africa. Transactions, Institute of Mining and Metallurgy, 114, 208–224.

Huthmann, F.M., Yudovskaya, M.A., Frei, D., Kinnaird, J.A., 2016. Geochronology evidence for an extension of the Northern Lobe of the Bushveld Complex, Limpopo Province, South Africa. Precambrian Research, 280, 61-75.

Huthmann, F.M., Yudovskaya, M.A., Elburg, M.A., Kinnaird, J.A., 2017. The Sr isotopic stratigraphy of the far northern Bushveld Complex. S.Afr.J.Geol.120.

Huthmann, F.M., Yudovskaya, M.A., Kinnaird, J.A., McCreesh, M.J.G., McDonald, I., 2018. Petrogenesis and PGE of the lower mineralized zone of the Waterberg Project, South Africa. Ore Geology Reviews, 92, 161-185.

Jansen, H., 1982. The geology of the Waterberg Basins in the Transvaal, Republic of South Africa. Geological Survey of South Africa Memorandum.

Kekana, S.M., 2014. An investigation of mineralisation controls in the upper section of the Platreef in the southern sector, on Turfspruit, Northern Limb, Bushveld Complex, South Africa. Msc thesis (unpublished), University of the Witwatersrand, 1-143.

Kinnaird, J.A., 2005. The Bushveld Large Igneous Province. School of Geoscience, University of the Witwatersrand, 39.

Kinnaird, J.A., and Nex, P.A.M., 2012. An Overview of the Platreef. Council for Geosciences (in press).

Kinnaird, J.A., Yudovskaya, M., McCreesh, M., Huthmann, F., Botha T.J., 2017. The Waterberg PGE Deposit – atypical magmatism and mineralisation. Economic Geology, 112, 1267-1394.

Kruger, F.J., 1994. The Sr-isotopic stratigraphy of the western Bushveld Complex. South African Journal of Geology, 97, 393-398.

Lee, C.A., 1996. A review of mineralisation in the Bushveld Complex and some other layered mafic intrusions. 103-146 in: Layered Intrusions (R.G. Cawthorn, editor). Elsevier Science.

Lomberg, K. and Goldschmidt, A., 2014. Platinum Group Metals Ltd. Technical Report for the Update on Exploration Drilling at the Waterberg Joint Venture and Waterberg Extension Project, South Africa (Latitude 23° 14’ 11’’ S, Longitude 28° 54’ 42’’ E) Platinum Group Metals (RSA)(Pty)Ltd (Internal report).

Maier, W.D., Barnes, S.J., de Waal, S.A., 1998. Exploration for magmatic Ni-Cu-PGE sulphide deposits: a review of recent advances in the use of geochemical tools, and their application to some South African ores. South African Journal of Geology, 101(3), 237-253.

Maier, W.D., Barnes, S.J., Teigler, B., De Klerk, W.J., Mitchell, A.A., 1996. Cu/Pd and Cu/Pt of silicate rocks in the Bushveld Complex: Implications for platinum-group element exploration. Economic Geology, 91, 1151-1158.

Maier, W.D., Gomwe, T., Barens, S.J., Li, C. & Theart, H. (2004). Platinum group elements in the Uitkomst Complex, South Africa. Economic Geology 99, 499–516.

Maier WD, de Klerk L, Blaine J, Manyeruke T, Barnes SJ, Stevens MVA, Mavrogenes JA (2008) Petrogenesis of contact-style PGE mineralization in the northern lobe of the Bushveld Complex: comparison of data from the farms Rooipoort, Townlands, Drenthe and Nonnenwerth. Miner Deposita 43:255–280

Manyeruke TD, Maier WD, Barnes SJ (2005) Major and trace element geochemistry of the Platreef on the farm Townlands, northern Bushveld complex. South Afr J Geol 108:381–396

Manyeruke, T.D., 2007. Geochemical Variations of the Platreef in the Northern Limb of the Bushveld Complex: Implications for the Origin of the PGE Mineralisation. Doctoral thesis, University of Pretoria, 1-206.

McCreesh, M.J.G., 2013. A study of the Main Zone-Upper Zone boundary beneath a thick succession of Waterberg sediments in the far north of the Northern limb of the Bushveld Complex. Bsc. Hons thesis, University of the Witwatersrand, 1-148.

McCreesh, M.J.G., 2016. An investigation of the mineralisation in the Waterberg platinum-group element deposit, South Africa. Msc thesis, University of the Witwatersrand, South Africa, 489pp.

McCreesh, M.J.G., Yudovskaya, M.A., Kinnaird, J.A., Reinke, C., 2018. Platinum-group minerals of the F and T zones, Waterberg Project, far northern Bushveld Complex: implication for the formation of the PGE mineralisation. Mineralogical Magazine, 82(3), 539-575.

McDonald, I., Holwell, D.A., 2011. Geology of the northern Bushveld Complex and the setting and genesis of the Platreef Ni-Cu-PGE deposit. Rev Econ Geol 17:297–327.

McDonald, I., Harmer, R.E., Holwell, D.A., Hughes, H.S.R., Boyce, A.J., 2017. Cu-Ni-PGE Mineralisation at the Aurora Project and potential for nrew PGE province in the Northern Bushveld Main Zone. Ore Geology Reviews, 80, 1135-1159.

McFall, K., McDonald, I., Tanner, D., Harmer, R.E., 2019. The mineralogy and mineral associations of platinum-group elements and precious metals in the Aurora Cu-Ni-Au-PGE deposit, Northern Limb, Bushveld Complex. Ore Geol Rev 106:403-422.

Meyer, R. and De Beer, H., 1987. Structure of the Bushveld Complex- from resistivity measurements. Nature, 325, 610-612.

Mitchell, A.A., 1990. The stratigraphy, petrology and mineralogy of the Main Zone of the north eastern Bushveld Complex. South African Journal of Geology, 93, 818-831.

Molyneux, T.G., 1974. A grological investigation of the Bushveld Complex in the Sekhukhuneland and part of the Steelpoort valley. Trans. Geological Society of South Africa, 77, 329-338.

Murphy, M., Muller, C.M.J., Cunningham, G., 2019. Independent Technical Report, Waterberg Project Definitive Feasibility Study and Mineral Resource Update, Bushveld Complex, South Africa. Waterberg JV Resources (Pty)Ltd, 1-604.

Naldrett, A.J., Asif, M., Krstic, S., Li, C., 2000. The composition of ore at the Voisey's Bay Ni-Cu sulphide deposit, with special reference to platinum-group elements. Economic Geology, 95, 845-866.

Naldrett, A.J., 2004. Magmatic Sulphide Deposits, Geology, Geochemistry and Exploration. Springer Berlin Heidelberg New York, 1-743.

Naldrett, A.J., Wilson, A., Kinnaird, J.A., and Chunnett, G., 2009. PGE Tenor and Metal Ratios within and below the Merensky Reef, Bushveld Complex: Implications for its Genesis. Journal of Petrology, 50, 625-659.

Naldrett, A.J., Kinnaird, J.A., Wilson, A., Yudovskaya, M., Chunnett, G., 2011. Genesis of the PGE-Enriched Merensky Reef and Chromitite Seams of the Bushveld Complex. Society of Economic Geologists, 17, 235-296.

Nex, P.A.M., Kinnaird, J.A., Vyver, B.A., van der Ingle, L.J., Cawthorn, R.G., 1998. A new stratigraphy for the Main Zone of the Bushveld Complex, in the Rustenburg area. South African Journal of Geology, 101, 215-223.

Peters, B., Parker, H., Kuhl, T., Joughin, W., Lawson, M., Coetzee, V., Simith, G., 2016. Platreef Project. 2016 Resource Technical Report, Ivanhoe Mines, New Horizons, 1-538.

Reynolds, I.M., 1985. Contrasted mineralogy and textural relations in the uppermost Ti-magnetite layers of the Bushveld Complex in the Bierkraal area north of Rustenburg. Economic Geology, 80, 1027-1048.

SACS (South African Committee for Stratigraphy)., 1980. Stratigraphy of South Africa. Part 1 (Kent, L.E., Comp.), Lithostratigraphy of the Republic of South Africa, Southwest Africa/Namibia, and the Republic of Bophuthatswana, Transkei and Venda. Handb. Geol. Surv. S. Afr., 8, 690 pp.

SAMREC (The South African Mineral Resource Committee)., 2007. The South African Code for the reporting of Exploration Results, Mineral Resources and Mineral Reserves. 2007 edition, 2-49.

Schuurman, L.W., Grabe, P.J., Steenkamp, C.J., 1998. Chromium. In: Wilson, M.G.C. and Anhaeusser, C.R (Eds.), The mineral Resource of South Africa. Handbook. Council for Geoscience, 16, 90-105.

Schweitzer, J.K., Hatton, C.J., De Waal, S.A., 1995a. Regional lithochemical stratigraphy of the Rooiberg Group, upper Transvaal Supergroup: a proposed new subdivision. South African Journal for Geology, 98, 245-255.

Schweitzer, J.K., Hatton, C.J., De Vaal, S.A., 1995b. Economic potential of the Rooiberg Group-volcanic rocks in the floor and roof of the Bushveld Complex. Mineral Deposita, 30, 168-177.

Uken, R. and Watkeys, M.K., 1997. Diapirism initiated by the Bushveld Complex, South Africa. Geology, 25, 723-726.

van der Merwe, M.J., 1976. The layered sequence of the Potgietersrus Limb of the Bushveld Complex. Economic Geology, 71, 1337-1351.

van Scheltema, J., 2019. Mineralisation of the northern limb: Harriet's Wish farm. Msc thesis (unpublished), University of the Witwatersrand, 1-298.

Vermaak, C.F and van der Merwe, M.J., 1986. Introduction to the Bushveld Complex. In: Anhaeusser, C.R., Maske, S (editors), Mineral Deposits of Southern Africa. The Geological Society of South Africa, 1021-1029.

von Gruenewaldt, G., 1973. The Main and Upper Zone of the Bushveld Complex in the Roossenekal area, Eastern Transvaal. Transactions of the Geological Society of South Africa, 76, 207-227.

von Gruenewaldt, G., Sharpe, M.R., Hatton, C.J., 1985. The Bushveld Complex, introduction and review. Economic Geology, 80, 803-812.

Walraven, F., 1986. A note on the stratigraphic terminology of the Bushveld Complex. In: Anhaeusser, C.R. and Maske, S. (eds.), Mineral Deposits of Southern Africa, Vol. II. Geological Society of South Africa, 1039-1040.

Willemse, J., 1969. The geology of the Bushveld Complex Igneous Complex, the largest repository of magmatic ore deposits in the world. In: Magmatic Ore Deposits – A symposium, 1-22.

Wilson, A.H., 2015. The Earliest Stages of Emplacement of the Eastern Bushveld Complex: Development of the Lower Zone, Marginal Zone and Basal Ultramafic Sequence. J. Petrol. 56, 347-388.

Yudovskaya, M.A., and Kinnaird, J.A., (2010). Chromite in the Platreef (Bushveld Complex, South Africa): occurrence and evolution of its chemical composition. Miner Deposita, 2010.

Yudovskaya, M.A., Kinnaird, J.A., Sobolev, A.V., Kuzmin, D.V., McDonald, I., Wilson, A.H., 2013. Petrogenesis of the Lower Zone olivine-rich cumulates beneath the Platreef and their correlation with recognized occurrence in the Bushveld Complex. Economic Geology, 108, 1923-1952.

Zeh A, Ovtcharova M, Wilson AH and Schaltegger U (2015) The Bushveld Complex was emplaced and cooled in less than one million years – results of zirconology, and geotectonic implications. Earth Planet Sci Lett 418:103-114

Appendix 1

A LIST OF SAMPLES FOR POLISHED SECTIONS

BHID	SAMPLE ID	FROM	TO	ZONE	WIDTH
WB222D1	AM-WITS-01	302.28	302.36	T ZONE	0.08
WB222D1	AM-WITS-02	307.15	307.21	T ZONE	0.06
WB222D1	AM-WITS-03	296.08	296.18	T ZONE	0.1
WB213D0	AM-WITS-04	198.28	198.41	T ZONE	0.13
WB213D0	AM-WITS-05	256.38	256.49	T ZONE	0.11
WB213D0	AM-WITS-06	282.22	283.35	T ZONE	1.13
WB230D0	AM-WITS-07	232	232.14	T ZONE	0.14
WB230D0	AM-WITS-08	238.14	238.27	T ZONE	0.13
WB230D0	AM-WITS-09	253.7	253.77	T ZONE	0.07
WB230D0	AM-WITS-10	357.8	357.88	T ZONE	0.08
WB215D0	AM-WITS-11	208.39	208.48	T ZONE	0.09
WB215D0	AM-WITS-12	229.23	229.39	T ZONE	0.16
WB215D0	AM-WITS-13	246.76	246.87	T ZONE	0.11
WB264D1	AM-WITS-14	431.8	431.92	F ZONE	0.12
WB264D1	AM-WITS-15	470.56	470.65	F ZONE	0.09
WB264D1	AM-WITS-16	400.8	400.92	F ZONE	0.12
WB264D1	AM-WITS-17	472.16	472.28	F ZONE	0.12
WB261D0	AM-WITS-18	329.08	329.25	F ZONE	0.17
WB261D0	AM-WITS-19	264.78	264.94	F ZONE	0.16
WB261D0	AM-WITS-20	371.5	371.6	F ZONE	0.1
WB261D0	AM-WITS-21	278.69	278.87	F ZONE	0.18
WB259D0	AM-WITS-22	323.25	323.36	F ZONE	0.11
WB259D0	AM-WITS-23	255	255.19	F ZONE	0.19
WB259D0	AM-WITS-24	281.46	281.56	F ZONE	0.1
WB259D0	AM-WITS-25	421.16	421.31	F ZONE	0.15
WE120D0	AM-WITS-26	411.76	411.89	F ZONE	0.13
WE120D0	AM-WITS-27	440.62	440.78	F ZONE	0.16
WE120D0	AM-WITS-28	416.59	416.71	F ZONE	0.12
WE120D0	AM-WITS-29	448.69	448.83	F ZONE	0.14

Appendix 2

EXHIBIT ROCK SAMPLES FOR LITHOSTRATIGRAPHY

BHID	FROM	TO	STRATIGRAPHY	CORE SIZE	FIGURE
WB154D0	482.46	482.63	BASEMENT	NQ	Figure 3.3A
WE005D0	326	326.2	BASEMENT	NQ	Figure 3.3B
WB136D0	866	866.22	TRNZ	NQ	Figure 3.4A
WE120D0	458.52	458.76	TRNZ	NQ	Figure 3.4B
WB176D0	661.18	661.3	TRNZ	NQ	Figure 3.4C
WB176D0	749.52	749.71	TRNZ	NQ	Figure 3.4D
WB264D1	382.2	382.41	FH/F -ZONE	NQ	Figure 3.5A
WB264D1	402.26	402.47	FH/F -ZONE	NQ	Figure 3.5B
WE120D0	415.5	515.68	FP/F -ZONE	NQ	Figure 3.5C
WB165D0	898.08	898.26	TGA/MAIN ZONE	NQ	Figure 3.6A
WB132D0	499.1	499.27	TGA/MAIN ZONE	NQ	Figure 3.6B
WB132D0	575.17	575.35	TGA/MAIN ZONE	NQ	Figure 3.6C
WB132D0	607.68	607.85	TGA/MAIN ZONE	NQ	Figure 3.6D
WB132D0	675	692	TGA/MAIN ZONE	NQ	Figure 3.6E
WB132D0	678.13	678.25	TGA/F -ZONE	NQ	Figure 3.6F
WB132D0	679	679.13	TGA/F -ZONE	NQ	Figure 3.6F
WB165D0	754.29	754.59	TGA/MAIN ZONE	NQ	Figure 3.7A
WB115D0	237.4	237.56	TGA/MAIN ZONE	NQ	Figure 3.7B
WB115D0	231.77	231.91	TGA/MAIN ZONE	NQ	Figure 3.7C
WB128D0	300.19	300.35	TGA/MAIN ZONE	NQ	Figure 3.7D
WB230D0	358	358.2	T ZONE/UPA	NQ	Figure 3.8A
WB237D0	213.19	213.33	T ZONE/ T1	NQ	Figure 3.8B
WB222D1	293.1	293.34	T ZONE/ LPA	NQ	Figure 3.8C
WB213D0	277	277.25	T ZONE/LPP	NQ	Figure 3.8D
WB222D1	302.16	302.36	T ZONE/ T2	NQ	Figure 3.8E
WB001D0	399.09	399.28	UPPER ZONE	BQ	Figure 3.9A
WB208D0	741	741.2	UPPER ZONE	NQ	Figure 3.9B
WB237D0	127.91	128.16	WB/BC CONTACT	NQ	Figure 3.11
WE120D0	50.52	50.79	WATERBERG SED	NQ	Figure 3.12A
WB261D0	179.19	179.34	WATERBERG SED	NQ	Figure 3.12B
WB222D0	131.55	131.84	WATERBERG SED	NQ	Figure 3.12C
WB199D0	174	174.19	SILL	NQ	Figure 3.13A
WB159D0	181.5	181.69	DYKE	NQ	Figure 3.13B

Appendix 3

Tenor data for T Zone and F Zone

Hole_ID	From	To	Pd_Tenor (ppm)	Pt_Tenor (ppm)	Au_Tenor (ppm)	% Total Sulphide
WB226D0	247	248	14.0	14.0	14.0	0.14
WB226D0	248	248.5	13.6	13.6	20.3	0.15
WB226D0	248.5	249	12.5	22.0	25.1	0.32
WB226D0	249	249.39	10.0	15.1	42.3	1.39
WB226D0	249.39	250	9.8	14.3	55.1	3.36
WB226D0	250	250.42	9.1	13.8	29.3	3.41
WB226D0	250.42	251	11.6	20.6	43.0	1.12
WB226D0	251	251.5	4.7	9.3	28.0	0.21
WB226D0	251.5	252	5.3	5.3	37.1	0.38
WB226D0	252	252.5	10.8	23.3	71.8	0.56
WB226D0	252.5	253	7.3	7.3	21.8	0.14
WB226D0	253	253.5	16.3	108.9	141.5	0.18
WB226D0	253.5	254	3.4	6.8	17.1	0.29
WB226D0	254	254.39	12.9	19.3	24.1	1.24
WB226D0	254.39	254.64	12.0	15.4	18.8	0.58
WB226D0	254.64	255	6.7	20.0	13.3	0.15
WB226D0	255	255.52	7.6	7.6	15.3	0.13
WB226D0	255.52	255.81	5.7	5.7	5.7	0.18
WB226D0	255.81	256.5	10.0	15.0	15.0	0.40
WB226D0	256.5	257.15	5.6	16.8	16.8	0.18
WB226D0	257.15	257.4	771.4	691.0	32.4	1.60
WB226D0	257.4	258	191.3	156.5	17.4	0.06
WB226D0	258	258.5	56.7	102.1	22.7	0.09
WB226D0	258.5	259	12.8	19.2	22.5	0.31
WB226D0	259	259.39	5.7	5.7	17.2	0.17
WB226D0	259.39	260	10.2	10.2	15.2	0.20
WB226D0	260	260.84	17.1	21.4	32.1	0.47
WB226D0	260.84	261.5	969.8	594.0	145.0	1.28
WB226D0	261.5	262	544.7	408.5	81.7	0.11
WB226D0	262	263	68.8	86.0	17.2	0.06
WB226D0	263	264	76.1	121.8	15.2	0.07
WB226D0	319	319.48	62.7	62.7	7.8	0.13
WB226D0	320	320.5	89.7	44.9	15.0	0.07
WB226D0	321	321.5	296.4	111.1	37.0	0.03
WB226D0	321.5	322	474.5	341.6	38.0	0.05
WB226D0	322	322.5	215.6	71.9	7.2	0.14
WB226D0	322.5	323	2007.3	805.9	59.7	0.13
WB226D0	323	323.5	748.3	272.1	68.0	0.07
WB226D0	323.5	324	504.2	121.0	40.3	0.05
WB226D0	324	324.5	513.1	182.4	45.6	0.09
WB226D0	324.5	325	1997.3	832.8	59.7	0.30
WB226D0	325	325.5	1044.0	388.5	136.2	0.54
WB226D0	325.5	326	881.6	382.6	149.7	0.30

WB226D0	326	326.42	114.3	91.5	45.7	0.04
WB226D0	326.42	326.8	72.0	20.6	30.9	0.10
WB226D0	326.8	327.5	608.1	230.2	105.9	0.81
WB226D0	327.5	328	783.6	291.1	162.3	0.18
WB226D0	328	328.5	631.7	240.6	157.9	0.13
WB226D0	328.5	329	410.0	90.3	41.7	0.14
WB226D0	329	329.76	374.5	181.5	80.7	0.35
WB226D0	330.08	330.5	420.9	185.7	143.5	0.83
WB226D0	330.5	331	54.5	32.3	48.5	0.50
WB226D0	331	331.5	13.8	20.7	17.2	0.29
WB226D0	331.5	332	18.4	36.8	30.7	0.16
WB226D0	332.5	333	9.5	15.8	12.7	0.32
WB226D0	333	333.85	90.1	72.0	36.0	0.11
WB226D0	333.85	334.5	19.9	33.1	13.2	0.15
WB243D0	228	229	9.9	9.9	19.7	0.10
WB243D0	229	230	8.5	8.5	8.5	0.12
WB243D0	230	231	4.4	4.4	4.4	0.23
WB243D0	231	231.5	1.6	1.6	3.3	0.61
WB243D0	231.5	232	4.9	4.9	4.9	0.20
WB243D0	232	232.5	5.2	5.2	5.2	0.19
WB243D0	232.5	233	7.2	7.2	7.2	0.14
WB243D0	233	233.5	10.6	10.6	10.6	0.09
WB243D0	233.5	234	13.2	8.8	8.8	0.23
WB243D0	234	234.5	47.5	31.0	64.1	0.48
WB243D0	234.5	235	7.5	9.4	32.1	0.53
WB243D0	235	235.5	53.9	67.6	50.9	1.32
WB243D0	235.5	236	126.0	87.7	200.0	1.09
WB243D0	236	236.5	7.7	6.4	9.0	0.78
WB243D0	236.5	237	25.3	17.7	30.3	0.40
WB243D0	237	237.5	24.8	18.0	36.1	0.44
WB243D0	237.5	238	22.2	16.6	25.0	0.36
WB243D0	238	238.5	28.9	18.1	25.3	0.28
WB243D0	238.5	239	22.7	22.7	11.3	0.26
WB243D0	239	239.5	21.0	21.0	26.2	0.19
WB243D0	239.5	240	19.6	19.6	26.1	0.15
WB243D0	240	240.7	12.3	12.3	18.5	0.16
WB243D0	240.7	241.7	27.3	16.4	27.3	0.18
WB243D0	241.7	242.7	37.8	30.2	15.1	0.13
WB243D0	242.7	243.7	46.7	28.0	18.7	0.11
WB243D0	243.7	244.7	53.3	44.4	8.9	0.11
WB243D0	244.7	245.7	354.5	301.9	45.9	0.15
WB243D0	245.7	246.7	188.6	98.0	22.6	0.13
WB243D0	246.7	247.7	1259.4	895.7	53.9	0.15
WB243D0	247.7	248.7	44.2	34.4	4.9	0.20
WB243D0	248.7	249.7	188.2	92.0	37.6	0.24
WB243D0	249.7	250.7	438.9	245.0	89.3	0.39
WB243D0	250.7	251.7	1042.5	622.8	182.8	0.15
WB243D0	251.7	252.7	65.2	78.2	26.1	0.08

WB243D0	252.7	253.7	36.9	55.3	18.4	0.05
WB243D0	253.7	254.7	63.3	126.6	21.1	0.05
WB243D0	254.7	255.7	96.0	216.0	24.0	0.04
WB243D0	255.7	256.7	87.3	122.3	17.5	0.06
WB243D0	256.7	257.7	57.0	99.8	14.3	0.07
WB243D0	257.7	258.7	29.2	38.9	9.7	0.10
WB243D0	258.7	259.7	103.1	93.7	75.0	0.11
WB243D0	259.7	260.7	83.0	124.5	20.8	0.05
WB243D0	260.7	261.09	125.3	88.2	65.4	0.92
WB243D0	261.59	262.09	43.8	43.8	7.3	0.14
WB243D0	262.09	262.59	51.9	29.6	14.8	0.13
WB243D0	263.41	264.41	103.2	37.5	9.4	0.11
WB243D0	264.41	265.41	124.8	58.7	22.0	0.14
WB243D0	265.41	266.41	48.3	29.0	9.7	0.10
WB243D0	266.41	267.41	41.3	34.4	13.8	0.15
WB243D0	267.41	268.41	54.3	30.2	12.1	0.17
WB243D0	268.41	269.41	83.7	50.2	16.7	0.12
WB243D0	269.41	270.41	102.2	55.8	18.6	0.11
WB243D0	270.41	271.41	356.7	123.5	27.4	0.07
WB243D0	271.41	272.3	805.7	244.4	63.4	0.11
WB243D0	299.62	300.33	42.8	36.7	9.2	0.33
WB243D0	300.33	300.83	49.1	32.7	8.2	0.12
WB243D0	300.83	301.33	122.2	150.0	11.1	0.18
WB243D0	301.33	301.81	16.7	5.6	5.6	0.18
WB243D0	302.6	303.1	11.5	7.6	3.8	0.26
WB243D0	303.1	303.6	47.9	47.9	23.9	0.04
WB243D0	303.6	304.1	34.1	34.1	34.1	0.03
WB243D0	304.1	304.6	17.3	34.5	17.3	0.06
WB243D0	304.6	305.1	95.3	95.3	23.8	0.04
WB243D0	305.1	305.6	43.8	21.9	43.8	0.05
WB243D0	305.6	306.1	8.3	8.3	6.2	0.48
WB243D0	306.1	306.6	156.5	193.2	103.3	0.30
WB243D0	306.6	307.1	134.5	149.4	298.8	2.01
WB243D0	307.1	307.6	121.8	146.7	81.7	0.72
WB243D0	307.6	308.1	30.5	30.5	45.8	0.07
WB243D0	308.1	308.6	327.8	483.7	219.6	0.31
WB243D0	308.6	309.1	142.1	201.6	143.7	1.25
WB243D0	309.1	309.41	220.9	263.1	132.9	3.81
WB243D0	309.41	309.91	95.5	148.5	126.6	1.51
WB243D0	309.91	310.41	58.7	85.1	76.0	0.99
WB243D0	310.41	310.91	52.2	74.2	107.6	1.91
WB243D0	310.91	311.41	36.6	39.6	64.0	0.33
WB243D0	311.41	311.91	71.0	125.3	108.7	1.32
WB243D0	311.91	312.41	54.7	81.5	86.9	2.05
WB243D0	312.41	312.91	76.4	95.2	122.1	1.86
WB243D0	312.91	313.41	53.7	72.3	83.6	0.97
WB243D0	313.41	313.91	39.8	60.5	58.9	0.63
WB243D0	313.91	314.41	9.4	12.2	10.1	1.39

WB243D0	314.41	314.91	41.1	56.6	69.4	1.09
WB243D0	314.91	315.35	104.8	202.7	270.5	2.17
WB243D0	315.35	315.85	64.2	69.7	95.4	0.55
WB243D0	315.85	316.35	56.3	83.2	106.0	0.75
WB243D0	316.35	316.85	49.5	85.2	87.2	0.50
WB243D0	316.85	317.35	15.2	30.3	60.6	0.13
WB243D0	317.35	317.85	66.2	84.4	462.2	2.25
WB243D0	317.85	318.35	83.4	103.6	193.6	2.27
WB243D0	318.35	318.85	53.8	83.5	112.3	1.25
WB243D0	318.85	319.2	64.2	85.6	100.9	0.33
WB243D0	319.2	319.7	7.6	15.1	30.3	0.13
WB243D0	320.5	320.9	1.4	1.4	5.7	0.70
WB243D0	324.9	325.9	18.2	18.2	27.3	0.11
WB243D0	325.9	326.43	20.2	40.4	30.3	0.10
WB243D0	326.43	326.93	65.2	54.8	75.6	0.38
WB243D0	326.93	327.43	43.7	38.9	36.6	0.85
WB243D0	327.43	327.93	18.1	27.1	36.1	0.11
WB243D0	327.93	328.43	83.2	89.6	121.6	0.16
WB243D0	328.43	328.93	80.9	72.6	79.0	1.09
WB243D0	328.93	329.43	65.9	63.1	76.6	1.77
WB243D0	329.43	329.93	78.6	71.7	79.9	0.73
WB243D0	329.93	330.43	67.1	55.3	75.0	0.25
WB243D0	330.43	330.93	78.8	73.6	73.6	1.52
WB243D0	330.93	331.43	165.4	208.6	86.3	0.14
WB243D0	331.43	331.7	154.4	133.8	30.9	0.10
WB243D0	331.7	332	99.0	66.0	44.8	0.42
WB243D0	332	333	300.3	60.1	15.0	0.07
WB243D0	336	337	79.1	13.2	13.2	0.08
WB243D0	337	338	30.9	10.3	41.2	0.10
WB243D0	338	339	111.0	101.9	89.2	0.55
WB243D0	339	340	255.4	296.2	40.9	0.10
WB243D0	340	341	238.6	145.8	13.3	0.08
WB243D0	342	342.75	526.8	862.0	9.6	0.10
WB243D0	342.75	343.25	181.5	191.0	9.6	0.10
WB243D0	343.25	343.75	132.1	79.3	13.2	0.08
WB243D0	343.75	344.3	94.9	89.9	93.3	1.20
WB243D0	344.3	345.3	124.0	173.6	24.8	0.08
WB243D0	345.3	346.3	118.2	219.5	16.9	0.06
WB243D0	346.3	347.3	62.2	111.9	99.5	0.08
WB243D0	347.3	348.3	42.7	85.4	32.0	0.09
WB243D0	348.3	349	65.5	131.1	13.1	0.08
WB238D0	224	224.5	4.1	4.1	4.1	0.24
WB238D0	224.5	225	9.8	9.8	9.8	0.10
WB238D0	225	225.5	12.5	12.5	12.5	0.08
WB238D0	225.5	226	13.4	13.4	13.4	0.07
WB238D0	226	226.5	6.2	6.2	6.2	0.16
WB238D0	226.5	227	6.2	6.2	6.2	0.16
WB238D0	227	227.5	3.3	3.3	6.7	0.30

WB238D0	227.5	227.93	6.0	3.0	9.0	0.33
WB238D0	227.93	228.5	16.5	3.3	9.9	0.30
WB238D0	228.5	229.08	23.7	14.2	21.3	0.84
WB238D0	229.08	229.5	17.4	9.9	19.9	0.40
WB238D0	229.5	230	40.2	40.2	28.7	0.17
WB238D0	230	230.52	43.1	37.7	16.1	0.19
WB238D0	230.52	231	35.1	26.3	17.5	0.11
WB238D0	231	232	27.0	20.2	13.5	0.15
WB238D0	232	232.5	20.8	15.6	5.2	0.19
WB238D0	232.5	233.07	35.8	26.0	22.8	0.31
WB238D0	233.07	233.5	24.6	16.4	32.8	1.10
WB238D0	233.5	234	21.0	12.3	28.0	1.14
WB238D0	234	234.5	14.1	6.1	20.2	0.50
WB238D0	234.5	235	22.5	15.5	25.3	0.71
WB238D0	235	235.5	13.3	8.0	16.0	0.75
WB238D0	235.5	236	17.9	14.3	25.1	0.56
WB238D0	236	236.52	12.2	8.2	18.3	0.49
WB238D0	236.52	237	18.0	7.7	15.4	0.39
WB238D0	237	237.59	20.0	11.1	13.3	0.90
WB238D0	237.59	238	113.0	105.6	20.4	0.54
WB238D0	238	239	115.7	84.1	21.0	0.29
WB238D0	250	250.5	157.3	57.2	14.3	0.07
WB238D0	250.5	251	127.8	42.6	8.5	0.12
WB238D0	251	251.5	182.5	48.0	19.2	0.10
WB238D0	251.5	251.75	189.7	70.3	28.1	0.28
WB238D0	251.75	252	20.2	20.2	2.5	0.40
WB238D0	254.5	255	61.2	40.8	18.8	0.64
WB238D0	255	255.5	63.7	42.0	17.6	0.74
WB238D0	270	271	290.6	92.5	39.6	0.08
WB238D0	272	273	138.4	46.1	46.1	0.02
WB238D0	274	275	31.9	31.9	31.9	0.03
WB238D0	275	276	34.4	17.2	17.2	0.06
WB238D0	276	277	22.4	22.4	22.4	0.04
WB238D0	277	278	56.7	14.2	14.2	0.07
WB238D0	279	280	821.0	469.2	70.4	0.04
WB238D0	280	281	246.5	117.1	43.1	0.16
WB238D0	281	282	358.8	196.6	167.1	0.20
WB238D0	282	282.9	206.8	126.4	139.8	0.52
WB238D0	282.9	283.2	124.4	94.0	98.7	1.29
WB238D0	283.6	284	128.0	82.3	109.8	0.22
WB238D0	284	284.45	141.3	72.9	59.3	0.22
WB238D0	284.45	284.91	65.1	60.8	59.3	0.69
WB238D0	284.91	285.5	86.3	83.3	206.6	0.32
WB238D0	285.5	286	79.3	63.5	84.6	0.19
WB238D0	289.5	290.17	4.4	4.4	4.4	0.23
WB238D0	290.17	291.17	9.4	9.4	9.4	0.11
WB238D0	291.17	292.17	7.5	7.5	7.5	0.13
WB238D0	293	294	10.3	10.3	10.3	0.10

WB238D0	294	295	11.9	11.9	11.9	0.08
WB244D0	191	191.5	16.5	8.3	8.3	0.12
WB244D0	191.5	192	14.6	7.3	7.3	0.14
WB244D0	192	192.5	6.4	6.4	6.4	0.16
WB244D0	192.5	193	12.4	6.2	12.4	0.16
WB244D0	193	193.5	3.0	3.0	6.0	0.33
WB244D0	193.5	194	6.8	6.8	20.4	0.15
WB244D0	194	194.26	7.5	7.5	15.1	0.13
WB244D0	194.26	194.76	15.3	10.2	17.9	0.39
WB244D0	194.76	195.26	39.2	24.4	36.1	1.97
WB244D0	195.26	195.76	20.7	15.6	41.5	0.19
WB244D0	195.76	196.26	9.2	5.1	18.4	0.98
WB244D0	196.26	196.76	9.8	4.9	24.6	0.20
WB244D0	196.76	197.26	10.6	5.3	31.7	0.19
WB244D0	197.26	197.76	9.3	4.6	23.2	0.22
WB244D0	197.76	198.26	18.7	11.2	22.5	0.27
WB244D0	198.26	198.76	20.5	20.5	30.8	0.20
WB244D0	198.76	199.26	36.2	36.2	31.1	0.19
WB244D0	199.26	199.76	46.6	46.6	23.3	0.13
WB244D0	199.76	200.26	33.1	24.8	16.5	0.12
WB244D0	200.26	200.76	36.6	27.5	18.3	0.11
WB244D0	200.76	201.53	43.0	28.7	14.3	0.14
WB244D0	201.53	201.8	74.0	81.4	14.8	0.14
WB244D0	201.8	202.3	116.0	58.0	19.3	0.16
WB244D0	202.3	202.8	26.5	13.3	26.5	0.30
WB244D0	202.8	203.3	17.2	11.5	30.2	0.70
WB244D0	203.3	203.8	15.0	15.0	27.6	0.40
WB244D0	203.8	204.3	10.7	8.0	18.7	0.37
WB244D0	204.3	204.8	12.6	6.3	18.9	0.32
WB244D0	204.8	205.3	11.3	8.4	16.9	0.36
WB244D0	205.3	205.8	10.4	8.3	16.6	0.48
WB244D0	205.8	206.3	14.7	9.8	19.6	0.41
WB244D0	206.3	206.8	16.3	9.8	19.6	0.31
WB244D0	206.8	207.3	16.5	12.0	19.6	0.66
WB244D0	207.3	207.8	21.6	14.9	21.6	1.48
WB244D0	207.8	208.45	28.4	17.1	15.6	0.70
WB244D0	208.45	208.95	86.6	89.8	38.5	0.31
WB244D0	208.95	209.45	35.1	28.1	14.1	0.14
WB244D0	209.45	209.95	358.6	44.8	7.5	0.13
WB244D0	209.95	210.45	271.6	297.3	29.4	0.27
WB244D0	210.45	210.95	373.2	443.9	31.4	0.25
WB244D0	210.95	211.45	205.5	154.1	34.2	0.06
WB244D0	211.45	211.95	200.3	96.1	16.0	0.12
WB244D0	211.95	212.45	147.5	118.0	14.7	0.07
WB244D0	212.45	212.95	384.8	188.5	31.4	0.13
WB244D0	212.95	213.45	38.1	38.1	12.7	0.08
WB244D0	213.45	213.95	564.9	461.8	58.0	0.47
WB244D0	213.95	214.45	257.1	126.2	21.4	0.84

WB244D0	214.45	214.95	129.3	142.3	25.9	0.08
WB244D0	214.95	215.45	101.1	67.4	16.8	0.06
WB244D0	215.45	215.95	63.6	79.5	15.9	0.06
WB244D0	215.95	216.45	87.2	116.2	29.1	0.03
WB244D0	216.45	216.95	185.9	59.2	16.9	0.12
WB244D0	216.95	217.45	115.5	53.3	17.8	0.11
WB244D0	217.45	217.95	19.1	19.1	4.8	0.21
WB244D0	217.95	218.45	419.2	204.4	83.2	0.29
WB244D0	218.45	218.88	385.6	205.9	89.9	0.34
WB244D0	218.88	219.38	157.3	77.0	65.2	1.52
WB244D0	219.38	219.88	194.9	91.4	49.2	1.00
WB244D0	219.88	220.38	231.8	130.0	75.5	1.71
WB244D0	220.38	220.88	134.7	68.9	62.6	0.32
WB244D0	220.88	221.38	100.7	30.7	56.9	0.23
WB244D0	221.38	221.7	108.1	32.1	68.9	0.84
WB244D0	221.7	222.2	33.4	10.8	9.7	0.93
WB244D0	222.2	222.7	138.1	62.6	71.7	1.33
WB244D0	222.7	223.2	21.3	9.0	15.4	1.88
WB244D0	223.2	223.7	13.8	5.8	11.6	2.24
WB244D0	223.7	224.2	20.0	9.3	13.0	2.15
WB244D0	224.2	224.7	12.0	5.8	6.2	2.08
WB244D0	224.7	225.2	10.6	5.1	8.1	1.97
WB244D0	225.2	225.7	9.0	3.8	6.0	2.34
WB244D0	225.7	226.2	10.4	5.2	9.9	2.12
WB244D0	226.2	226.7	17.2	10.9	11.3	2.21
WB244D0	226.7	227.2	19.5	10.0	10.7	2.61
WB244D0	227.2	227.7	26.7	12.7	10.9	2.28
WB244D0	227.7	228.2	42.9	26.6	12.7	3.31
WB244D0	228.2	228.7	57.0	37.2	20.5	1.56
WB244D0	228.7	229.2	29.7	15.4	21.6	1.62
WB244D0	229.2	229.7	51.0	30.7	19.6	1.63
WB244D0	229.7	230.2	56.5	32.1	25.4	3.27
WB244D0	230.2	230.7	62.3	36.0	22.4	2.05
WB244D0	230.7	231.2	51.5	43.1	17.9	0.95
WB244D0	231.2	231.7	102.9	32.4	47.0	2.47
WB244D0	231.7	232.2	69.1	52.0	22.3	1.75
WB244D0	232.2	232.7	71.1	36.4	29.9	1.84
WB244D0	232.7	233.2	72.3	45.9	28.2	2.27
WB244D0	233.2	233.7	87.0	48.3	28.2	2.48
WB244D0	233.7	234.2	103.1	48.0	38.0	1.81
WB244D0	234.2	234.7	84.7	52.1	26.5	1.13
WB244D0	234.7	235.2	104.0	63.6	24.3	1.81
WB244D0	235.2	235.7	95.3	66.4	24.5	0.69
WB244D0	235.7	236.2	76.7	50.0	16.7	0.60
WB244D0	236.2	236.7	94.6	61.0	25.2	0.48
WB244D0	236.7	237.2	93.1	59.7	25.3	0.99
WB244D0	237.2	237.7	107.3	72.7	28.1	1.21
WB244D0	237.7	238.2	90.9	62.6	26.8	0.67

WB244D0	238.2	238.59	92.6	63.6	26.0	0.35
WB244D0	238.59	239.09	126.1	81.5	28.6	1.19
WB244D0	239.09	239.59	32.8	19.2	21.5	2.56
WB244D0	239.59	240.09	166.6	119.0	43.2	1.13
WB244D0	240.09	240.59	124.1	127.4	32.7	0.31
WB244D0	240.59	241.09	62.7	40.7	16.5	0.91
WB244D0	241.09	241.59	77.3	62.2	12.1	1.32
WB244D0	241.59	242.09	32.9	12.4	8.2	0.24
WB244D0	242.09	242.59	63.8	51.0	17.0	0.24
WB244D0	242.59	243.09	80.8	40.7	30.9	1.42
WB244D0	243.09	243.59	198.6	191.0	7.6	0.13
WB244D0	243.59	244.09	72.7	31.2	10.4	0.10
WB244D0	244.09	244.59	214.0	278.2	10.7	0.09
WB244D0	244.59	245.09	201.3	106.6	23.7	0.08
WB244D0	245.09	245.59	23.5	5.9	5.9	0.17
WB244D0	245.59	246.09	14.0	7.0	7.0	0.14
WB244D0	246.09	246.59	21.5	21.5	43.1	0.05
WB244D0	246.59	247.09	21.9	10.9	10.9	0.09
WB244D0	247.09	247.59	89.1	53.5	17.8	0.06
WB244D0	247.59	248.09	441.0	388.5	31.5	0.10
WB244D0	248.09	248.59	594.4	439.3	77.5	0.08
WB244D0	248.59	249.09	174.3	104.6	34.9	0.06
WB244D0	249.09	249.59	1525.6	1063.0	78.7	0.10
WB244D0	249.59	250.09	593.1	294.0	50.7	0.20
WB244D0	250.09	250.59	571.5	405.1	21.7	0.28
WB244D0	250.59	251.09	473.6	224.9	47.4	0.17
WB244D0	251.09	251.59	153.9	56.0	14.0	0.07
WB244D0	251.59	252.09	123.6	30.9	15.5	0.06
WB244D0	252.09	252.59	89.5	44.7	19.2	0.16
WB244D0	252.59	253.09	53.1	10.6	21.3	0.09
WB244D0	253.09	253.59	523.1	403.0	56.6	0.14
WB244D0	253.59	254.09	43.0	32.3	43.0	0.09
WB244D0	254.09	254.59	167.6	188.5	167.6	0.10
WB244D0	254.59	255.09	174.6	266.5	147.0	0.33
WB244D0	255.09	255.53	159.9	116.7	28.2	0.53
WB244D0	255.53	256.03	6.7	3.3	6.7	0.30
WB244D0	256.03	256.53	6.4	6.4	12.9	0.16
WB244D0	256.53	257.03	14.0	9.3	18.6	0.21
WB244D0	257.03	257.53	4.9	4.9	24.7	0.20
WB244D0	257.53	258.03	9.7	9.7	19.4	0.10
WB244D0	258.03	258.53	14.8	14.8	22.2	0.13
WB244D0	258.53	259.05	110.2	88.2	36.7	1.23
WB244D0	259.05	259.55	161.6	95.5	290.1	0.27
WB244D0	259.55	260.36	65.3	32.7	39.2	0.15
WB244D0	260.36	260.86	80.8	34.4	50.9	0.67
WB244D0	260.86	261.36	249.6	86.3	200.7	0.96
WB244D0	261.36	261.86	113.2	79.6	47.7	1.13
WB244D0	261.86	262.15	89.3	61.7	48.0	1.81

WB244D0	262.15	262.65	57.2	19.1	146.2	0.16
WB244D0	262.65	263.15	178.7	79.3	79.3	0.69
WB244D0	264.85	265.35	9.9	9.9	9.9	0.10
WB244D0	265.35	265.85	124.6	83.0	62.3	0.05
WB244D0	265.85	266.35	52.4	39.3	52.4	0.08
WB244D0	266.35	266.94	115.3	43.9	49.4	0.18
WB244D0	266.94	267.44	379.8	104.0	57.5	1.53
WB244D0	267.44	267.94	164.7	81.7	110.3	0.77
WB244D0	267.94	268.44	167.2	93.1	82.5	0.47
WB244D0	268.44	268.94	213.2	118.4	86.8	0.13
WB244D0	269.6	270.1	12.1	12.1	12.1	0.08
WB244D0	270.1	271.1	63.3	37.4	31.7	0.35
WB244D0	271.1	272.1	56.2	5.8	9.7	0.52
WB244D0	272.1	273.1	21.1	26.3	15.8	0.19
WB244D0	273.1	274.1	14.6	7.3	14.6	0.14
WB244D0	274.1	275.1	23.9	8.0	16.0	0.13
WB244D0	275.1	275.5	8.4	8.4	8.4	0.12
WB244D0	275.5	276.5	9.3	9.3	9.3	0.11
WB244D0	276.5	277.5	11.8	11.8	11.8	0.08
WB244D0	281.5	282.5	86.4	43.2	14.4	0.07
WB244D0	282.5	283.5	102.1	43.8	14.6	0.07
WB215D0	205	206	255.5	154.2	39.7	0.23
WB215D0	206	207	304.6	137.7	72.3	0.72
WB215D0	207	207.5	219.0	158.1	48.7	0.08
WB215D0	207.5	208	296.3	89.4	96.8	0.67
WB215D0	208	208.5	434.2	207.6	82.6	0.47
WB215D0	208.5	209	250.7	136.8	45.6	0.04
WB215D0	209	209.5	63.9	31.9	53.2	0.09
WB215D0	209.5	210	195.8	80.0	108.5	1.09
WB215D0	210	210.5	188.1	118.7	138.9	0.89
WB215D0	210.5	211	135.6	71.3	56.9	2.16
WB215D0	211	211.5	83.2	67.1	33.4	3.29
WB215D0	211.5	212	193.6	129.6	218.0	0.66
WB215D0	212	212.5	127.6	151.9	42.5	0.16
WB215D0	212.5	213	31.3	10.4	5.2	0.19
WB215D0	213	213.5	117.6	70.5	36.1	0.64
WB215D0	213.5	214	59.4	33.9	17.0	0.12
WB215D0	214	214.5	123.4	74.0	32.1	0.41
WB215D0	214.5	215	92.0	61.4	21.9	1.37
WB215D0	215	215.5	109.8	118.9	27.4	0.11
WB215D0	215.5	216	79.6	47.6	10.7	1.03
WB215D0	216	216.5	75.4	58.5	11.1	1.54
WB215D0	216.5	217	92.6	61.5	78.7	1.51
WB215D0	217	217.5	80.7	52.9	20.0	1.80
WB215D0	217.5	218	74.2	44.6	37.9	2.98
WB215D0	218	218.74	138.7	80.6	48.7	1.07
WB215D0	218.74	219.05	198.6	126.7	46.8	0.88
WB215D0	219.05	219.5	40.5	24.4	14.0	1.43

WB215D0	219.5	220	23.9	23.9	7.2	0.42
WB215D0	220	220.5	100.0	60.0	35.2	1.25
WB215D0	220.5	221	99.7	56.0	43.7	0.73
WB215D0	221	221.5	104.6	63.5	35.5	0.54
WB215D0	221.5	222	109.7	61.2	39.3	0.87
WB215D0	227	228	169.7	73.8	44.3	0.14
WB215D0	228	229	94.0	35.9	9.8	1.84
WB215D0	229	230	744.0	303.4	21.7	0.14
WB215D0	230	231	132.2	66.1	16.5	0.06
WB215D0	231	232	106.2	38.6	9.7	0.10
WB215D0	232	233	306.3	209.6	16.1	0.06
WB215D0	233	234	316.3	265.7	12.7	0.08
WB215D0	234	235	565.6	342.3	14.9	0.07
WB215D0	235	236	551.5	318.6	12.3	0.08
WB215D0	236	237	370.1	142.3	14.2	0.07
WB215D0	237	238	94.1	38.7	5.5	0.18
WB215D0	238	238.53	55.2	20.7	6.9	0.15
WB215D0	238.53	239	72.7	36.4	36.4	0.08
WB215D0	239	240	190.6	119.3	110.2	0.77
WB215D0	240	240.5	179.2	177.2	202.8	0.51
WB215D0	240.5	241	48.7	16.2	40.5	0.12
WB215D0	241	241.5	177.7	132.6	110.7	0.69
WB215D0	241.5	242	140.8	109.0	95.3	0.22
WB215D0	242	242.5	182.3	119.5	121.3	1.11
WB215D0	242.5	243	176.8	121.5	167.9	0.45
WB215D0	243	243.5	326.3	232.0	158.1	0.39
WB215D0	243.5	244	126.5	63.2	47.4	0.32
WB215D0	244	244.5	185.6	109.4	91.0	0.81
WB215D0	244.5	245	366.5	278.5	129.0	0.34
WB215D0	245	245.5	58.6	50.2	58.6	0.12
WB215D0	245.5	246	30.8	30.8	30.8	0.13
WB215D0	246	246.5	5.6	5.6	16.9	0.18
WB215D0	246.5	247	19.9	14.9	29.8	0.20
WB215D0	247	247.68	106.3	119.8	127.1	1.11
WB215D0	247.68	248	115.9	128.5	1116.4	0.47
WB215D0	249	250	179.9	57.6	50.4	0.14
WB215D0	251	251.5	56.7	18.9	18.9	0.11
WB215D0	253.17	254	16.1	16.1	16.1	0.06
WB215D0	254	254.36	9.4	9.4	9.4	0.11
WB222D0	162	163	16.7	8.3	8.3	0.12
WB222D0	163	163.64	19.6	9.8	9.8	0.10
WB222D0	163.64	164.12	7.3	3.7	3.7	0.27
WB222D0	164.12	164.6	15.7	7.9	7.9	0.13
WB222D0	164.6	165	13.3	6.6	6.6	0.15
WB222D0	165	165.5	22.8	17.8	7.6	0.39
WB222D0	165.5	166	40.0	30.5	22.9	1.05
WB222D0	166	166.5	24.9	22.4	21.4	2.01
WB222D0	166.5	167	19.2	14.4	38.3	0.21

WB222D0	167	167.5	223.2	154.5	34.3	0.12
WB222D0	167.5	168	68.5	22.8	22.8	0.09
WB222D0	168	168.5	1036.8	542.8	42.3	0.31
WB222D0	168.5	169	365.7	106.4	33.2	0.15
WB222D0	169	169.5	26.8	26.8	26.8	0.11
WB222D0	169.5	170	102.4	51.2	51.2	0.04
WB222D0	170	170.5	56.6	56.6	28.3	0.07
WB222D0	170.5	171	128.8	128.8	42.9	0.05
WB222D0	171	172	88.6	73.9	14.8	0.07
WB222D0	172	173	48.3	48.3	24.2	0.08
WB222D0	173	174	46.2	46.2	15.4	0.06
WB222D0	174	174.5	20.6	13.8	6.9	0.29
WB222D0	174.5	175	71.4	53.6	17.9	0.11
WB222D0	175	175.5	112.6	70.4	28.2	0.07
WB222D0	175.5	176	31.3	25.0	12.5	0.16
WB222D0	176	176.5	7.9	3.9	7.9	0.25
WB222D0	176.5	177	11.4	11.4	11.4	0.18
WB222D0	177	177.5	24.1	8.0	24.1	0.12
WB222D0	177.5	178	9.2	4.6	9.2	0.22
WB222D0	178.5	179	7.8	7.8	15.5	0.13
WB222D0	179.5	180	9.6	4.8	9.6	0.21
WB222D0	180	180.5	10.9	5.5	16.4	0.18
WB222D0	180.5	181	13.0	6.5	13.0	0.15
WB222D0	181	181.5	7.3	3.6	7.3	0.28
WB222D0	181.5	182	2.8	5.5	8.3	0.36
WB222D0	182	182.5	5.8	5.8	5.8	0.34
WB222D0	182.5	183	7.1	7.1	7.1	0.14
WB222D0	183	183.5	4.7	2.4	2.4	0.42
WB222D0	183.5	184	16.4	16.4	16.4	0.06
WB222D0	184	184.5	9.6	19.1	19.1	0.10
WB222D0	184.5	184.93	16.9	25.4	16.9	0.12
WB222D0	185.2	185.5	5.4	10.9	5.4	0.18
WB222D0	185.5	186	12.0	30.0	12.0	0.17
WB222D0	186	186.5	10.2	20.3	20.3	0.10
WB222D0	186.5	187	6.1	18.4	12.2	0.16
WB222D0	187	187.5	9.8	19.7	9.8	0.10
WB222D0	187.5	188	2.0	4.0	2.0	0.50
WB222D0	188	189	22.0	22.0	11.0	0.09
WB222D0	217	218	65.7	26.3	13.1	0.08
WB222D0	218	218.5	80.3	50.2	10.0	0.10
WB222D0	218.5	219	62.1	34.5	9.2	0.43
WB222D0	219	219.5	21.6	10.8	10.8	0.09
WB222D0	219.5	220	24.4	16.3	8.1	0.25
WB222D0	220	220.5	111.4	82.1	20.5	0.34
WB222D0	220.5	221	72.8	62.4	15.6	0.19
WB222D0	221	221.5	104.4	103.5	25.6	1.13
WB222D0	221.5	222	130.9	114.4	23.6	3.09
WB222D0	222	222.5	117.7	84.6	31.8	2.39

WB222D0	222.5	222.88	91.0	76.8	20.2	2.18
WB222D0	222.88	223.5	92.5	66.4	18.7	1.76
WB222D0	223.5	224.24	119.2	83.2	26.7	0.97
WB222D0	224.24	224.6	155.0	70.9	18.7	0.54
WB222D0	224.6	225.08	97.4	55.8	14.3	0.70
WB222D0	225.5	226	129.3	112.6	20.9	0.48
WB222D0	226.36	227	80.7	57.6	11.5	0.09
WB222D0	227	228	110.4	110.4	27.6	0.04
WB222D0	294	295	320.1	166.0	59.3	0.08
WB222D0	295	295.33	206.8	113.2	68.9	0.20
WB222D0	295.33	296	399.7	246.1	151.7	1.05
WB222D0	296	296.5	680.4	446.2	170.9	0.63
WB222D0	296.5	297	163.4	83.1	75.9	1.12
WB222D0	297	297.5	204.7	92.9	72.4	1.27
WB222D0	297.5	298	230.8	104.1	75.0	1.72
WB222D0	298	298.5	174.4	76.0	45.8	0.89
WB222D0	298.5	299	129.0	49.5	39.2	0.87
WB222D0	299	299.5	195.9	80.9	48.8	1.84
WB222D0	299.5	300	227.6	96.1	56.4	2.04
WB222D0	300	300.5	218.5	94.6	59.1	1.44
WB222D0	300.5	301	143.2	56.9	32.5	0.98
WB222D0	301	301.5	154.4	67.1	49.7	1.89
WB222D0	301.5	302	128.5	65.6	13.1	1.07
WB222D0	302	302.5	226.4	74.9	43.5	0.57
WB222D0	302.5	303	138.8	66.0	34.8	1.89
WB222D0	303.5	304	23.0	17.9	6.4	0.78
WB222D0	304	304.5	103.6	32.6	63.6	2.45
WB222D0	304.5	305	141.8	27.1	33.4	0.48
WB222D0	305	305.5	113.9	18.6	43.7	3.39
WB222D0	307	307.5	241.9	110.4	99.9	0.19
WB222D0	307.5	308	96.1	50.9	28.3	0.18
WB222D0	308	308.52	118.4	52.6	34.2	0.38
WB222D0	309	309.5	28.8	38.4	9.6	0.10
WB222D0	310.5	310.88	95.1	111.0	15.9	0.13
WB222D0	310.88	311.13	177.4	67.5	174.5	1.36
WB222D0	311.13	312	174.4	195.3	41.9	0.14
WB222D0	312	312.5	72.9	72.9	36.5	0.14
WB222D0	312.5	313	139.7	72.3	32.4	0.40
WB222D0	313	313.5	85.1	85.1	17.0	0.12
WB222D0	313.5	314	64.8	97.1	10.8	0.09
WB222D0	314	315	52.8	63.3	21.1	0.09
WB222D0	315.3	315.55	43.8	27.7	103.7	0.68
WB222D0	315.55	315.91	55.6	20.2	36.2	1.44
WB222D0	315.91	316.59	178.7	90.0	54.8	0.77
WB222D0	316.59	317.17	75.7	66.3	28.4	0.11
WB222D0	317.17	317.63	46.4	38.7	23.2	0.13
WB222D0	317.63	318	45.1	36.1	18.0	0.11
WB222D1	272	273	66.1	37.8	9.4	0.11

WB222D1	273	273.4	127.4	79.6	15.9	0.06
WB222D1	273.4	273.86	120.0	60.0	12.0	0.08
WB222D1	276.38	277	23.3	31.1	7.8	0.13
WB222D1	287	288	132.3	132.3	33.1	0.03
WB222D1	288	289	164.9	164.9	33.0	0.03
WB222D1	294	295	77.4	77.4	19.3	0.05
WB222D1	295	295.5	639.6	539.7	60.0	0.05
WB222D1	295.5	296.08	547.0	247.2	105.1	0.32
WB222D1	296.08	296.5	659.9	188.2	95.3	0.40
WB222D1	296.5	297	226.4	94.0	65.4	1.82
WB222D1	297	297.5	225.3	69.7	87.3	2.21
WB222D1	297.5	298	235.2	90.3	53.2	1.37
WB222D1	298	298.5	143.1	88.5	26.8	1.94
WB222D1	298.5	299	138.9	53.6	26.8	1.64
WB222D1	299	299.5	194.8	78.3	39.4	1.83
WB222D1	299.5	300	172.1	81.4	34.1	2.05
WB222D1	300	300.5	187.5	69.9	42.1	2.87
WB222D1	300.5	301	203.5	72.1	46.6	1.57
WB222D1	301	301.58	151.3	61.2	47.9	2.32
WB222D1	301.58	302	213.0	86.2	41.4	2.37
WB222D1	302	302.5	155.0	32.6	279.3	5.73
WB222D1	302.5	303	205.5	80.4	64.8	0.45
WB222D1	303	303.5	205.3	86.9	50.0	0.38
WB222D1	303.5	304	164.9	76.4	40.2	0.25
WB222D1	305.5	306	96.0	54.9	13.7	0.15
WB222D1	306	306.5	146.8	76.1	21.7	0.18
WB222D1	306.5	307	84.8	60.6	36.4	0.08
WB222D1	307	307.5	29.7	44.6	14.9	0.07
WB222D1	307.5	308	36.3	36.3	12.1	0.08
WB222D1	310	310.5	41.6	77.2	5.9	0.17
WB222D1	310.5	311	115.5	96.2	28.9	0.10
WB222D1	311	311.32	180.1	85.4	34.6	0.43
WB222D1	312.5	313	105.2	57.2	22.9	0.44
WB222D1	313	314	68.8	103.2	22.9	0.09
WB222D1	314	315	70.3	54.1	10.8	0.18
WB221D0	158	158.89	6.9	13.8	6.9	0.14
WB221D0	158.89	159.5	6.5	13.1	6.5	0.15
WB221D0	159.5	160	7.5	7.5	7.5	0.13
WB221D0	160	161	6.7	6.7	6.7	0.15
WB221D0	161	162	7.1	7.1	7.1	0.14
WB221D0	162	162.5	5.4	5.4	5.4	0.19
WB221D0	162.5	163.16	3.0	3.0	3.0	0.34
WB221D0	163.16	163.5	8.7	8.7	8.7	0.11
WB221D0	163.5	164	10.5	10.5	10.5	0.10
WB221D0	164	164.5	4.9	4.9	4.9	0.20
WB221D0	165	165.5	31.2	31.2	31.2	0.03
WB221D0	165.5	166	6.4	6.4	6.4	0.16
WB221D0	166	166.5	5.8	5.8	5.8	0.17

WB221D0	166.5	167.23	5.9	5.9	5.9	0.17
WB221D0	167.23	167.6	8.2	4.1	4.1	0.24
WB221D0	167.6	168	10.3	10.3	10.3	0.10
WB221D0	168	168.5	15.4	0.3	0.3	3.90
WB221D0	168.5	169	7.5	7.5	7.5	0.13
WB221D0	169	169.45	28.7	14.8	2.5	2.37
WB221D0	169.45	170	183.5	83.1	33.5	0.93
WB221D0	170	170.5	39.2	23.0	5.3	2.65
WB221D0	170.5	171	14.5	14.5	7.2	0.14
WB221D0	171	171.5	28.5	19.0	19.0	0.11
WB221D0	171.5	172	49.1	36.8	24.5	0.08
WB221D0	172	172.5	52.7	52.7	26.3	0.08
WB221D0	172.5	173	72.7	101.8	29.1	0.07
WB221D0	173	173.5	52.8	52.8	23.5	0.17
WB221D0	173.5	174	45.9	52.5	19.7	0.15
WB221D0	174	174.5	19.2	21.1	11.5	0.52
WB221D0	174.5	175	73.4	73.4	45.9	0.11
WB221D0	175	175.5	103.4	137.9	57.4	0.09
WB221D0	175.5	176	88.0	73.5	47.2	1.10
WB221D0	176	176.25	63.9	57.7	20.3	1.77
WB221D0	176.25	177	64.0	44.3	23.0	0.61
WB221D0	177	178	4.3	8.6	12.8	0.23
WB221D0	178	179	12.0	6.0	12.0	0.17
WB221D0	225	226	22.6	56.6	11.3	0.09
WB221D0	226	227	21.3	42.6	10.7	0.09
WB221D0	227	228	22.6	33.9	11.3	0.09
WB221D0	228	229	25.9	38.8	12.9	0.08
WB221D0	229	230	34.1	45.4	11.4	0.09
WB221D0	230	231	20.4	51.0	10.2	0.10
WB221D0	231	232	24.4	48.7	12.2	0.08
WB221D0	232	233	19.6	29.5	9.8	0.10
WB221D0	233	233.68	28.8	38.4	9.6	0.10
WB221D0	233.68	234	29.6	29.6	9.9	0.10
WB221D0	234	235	50.9	20.4	10.2	0.10
WB221D0	235	236	103.7	34.6	11.5	0.09
WB221D0	236	236.71	105.6	46.9	11.7	0.09
WB221D0	236.71	237	97.9	32.6	10.9	0.09
WB221D0	237	238	116.7	46.7	11.7	0.09
WB221D0	238	239	106.9	38.9	9.7	0.10
WB221D0	239	240	114.4	35.2	8.8	0.11
WB221D0	240	241	92.0	40.9	10.2	0.10
WB221D0	244	245	46.2	46.2	9.2	0.11
WB221D0	245	245.3	28.6	28.6	9.5	0.11
WB221D0	245.3	245.97	36.8	36.8	12.3	0.08
WB221D0	245.97	246.5	40.6	40.6	13.5	0.07
WB221D0	246.5	247	28.4	47.3	18.9	0.11
WB221D0	247	248	38.4	38.4	9.6	0.10
WB221D0	248	249	44.4	37.0	7.4	0.14

WB221D0	249	250	66.0	56.6	9.4	0.11
WB221D0	250	251	50.3	50.3	12.6	0.08
WB221D0	251	252	50.3	50.3	12.6	0.08
WB221D0	252	253	50.3	50.3	12.6	0.08
WB221D0	253	254	36.9	36.9	9.2	0.11
WB221D0	254	255	47.6	35.7	11.9	0.08
WB221D0	255	256	49.6	49.6	12.4	0.08
WB221D0	256	257	51.0	63.8	12.8	0.08
WB221D0	257	258	83.8	95.7	12.0	0.08
WB221D0	258	259	133.2	116.5	16.6	0.06
WB221D0	263	264	66.9	61.3	5.6	0.18
WB221D0	264	265	112.4	158.7	13.2	0.15
WB221D0	266.1	266.7	71.1	71.1	6.5	0.15
WB221D0	267.28	268	46.2	46.2	5.1	0.19
WB221D0	268	269	48.4	48.4	6.9	0.14
WB221D0	269	270	59.7	59.7	8.5	0.12
WB221D0	271.82	272.5	69.3	46.2	11.5	0.09
WB221D0	272.5	273	46.3	38.6	7.7	0.13
WB221D0	273	274	41.0	24.6	8.2	0.12
WB221D0	276	277	57.1	57.1	9.5	0.10
WB221D0	286	287	17.1	17.1	8.6	0.23
WB221D0	287	287.4	19.2	19.2	7.7	0.26
WB221D0	296	297	31.4	17.9	22.4	0.22
WB221D0	297	297.25	164.5	100.8	47.8	0.19
WB221D0	297.25	297.75	189.6	105.4	73.7	0.38
WB221D0	297.75	298	287.7	173.9	136.6	0.48
WB221D0	298	298.5	351.9	205.9	112.3	0.53
WB221D0	298.5	299	14.7	4.9	9.8	0.61
WB221D0	299	299.5	11.8	15.7	15.7	0.26
WB221D0	299.5	300.12	127.6	61.0	44.4	0.18
WB221D0	301.02	301.5	14.5	14.5	43.4	0.07
WB221D0	301.5	302	12.6	12.6	25.1	0.08
WB213D0	178	178.521	10.9	10.9	10.9	0.09
WB213D0	178.521	179	6.9	6.9	6.9	0.14
WB213D0	179	179.5	8.9	8.9	8.9	0.11
WB213D0	179.5	179.9	13.8	13.8	13.8	0.07
WB213D0	179.9	180.2	13.0	13.0	13.0	0.08
WB213D0	180.2	180.68	4.3	4.3	4.3	0.23
WB213D0	180.68	181	15.1	15.1	15.1	0.07
WB213D0	181	181.5	4.6	4.6	4.6	0.22
WB213D0	181.5	182	7.6	7.6	7.6	0.13
WB213D0	182	182.5	11.6	11.6	11.6	0.09
WB213D0	182.5	183	10.1	10.1	10.1	0.10
WB213D0	183	183.6	8.3	8.3	8.3	0.12
WB213D0	183.6	184.3	1.1	1.1	1.1	0.87
WB213D0	184.3	185	2.6	0.0	2.6	0.39
WB213D0	185	185.67	7.2	7.2	7.2	0.14
WB213D0	185.67	186	7.5	7.5	7.5	0.13

WB213D0	186	186.5	10.8	10.8	10.8	0.09
WB213D0	186.5	186.97	10.4	10.4	31.1	0.10
WB213D0	186.97	187.5	11.3	7.5	33.8	0.53
WB213D0	187.5	187.84	8.0	4.8	19.2	0.63
WB213D0	187.84	188.5	15.5	9.9	36.4	0.91
WB213D0	188.5	188.9	12.2	10.1	28.4	1.48
WB213D0	188.9	189.2	13.0	10.4	32.5	2.31
WB213D0	189.2	189.5	17.4	14.2	32.3	2.88
WB213D0	189.5	190	17.6	14.1	40.6	1.13
WB213D0	190	190.5	103.6	144.6	43.4	0.41
WB213D0	190.5	191	23.8	22.2	37.8	1.22
WB213D0	191	191.5	29.9	41.0	43.1	1.97
WB213D0	191.5	192	27.6	25.9	71.1	1.19
WB213D0	192	192.5	12.9	9.7	30.6	0.62
WB213D0	192.5	193	12.1	9.1	39.4	0.33
WB213D0	193	193.5	14.7	11.3	21.7	1.15
WB213D0	193.5	194	13.6	8.3	28.5	1.69
WB213D0	194	194.3	15.5	9.5	18.5	3.68
WB213D0	194.3	195	7.3	7.3	25.4	0.28
WB213D0	195	195.5	18.6	15.5	27.9	0.32
WB213D0	195.5	195.94	27.7	38.1	17.3	0.29
WB213D0	195.94	196.5	233.8	190.0	70.0	0.80
WB213D0	196.5	197	64.6	41.7	31.6	0.70
WB213D0	197	197.5	182.3	118.3	46.3	2.14
WB213D0	197.5	198	219.3	124.2	25.2	0.52
WB213D0	198	198.5	352.4	283.4	52.9	1.06
WB213D0	198.5	199	228.2	184.5	43.7	0.21
WB213D0	199	199.5	17.2	15.0	4.3	0.47
WB213D0	199.5	200	21.0	21.0	12.6	0.24
WB213D0	200	200.5	21.3	31.9	5.3	0.19
WB213D0	200.5	201	64.3	55.1	27.5	0.11
WB213D0	201	201.5	18.2	27.2	9.1	0.11
WB213D0	201.5	202	32.1	42.8	10.7	0.09
WB213D0	250	250.51	43.4	32.5	10.8	0.09
WB213D0	250.51	251	53.7	53.7	23.0	0.13
WB213D0	251	251.61	110.4	78.9	31.6	0.13
WB213D0	251.61	251.93	45.7	41.5	12.5	0.24
WB213D0	251.93	252.5	77.4	61.9	23.2	0.13
WB213D0	252.5	253	105.8	95.2	31.7	0.09
WB213D0	253	253.5	142.2	124.4	35.5	0.06
WB213D0	253.5	254	69.1	61.5	15.4	0.13
WB213D0	254	254.5	63.5	50.8	19.0	0.16
WB213D0	254.5	255	31.9	19.2	12.8	0.16
WB213D0	255	255.5	16.1	10.8	16.1	0.19
WB213D0	255.5	256.15	45.7	34.3	45.7	0.09
WB213D0	256.15	256.69	431.6	215.8	86.3	0.02
WB213D0	256.69	257	147.5	73.7	73.7	0.01
WB213D0	257	258	160.8	80.4	80.4	0.01

WB213D0	258	259	83.4	41.7	41.7	0.02
WB213D0	259	260	26.9	13.5	13.5	0.07
WB213D0	260	261	53.9	27.0	27.0	0.04
WB213D0	261	262	68.4	22.8	22.8	0.04
WB213D0	262	263	50.1	16.7	16.7	0.06
WB213D0	263	264	117.3	39.1	39.1	0.03
WB213D0	264	265	85.7	21.4	21.4	0.05
WB213D0	265	266	116.1	19.4	19.4	0.05
WB213D0	266	267	63.8	10.6	10.6	0.09
WB213D0	267	268	68.8	13.8	13.8	0.07
WB213D0	268	269	30.5	10.2	10.2	0.10
WB213D0	269	270	51.2	17.1	17.1	0.06
WB213D0	270	271	23.0	23.0	11.5	0.09
WB213D0	271	272	20.2	20.2	10.1	0.10
WB213D0	272	273	27.1	13.6	13.6	0.07
WB213D0	273	274	38.2	19.1	19.1	0.05
WB213D0	274	275	28.4	14.2	14.2	0.07
WB213D0	275	276	16.6	16.6	16.6	0.06
WB213D0	276	276.5	60.9	20.3	20.3	0.05
WB213D0	276.5	277.25	36.8	12.3	12.3	0.08
WB213D0	278	279	60.1	51.5	34.3	0.12
WB213D0	279.35	279.62	19.4	32.3	38.7	0.16
WB213D0	281.8	283.35	6.4	4.3	10.7	0.47
WB213D0	284	284.5	27.2	57.7	101.9	0.88
WB213D0	284.5	285	41.2	70.5	99.8	1.26
WB213D0	285	285.5	76.3	111.6	129.9	0.88
WB213D0	285.5	286	41.2	71.8	106.3	0.75
WB213D0	286	286.5	43.5	76.5	91.8	2.87
WB213D0	286.5	287	42.9	71.0	56.4	4.66
WB213D0	287	287.5	77.7	158.0	149.4	1.99
WB213D0	287.5	288	68.5	133.6	114.5	0.89
WB213D0	288	288.57	80.1	130.7	149.3	1.56
WB213D0	288.57	289	52.2	69.6	116.0	0.17
WB213D0	289	289.5	45.8	58.8	71.9	0.15
WB213D0	289.5	290	40.2	13.4	53.7	0.07
WB213D0	290	290.5	135.1	189.2	108.1	0.11
WB213D0	290.5	291	8.3	8.3	83.3	0.12
WB213D0	291	291.5	13.8	13.8	41.3	0.07
WB213D0	291.5	292	8.8	8.8	17.5	0.11
WB213D0	292	292.5	12.6	12.6	12.6	0.08
WB213D0	292.5	293	10.1	10.1	20.2	0.10
WB213D0	293	293.5	81.6	183.2	107.0	0.55
WB213D0	293.5	294	87.6	219.1	125.2	0.32
WB213D0	294	294.5	9.1	27.2	18.1	0.11
WB213D0	294.5	295	10.6	21.2	10.6	0.09
WB235D0	199	199.5	11.6	11.6	23.3	0.09
WB235D0	199.5	200	350.7	185.2	39.6	0.56
WB235D0	200	200.5	112.3	70.2	56.2	0.14

WB235D0	200.5	201	91.9	84.2	38.3	0.13
WB235D0	201	201.5	94.3	134.8	27.0	0.07
WB235D0	201.5	202	39.3	58.9	19.6	0.10
WB235D0	202	202.5	82.4	137.4	27.5	0.04
WB235D0	202.5	203	92.0	110.3	18.4	0.05
WB235D0	203	203.5	419.8	190.1	109.5	0.66
WB235D0	203.5	204	341.7	137.5	66.7	0.75
WB235D0	204	204.5	234.4	200.9	75.3	0.60
WB235D0	204.5	205	270.0	145.8	44.7	0.60
WB235D0	205	206	451.4	230.9	63.0	0.10
WB235D0	206	207	53.6	80.4	26.8	0.04
WB235D0	207	207.45	32.4	64.8	32.4	0.03
WB235D0	207.45	208	311.2	173.7	61.1	2.18
WB235D0	208	208.5	207.3	100.3	30.8	1.65
WB235D0	208.5	208.89	60.1	60.1	24.0	0.08
WB235D0	208.89	209.14	64.8	33.4	12.2	0.99
WB235D0	209.14	209.8	365.4	156.0	45.2	0.24
WB235D0	209.8	210.36	1090.5	648.2	153.3	0.23
WB235D0	210.36	210.62	18.5	12.3	15.4	0.32
WB235D0	210.62	211	699.8	442.7	128.5	0.07
WB235D0	211	211.38	845.4	482.2	142.9	0.50
WB235D0	211.38	212	160.5	117.3	74.1	0.16
WB235D0	212	212.5	179.9	135.0	172.5	0.13
WB235D0	212.5	213	322.1	150.2	96.8	0.60
WB235D0	213	213.5	66.2	66.2	40.7	0.20
WB235D0	213.5	214	895.0	834.7	163.4	1.26
WB235D0	214	214.5	1575.1	1214.6	185.5	1.03
WB235D0	214.5	215	117.0	99.0	69.7	0.44
WB235D0	215	216	37.1	41.3	24.8	0.24
WB235D0	216	217	98.0	73.5	49.0	0.16
WB235D0	217	218	27.6	27.6	18.4	0.11
WB235D0	218	219	28.9	19.2	19.2	0.10
WB235D0	219.5	220	46.2	30.8	76.9	0.06
WB235D0	220	221	22.5	22.5	15.0	0.13
WB235D0	263	264	83.8	27.9	27.9	0.04
WB235D0	264	265	35.7	35.7	35.7	0.03
WB235D0	265	265.5	13.8	13.8	13.8	0.07
WB235D0	265.5	265.85	7.9	7.9	7.9	0.13
WB235D0	265.85	266.5	1.7	1.7	1.7	0.59
WB235D0	266.5	267.35	9.6	4.8	9.6	0.21
WB235D0	267.35	267.7	78.7	31.5	15.7	0.06
WB235D0	267.7	268.15	15.9	15.9	15.9	0.06
WB235D0	268.15	268.45	22.6	7.5	7.5	0.27
WB235D0	268.45	269	663.4	333.5	48.2	0.27
WB235D0	269	269.5	516.0	419.3	21.5	0.19
WB235D0	269.5	269.85	69.9	35.0	35.0	0.03
WB235D0	269.85	270.36	17.6	5.9	5.9	0.17
WB235D0	270.36	270.8	38.4	9.6	28.8	0.10

WB235D0	271.18	271.75	165.5	110.6	96.4	2.53
WB235D0	271.75	272.08	208.4	122.8	113.3	1.47
WB235D0	272.08	272.5	100.9	45.8	82.5	0.22
WB235D0	272.5	273	83.5	62.7	112.2	0.38
WB235D0	273	273.5	97.9	55.3	780.1	0.87
WB235D0	273.5	274	24.4	21.4	51.9	0.33
WB235D0	274	274.5	30.5	36.6	140.4	0.16
WB235D0	275	275.5	34.9	35.9	154.3	0.95
WB235D0	277.5	278	62.7	38.9	41.0	0.93
WB235D0	278	278.28	70.4	44.5	137.1	0.27
WB235D0	278.28	278.78	159.7	108.5	173.6	1.15
WB235D0	278.78	279.08	93.9	85.7	85.7	0.25
WB235D0	279.08	279.38	129.1	128.3	99.5	1.25
WB235D0	279.38	280	102.1	81.7	91.9	0.29
WB235D0	285.58	286	13.4	6.7	13.4	0.15
WB235D0	286	286.65	18.3	12.2	12.2	0.16
WB237D0	180	181	12.4	6.2	6.2	0.16
WB237D0	181	182	6.4	6.4	6.4	0.16
WB237D0	182	182.68	5.1	5.1	5.1	0.19
WB237D0	182.68	183	8.8	7.8	17.6	1.02
WB237D0	183	183.5	9.2	7.2	31.9	0.97
WB237D0	183.5	184	14.9	13.2	28.5	2.35
WB237D0	184	184.35	63.3	35.9	66.1	0.70
WB237D0	184.35	185	9.8	14.7	29.5	0.20
WB237D0	185	185.5	8.6	4.3	17.2	0.23
WB237D0	185.5	186	8.6	8.6	17.2	0.23
WB237D0	186	186.5	5.7	11.3	17.0	0.18
WB237D0	186.5	187	5.4	5.4	16.2	0.19
WB237D0	187	187.5	9.2	9.2	13.8	0.22
WB237D0	187.5	188	22.2	22.2	22.2	0.18
WB237D0	188	188.63	34.5	51.8	17.3	0.12
WB237D0	188.63	189	57.7	69.3	23.1	0.09
WB237D0	189	189.5	28.5	34.2	11.4	0.18
WB237D0	189.5	190	37.5	32.8	9.4	0.21
WB237D0	190	190.44	65.0	50.0	10.0	0.20
WB237D0	190.44	191	41.5	24.9	22.8	0.48
WB237D0	191	191.5	43.9	25.9	25.9	0.50
WB237D0	191.5	192	35.0	21.5	24.2	0.37
WB237D0	192	192.5	20.6	16.5	41.1	0.49
WB237D0	192.5	193	25.2	21.6	25.2	0.28
WB237D0	193	193.5	15.2	11.4	26.6	0.26
WB237D0	193.5	194	21.7	24.4	21.7	0.37
WB237D0	194	194.5	17.2	11.5	19.2	1.04
WB237D0	194.5	195	23.4	14.0	23.4	0.43
WB237D0	195	195.5	19.0	14.2	21.3	0.42
WB237D0	195.5	196	13.0	10.4	18.2	0.38
WB237D0	196	196.5	15.6	10.7	18.5	1.03
WB237D0	196.5	197	22.2	16.3	26.0	3.69

WB237D0	197	197.5	23.5	17.4	28.7	2.47
WB237D0	197.5	198	18.8	15.1	27.1	1.92
WB237D0	198	198.5	14.8	13.0	18.5	0.54
WB237D0	198.5	199	23.2	15.9	22.7	2.20
WB237D0	199	199.5	23.2	17.3	23.9	3.88
WB237D0	199.5	200	22.1	17.2	28.8	3.61
WB237D0	200	200.5	19.3	15.4	31.1	2.28
WB237D0	200.5	201	19.7	16.0	32.5	2.18
WB237D0	201	201.76	19.8	14.8	23.9	1.21
WB237D0	202.05	202.5	216.9	344.5	38.3	0.08
WB237D0	202.5	203	528.5	639.8	41.7	0.07
WB237D0	203	203.5	737.9	345.0	67.1	0.10
WB237D0	203.5	204	519.2	167.2	52.8	0.11
WB237D0	204	204.5	39.2	39.2	29.4	0.10
WB237D0	204.5	205	128.2	149.6	14.2	0.14
WB237D0	205	205.5	562.4	321.9	93.7	0.25
WB237D0	205.5	206	334.6	175.3	93.5	0.68
WB237D0	206	206.5	224.2	117.7	74.1	1.08
WB237D0	206.5	207	383.9	195.7	128.0	0.13
WB237D0	207	207.5	223.7	150.9	82.2	2.21
WB237D0	207.5	208	216.9	146.5	75.3	2.26
WB237D0	208	208.5	210.0	152.0	83.3	0.83
WB237D0	208.5	209	192.9	135.8	95.8	4.15
WB237D0	209	209.37	144.0	96.5	70.3	3.47
WB237D0	209.37	210.1	144.4	73.8	66.7	2.79
WB237D0	210.1	210.5	171.2	96.1	50.2	2.57
WB237D0	210.5	211	134.7	102.5	49.1	2.32
WB237D0	211	211.5	126.2	70.5	90.3	0.81
WB237D0	211.5	212	261.5	177.4	68.9	0.86
WB237D0	212	212.46	241.1	133.9	47.0	0.98
WB237D0	212.46	213	115.0	69.0	58.9	1.48
WB237D0	213	213.7	162.6	59.7	81.0	2.83
WB237D0	213.7	214	67.4	33.7	39.4	1.93
WB237D0	214	214.6	115.0	69.6	42.8	2.24
WB237D0	214.6	215	189.0	72.6	36.5	2.58
WB237D0	215	215.5	130.2	77.1	57.3	1.41
WB237D0	215.5	215.81	144.7	61.7	26.2	2.03
WB237D0	215.81	216.16	14.1	25.0	7.8	0.64
WB237D0	216.5	217	65.1	5.0	4.5	2.00
WB237D0	217	217.5	47.2	28.3	28.3	0.11
WB237D0	217.5	217.98	183.4	75.0	108.4	0.36
WB237D0	220.02	220.5	59.1	42.2	38.0	0.24
WB237D0	220.5	221	61.6	30.8	13.2	0.23
WB237D0	221	221.5	86.8	52.1	48.6	0.58
WB237D0	221.5	221.9	90.7	60.4	50.4	0.20
WB237D0	221.9	222.5	74.3	45.1	25.6	1.13
WB237D0	222.5	223	61.7	34.3	19.8	1.72
WB237D0	223	223.5	61.3	38.5	24.5	2.28

WB237D0	223.5	224	55.3	37.2	17.4	1.66
WB237D0	224	224.5	79.6	51.3	28.9	1.52
WB237D0	224.5	225	77.2	55.1	18.7	0.91
WB237D0	225.5	226.08	161.7	72.2	17.2	0.29
WB237D0	226.5	227.16	82.0	55.7	20.5	0.34
WB237D0	227.16	227.5	78.2	53.7	23.5	1.06
WB237D0	227.5	228.05	54.6	34.1	5.5	2.20
WB237D0	228.05	228.5	63.0	49.5	13.5	0.22
WB237D0	229	229.5	60.3	56.9	13.4	0.30
WB237D0	229.5	230	43.5	36.0	9.5	1.06
WB237D0	230	230.5	70.0	45.0	18.4	1.36
WB237D0	231	231.5	72.2	47.5	22.8	1.05
WB237D0	231.5	232	73.0	45.9	28.7	1.22
WB237D0	232.71	233.3	151.3	86.5	13.0	0.23
WB237D0	233.3	234	144.1	82.3	20.6	0.05
WB237D0	234	234.5	122.0	86.0	34.4	0.64
WB237D0	234.5	235	72.7	43.6	28.0	1.86
WB237D0	235	235.5	49.6	31.5	14.1	1.49
WB237D0	235.5	236	120.0	77.3	72.0	0.38
WB237D0	236	236.5	54.2	33.7	14.6	2.20
WB237D0	236.5	237	63.8	46.0	19.6	3.21
WB237D0	237	237.5	108.0	129.6	21.6	0.09
WB237D0	237.5	238	54.1	18.0	36.1	0.06
WB237D0	238	238.5	71.3	89.1	17.8	0.06
WB237D0	238.5	239	12.4	12.4	12.4	0.08
WB237D0	239	239.5	38.4	38.4	19.2	0.05
WB237D0	239.5	240	117.7	78.4	19.6	0.05
WB237D0	240	240.5	141.6	35.4	35.4	0.03
WB237D0	240.5	241	506.2	415.8	36.2	0.06
WB237D0	241	241.5	1013.8	392.7	82.2	0.11
WB237D0	241.5	242	584.3	324.6	117.7	0.25
WB237D0	242	242.5	59.9	37.2	33.0	0.48
WB237D0	242.5	243	130.0	43.3	43.3	0.05
WB237D0	243	243.5	471.8	233.3	146.8	0.38
WB237D0	243.5	244	314.2	221.5	140.1	1.86
WB237D0	244	244.5	337.8	199.0	141.2	2.02
WB237D0	244.5	245	183.7	108.9	85.1	1.55
WB237D0	245	245.5	276.3	142.6	112.9	0.34
WB237D0	245.5	246	74.2	38.9	151.9	0.28
WB237D0	246	246.5	91.5	57.2	45.7	0.09
WB237D0	246.5	247	60.3	34.5	43.1	0.12
WB237D0	247	247.5	46.0	30.7	30.7	0.07
WB237D0	247.5	248	122.7	106.6	92.0	0.68
WB237D0	248	248.5	108.4	84.7	86.0	3.21
WB237D0	248.5	249	86.0	74.3	83.4	0.77
WB237D0	249	249.5	93.9	71.6	80.3	2.21
WB237D0	249.5	250	96.4	67.1	75.6	1.30
WB237D0	250	250.5	113.2	79.2	92.0	1.17

WB237D0	250.5	251	107.3	80.5	66.6	1.01
WB237D0	251	251.5	152.3	115.8	149.3	0.66
WB237D0	251.5	252	117.8	73.8	100.9	0.77
WB237D0	252.5	253	113.5	79.5	158.9	0.18
WB237D0	253	253.5	54.1	38.6	43.8	0.39
WB237D0	253.5	254	85.0	75.4	68.3	0.84
WB237D0	254	254.5	154.2	98.8	101.2	0.42
WB237D0	254.5	255	10.5	10.5	41.8	0.10
WB237D0	255	255.5	4.7	4.7	18.7	0.21
WB237D0	255.5	256.07	57.3	40.1	51.5	0.17
WB237D0	256.4	257	75.8	53.9	37.9	0.69
WB237D0	258	258.5	262.6	192.6	166.3	0.11
WB237D0	258.5	259	19.9	39.8	19.9	0.05
WB237D0	259	259.5	1045.2	333.3	212.1	0.07
WB237D0	259.5	259.96	18.8	18.8	18.8	0.11
WB237D0	263	263.5	99.0	79.7	72.5	0.41
WB237D0	263.5	263.75	100.0	77.3	75.0	0.88
WB237D0	265	265.5	13.7	13.7	13.7	0.07
WB237D0	265.5	266	34.8	43.6	26.1	0.11
WB237D0	266	266.5	68.8	58.5	55.1	0.58
WB237D0	266.5	267	45.5	22.7	15.2	0.13
WB237D0	267.5	268	32.8	43.7	32.8	0.09
WB228D0	239	239.5	7.2	7.2	7.2	0.14
WB228D0	239.5	240	6.3	6.3	6.3	0.16
WB228D0	240	240.5	7.8	7.8	7.8	0.13
WB228D0	240.5	241	7.1	7.1	7.1	0.14
WB228D0	241	241.7	4.4	4.4	8.7	0.23
WB228D0	241.7	242	35.6	11.2	13.1	0.53
WB228D0	242	242.5	17.3	4.7	7.9	0.64
WB228D0	242.5	243	2.9	2.9	21.7	0.69
WB228D0	243	243.5	44.0	30.2	35.4	1.16
WB228D0	243.5	244	64.9	31.7	85.1	0.69
WB228D0	244	244.5	30.2	21.6	27.4	0.69
WB228D0	244.5	245	49.8	58.1	16.6	0.12
WB228D0	245	245.5	17.1	17.1	4.3	0.23
WB228D0	245.5	246	30.6	20.4	10.2	0.20
WB228D0	246	246.5	14.0	27.9	7.0	0.14
WB228D0	246.5	247	32.7	24.5	16.3	0.12
WB228D0	430	430.5	129.4	86.3	21.6	0.05
WB228D0	430.5	431	219.6	50.7	33.8	0.06
WB228D0	431	431.5	903.9	440.6	22.6	0.09
WB228D0	431.5	432	1417.3	658.6	114.5	0.28
WB228D0	432	432.5	95.7	47.8	23.9	0.04
WB228D0	432.5	433	38.6	12.9	12.9	0.08
WB228D0	433	433.5	29.8	6.0	23.9	0.17
WB228D0	433.5	434	187.1	114.3	76.9	0.48
WB228D0	434	434.5	1053.1	470.0	95.7	0.11
WB228D0	434.5	435.21	63.4	63.4	31.7	0.16

WB228D0	435.21	435.6	232.7	98.8	61.5	0.91
WB228D0	435.6	436	361.7	196.8	89.3	1.76
WB228D0	436	436.5	211.8	114.3	70.6	0.78
WB228D0	436.5	437	180.6	106.6	72.2	0.58
WB228D0	437	437.5	138.0	70.2	133.0	1.59
WB228D0	437.5	438	58.5	15.6	19.5	0.26
WB228D0	438	438.35	209.9	134.9	78.4	0.87
WB228D0	440	440.5	59.5	44.6	14.9	0.07
WB228D0	440.5	441	68.6	51.5	17.2	0.06
WB230D0	227	228	93.1	4.4	4.4	0.23
WB230D0	228	228.82	48.2	30.7	13.1	0.68
WB230D0	228.82	229.5	202.1	38.5	9.6	0.10
WB230D0	229.5	230	188.4	103.4	78.5	1.68
WB230D0	230	230.5	238.8	139.4	69.9	4.05
WB230D0	230.5	230.83	244.3	151.4	52.7	3.09
WB230D0	230.83	231.5	284.9	166.7	73.5	2.64
WB230D0	231.5	232	272.7	136.5	59.3	2.68
WB230D0	232	232.5	376.9	182.3	77.9	2.53
WB230D0	232.5	233	370.1	222.9	79.5	3.28
WB230D0	233	233.5	341.6	163.9	73.5	3.98
WB230D0	233.5	234	330.4	133.3	68.5	3.27
WB230D0	234	234.5	312.1	151.9	64.8	3.04
WB230D0	234.5	235	232.0	87.3	49.0	2.25
WB230D0	235	235.5	279.5	105.5	50.2	2.19
WB230D0	235.5	236	127.7	78.8	32.6	0.74
WB230D0	236	236.5	203.4	107.1	39.3	0.56
WB230D0	236.5	237	51.6	28.7	11.5	0.17
WB230D0	237	237.5	15.3	7.6	7.6	0.26
WB230D0	237.5	238	11.9	4.0	4.0	0.25
WB230D0	238	238.37	434.1	32.2	6.6	1.06
WB230D0	238.37	238.62	49.3	19.1	23.2	0.99
WB230D0	238.62	239	223.4	96.0	36.6	2.49
WB230D0	239	240	150.7	46.6	21.5	0.28
WB230D0	240	240.51	67.2	28.8	9.6	0.10
WB230D0	240.51	241	85.2	28.4	14.2	0.07
WB230D0	241	242	101.7	33.9	16.9	0.06
WB230D0	346	346.44	45.7	28.6	5.7	0.18
WB230D0	347.5	348	53.7	26.8	26.8	0.04
WB230D0	348.55	348.82	52.4	37.4	3.7	0.27
WB230D0	350.5	351	380.2	145.7	87.9	1.23
WB230D0	351	351.4	230.6	95.9	44.0	2.27
WB230D0	351.4	352	141.6	57.8	43.3	2.89
WB230D0	352	352.5	341.4	131.9	67.0	0.94
WB230D0	352.5	353	217.2	76.6	48.4	0.64
WB230D0	353	353.4	321.4	101.2	76.1	1.35
WB230D0	353.4	353.77	414.7	163.5	89.6	1.02
WB230D0	353.77	354.5	59.9	39.9	17.1	0.35
WB230D0	354.5	355	14.4	5.7	8.6	0.35

WB230D0	355	356	4.7	4.7	14.1	0.21
WB230D0	356	357	3.8	3.8	11.4	0.26
WB230D0	357	358	5.7	11.4	22.8	0.18
WB230D0	358	358.9	4.8	4.8	23.8	0.21
WB230D0	358.9	359.3	133.4	36.4	61.3	1.57
WB230D0	359.3	359.87	44.4	14.8	25.9	0.27
WB230D0	359.87	360.17	83.7	25.7	6.4	0.16
WB230D0	361	362	15.6	20.8	2.6	0.38
WB230D0	362	363	65.7	56.3	9.4	0.11
WB230D0	363	363.34	19.9	54.9	5.0	0.20
WB230D0	363.34	364	101.5	63.4	12.7	0.08
WB276D0	392	392.35	13.2	19.9	6.6	0.418
WB276D0	396.92	397.5	18.5	37.1	7.4	0.727
WB276D0	404.63	405	61.1	67.9	6.8	0.877
WB276D0	415	415.43	375.2	164.7	27.0	0.667
WB276D0	415.43	415.9	299.4	116.2	13.9	1.898
WB276D0	416.8	417.36	347.9	170.5	16.4	0.893
WB276D0	419.5	420	238.0	124.0	7.6	0.719
WB276D0	420	420.5	308.6	122.2	29.6	0.671
WB276D0	420.5	420.86	281.2	114.4	28.6	1.149
WB276D0	421.11	421.37	128.5	103.2	17.2	0.731
WB276D0	422.17	422.6	230.2	58.0	11.9	0.369
WB276D0	422.6	423	184.8	51.2	9.1	0.354
WB276D0	424.11	424.88	158.3	92.6	9.0	0.387
WB276D0	428.32	429	257.1	120.2	22.4	0.550
WB276D0	429	429.72	374.9	143.2	24.2	0.189
WB276D0	429.72	430	612.3	296.5	42.5	1.001
WB276D0	430	430.5	476.4	205.1	34.2	0.993
WB276D0	431	431.74	519.0	338.3	19.5	0.553
WB276D0	431.74	432	162.0	88.0	13.9	1.570
WB276D0	432.4	432.84	192.1	74.4	14.9	1.601
WB276D0	432.84	433.09	261.7	97.5	22.3	1.349
WB276D0	433.09	433.5	442.1	186.6	36.8	1.141
WB276D0	433.5	434	503.2	200.7	47.3	1.033
WB276D0	434	434.5	604.5	264.3	42.1	1.659
WB276D0	434.5	435	378.9	244.5	17.5	0.694
WB276D0	453.5	454	119.1	42.8	48.9	0.454
WB276D0	454	454.5	192.2	97.0	12.6	1.075
WB276D0	454.5	455	197.2	76.7	21.9	2.140
WB276D0	457	457.5	318.4	173.7	7.2	1.101
WB276D0	457.5	458	46.3	23.2	2.6	2.374
WB276D0	463.8	464.4	169.2	60.6	12.5	1.652
WB276D0	464.4	464.72	178.6	62.3	12.5	1.668
WB276D0	468.6	469	302.5	118.6	18.9	1.840
WB276D0	469	469.47	393.2	163.0	25.2	1.833
WB276D0	477	477.5	238.8	83.0	15.6	0.821
WB276D0	477.5	477.75	333.7	138.2	16.9	0.512
WB276D0	477.75	478.4	429.9	178.8	26.6	0.787

WB276D0	478.4	478.9	434.4	175.2	25.6	0.634
WB276D0	478.9	479.25	434.2	177.6	31.6	0.810
WB276D0	479.25	479.54	313.5	118.6	22.6	1.725
WB276D0	480	480.47	293.0	127.8	15.3	0.424
WB276D0	481.07	481.32	454.4	193.9	38.2	0.636
WB276D0	481.32	481.89	19.2	7.7	3.8	0.458
WB276D0	481.89	482.5	236.1	90.8	15.7	1.038
WB276D0	482.5	483	368.0	151.1	21.7	0.591
WB276D0	483	483.5	318.9	131.9	20.4	0.742
WB276D0	483.5	484	294.5	128.2	19.1	0.220
WB276D0	484	484.5	279.2	111.7	16.7	0.266
WB276D0	484.5	485	225.3	90.6	15.9	0.684
WB276D0	485	485.4	259.1	98.0	16.3	0.410
WB276D0	485.4	485.78	207.1	90.3	11.6	0.818
WB276D0	486.03	486.5	279.2	103.9	16.6	1.354
WB276D0	486.5	487	268.3	118.4	13.7	1.868
WB276D0	487	487.56	286.9	106.9	16.9	2.209
WB276D0	487.81	488.2	217.9	80.4	9.5	1.376
WB276D0	488.2	488.6	267.8	91.7	21.6	1.164
WB276D0	488.6	489.08	274.6	123.9	20.6	1.071
WB276D0	489.08	489.6	176.8	63.7	11.8	1.385
WB276D0	489.6	490.07	257.6	91.3	14.1	1.203
WB276D0	490.07	490.67	223.3	88.8	15.7	1.401
WB276D0	490.67	490.93	276.2	100.4	18.4	1.178
WB276D0	490.93	491.19	258.3	107.3	17.0	0.915
WB276D0	491.19	491.7	282.4	111.7	14.8	0.855
WB276D0	491.7	492.13	248.8	92.0	14.2	0.961
WB276D0	492.13	492.83	212.7	77.9	13.3	0.861
WB276D0	492.83	493.22	317.9	126.8	25.4	0.618
WB276D0	494.56	495	233.6	127.0	17.0	0.628
WB276D0	495.3	495.67	267.6	182.2	19.7	0.468
WB276D0	495.67	496.34	205.5	82.1	12.4	0.600
WB276D0	496.34	497	332.7	114.5	14.5	0.441
WB276D0	497.5	498	289.0	120.5	17.8	1.350
WB276D0	498	498.68	326.5	113.1	13.5	0.846
WB276D0	498.68	499.07	529.6	204.6	32.1	1.650
WB276D0	499.07	499.5	95.5	37.4	5.8	0.913
WB276D0	499.5	500	139.1	64.4	10.2	1.510
WB276D0	500	500.41	169.3	50.5	11.9	0.380
WB276D0	501	501.33	187.7	46.9	11.7	0.369
WB276D0	501.33	501.69	148.2	57.4	8.0	0.348
WB276D0	501.69	502.04	290.6	210.0	19.0	0.356
WB276D0	502.04	502.48	22.0	15.4	4.4	1.054
WB276D0	502.48	502.95	298.4	115.2	18.3	0.583
WB276D0	503.34	503.58	325.9	66.7	12.2	0.724
WB276D0	503.83	504.66	300.4	117.0	28.1	0.501
WB276D0	504.66	505.22	295.2	120.1	18.9	0.646
WB276D0	505.22	505.5	300.0	111.1	19.4	1.313

WB276D0	505.5	505.9	294.5	105.4	18.0	0.674
WB276D0	505.9	506.27	388.2	140.7	22.5	0.846
WB276D0	506.27	506.9	325.7	133.5	21.4	0.720
WB276D0	506.9	507.55	304.1	133.4	17.1	0.902
WB276D0	507.55	508.05	284.9	80.7	12.6	1.027
WB276D0	508.05	508.5	443.6	118.0	22.8	0.734
WB276D0	508.5	508.92	433.4	165.9	21.9	1.251
WB276D0	508.92	509.65	51.4	18.4	7.3	0.522
WB276D0	509.65	510.17	428.1	97.1	19.8	0.434
WB276D0	510.17	510.42	328.6	125.7	23.3	0.626
WB276D0	510.42	511	308.6	112.8	23.6	0.836
WB276D0	511	511.38	211.1	74.6	11.7	1.657
WB276D0	511.88	512.25	264.8	92.2	15.0	0.792
WB276D0	512.25	512.75	95.5	32.5	10.2	1.658
WB276D0	512.75	513.21	201.2	78.3	14.5	1.391
WB276D0	513.21	513.98	125.4	41.8	9.4	0.558
WB276D0	513.98	514.23	349.4	116.5	15.3	0.329
WB276D0	514.23	514.86	250.7	104.6	15.4	1.384
WB276D0	514.86	515.16	240.3	92.4	21.1	1.002
WB276D0	515.16	515.41	73.3	32.3	11.7	1.725
WB276D0	515.41	515.95	263.2	115.7	21.2	1.350
WB276D0	516.59	517.11	270.5	116.4	19.4	1.258
WB276D0	517.11	517.36	234.1	94.5	15.0	0.611
WB276D0	517.36	517.63	174.2	67.4	14.0	0.564
WB276D0	517.63	518.2	254.1	96.1	16.3	0.903
WB276D0	518.2	518.87	290.8	106.6	18.6	0.854
WB276D0	518.87	519.5	247.4	91.4	18.5	1.328
WB276D0	519.5	520	256.4	92.4	17.5	0.864
WB276D0	520	520.46	328.4	99.0	15.1	1.246
WB276D0	520.46	521	269.2	108.8	16.6	1.517
WB276D0	521	521.6	260.2	119.2	20.5	2.029
WB276D0	521.6	522.17	313.4	117.5	18.2	0.749
WB276D0	522.17	522.48	378.1	93.3	15.6	0.978
WB276D0	522.48	522.83	273.0	113.1	21.5	1.374
WB276D0	522.83	523.57	270.2	87.4	24.1	1.219
WB276D0	523.57	524.05	258.3	81.6	17.2	1.957
WB276D0	524.05	524.44	409.3	150.2	22.9	0.964
WB276D0	524.44	524.83	170.9	74.7	13.8	0.422
WB276D0	524.83	525.5	228.6	140.7	20.3	0.685
WB276D0	525.5	526	546.1	191.1	43.7	0.309
WB276D0	526	526.5	454.4	256.3	20.4	1.035
WB276D0	526.5	527	373.3	87.8	19.2	0.873
WB276D0	527	527.5	373.3	136.0	26.0	0.962
WB276D0	527.5	528	342.5	143.9	27.4	0.927
WB276D0	528	528.5	267.3	120.3	20.1	0.564
WB276D0	528.5	529	375.8	106.2	24.5	0.507
WB276D0	531	532	39.3	15.7	7.9	0.415
WB264D0	390.76	391.5	67.6	19.9	4.0	0.755

WB264D0	391.5	391.9	272.5	101.9	26.6	1.092
WB264D0	391.9	392.4	293.1	104.8	21.4	0.405
WB264D0	392.4	392.9	304.1	117.1	24.5	0.898
WB264D0	392.9	393.2	279.0	142.4	22.2	0.569
WB264D0	393.7	394.7	424.8	204.9	28.6	0.694
WB264D0	394.7	395.7	410.7	183.7	28.1	0.180
WB264D0	395.7	396.45	306.4	129.9	16.1	0.157
WB264D0	400.1	400.6	506.3	246.8	27.6	0.222
WB264D0	400.6	401.1	415.1	165.5	24.3	0.171
WB264D0	401.1	401.6	511.6	199.4	44.4	0.358
WB264D0	401.6	402.36	435.9	165.4	27.9	0.169
WB264D0	402.36	403.36	220.9	86.4	9.6	0.155
WB264D0	403.36	404.36	254.8	114.2	15.3	0.119
WB264D0	404.36	405.36	255.1	73.8	18.1	0.197
WB264D0	405.36	405.8	126.6	39.4	6.2	0.069
WB264D0	405.8	406.3	34.9	11.6	2.9	0.210
WB264D0	406.3	406.8	175.2	73.3	14.9	0.087
WB264D0	406.8	407.39	178.5	62.2	36.0	0.074
WB264D0	407.39	407.72	154.6	68.6	21.5	0.205
WB264D0	408.72	409.72	296.3	170.7	7.1	0.143
WB264D0	409.72	410.72	167.6	70.3	35.1	0.178
WB264D0	411.72	412.72	236.7	81.5	11.6	0.116
WB264D0	412.72	413	402.4	180.3	22.8	0.066
WB264D0	413	413.62	321.3	134.8	17.6	0.102
WB264D0	413.62	414.62	181.0	81.7	11.7	0.070
WB264D0	416.07	416.38	277.3	115.4	24.4	0.354
WB264D0	416.82	417.32	392.1	310.0	17.8	0.686
WB264D0	417.32	417.57	263.4	212.1	30.3	1.296
WB264D0	418.07	418.57	296.8	141.1	12.5	0.720
WB264D0	419.07	419.91	226.2	169.1	9.9	0.735
WB264D0	419.91	420.16	204.5	84.6	13.8	0.577
WB264D0	420.16	420.66	204.1	150.2	19.9	0.601
WB264D0	420.66	421.16	228.7	74.6	15.7	0.438
WB264D0	421.16	421.66	540.9	273.1	43.5	0.744
WB264D0	425.55	426.05	314.7	139.5	26.0	0.362
WB264D0	426.05	426.55	346.5	130.3	23.4	0.273
WB264D0	426.55	427.05	347.2	227.4	15.4	0.697
WB264D0	427.05	427.55	211.6	89.7	13.8	1.088
WB264D0	428.05	428.55	383.0	136.8	23.9	1.002
WB264D0	428.55	429.05	691.6	272.5	29.5	2.228
WB264D0	429.05	429.55	651.3	307.8	33.5	0.645
WB264D0	430.05	430.55	376.2	157.9	25.7	0.288
WB264D0	430.55	431.05	487.2	197.1	26.9	0.374
WB264D0	431.05	431.55	428.9	173.2	30.8	0.419
WB264D0	431.55	432.05	358.8	146.0	25.9	0.187
WB264D0	432.05	432.65	375.3	160.9	23.0	0.361
WB264D0	432.94	433.44	240.8	97.3	15.6	0.369
WB264D0	433.44	433.86	391.8	170.2	37.1	0.682

WB264D0	434.21	434.71	644.3	165.8	22.9	0.064
WB264D0	434.71	435.21	248.5	102.1	14.7	0.541
WB264D0	435.21	435.71	366.3	150.0	24.8	0.496
WB264D0	435.71	436.21	323.9	129.8	18.0	0.390
WB264D0	436.21	436.71	318.4	138.5	27.7	0.942
WB264D0	436.71	437.21	346.9	160.2	19.0	0.566
WB264D0	437.21	437.71	273.4	112.0	18.3	0.503
WB264D0	437.71	438.21	316.3	125.1	22.9	0.997
WB264D0	438.21	438.71	284.7	120.6	20.1	0.732
WB264D0	438.71	439.21	343.7	134.5	24.2	0.648
WB264D0	439.21	439.71	269.7	120.6	13.0	0.595
WB264D0	439.71	440.21	280.9	120.4	19.9	0.811
WB264D0	440.21	440.71	217.7	91.8	12.3	0.612
WB264D0	441.71	442.21	219.9	86.5	14.4	0.415
WB264D0	443.43	443.93	339.8	164.2	19.3	0.900
WB264D0	443.93	444.43	280.7	109.0	18.3	1.035
WB264D0	444.43	444.93	297.2	115.9	20.0	1.098
WB264D0	444.93	445.43	227.0	80.5	18.7	1.660
WB264D0	445.43	445.93	309.5	115.5	25.9	0.789
WB264D0	445.93	446.43	296.0	123.1	24.8	2.101
WB264D0	446.43	446.93	415.6	178.5	26.4	1.427
WB264D0	446.93	447.43	428.0	178.5	29.4	1.322
WB264D0	447.43	447.93	324.3	141.1	16.3	0.806
WB264D0	447.93	448.43	312.2	109.1	15.2	0.410
WB264D0	448.43	448.93	335.4	117.0	18.4	1.205
WB264D0	449.25	449.75	358.0	142.4	24.7	1.014
WB264D0	449.75	450.25	326.0	135.2	30.8	0.772
WB264D0	451.25	451.54	230.9	98.2	13.8	0.751
WB264D0	456.29	457.29	298.5	110.9	20.0	0.773
WB264D0	457.29	457.71	244.0	94.1	15.9	1.047
WB264D0	457.71	458.71	318.2	119.1	18.5	0.870
WB264D0	458.71	459.71	216.8	67.0	15.8	1.187
WB264D0	459.96	460.27	262.1	79.5	15.7	1.387
WB264D0	460.27	460.88	212.7	84.2	13.3	0.877
WB264D0	460.88	461.4	288.2	92.9	14.3	0.843
WB264D0	461.4	461.94	114.6	36.0	9.8	1.304
WB264D0	461.94	462.38	229.3	94.9	15.4	0.615
WB264D0	462.38	463	225.9	93.7	16.9	0.901
WB264D0	463.38	463.88	124.8	52.7	12.3	1.743
WB264D0	464.38	464.94	116.3	33.6	8.4	1.178
WB264D0	465.22	465.54	158.0	44.4	9.7	0.907
WB264D0	465.54	466.04	235.4	98.2	15.4	0.873
WB264D0	466.04	466.54	229.9	38.4	11.0	1.260
WB264D0	466.54	467.04	197.5	79.2	15.4	0.579
WB264D0	467.04	467.44	259.0	107.8	18.1	1.756
WB264D0	467.44	468.21	133.8	52.1	7.4	1.079
WB264D0	468.21	468.71	183.1	80.3	11.8	0.698
WB264D0	468.71	469.21	141.3	59.3	9.4	0.693

WB264D0	469.21	469.66	175.6	66.2	12.9	0.994
WB264D0	469.66	470.01	204.4	68.7	21.5	0.670
WB264D0	470.01	470.46	99.9	40.4	7.6	0.551
WB264D0	470.46	470.82	212.8	84.4	17.4	1.050
WB264D0	470.82	471.32	381.3	141.4	17.1	1.768
WB264D0	471.32	471.82	414.8	166.6	30.8	0.681
WB264D0	471.82	472.32	308.3	168.7	24.5	1.298
WB264D0	472.32	472.82	441.5	181.0	27.1	1.268
WB264D0	472.82	473.32	296.3	140.4	20.9	1.906
WB264D0	473.32	473.82	227.0	101.6	14.4	2.142
WB264D0	473.82	474.32	400.6	171.4	26.3	1.157
WB264D0	474.32	474.82	339.6	148.6	17.0	1.242
WB264D0	474.82	475.32	231.4	88.5	13.9	1.909
WB264D0	475.32	475.82	204.2	86.5	12.1	0.237
WB264D0	475.82	476.32	212.8	81.8	18.1	0.556
WB264D0	476.32	476.82	226.0	92.3	15.3	0.563
WB264D0	476.82	477.32	244.6	111.7	19.7	0.318
WB264D0	477.32	477.82	244.4	124.8	17.1	1.240
WB264D0	477.82	478.32	183.1	71.6	15.1	0.555
WB264D0	478.32	478.82	187.9	53.8	9.6	0.471
WB264D0	478.82	479.32	173.1	61.5	20.5	1.246
WB264D0	479.32	480	220.5	86.7	24.3	0.748
WB264D0	480	480.56	182.2	75.8	16.0	0.725
WB264D0	480.56	481.06	189.5	83.4	12.1	0.867
WB264D0	481.06	481.56	227.8	127.4	14.5	0.590
WB264D0	481.56	482.35	175.5	61.0	10.8	0.874
WB264D0	482.35	482.85	236.7	119.0	13.8	0.310
WB264D0	482.85	483.2	236.8	111.6	8.4	0.561
WB264D0	483.2	483.7	127.4	58.5	26.4	0.665
WB264D0	483.7	484.2	166.6	71.5	9.9	0.982
WB264D0	484.2	484.7	186.0	68.4	10.0	0.768
WB264D0	484.7	485.2	277.2	113.0	29.4	0.432
WB264D0	485.2	485.7	305.4	127.5	16.8	1.768
WB264D0	485.7	486.4	242.8	91.8	16.9	0.958
WB264D0	486.4	486.9	210.9	74.1	18.4	0.507
WB264D0	486.9	487.4	277.3	94.7	13.2	0.352
WB264D0	487.4	487.9	187.6	90.0	12.1	0.369
WB264D0	487.9	488.4	168.2	74.3	13.4	0.366
WB264D0	488.4	488.77	150.8	70.7	12.2	0.827
WB264D0	488.77	489.27	245.6	105.3	16.6	1.047
WB264D0	489.27	489.77	399.5	165.6	24.9	0.651
WB264D0	489.77	490.27	371.7	165.0	31.6	0.401
WB264D0	490.27	490.77	359.2	157.7	26.2	0.452
WB264D0	490.77	491.13	289.0	135.1	30.4	0.527
WB264D0	491.13	491.63	404.5	166.4	30.1	1.114
WB264D0	491.63	492.13	297.9	118.6	21.2	0.987
WB264D0	492.13	492.63	246.5	105.4	14.6	1.265
WB264D0	492.63	493.4	203.9	84.1	12.7	0.344

WB264D0	493.4	493.9	237.2	110.9	15.9	0.459
WB264D0	493.9	494.4	436.5	173.8	27.7	0.403
WB264D0	494.4	494.9	310.8	143.2	20.7	0.388
WB264D0	494.9	495.55	197.1	82.2	14.0	0.538
WB264D0	495.55	496.05	116.6	53.9	5.8	0.948
WB264D0	496.05	496.55	280.1	103.5	16.6	0.386
WB264D0	496.55	497.03	230.9	65.3	11.1	0.619
WB264D0	497.03	497.53	237.6	94.4	15.9	0.411
WB264D0	497.53	498.03	238.7	95.0	12.8	0.415
WB264D0	498.03	498.82	300.2	149.8	15.9	0.381
WB264D0	498.82	499.32	195.8	85.7	13.4	0.759
WB264D0	499.32	499.82	279.3	87.5	13.1	0.138
WB264D0	499.82	500.35	242.6	108.5	23.5	0.159
WB264D0	500.35	500.85	156.2	49.5	8.8	0.159
WB264D0	501.52	502.02	235.2	89.2	12.0	0.584
WB264D0	502.02	502.88	221.0	124.5	16.5	0.443
WB264D0	502.88	503.38	164.3	64.3	7.8	1.267
WB264D0	503.38	503.88	235.9	90.3	12.3	1.071
WB264D0	503.88	504.38	274.0	101.1	22.5	1.056
WB264D0	504.38	504.88	167.9	67.2	9.9	0.374
WB264D0	504.88	505.16	236.5	95.0	15.5	3.918
WB264D0	505.66	506.66	174.6	87.8	8.9	0.641
WB264D0	506.66	507.66	211.9	72.8	9.1	0.598
WB264D0	507.66	508.66	222.9	87.7	14.0	0.743
WB264D0	508.66	509.66	312.8	120.2	20.3	2.679
WB264D0	509.66	510.66	272.3	121.6	25.4	10.211
WB264D0	510.66	511.66	274.6	111.9	10.5	0.429
WB264D0	511.66	512.66	219.0	80.3	19.5	0.751
WB264D0	512.66	513.66	191.5	58.8	13.1	0.458
WB264D0	513.66	514	216.2	53.1	20.7	0.765
WB264D0	514	514.8	69.5	26.1	8.7	6.421
WB264D1	388.85	389.5	791.2	527.4	263.7	1.869
WB264D1	389.5	390.5	275.3	125.9	15.1	0.465
WB264D1	391.5	391.82	105.6	56.3	24.6	0.676
WB264D1	391.82	392.32	299.8	125.2	24.7	0.575
WB264D1	392.32	392.82	403.0	167.3	35.9	0.687
WB264D1	394.82	395.32	401.2	156.2	23.8	1.281
WB264D1	395.32	395.9	232.0	110.6	19.6	3.660
WB264D1	400.25	400.51	184.1	82.9	11.2	1.904
WB264D1	400.77	401.28	570.7	234.7	40.0	2.976
WB264D1	401.28	401.76	472.7	194.0	35.3	1.062
WB264D1	401.76	402.26	493.0	299.9	59.1	0.991
WB264D1	402.26	402.76	428.6	220.6	24.5	0.395
WB264D1	402.76	403.32	278.3	109.5	13.9	0.417
WB264D1	403.86	404.36	257.4	117.3	17.4	0.738
WB264D1	404.36	404.9	330.6	146.0	18.1	0.607
WB264D1	405.4	405.65	204.2	98.3	11.3	0.746
WB264D1	406	406.5	334.8	191.9	37.9	0.997

WB264D1	406.98	407.98	140.0	47.7	26.8	1.646
WB264D1	408.98	409.98	162.2	51.8	10.4	0.444
WB264D1	412.98	413.27	78.7	37.3	8.3	0.908
WB264D1	413.27	413.77	215.1	99.4	28.9	0.581
WB264D1	413.77	414.25	284.3	135.5	15.3	2.966
WB264D1	414.25	414.5	134.4	70.3	8.3	0.401
WB264D1	414.5	415.05	2.2	4.4	4.4	0.652
WB264D1	418.72	419.22	268.6	97.0	18.1	1.329
WB264D1	419.22	419.72	268.0	87.3	25.6	0.226
WB264D1	419.72	420.22	269.1	99.2	22.5	0.214
WB264D1	420.22	420.84	240.4	102.5	15.6	1.480
WB264D1	421.2	421.45	301.6	131.2	15.4	2.703
WB264D1	421.45	421.8	346.5	167.4	19.3	2.286
WB264D1	421.8	422.44	348.1	176.7	11.8	1.173
WB264D1	425.5	426	183.6	61.2	14.3	6.832
WB264D1	426	426.5	348.6	145.7	20.8	1.679
WB264D1	426.5	427	381.8	185.1	22.4	1.148
WB264D1	427.5	428	384.6	161.4	33.2	2.006
WB264D1	428	428.31	445.9	172.5	28.0	0.575
WB264D1	428.65	429.07	324.3	140.0	20.6	2.420
WB264D1	430.15	430.61	290.3	118.9	20.9	1.535
WB264D1	430.61	431.11	328.6	122.9	24.4	0.646
WB264D1	431.11	431.61	381.0	158.5	24.5	0.415
WB264D1	431.61	432.11	716.3	272.3	33.2	0.429
WB264D1	432.11	432.57	339.9	134.6	15.8	0.573
WB264D1	432.57	433.07	406.0	222.6	35.5	0.568
WB264D1	434.07	434.57	372.5	170.8	28.7	0.449
WB264D1	434.57	435.07	517.3	160.6	13.1	0.835
WB264D1	435.57	436.07	453.0	195.4	44.1	0.310
WB264D1	436.57	437.1	372.1	122.1	23.4	0.545
WB264D1	437.1	437.6	311.9	125.9	19.5	0.404
WB264D1	437.6	438.16	316.8	121.4	19.8	0.657
WB264D1	439.67	440.45	374.2	131.0	15.4	0.977
WB264D1	440.45	440.93	215.3	107.0	13.6	0.686
WB264D1	440.93	441.65	223.9	87.9	8.3	0.506
WB264D1	441.65	442.04	298.6	137.5	18.7	0.753
WB264D1	442.34	442.59	292.6	116.1	17.8	1.578
WB264D1	442.59	442.84	246.1	59.4	8.8	0.759
WB264D1	442.84	443.34	298.4	118.6	21.7	0.440
WB264D1	443.34	444.07	354.1	138.1	79.6	0.505
WB264D1	444.07	444.57	282.6	129.6	14.6	0.634
WB264D1	444.57	445.22	456.2	182.1	24.9	0.638
WB264D1	445.22	445.7	310.6	59.1	4.0	0.470
WB264D1	445.7	446.19	344.6	152.3	23.7	0.512
WB264D1	446.51	447.01	316.5	146.5	18.7	0.432
WB264D1	447.51	448.01	398.9	130.6	25.4	0.522
WB264D1	448.51	449.01	337.4	140.0	24.1	1.175
WB264D1	449.01	449.51	322.1	132.3	19.8	0.628

WB264D1	449.51	450.01	333.7	138.0	21.6	0.641
WB264D1	450.01	450.55	313.2	133.7	21.5	0.632
WB264D1	451.55	452.05	187.7	65.7	6.3	0.474
WB264D1	452.05	452.55	195.7	73.7	7.6	0.614
WB264D1	453.57	454.07	248.3	108.2	17.5	0.421
WB264D1	454.07	454.34	250.6	101.5	17.8	0.617
WB264D1	455.22	455.73	260.1	103.2	16.4	0.369
WB264D1	456.08	456.41	201.8	86.1	13.5	0.537
WB264D1	456.91	457.41	328.8	123.5	22.3	0.515
WB264D1	457.41	457.91	286.3	119.8	22.7	0.737
WB264D1	457.91	458.41	29.1	19.4	9.7	0.133
WB264D1	458.41	458.91	128.0	101.2	3.8	0.098
WB264D1	459.42	460.04	191.3	80.4	10.6	0.064
WB264D1	460.04	460.4	263.4	134.0	14.7	0.733
WB264D1	460.8	461.11	234.5	104.9	16.0	1.217
WB264D1	461.11	461.61	260.9	116.6	17.6	1.918
WB264D1	461.61	462.11	285.1	110.9	16.8	1.128
WB264D1	462.11	462.61	232.8	100.4	16.1	1.316
WB264D1	462.61	463.11	251.5	104.4	15.9	0.787
WB264D1	463.11	463.61	305.6	164.5	19.6	0.589
WB264D1	463.61	464.11	209.0	95.9	20.0	0.166
WB264D1	464.11	464.78	259.7	98.2	18.8	0.297
WB264D1	464.78	465.04	220.2	103.4	6.1	0.448
WB264D1	465.04	465.88	216.8	90.9	21.0	0.328
WB264D1	465.88	466.19	249.4	103.3	16.9	1.050
WB264D1	467.9	468.4	195.4	78.6	13.8	1.093
WB264D1	468.4	468.9	139.7	85.1	9.5	0.370
WB264D1	468.9	469.4	278.6	135.4	17.2	0.362
WB264D1	469.4	469.9	229.6	88.4	12.6	0.654
WB264D1	469.9	470.4	280.3	113.9	21.7	0.431
WB264D1	470.4	470.65	2.1	1.1	0.4	0.334
WB264D1	470.92	471.38	174.7	79.1	12.9	0.641
WB264D1	471.38	471.88	466.0	212.0	27.1	0.402
WB264D1	471.88	472.38	547.7	156.6	28.1	0.212
WB264D1	472.38	472.88	390.3	174.4	27.5	0.514
WB264D1	472.88	473.38	294.5	116.6	27.7	0.317
WB264D1	473.38	473.88	260.4	120.1	21.7	0.834
WB264D1	473.88	474.38	291.0	95.7	21.8	1.102
WB264D1	474.38	474.88	171.6	179.5	22.3	0.357
WB264D1	474.88	475.38	173.1	74.9	12.0	0.622
WB264D1	475.38	475.88	169.5	66.6	10.3	0.329
WB264D1	475.88	476.38	213.2	96.4	19.2	0.952
WB264D1	476.38	476.88	222.2	86.2	16.9	0.946
WB264D1	476.88	477.38	264.3	118.9	16.6	0.430
WB264D1	477.38	477.88	205.6	79.9	17.0	0.315
WB264D1	477.88	478.38	171.1	64.5	14.4	0.685
WB264D1	478.38	478.88	311.2	119.5	8.2	0.701
WB264D1	478.88	479.38	186.0	48.7	5.5	0.366

WB264D1	479.38	479.88	210.8	100.4	10.1	0.461
WB264D1	479.88	480.55	185.5	71.3	12.9	0.500
WB264D1	480.78	481.05	209.0	84.4	16.5	0.436
WB264D1	481.05	481.55	204.5	86.2	18.0	1.287
WB264D1	481.55	482.05	224.7	89.6	18.4	0.396
WB264D1	482.05	482.55	225.8	91.3	17.4	0.770
WB264D1	482.55	483.05	225.3	101.0	15.5	0.231
WB264D1	483.05	483.55	226.8	88.2	19.7	0.495
WB264D1	483.55	484.05	247.6	105.8	14.2	0.248
WB264D1	484.05	484.19	198.8	100.6	16.8	0.488
WB264D1	484.19	484.69	155.9	65.6	10.9	0.742
WB264D1	485.29	485.55	294.0	125.7	14.2	1.251
WB264D1	485.55	486.05	243.0	98.9	20.8	0.927
WB264D1	486.05	486.55	251.6	43.8	6.2	0.463
WB264D1	486.55	487.05	212.4	80.6	15.7	0.397
WB264D1	487.05	487.72	215.6	89.4	14.9	0.183
WB264D1	488.22	488.72	111.9	55.9	4.5	0.258
WB264D1	488.72	489.23	174.2	84.3	14.3	0.563
WB264D1	489.23	489.73	254.4	94.8	37.5	0.482
WB264D1	489.73	490.23	362.3	160.2	24.8	0.440
WB264D1	490.23	490.84	449.2	172.6	28.2	0.445
WB264D1	490.84	491.56	155.4	66.4	11.0	0.383
WB264D1	492.06	492.56	81.6	30.2	3.0	0.314
WB264D1	493.67	494.1	394.2	272.6	20.6	2.292
WB264D1	494.1	494.67	165.5	63.1	17.8	0.317
WB264D1	494.9	495.17	305.7	121.6	21.9	0.511
WB264D1	495.17	495.67	252.2	110.7	18.1	0.170
WB264D1	495.67	496.17	301.0	128.1	20.8	1.249
WB264D1	496.17	496.67	268.3	102.2	18.9	1.849
WB264D1	496.67	497.17	298.7	128.2	25.4	1.061
WB264D1	497.17	497.67	429.2	296.9	20.8	0.960
WB264D1	497.67	498.17	385.2	147.9	24.0	0.750
WB264D1	498.17	498.67	232.7	92.3	17.1	1.874
WB264D1	498.67	499.17	316.3	135.8	23.9	0.670
WB264D1	499.17	499.67	262.1	105.5	16.6	1.507
WB264D1	499.67	500.17	236.6	98.0	14.9	1.745
WB264D1	500.17	500.67	221.1	85.6	18.4	0.760
WB264D1	500.67	501.5	246.4	128.5	10.5	0.856
WB264D1	501.5	502.07	316.8	112.8	14.2	1.764
WB264D1	502.07	502.88	306.4	147.9	15.3	1.955
WB264D1	502.88	503.38	244.7	103.0	19.4	1.962
WB264D1	503.38	503.8	205.4	89.2	11.7	0.852
WB264D1	503.8	504.05	144.0	19.6	3.1	1.277
WB264D1	504.05	504.45	301.5	119.5	18.7	1.390
WB264D1	504.45	505	86.0	33.4	5.6	1.615
WB264D1	505	505.5	169.4	64.0	11.9	2.609
WB264D1	505.5	506	288.7	130.9	28.9	1.451
WB264D1	506	506.5	322.9	134.1	22.9	1.006

WB264D1	506.5	507	238.4	93.3	15.4	1.619
WB264D1	507	507.5	335.2	135.1	24.6	0.814
WB264D1	507.5	508	318.4	126.0	19.9	0.302
WB264D1	508	508.53	204.4	88.0	15.7	0.318
WB264D1	509.53	510.03	249.2	105.7	18.5	1.192
WB264D1	510.03	510.53	193.4	81.6	10.6	0.563
WB264D1	511.03	511.53	338.2	126.2	31.2	0.769
WB264D1	512.55	512.89	268.3	107.3	19.6	0.764
WB264D1	512.89	513.39	228.0	100.5	14.4	0.557
WB264D1	513.39	513.88	271.1	113.8	17.1	0.642
WB264D1	513.88	514.22	290.2	128.7	21.1	0.427
WB264D1	514.22	514.53	240.8	109.3	15.8	0.631
WB264D1	514.71	515.42	219.3	88.1	12.6	0.556
WB264D1	515.42	515.92	334.2	92.5	17.5	1.200
WB264D1	515.92	516.42	197.0	105.8	18.2	0.274
WB264D1	516.42	516.92	277.0	126.4	13.4	0.744
WB264D1	516.92	517.3	160.0	68.6	15.2	0.131
WB264D1	517.3	517.8	40.4	32.4	16.2	0.124
WB264D1	517.8	518.8	32.0	10.7	10.7	0.094
WB264D1	518.8	519.8	11.0	11.0	11.0	0.091
WB264D1	519.8	520.8	29.2	29.2	29.2	0.034
WB261D0	239.5	240.13	2.4	2.4	4.8	0.415
WB261D0	240.13	241	4.1	4.1	4.1	0.246
WB261D0	254.5	254.94	464.8	189.8	19.8	1.818
WB261D0	254.94	255.31	453.3	196.1	26.3	0.836
WB261D0	255.31	256	625.1	272.3	38.7	1.678
WB261D0	256	256.5	528.4	236.9	28.2	1.558
WB261D0	256.5	257	529.2	215.0	27.3	1.321
WB261D0	257	257.5	435.2	197.0	28.7	1.742
WB261D0	257.5	257.81	507.0	229.2	35.5	1.663
WB261D0	257.81	258.17	520.6	227.3	36.7	0.955
WB261D0	258.17	259	515.4	216.9	35.5	1.692
WB261D0	259	259.5	633.7	214.1	44.9	2.447
WB261D0	259.5	260	551.9	254.2	37.9	1.794
WB261D0	260	260.5	436.1	183.7	16.1	0.931
WB261D0	260.5	261	447.5	177.8	24.5	1.305
WB261D0	261	261.5	447.6	199.7	24.7	1.577
WB261D0	261.5	262	478.1	232.7	28.2	2.269
WB261D0	262	262.27	244.6	106.7	12.7	1.885
WB261D0	262.27	263	50.8	33.9	16.9	0.059
WB261D0	263	263.42	165.2	82.6	16.5	0.061
WB261D0	263.85	264.61	468.2	177.3	24.1	1.286
WB261D0	264.61	265	660.8	158.7	23.9	2.010
WB261D0	265	265.77	478.4	188.2	29.0	1.860
WB261D0	265.77	266.23	411.8	180.7	40.6	2.535
WB261D0	266.23	267	393.2	155.9	30.6	1.635
WB261D0	267.5	268.14	355.1	150.9	22.1	0.544
WB261D0	268.14	268.5	280.6	140.3	16.5	0.364

WB261D0	269	270	243.6	89.6	22.7	0.792
WB261D0	278.27	278.63	355.5	150.4	147.5	1.024
WB261D0	278.63	279	656.0	188.5	47.1	0.276
WB261D0	279	279.5	69.4	31.5	18.9	0.159
WB261D0	279.5	280	337.9	130.7	22.1	0.497
WB261D0	280	280.32	312.8	136.0	14.8	0.809
WB261D0	280.32	281	371.6	141.7	24.1	0.374
WB261D0	281	281.5	671.6	463.1	31.8	0.283
WB261D0	281.5	282	163.1	88.8	10.7	1.024
WB261D0	282	282.41	367.0	135.0	23.8	1.599
WB261D0	282.41	282.79	710.4	301.2	40.5	0.667
WB261D0	282.79	283.5	624.3	271.0	36.9	1.166
WB261D0	283.5	284.31	417.3	188.9	22.6	1.016
WB261D0	285.4	286.19	577.6	198.3	28.3	0.459
WB261D0	286.19	286.64	428.4	178.7	34.1	0.733
WB261D0	286.64	287	254.5	104.8	13.3	1.049
WB261D0	287	287.47	62.5	27.2	5.4	0.368
WB261D0	287.47	287.92	427.3	171.5	21.8	0.321
WB261D0	287.92	288.5	257.3	115.2	16.6	0.781
WB261D0	289.5	290	208.0	88.1	19.6	0.409
WB261D0	290	290.34	560.4	367.0	28.9	0.760
WB261D0	290.34	290.8	139.4	65.5	29.6	0.473
WB261D0	290.8	291.29	60.0	32.1	4.3	0.467
WB261D0	307.44	307.89	40.1	28.6	5.7	0.349
WB261D0	307.89	308.35	217.3	103.8	13.0	0.308
WB261D0	327.6	328	69.1	34.6	11.5	0.174
WB261D0	329	329.5	659.8	332.6	32.4	0.370
WB261D0	329.5	330	390.3	183.0	21.3	0.328
WB261D0	330	330.7	111.0	50.5	10.1	0.198
WB261D0	331.5	332	39.1	21.0	3.0	0.333
WB261D0	333.03	333.75	143.1	78.7	7.2	0.280
WB261D0	333.75	334.33	889.4	373.1	21.7	0.230
WB261D0	334.33	335.33	161.4	73.7	5.6	0.719
WB261D0	335.33	335.69	325.4	163.6	21.1	0.569
WB261D0	335.69	336	285.0	115.1	27.4	0.547
WB261D0	336	336.5	485.2	147.0	18.7	0.748
WB261D0	337.5	338	41.2	13.7	4.6	0.218
WB261D0	338	338.5	100.7	53.0	10.6	0.189
WB261D0	338.5	339	198.5	117.1	15.3	0.196
WB261D0	339	339.55	572.2	258.1	28.0	0.322
WB261D0	345	346	530.1	226.2	36.6	0.438
WB261D0	346	347	286.7	110.6	24.4	0.534
WB261D0	348.9	349.5	479.1	177.2	28.5	1.332
WB261D0	349.5	350	289.3	107.3	23.0	0.522
WB261D0	352.5	353	217.6	88.0	18.5	0.864
WB261D0	353	353.5	150.9	80.2	26.7	0.524
WB261D0	353.5	354	169.1	71.4	12.9	1.555
WB261D0	354	354.5	201.8	82.5	16.5	1.031

WB261D0	359	359.5	234.4	142.9	22.9	0.350
WB261D0	363	363.5	446.4	205.5	38.5	0.311
WB261D0	363.5	364.19	414.5	153.9	76.0	0.552
WB261D0	364.19	364.5	358.6	159.1	30.2	0.993
WB261D0	366.5	366.95	222.6	101.4	15.4	0.907
WB261D0	366.95	367.21	221.7	107.6	22.0	1.227
WB261D0	367.86	368.5	311.4	141.3	17.7	1.076
WB261D0	368.5	369	194.0	99.6	13.5	0.593
WB261D0	369	369.33	191.2	86.4	11.0	0.544
WB261D0	369.33	369.59	266.9	109.5	17.0	0.648
WB261D0	369.59	370	333.2	148.2	21.0	1.141
WB261D0	370	370.5	312.9	142.0	18.5	0.866
WB261D0	370.5	371	314.0	131.5	19.6	1.376
WB261D0	371	371.5	307.0	401.9	30.0	0.401
WB261D0	371.5	372	83.2	44.2	5.2	0.385
WB261D0	372	372.5	279.8	113.9	22.0	0.500
WB261D0	372.5	373	325.1	100.2	19.3	0.569
WB261D0	374.5	375	348.3	142.7	18.2	0.603
WB261D0	376	376.5	310.7	175.4	21.7	1.197
WB261D0	376.5	377	352.1	193.0	22.0	0.591
WB261D0	377	377.5	389.4	127.1	20.7	0.629
WB261D0	377.5	378	408.6	152.9	54.6	0.915
WB261D0	380	380.6	376.5	152.2	22.6	0.486
WB261D0	383	383.5	634.9	146.4	49.3	0.628
WB261D0	386	386.5	325.6	143.1	24.5	0.734
WB261D0	387	387.5	593.6	260.8	35.3	0.652
WB261D0	387.5	388	495.5	206.0	34.8	1.150
WB261D0	388	388.5	543.6	169.7	26.6	1.126
WB261D0	388.5	389	476.7	198.2	13.4	0.747
WB261D0	389	389.5	535.3	248.0	36.1	1.302
WB261D0	389.5	390	548.9	217.1	31.1	1.124
WB261D0	390	390.5	503.7	223.4	24.3	1.070
WB261D0	390.5	391	376.3	159.7	20.5	0.877
WB261D0	391	391.5	96.2	39.0	5.2	2.309
WB261D0	395	396	306.5	137.2	20.4	0.343
WB261D0	396	396.36	254.8	103.7	14.8	0.338
WB261D0	397	397.5	242.1	106.1	13.3	0.301
WB261D0	397.5	398	201.6	92.8	12.8	0.312
WB261D0	398.5	399	180.9	73.3	12.2	0.409
WB261D0	399	399.31	153.6	65.1	5.2	0.384
WB261D0	399.31	400	229.0	116.0	17.8	0.336
WB261D0	400	400.5	312.9	150.8	14.2	0.351
WB261D0	400.5	401	266.5	121.1	13.5	0.371
WB261D0	401	401.5	282.0	129.1	18.4	0.379
WB261D0	401.5	402	289.8	138.6	17.6	0.397
WB261D0	402	402.5	298.9	139.0	18.5	0.432
WB261D0	402.5	403	258.7	128.1	17.2	0.406
WB280D0	350	350.5	428.1	165.0	23.9	0.42

WB280D0	350.5	351	363.3	151.4	22.0	0.73
WB280D0	351	351.5	285.0	127.7	16.0	0.88
WB280D0	351.5	352	275.7	95.9	16.5	0.67
WB280D0	352.5	353	461.0	190.2	32.1	1.90
WB280D0	353	353.5	328.0	132.1	23.5	0.89
WB280D0	353.5	354	341.9	147.3	20.8	0.72
WB280D0	354	354.5	260.9	120.7	25.3	0.67
WB280D0	354.5	355	310.8	125.4	19.2	1.15
WB280D0	355	355.62	340.6	162.8	21.9	0.73
WB280D0	356	356.5	78.7	21.7	5.4	0.37
WB280D0	356.5	357	253.9	81.8	31.0	0.35
WB280D0	357	357.36	108.6	38.8	7.8	0.39
WB280D0	357.36	358	112.8	45.5	9.1	0.55
WB280D0	358	358.5	84.9	42.4	15.9	0.19
WB280D0	358.5	359	304.5	127.8	19.0	1.00
WB280D0	359	359.5	342.4	139.0	23.2	0.99
WB280D0	359.5	360	215.1	90.4	10.8	0.55
WB280D0	360	360.5	192.3	73.2	10.8	1.57
WB280D0	360.5	361	234.8	101.8	13.7	1.60
WB280D0	361	361.28	300.2	121.6	18.5	1.35
WB280D0	361.28	361.62	217.3	102.5	17.5	1.14
WB280D0	361.62	362.11	278.7	98.7	17.4	1.03
WB280D0	362.11	362.4	269.4	97.6	15.7	1.66
WB280D0	362.4	362.83	187.4	73.5	11.5	0.69
WB280D0	364	364.68	160.8	59.5	17.6	0.45
WB280D0	364.68	365	356.2	129.3	18.6	1.08
WB280D0	365	365.41	196.3	76.2	18.7	2.14
WB280D0	365.41	365.82	220.6	88.1	14.5	1.10
WB280D0	365.82	366.47	301.1	104.5	16.4	2.37
WB280D0	366.47	367	293.6	119.9	21.2	1.65
WB280D0	367	367.5	243.4	108.5	14.4	1.67
WB280D0	367.5	368	275.5	106.0	13.0	1.84
WB280D0	368	368.5	304.9	119.5	18.5	1.83
WB280D0	368.5	369	251.0	114.5	14.6	0.82
WB280D0	369	369.5	236.2	68.3	13.7	0.51
WB280D0	370.5	371	403.9	127.0	6.4	0.79
WB280D0	374.5	375	236.5	121.4	11.0	0.63
WB280D0	375.5	375.87	302.4	138.2	32.1	0.81
WB280D0	378.86	379.5	313.7	113.1	17.4	1.72
WB280D0	379.5	380	391.2	146.1	23.6	0.42
WB280D0	380	380.5	264.3	100.7	9.4	0.64
WB280D0	380.5	381	87.3	30.5	4.4	0.46
WB280D0	382.77	383.1	454.8	197.5	25.1	1.04
WB280D0	383.1	383.72	314.7	101.5	8.5	0.59
WB280D0	383.72	384	566.4	258.9	16.2	0.74
WB280D0	384	384.5	245.9	141.1	18.2	0.22
WB280D0	384.5	385	26.3	15.1	3.8	0.27
WB280D0	386.35	386.77	285.3	152.2	19.0	0.68

WB280D0	388	388.5	328.9	182.7	17.1	0.41
WB280D0	388.5	389	355.6	133.2	20.8	0.82
WB280D0	389.5	389.91	419.4	172.8	19.2	1.35
WB280D0	389.91	390.24	298.2	115.1	16.1	1.87
WB280D0	390.24	391	312.3	122.7	19.9	2.21
WB280D0	391	391.7	294.2	121.3	17.4	1.38
WB280D0	391.7	392	347.9	128.9	18.9	1.16
WB280D0	392	392.5	283.0	154.1	27.1	1.07
WB280D0	392.5	392.94	325.7	161.8	33.9	1.38
WB280D0	392.94	393.6	288.5	102.2	16.6	1.20
WB280D0	393.6	394	306.2	126.3	17.8	1.40
WB280D0	394	394.5	370.9	130.7	17.8	1.18
WB280D0	395	395.5	416.3	119.1	17.5	0.92
WB280D0	395.5	396	327.4	133.3	11.7	0.86
WB280D0	396	396.68	468.4	177.0	43.7	0.96
WB280D0	400	400.34	556.1	222.9	40.6	0.86
WB280D0	400.34	400.96	865.5	349.4	43.7	0.62
WB280D0	402.5	403	372.4	154.4	17.5	0.63
WB280D0	403	403.5	290.6	119.7	15.0	0.47
WB280D0	403.5	404	273.3	98.3	16.7	0.60
WB280D0	406.5	407	303.8	79.3	11.3	0.44
WB280D0	410.82	411.19	211.1	34.1	27.4	1.35
WB280D0	417.28	417.7	289.6	61.5	14.2	0.85
WB280D0	417.7	418.11	425.0	228.5	23.0	1.65
WB280D0	418.11	418.56	454.7	187.3	27.4	0.91
WB280D0	419.11	419.71	409.3	181.5	22.5	1.51
WB280D0	422.88	423.5	192.1	86.9	10.5	0.38
WB280D0	424.5	425	287.0	178.7	37.9	0.37
WB280D0	425	425.5	954.8	186.9	34.5	0.35
WB280D0	436.68	437	146.1	92.7	2.8	0.36
WB280D0	437	437.59	95.9	43.7	4.7	1.05
WB280D0	437.59	438	627.4	241.7	36.0	0.58
WB280D0	438	438.54	165.7	71.8	8.3	0.72
WB280D0	438.54	439	932.3	349.4	71.9	0.50
WB280D0	439	439.5	991.0	418.1	52.6	0.65
WB280D0	439.5	440	1050.3	486.7	63.2	1.31
WB280D0	440	440.5	864.8	425.7	60.8	0.67
WB280D0	440.5	441	754.9	277.6	44.9	0.85
WB280D0	441	441.5	818.2	311.2	47.2	0.72
WB280D0	441.5	442	816.1	341.5	55.4	0.90
WB280D0	442	442.73	825.1	277.6	59.4	1.03
WB280D0	442.73	443	348.7	110.3	15.0	0.73
WB280D0	443	443.5	378.1	154.3	19.2	1.25
WB280D0	443.5	444	426.9	199.1	30.6	0.52
WB280D0	444	444.5	299.8	133.7	20.8	0.43
WB280D0	444.5	444.75	354.6	150.1	20.8	0.63
WB280D0	444.75	445.14	471.3	183.0	33.5	0.84
WB280D0	445.14	445.5	434.6	173.8	29.6	1.66

WB280D0	447.5	448	253.9	103.6	17.7	0.79
WB280D0	448	448.5	263.6	104.4	10.9	1.66
WB280D0	448.5	448.96	303.3	117.9	16.5	1.39
WB280D0	448.96	449.5	326.1	166.6	25.1	0.56
WB280D0	449.5	449.96	398.0	252.1	33.4	0.33
WB280D0	449.96	450.59	289.0	122.1	13.7	1.38
WB280D0	450.59	451	408.1	169.6	21.0	1.00
WB280D0	451	451.61	379.1	111.3	25.5	1.73
WB280D0	451.61	452	451.0	291.1	34.8	1.35
WB280D0	452	452.65	256.7	91.4	22.3	1.26
WB280D0	452.65	452.92	475.9	191.3	32.7	0.61
WB280D0	452.92	453.5	214.4	95.7	16.0	0.56
WB280D0	453.5	454.25	219.2	98.5	13.3	0.90
WB280D0	454.25	455	467.1	185.0	28.1	0.85
WB280D0	455	455.54	432.9	161.1	24.8	1.33
WB280D0	456.76	457.1	378.6	152.8	20.8	0.86
WB280D0	457.1	457.5	226.3	90.7	14.4	1.25
WB280D0	457.5	457.81	330.2	132.5	19.1	1.52
WB280D0	457.81	458.16	251.8	97.1	16.8	2.03
WB280D0	458.16	458.8	397.7	141.5	21.4	0.75
WB280D0	458.8	459.26	324.0	111.4	17.4	0.98
WB280D0	459.26	459.62	328.4	104.8	22.6	1.37
WB280D0	460.1	460.35	354.4	138.7	19.7	1.22
WB280D0	461.39	462	351.5	122.6	18.9	1.96
WB280D0	462	462.3	313.1	107.8	17.6	0.96
WB280D0	466.7	467	277.0	118.4	16.6	0.42
WB280D0	467	467.49	332.8	159.1	21.9	0.69
WB280D0	467.49	467.75	168.1	77.6	9.7	0.31
WB280D0	467.75	468	422.4	177.8	26.1	1.03
WB280D0	468	468.75	435.4	168.4	36.7	0.87
WB280D0	468.75	469.15	376.4	136.2	18.7	0.96
WB280D0	469.15	469.4	313.0	131.7	19.4	0.93
WB280D0	470.8	471.08	471.2	352.6	19.5	0.56
WB280D0	471.78	472.29	329.6	96.7	17.8	0.51
WB280D0	473.5	474	296.6	118.2	14.5	0.41
WB280D0	474	474.36	287.5	106.0	22.5	0.75
WB280D0	474.36	474.75	126.4	44.9	22.9	1.09
WB280D0	476	476.5	244.5	81.5	17.3	0.40
WB280D0	479.82	480.66	363.1	132.5	22.3	0.90
WB280D0	480.66	481	374.2	161.6	31.6	0.57
WB280D0	481	481.48	284.0	93.7	15.9	0.69
WB280D0	482	482.5	160.7	55.4	11.1	0.18
WB280D0	482.5	483	44.7	25.6	12.8	0.16
WB280D0	483	483.5	58.4	31.5	4.5	0.22
WB280D0	483.5	484	17.6	23.4	11.7	0.17
WB280D0	484	485	78.2	14.0	5.6	0.36
WB280D0	485	486	29.5	11.8	5.9	0.17
WB259D0	259	260	25.8	19.3	6.4	0.16

WB259D0	260	261	8.4	25.1	8.4	0.12
WB259D0	261	262	5.1	15.2	5.1	0.20
WB259D0	262	262.5	14.5	43.4	14.5	0.07
WB259D0	262.5	263.11	9.5	14.3	4.8	0.21
WB259D0	263.11	264	22.9	45.8	11.5	0.09
WB259D0	264	265	40.6	54.2	13.5	0.07
WB259D0	265	266	4.9	9.8	4.9	0.20
WB259D0	266	267	7.0	7.0	7.0	0.14
WB259D0	267	267.63	5.6	5.6	5.6	0.18
WB259D0	267.63	268	8.6	25.8	8.6	0.12
WB259D0	268	269	30.4	45.6	15.2	0.07
WB259D0	269	270	9.8	19.6	9.8	0.10
WB259D0	270	271	14.3	28.7	14.3	0.07
WB259D0	285.5	286	296.4	112.9	48.0	0.35
WB259D0	287	287.5	443.4	186.7	45.2	0.69
WB259D0	287.5	288	478.5	196.0	33.2	1.30
WB259D0	288	288.5	312.3	136.0	23.6	0.72
WB259D0	288.5	289	282.8	126.5	25.8	0.74
WB259D0	289	289.5	71.1	45.1	17.3	0.58
WB259D0	292	292.54	66.5	46.6	5.0	0.60
WB259D0	292.54	293	25.1	13.7	2.3	0.44
WB259D0	293	293.5	10.8	5.4	2.7	0.74
WB259D0	293.5	294	49.7	49.7	2.8	0.36
WB259D0	310.07	310.5	51.3	36.6	7.3	0.27
WB259D0	311	311.5	453.2	196.5	31.6	0.70
WB259D0	311.5	312	441.2	164.5	69.9	1.09
WB259D0	312	312.5	457.1	189.6	37.9	1.00
WB259D0	313	313.5	417.5	200.7	31.9	2.23
WB259D0	313.5	314	288.4	99.2	17.1	0.65
WB259D0	314	314.5	312.4	156.2	6.9	0.29
WB259D0	314.5	315	259.6	141.9	18.7	0.37
WB259D0	315.5	316.1	420.5	176.8	28.7	0.42
WB259D0	316.1	316.36	80.3	48.2	10.7	0.19
WB259D0	321	321.5	423.5	168.8	33.2	0.36
WB259D0	321.5	322	455.3	197.8	40.7	0.37
WB259D0	322.5	323	203.8	95.3	17.6	0.68
WB259D0	323	323.5	629.7	330.6	31.5	0.06
WB259D0	324.96	325.5	506.4	231.0	25.9	0.54
WB259D0	325.5	326	453.6	215.7	26.2	0.50
WB259D0	326.5	327	223.1	100.0	28.2	0.39
WB259D0	327.5	328	251.5	105.1	22.3	0.94
WB259D0	328	328.62	192.6	97.2	15.9	0.57
WB259D0	329.8	330.5	208.7	95.4	15.9	0.50
WB259D0	330.5	331	132.3	62.2	12.0	1.00
WB259D0	349.5	349.92	20.5	13.7	4.1	0.73
WB259D0	352.52	353	378.3	171.4	26.2	0.65
WB259D0	353	353.5	8.4	6.7	1.7	0.60
WB259D0	353.5	353.98	1.2	1.2	1.2	0.81

WB259D0	353.98	354.48	124.3	50.7	6.5	0.61
WB259D0	354.48	355	359.1	161.5	26.5	0.41
WB259D0	355	355.5	593.2	295.5	32.2	0.90
WB259D0	365	365.5	299.4	148.7	16.4	1.04
WB259D0	365.5	366	271.3	153.0	17.3	1.10
WB259D0	366	366.5	281.3	104.2	20.5	1.66
WB259D0	366.5	367	226.9	95.1	12.7	0.79
WB259D0	367	367.5	304.2	138.1	14.3	2.10
WB259D0	367.5	368	370.8	152.1	25.9	1.43
WB259D0	368	368.5	269.3	114.2	22.7	1.32
WB259D0	368.5	369	236.8	99.2	19.8	0.81
WB259D0	369	369.5	236.3	131.5	12.2	0.41
WB259D0	369.5	370	321.9	135.2	18.3	1.21
WB259D0	370	370.46	472.4	213.0	42.4	1.01
WB259D0	370.46	371	168.4	71.3	13.0	0.77
WB259D0	371	371.48	282.1	115.8	17.3	0.75
WB259D0	371.48	372	253.7	97.1	15.5	0.77
WB259D0	372	372.5	333.3	129.9	23.9	1.05
WB259D0	373	373.5	193.2	47.2	5.8	0.87
WB259D0	376	376.5	358.9	122.2	17.7	1.19
WB259D0	376.5	377	7.9	4.3	1.4	1.39
WB259D0	377	377.5	1.1	1.1	1.1	0.88
WB259D0	377.5	378	1.2	1.2	1.2	0.84
WB259D0	379	379.62	495.5	174.9	29.9	1.30
WB259D0	379.62	380	387.0	151.2	29.3	0.62
WB259D0	380	380.3	350.8	144.3	21.1	0.90
WB259D0	381.07	381.58	472.3	277.2	23.5	1.74
WB259D0	381.58	381.88	468.7	223.3	32.3	1.18
WB259D0	381.88	382.15	386.9	184.1	26.5	0.91
WB259D0	383.5	384	371.0	147.7	24.0	0.87
WB259D0	386	386.44	417.4	139.7	11.1	1.26
WB259D0	387	387.5	255.8	119.3	13.8	0.58
WB259D0	387.78	388.3	314.9	142.4	18.8	1.76
WB259D0	388.3	388.75	426.2	224.2	21.3	1.08
WB259D0	388.75	389.3	164.7	40.1	8.6	0.70
WB259D0	389.3	390	233.9	135.7	10.1	0.69
WB259D0	390	390.5	288.6	111.6	19.1	0.99
WB259D0	390.5	391.15	376.0	199.9	34.3	0.67
WB259D0	391.15	391.83	265.0	112.5	14.5	0.55
WB259D0	391.83	392.27	377.1	144.8	26.7	1.05
WB259D0	393	393.5	292.5	119.9	13.0	1.77
WB259D0	393.5	394	425.7	183.5	17.6	0.68
WB259D0	394	394.5	463.9	103.3	13.9	1.30
WB259D0	394.5	395	402.1	191.6	27.6	1.27
WB259D0	395	395.5	472.2	189.4	27.3	1.91
WB259D0	395.5	396	492.1	187.7	25.2	2.14
WB259D0	396	396.42	346.6	147.8	17.3	1.16
WB259D0	397.37	398	189.2	110.3	6.4	1.24

WB259D0	398	398.5	431.7	167.7	28.3	1.91
WB259D0	404	404.5	25.3	12.6	4.2	0.24
WB259D0	404.5	405.11	203.2	48.6	16.2	0.56
WB259D0	408	408.5	328.5	346.2	101.2	0.56
WB259D0	408.5	409	6.3	15.7	6.3	0.32
WB259D0	410.5	411	31.5	16.1	3.2	1.24
WB259D0	411	411.5	95.5	34.2	7.2	0.55
WB259D0	414	414.5	178.5	46.8	8.5	0.47
WB259D0	414.5	415	498.3	133.2	27.3	1.25
WB259D0	415	415.69	437.1	115.0	42.8	0.75
WB259D0	417.52	417.8	335.3	129.7	22.1	0.72
WB259D0	417.8	418.15	207.7	84.2	11.5	0.87
WB259D0	418.15	419	186.5	83.1	10.2	0.59
WB259D0	419	419.35	361.5	143.0	29.7	0.87
WB259D0	421.07	421.5	6.5	9.7	3.2	0.31
WB259D0	425.5	426	403.2	265.8	26.8	0.56
WB259D0	426	426.5	375.8	133.8	27.1	0.67
WB259D0	426.5	427	375.9	547.0	45.8	0.98
WB259D0	427	427.5	385.7	191.5	26.1	0.77
WB259D0	432	432.5	48.6	25.5	4.6	0.43
WB259D0	432.5	432.94	218.4	79.2	9.6	1.77
WB259D0	432.94	433.5	228.6	103.4	21.9	0.96
WB259D0	433.5	434.05	238.6	169.6	13.8	0.51
WB259D0	438.07	438.5	175.9	85.1	8.5	0.35
WB259D0	438.5	439	103.1	57.0	5.4	0.37
WB259D0	439	439.63	300.5	136.6	21.9	0.37
WB259D0	439.63	440	322.9	158.4	19.4	0.83
WB259D0	440	440.39	213.9	104.1	13.4	1.05
WB259D0	440.39	441	235.2	119.9	15.4	0.65
WB259D0	445	445.53	137.1	74.8	5.0	0.40
WB259D0	445.53	445.78	402.5	216.7	26.5	0.45
WB259D0	446.31	447	284.6	129.0	15.2	0.53
WB259D0	447	447.5	392.3	162.5	15.3	1.11
WB259D0	447.5	448	301.0	114.5	18.2	0.99
WB259D0	448	448.39	415.7	188.9	27.7	1.27
WB259D0	448.73	449	220.9	93.0	11.6	0.34
WB259D0	449	449.33	400.4	158.9	32.6	0.46
WB259D0	449.98	450.5	265.6	126.6	14.9	0.40
WB259D0	450.5	451	412.8	188.3	28.4	0.39
WB259D0	453.5	454	617.1	316.0	42.7	0.54
WB259D0	454	454.5	371.2	160.3	25.3	0.95
WB259D0	456	456.5	227.8	93.2	18.1	0.39
WB259D0	456.5	457	192.1	72.7	12.9	0.62
WB259D0	457	457.5	226.5	90.1	12.2	0.41
WB259D0	465	466	81.8	31.3	4.8	0.42
WB259D0	466	467	84.0	26.2	7.9	0.38
WB259D0	467	468	131.7	21.1	2.6	0.76
WB259D0	468	469	14.5	7.2	7.2	0.14

WB259D0	469	470	6.3	6.3	6.3	0.16
WB259D0	470	471	6.3	6.3	6.3	0.16
WB257D0	225	225.25	13.7	12.0	1.7	0.58
WB257D0	226.1	227	2.3	2.3	2.3	0.44
WB257D0	227	228	1.6	0.8	0.8	1.27
WB257D0	228	228.5	0.9	0.9	0.9	1.07
WB257D0	228.5	229	2.8	1.9	0.9	1.06
WB257D0	229	229.5	2.7	8.0	2.7	0.37
WB257D0	229.5	230	0.3	0.3	0.3	3.92
WB257D0	230	230.5	1.6	4.7	1.6	0.64
WB257D0	230.5	231	3.3	5.0	1.7	0.60
WB257D0	231	231.5	18.8	6.7	1.3	0.74
WB257D0	231.5	232	0.7	1.5	0.4	2.68
WB257D0	232	232.3	0.2	0.2	0.1	10.21
WB257D0	232.3	233	9.3	4.7	2.3	0.43
WB257D0	233	233.5	2.7	4.0	1.3	0.75
WB257D0	243.42	243.77	233.8	124.5	6.6	0.46
WB257D0	247.5	248	56.2	30.1	2.6	0.77
WB257D0	248	248.6	0.9	0.6	0.3	6.42
WB257D0	248.6	249.2	17.7	7.5	1.1	1.87
WB257D0	251.05	252	34.4	8.6	2.1	0.47
WB257D0	252	253	26.6	16.3	1.5	0.68
WB257D0	256.8	257.5	179.0	76.5	10.4	0.58
WB257D0	260.5	261	394.2	151.3	18.9	0.69
WB257D0	261	261.5	187.3	101.5	10.9	1.28
WB257D0	261.5	262	34.2	18.6	2.2	3.66
WB257D0	262	262.53	62.0	27.3	3.2	1.90
WB257D0	262.8	263.57	111.9	56.1	6.0	2.98
WB257D0	263.82	264.4	364.5	169.5	17.9	1.06
WB257D0	264.4	264.86	273.5	116.1	18.2	0.99
WB257D0	265.3	266.08	172.0	68.3	7.6	0.40
WB257D0	266.08	266.33	222.9	81.5	21.6	0.42
WB257D0	266.33	266.84	717.9	310.2	40.6	0.74
WB257D0	266.84	267.5	722.9	370.5	36.2	0.61
WB257D0	267.5	268	65.7	36.2	4.0	0.75
WB257D0	268	268.5	111.4	84.3	7.0	1.00
WB257D0	268.5	269	134.9	110.6	6.1	1.65
WB257D0	269.5	270	193.7	67.6	13.5	0.44
WB257D0	270	270.5	343.7	141.0	17.6	0.91
WB257D0	271.5	272	36.2	13.8	1.7	0.58
WB257D0	272	272.5	68.4	28.0	3.4	2.97
WB257D0	272.5	273	15.0	7.5	2.5	0.40
WB257D0	273	273.5	171.8	61.4	6.1	0.65
WB257D0	273.5	274	43.6	26.3	3.0	1.33
WB257D0	274.5	275	8.8	8.8	4.4	0.23
WB257D0	275	275.5	23.4	14.0	9.4	0.21
WB257D0	275.5	276	18.2	8.8	0.7	1.48
WB257D0	276	276.5	29.6	9.2	2.2	2.70

WB257D0	276.5	277	163.2	66.5	11.8	2.29
WB257D0	277	277.5	80.1	32.4	4.3	1.17
WB257D0	277.5	278	25.5	9.7	1.6	6.83
WB257D0	278	278.5	374.0	154.3	22.0	1.68
WB257D0	278.5	279	312.6	213.3	18.3	1.15
WB257D0	279	279.5	197.4	85.2	10.5	2.01
WB257D0	279.5	280	153.2	64.4	10.4	0.57
WB257D0	281	282	138.4	60.7	8.7	2.42
WB257D0	282	282.58	416.3	174.0	25.4	1.53
WB257D0	282.58	283	359.4	159.6	17.0	0.65
WB257D0	283	283.5	238.7	118.2	19.3	0.41
WB257D0	283.5	284	251.8	109.6	16.3	0.43
WB257D0	284	284.5	368.0	153.5	20.9	0.57
WB257D0	284.5	285.21	306.5	125.0	17.6	0.57
WB257D0	285.62	286	343.3	127.1	13.4	0.45
WB257D0	286	286.66	432.3	172.4	22.8	0.84
WB257D0	288.2	288.86	435.6	100.0	9.7	0.31
WB257D0	288.86	289.66	399.7	174.2	22.0	0.55
WB257D0	292	292.5	525.4	213.1	27.3	0.40
WB257D0	299	299.5	197.7	80.6	18.3	0.66
WB257D0	299.5	300	345.1	153.6	22.5	0.98
WB257D0	303	303.5	281.5	125.4	16.0	0.69
WB257D0	303.5	304	320.2	132.4	17.8	0.51
WB257D0	304	304.5	305.4	171.3	27.9	0.75
WB257D0	306	306.5	541.9	218.7	34.9	1.58
WB257D0	306.5	307.1	292.5	130.4	19.8	0.76
WB257D0	307.44	307.92	261.1	109.0	18.2	0.44
WB257D0	309.5	310	338.9	128.8	25.8	0.50
WB257D0	311.49	312.1	381.8	138.9	23.7	0.63
WB257D0	312.1	312.93	338.7	161.5	17.2	0.64
WB257D0	312.93	313.27	266.2	102.2	17.0	0.47
WB257D0	314	314.61	209.2	93.8	7.8	0.51
WB257D0	315.1	315.72	289.1	108.7	20.8	0.43
WB257D0	315.72	316.06	348.8	120.7	23.0	0.52
WB257D0	318.52	318.77	345.5	141.3	23.0	1.17
WB257D0	318.77	319.46	202.3	100.4	12.7	0.63
WB257D0	319.96	320.33	355.7	157.6	15.6	0.64
WB257D0	320.92	321.28	329.1	129.7	23.7	0.63
WB257D0	321.28	321.74	415.4	172.9	19.0	0.47
WB257D0	323.75	324.4	61.9	24.4	13.0	0.61
WB257D0	324.4	324.96	80.7	35.6	7.1	0.42
WB257D0	324.96	325.74	307.9	119.9	14.6	0.62
WB257D0	325.74	326.04	214.0	84.0	16.3	0.37
WB257D0	326.04	326.5	523.3	158.3	31.7	0.54
WB257D0	326.5	327	359.5	132.1	17.5	0.51
WB257D0	327	327.55	373.1	134.3	23.1	0.74
WB257D0	327.55	328	165.5	67.7	7.5	0.13
WB257D0	328	329	30.6	20.4	10.2	0.10

WB257D0	329	329.62	46.5	46.5	15.5	0.06
WB257D0	329.62	329.87	337.0	129.6	20.5	0.73
WB257D0	330.18	330.48	478.3	107.7	23.8	1.22
WB257D0	330.48	331	222.1	43.8	21.9	1.92
WB257D0	331	331.46	301.4	103.7	19.5	1.13
WB257D0	331.46	331.76	376.9	178.6	40.3	1.32
WB257D0	331.76	332.03	321.4	141.0	24.1	0.79
WB257D0	332.03	332.6	256.4	90.0	18.7	0.59
WB257D0	332.6	333.25	78.4	30.2	6.0	0.17
WB257D0	334.86	335.53	208.5	94.1	10.1	0.30
WB257D0	336.7	337.04	223.0	145.0	20.1	0.45
WB257D0	339.26	339.62	127.9	54.8	9.1	0.33
WB257D0	340.32	341	168.6	66.7	14.3	1.05
WB257D0	341	341.66	154.6	63.1	9.1	1.09
WB257D0	345.36	345.78	35.1	10.8	2.7	0.37
WB257D0	345.78	346.4	107.8	44.2	5.5	0.36
WB257D0	346.4	347.1	123.9	41.3	9.2	0.65
WB257D0	347.1	347.86	109.1	30.2	7.0	0.43
WB257D0	347.86	348.26	119.8	47.9	6.0	0.33
WB257D0	348.26	348.59	146.7	60.9	7.8	0.64
WB257D0	348.59	349	59.7	27.3	5.0	0.40
WB257D0	349	349.27	170.1	75.6	4.7	0.21
WB257D0	349.27	350	91.5	40.9	5.8	0.51
WB257D0	350.5	351	170.1	69.3	6.3	0.32
WB257D0	351	351.65	128.2	55.1	20.4	0.83
WB257D0	351.65	352.34	126.1	59.9	11.8	1.10
WB257D0	352.34	352.67	126.2	50.5	5.6	0.36
WB257D0	352.67	353.04	107.6	51.4	8.0	0.62
WB257D0	353.04	353.5	133.9	54.8	9.1	0.33
WB257D0	353.5	353.75	218.6	90.4	12.6	0.95
WB257D0	354.1	354.63	133.2	62.4	9.5	0.95
WB257D0	354.63	354.88	81.4	37.2	4.7	0.43
WB257D0	354.88	355.53	95.3	38.1	6.4	0.31
WB257D0	356.05	356.55	291.8	129.8	14.6	0.69
WB257D0	356.55	357	198.2	95.5	15.7	0.70
WB257D0	361.27	361.52	205.0	93.0	13.7	0.37
WB257D0	363.81	364.3	219.2	82.5	15.2	0.46
WB257D0	364.3	364.74	122.0	48.0	12.0	0.50
WB257D0	364.74	365.08	156.0	61.9	18.4	0.44
WB257D0	365.08	365.4	170.1	62.1	12.4	1.29
WB257D0	366.6	367.15	262.8	113.7	12.6	0.40
WB257D0	367.15	367.6	133.8	51.9	15.6	0.77
WB257D0	369.66	370	56.3	26.0	4.3	0.23
WB257D0	370	370.42	173.6	84.8	6.1	0.50
WB257D0	370.83	371.5	60.5	28.2	4.0	0.25
WB257D0	371.5	372	356.8	164.0	28.7	0.49
WB257D0	373	374	421.9	231.8	27.0	0.74
WB257D0	374	374.79	455.5	187.0	25.6	1.25

WB257D0	374.79	375.5	87.4	32.4	7.6	0.93
WB257D0	376	377	13.0	6.5	2.2	0.46
WB257D0	377	378	45.4	30.3	5.0	0.40
WB257D0	378	379	49.1	32.7	5.5	0.18
WB257D0	379	379.76	58.1	19.4	3.9	0.26
WB257D0	379.76	380.5	266.4	101.2	16.0	0.56
WB257D0	381.35	382	47.7	14.5	4.1	0.48
WB257D0	382	383	63.6	25.0	4.5	0.44
WB257D0	384	385	67.4	22.5	2.2	0.44
WB257D0	386	387	65.2	20.9	5.2	0.38
WB257D0	387	387.8	12.7	9.5	3.2	0.31
WB257D0	387.8	388.5	3.5	1.3	0.4	2.29
WB257D0	388.5	389	12.6	12.6	3.2	0.32
WB257D0	389	390	5.9	5.9	2.0	0.51
WB257D0	390	391	17.7	17.7	5.9	0.17
WB254D0	329.6	330.2	9.7	9.7	9.7	0.10
WB254D0	330.2	330.7	17.4	17.4	17.4	0.06
WB254D0	330.7	331.42	18.4	27.6	9.2	0.11
WB254D0	331.42	331.94	34.7	34.7	11.6	0.09
WB254D0	331.94	332.25	16.8	16.8	16.8	0.06
WB254D0	332.25	333.25	14.5	14.5	14.5	0.07
WB254D0	334	334.79	13.6	13.6	13.6	0.07
WB254D0	335.4	335.7	7.7	7.7	7.7	0.13
WB254D0	341.5	342	1594.0	845.5	57.6	0.66
WB254D0	342	342.5	451.7	254.6	20.1	0.70
WB254D0	343.5	344	630.1	342.4	19.0	0.42
WB254D0	344	344.7	762.1	330.9	28.4	0.53
WB254D0	344.7	345	322.6	151.2	16.8	1.13
WB254D0	345.5	346	1173.4	628.4	84.9	0.75
WB254D0	346	346.5	117.5	47.9	17.4	0.69
WB254D0	346.5	347	420.5	277.2	60.7	0.64
WB254D0	347	347.5	347.0	165.4	32.5	0.99
WB254D0	347.5	348	322.5	137.5	21.1	2.28
WB254D0	348	348.5	207.2	92.6	17.8	1.63
WB254D0	348.5	349	277.7	123.6	24.2	1.12
WB254D0	349	349.5	129.4	58.6	8.1	0.49
WB254D0	349.5	350	188.6	76.2	12.2	1.72
WB254D0	350	350.5	171.7	91.0	12.3	1.55
WB254D0	350.5	350.84	13.9	11.6	25.5	0.43
WB254D0	350.84	351.5	340.8	154.2	18.7	1.76
WB254D0	351.5	352.17	169.7	79.2	22.6	0.44
WB254D0	352.17	352.62	383.0	241.8	35.8	1.03
WB254D0	352.62	353	277.4	121.5	18.0	2.62
WB254D0	353	353.5	457.7	159.3	17.4	1.09
WB254D0	353.5	354	346.6	144.4	75.1	2.37
WB254D0	354	354.72	257.2	78.9	24.1	3.61
WB254D0	354.72	355.1	373.7	163.6	33.5	0.54
WB254D0	355.1	355.44	165.5	89.5	20.1	0.45

WB254D0	355.44	356	286.6	89.9	24.6	1.06
WB254D0	356	356.64	154.5	59.0	42.6	1.95
WB254D0	356.64	357	121.4	57.5	13.0	2.31
WB254D0	357	357.58	259.7	129.1	13.1	0.69
WB254D0	357.58	357.84	182.0	54.1	15.0	0.67
WB254D0	357.84	358.22	196.6	70.7	6.6	0.45
WB254D0	358.22	358.68	407.2	80.8	9.9	2.41
WB254D0	358.68	359	301.5	109.5	18.2	1.15
WB254D0	359	359.5	112.2	47.6	8.1	1.11
WB254D0	359.5	360	196.2	141.3	11.7	1.11
WB254D0	360	360.37	82.0	39.7	10.6	0.38
WB254D0	360.37	360.62	26.1	10.4	4.5	1.34
WB254D0	360.62	361.22	150.0	52.9	7.6	0.93
WB254D0	362.07	362.6	42.2	21.1	3.8	0.52
WB254D0	362.6	363.22	7.9	10.5	2.6	0.38
WB254D0	363.22	363.55	93.0	66.4	13.3	0.08
WB254D0	363.55	364	181.4	90.7	7.0	0.43
WB254D0	364	364.4	52.7	35.1	2.5	0.80
WB254D0	364.4	364.83	56.3	33.3	7.7	0.39
WB254D0	364.83	365.5	59.0	33.3	7.7	0.39
WB254D0	365.5	366	40.7	28.5	4.1	0.25
WB254D0	366	366.5	7.0	3.5	7.0	0.28
WB254D0	367	367.5	1000.8	324.7	130.4	0.38
WB254D0	367.5	368	294.2	119.0	23.5	0.76
WB254D0	368	368.65	196.7	84.3	51.3	0.82
WB254D0	368.65	369	57.4	21.3	8.5	0.47
WB254D0	369	369.5	159.6	57.8	17.0	1.00
WB254D0	369.5	370	121.2	48.2	9.2	1.41
WB254D0	370	370.5	119.5	53.2	9.3	1.07
WB254D0	370.5	371	142.7	81.4	9.7	1.45
WB254D0	371	371.5	273.4	126.9	17.2	0.81
WB254D0	371.5	372	466.5	174.6	16.6	0.78
WB254D0	372	372.5	83.2	27.4	7.6	1.06
WB254D0	372.5	373	206.5	76.0	14.9	1.21
WB254D0	373	373.5	170.9	72.7	7.3	0.55
WB254D0	373.5	374	90.6	46.9	6.2	0.32
WB254D0	375	375.5	106.9	44.5	8.9	0.34
WB254D0	375.5	376	113.4	46.9	7.8	0.26
WB254D0	382.5	383	68.7	37.2	2.9	0.35
WB254D0	383	383.5	54.1	31.2	8.3	0.48
WB254D0	383.5	384	58.9	31.7	6.0	0.66
WB254D0	384	384.5	107.0	55.4	3.8	0.52
WB254D0	384.5	385.16	97.8	52.4	8.7	0.57
WB254D0	385.16	385.6	39.6	26.4	6.6	0.30
WB254D0	385.6	386	26.1	13.0	3.3	0.31
WB254D0	386	386.34	70.2	32.2	5.9	0.34
WB254D0	386.34	387	65.0	34.2	3.4	0.29
WB254D0	387	387.4	51.8	21.4	3.4	0.89

WB254D0	387.4	387.85	59.7	24.7	3.9	0.77
WB254D0	388.4	388.96	73.3	29.8	6.9	0.87
WB254D0	389.28	389.53	2.7	5.5	2.7	0.36
WB254D0	391	391.5	28.4	17.4	10.9	0.46
WB254D0	391.5	392	22.0	11.0	22.0	0.55
WB254D0	392	392.5	30.2	9.2	3.9	0.76
WB254D0	392.5	393	15.7	6.0	3.6	0.83
WB254D0	393	393.5	55.7	23.0	6.6	0.30
WB254D0	393.5	394	68.4	27.4	6.8	0.15
WB254D0	394.5	395	16.1	8.1	2.7	0.37
WB254D0	395	395.6	34.1	14.6	4.9	0.21
WB254D0	395.6	396.2	15.3	8.1	0.9	1.11
WB254D0	396.2	396.6	5.5	3.6	0.9	1.10
WB254D0	396.6	397	4.6	4.6	0.9	1.10
WB254D0	397	397.5	4.5	2.7	0.9	1.12
WB254D0	397.5	398	3.5	2.0	1.0	2.00
WB254D0	398	398.5	3.8	2.5	1.3	1.59
WB254D0	398.5	399	14.2	5.3	0.9	1.13
WB254D0	399	399.5	40.2	24.8	3.1	0.32
WB254D0	400	400.5	47.3	23.6	3.0	0.34
WB254D0	400.5	401.17	21.2	14.2	3.5	0.28
WB254D0	401.17	401.77	13.1	5.6	1.9	0.53
WB254D0	401.77	402.07	12.2	3.5	1.7	0.57
WB254D0	405.75	406.15	58.3	24.3	4.9	0.21
WB254D0	406.15	406.5	17.3	5.8	9.6	0.52
WB254D0	406.5	407	22.0	8.8	10.3	0.68
WB254D0	409.5	410	59.8	31.2	5.2	0.38
WB254D0	413.5	414	12.8	25.6	12.8	0.08
WB254D0	415	415.5	9.2	9.2	9.2	0.11
WB254D0	416	416.5	10.9	10.9	10.9	0.09
WB254D0	417	417.37	28.6	14.3	14.3	0.07
WB254D0	417.37	418	27.8	13.9	13.9	0.07
WB254D0	418	418.5	22.4	22.4	11.2	0.09
WB254D0	418.5	419	20.3	10.1	3.4	0.30
WB254D0	419	419.5	11.6	11.6	11.6	0.09
WB254D0	419.5	420	24.7	16.5	8.2	0.12
WB254D0	420	420.5	94.9	30.4	3.8	0.26
WB254D0	420.5	421	13.9	13.9	4.6	0.22
WB254D0	421	421.5	67.3	30.6	6.1	0.16
WB254D0	421.5	422	115.3	59.1	2.8	0.36
WB254D0	422	422.4	99.9	62.4	5.3	0.56
WB254D0	422.82	423.5	82.4	38.1	6.3	0.16
WB254D0	423.5	424	30.0	20.0	10.0	0.10
WB254D0	428.2	428.6	54.8	27.4	2.7	0.36
WB254D0	428.6	429	39.2	21.1	3.0	0.33
WB254D0	429	429.6	53.4	30.9	2.8	0.36
WB254D0	430.22	430.6	85.8	42.9	3.3	0.30
WB254D0	430.6	431	99.4	39.8	8.5	0.35

WB254D0	431	431.68	100.9	46.6	7.8	0.39
WB254D0	431.68	432.38	116.7	54.1	8.5	0.59
WB254D0	432.79	433.18	110.4	50.6	9.2	0.22
WB254D0	434.13	434.68	117.1	54.0	9.0	0.33
WB254D0	435.4	435.65	141.8	66.4	10.8	0.56
WB254D0	436.66	437.36	153.6	63.2	15.4	0.59
WB254D0	438	438.66	141.6	64.6	13.5	0.96
WB254D0	438.66	439	134.6	60.3	10.4	0.86
WB254D0	439	439.67	82.6	35.4	8.8	0.34
WB254D0	439.67	440.15	141.7	53.4	9.7	1.03
WB254D0	440.15	440.5	176.0	66.9	14.9	0.81
WB254D0	440.5	441	86.1	27.2	6.8	0.88
WB254D0	441	441.5	68.6	25.7	5.1	0.58
WB254D0	441.5	442	88.2	34.7	7.5	1.33
WB254D0	442	442.5	68.6	33.5	6.7	1.20
WB254D0	442.5	443	145.2	60.8	12.2	1.32
WB254D0	443	443.5	109.6	47.0	8.4	0.83
WB254D0	443.5	444	67.3	26.5	5.1	0.98
WB254D0	444	444.5	126.7	53.0	9.2	0.43
WB254D0	444.5	445	84.3	33.7	7.2	0.42
WB254D0	445	445.5	98.6	42.7	6.6	0.30
WB254D0	445.5	446	76.1	38.0	6.3	0.16
WB254D0	446	446.5	61.0	22.5	6.4	0.31
WB254D0	446.5	447	56.3	24.1	5.4	0.37
WB254D0	447	447.5	41.1	31.9	4.6	0.22
WB254D0	447.5	448	43.7	14.6	4.9	0.21
WB254D0	448	448.35	65.1	24.2	3.7	0.54
WB254D0	448.35	449	69.2	26.9	5.8	0.52
WB254D0	449.6	450	118.9	52.8	7.9	0.38
WB254D0	450	450.42	117.8	48.2	8.9	0.56
WB254D0	450.42	451	33.1	16.5	5.5	0.18
WB254D0	451	451.5	50.8	13.5	4.5	0.67
WB254D0	451.5	452	63.8	19.1	6.4	0.31
WB254D0	452	452.5	94.5	32.9	7.2	0.70
WB254D0	452.5	453	76.6	34.5	3.8	0.26
WB254D0	453	453.5	64.8	30.2	4.3	0.23
WB254D0	453.5	454	54.5	25.2	4.2	0.24
WB254D0	454	454.5	64.6	40.4	8.1	0.25
WB254D0	454.5	455	44.7	20.3	4.1	0.25
WB254D0	455	455.7	71.1	35.5	7.1	0.14
WB254D0	455.7	456.06	99.5	41.2	6.9	0.29
WB254D0	456.5	457.07	127.8	51.6	9.8	0.41
WB254D0	457.07	457.6	115.6	49.7	11.7	0.68
WB254D0	457.6	458.26	120.6	52.5	7.1	0.70
WB254D0	458.26	459	103.8	42.1	1.0	1.02
WB254D0	459	459.5	70.3	26.7	4.8	0.41
WB254D0	459.5	460	77.2	32.7	5.9	0.34
WB254D0	460	460.5	45.8	19.6	6.5	0.15

WB254D0	460.5	461.33	74.3	32.5	4.6	0.22
WB254D0	461.33	462	5.0	5.0	5.0	0.20
WB254D0	462	463	2.0	2.0	2.0	0.50
WB254D0	463	464	7.9	7.9	7.9	0.13
WB254D0	464	465	3.1	3.1	3.1	0.32
WB254D0	465	466	5.0	5.0	5.0	0.20
WB255D0	428.5	429	610.7	228.7	81.4	1.15
WB255D0	429	429.5	173.1	72.1	45.0	2.62
WB255D0	429.5	430	204.7	80.9	15.9	1.45
WB255D0	430	430.5	416.4	306.2	180.7	0.98
WB255D0	430.5	431	81.7	33.6	14.4	0.21
WB255D0	431	431.5	257.3	111.0	22.5	0.62
WB255D0	431.5	432	219.3	100.7	24.6	0.45
WB255D0	432	432.5	236.5	115.6	28.5	0.56
WB255D0	432.5	433	163.8	76.7	13.6	1.25
WB255D0	433	433.5	44.2	24.1	12.1	0.50
WB255D0	433.5	434	256.7	93.9	19.8	0.76
WB255D0	434	434.5	150.9	63.9	16.0	0.56
WB255D0	434.5	435	341.8	167.3	19.3	0.83
WB255D0	435	435.71	210.0	81.0	14.9	0.60
WB255D0	435.71	436	215.6	92.9	17.1	1.11
WB255D0	436	436.5	177.7	79.7	24.5	0.82
WB255D0	436.5	437	167.8	87.5	14.3	0.56
WB255D0	437	437.5	219.3	103.0	14.5	0.83
WB255D0	439	439.25	6.0	6.0	18.0	0.17
WB255D0	442.5	443	262.3	117.5	16.5	1.21
WB255D0	443	443.5	211.3	71.2	9.2	0.87
WB255D0	444	444.5	133.4	68.1	17.7	0.73
WB255D0	444.5	445	143.5	58.7	9.8	0.92
WB255D0	445	445.58	159.6	65.9	13.2	0.68
WB255D0	447	447.25	193.3	68.3	15.5	0.78
WB255D0	447.25	447.92	207.0	88.5	20.0	1.20
WB255D0	447.92	448.59	116.8	50.1	9.2	1.74
WB255D0	448.59	449.31	176.2	71.6	18.4	1.03
WB255D0	449.31	450.05	29.9	12.0	2.0	0.50
WB255D0	450.05	450.49	108.6	43.2	23.7	0.72
WB255D0	450.74	451	195.8	74.7	17.1	1.23
WB255D0	451	451.5	122.7	46.1	13.7	1.02
WB255D0	451.5	452	183.6	62.7	11.7	0.69
WB255D0	452	452.7	153.3	64.2	10.9	0.92
WB255D0	452.7	453.11	136.3	51.5	15.3	0.72
WB255D0	453.11	453.49	148.3	58.0	12.1	0.74
WB255D0	454.5	455.2	111.9	27.6	16.2	0.62
WB255D0	455.2	456	143.1	53.5	11.0	0.64
WB255D0	459.5	460	179.9	70.6	13.7	0.44
WB255D0	460.62	460.87	179.5	72.4	16.6	0.66
WB255D0	460.87	461.25	151.7	60.5	13.2	0.91
WB255D0	461.25	461.62	158.6	65.8	10.8	2.67

WB255D0	461.62	462	213.0	60.6	10.7	1.02
WB255D0	462	462.5	50.7	17.3	4.6	0.87
WB255D0	462.5	463	130.0	52.0	12.5	0.96
WB255D0	463	463.3	198.3	82.7	18.2	0.82
WB255D0	463.3	464	251.1	107.2	17.6	0.63
WB255D0	464.5	465	67.5	26.7	6.3	0.64
WB255D0	465	465.46	45.4	21.0	7.0	0.86
WB255D0	465.46	465.83	137.6	50.4	22.5	1.69
WB255D0	465.83	466.5	224.4	91.6	17.6	0.85
WB255D0	466.5	467.18	187.0	64.5	20.2	2.48
WB255D0	467.18	467.46	154.8	56.9	13.2	0.76
WB255D0	467.46	468	125.9	51.8	10.6	0.95
WB255D0	468	468.5	158.5	70.7	13.6	1.70
WB255D0	468.5	469.16	142.8	62.2	11.7	1.03
WB255D0	469.16	469.85	155.3	107.3	9.9	0.71
WB255D0	469.85	470.32	145.2	49.9	10.9	0.64
WB255D0	470.78	471.24	147.9	38.3	16.5	1.33
WB255D0	471.24	471.6	100.8	40.4	11.1	1.81
WB255D0	472	472.5	174.5	69.0	17.3	0.52
WB255D0	472.5	473	132.8	78.2	11.9	0.42
WB255D0	473	473.5	119.3	45.5	9.4	0.64
WB255D0	473.5	474	204.7	95.5	12.1	0.66
WB255D0	474	474.5	147.4	72.2	14.3	1.33
WB255D0	474.5	475	178.8	79.9	16.2	1.05
WB255D0	475	475.5	164.8	60.7	11.7	1.45
WB255D0	475.5	476	180.0	67.9	14.4	0.97
WB255D0	476	476.5	171.9	63.1	17.3	0.63
WB255D0	476.5	477	248.9	67.0	22.3	0.90
WB255D0	477	477.5	195.0	66.2	12.9	1.93
WB255D0	477.5	478	96.5	59.7	9.0	1.01
WB255D0	478	478.36	179.9	72.2	12.7	0.71
WB255D0	478.36	479	99.5	38.2	9.5	0.73
WB255D0	479	479.5	117.1	41.5	7.6	0.26
WB255D0	479.5	480	174.8	78.2	13.8	0.22
WB255D0	480	480.5	224.3	107.4	11.9	0.42
WB255D0	480.5	481	166.8	73.3	7.7	1.04
WB255D0	481	481.5	248.4	92.1	26.3	0.68
WB255D0	482	482.5	207.0	64.1	29.6	0.20
WB255D0	482.5	483	154.1	44.0	29.3	0.14
WB255D0	483	483.5	134.4	56.9	15.8	0.63
WB255D0	483.5	484	93.1	49.5	7.3	0.69
WB255D0	484	484.5	74.9	44.9	10.0	0.20
WB255D0	484.5	485	45.3	30.2	7.5	0.27
WB255D0	485	485.32	128.5	47.7	9.3	0.75
WB255D0	485.32	486	163.0	59.3	11.1	1.08
WB255D0	487	487.4	81.3	36.5	10.0	0.60
WB255D0	487.4	488	201.6	81.3	17.0	0.82
WB255D0	488	489	136.6	61.2	8.2	0.49

WB255D0	489	490	139.7	66.8	12.2	0.33
WB255D0	490	490.52	25.8	17.2	8.6	0.12
WB255D0	490.52	490.89	55.6	46.3	18.5	0.11
WB255D0	491.48	492	157.9	63.2	14.4	0.35
WB255D0	492	493	132.2	57.0	11.4	0.44
WB255D0	493	493.5	38.7	19.4	3.9	0.26
WB255D0	494	494.5	131.6	65.8	14.6	0.41
WB255D0	495	495.5	92.1	40.3	11.5	0.35
WB255D0	495.5	496	133.7	48.2	10.1	1.29
WB255D0	496	496.5	147.8	54.6	12.9	0.93
WB255D0	496.5	496.84	154.6	57.8	12.1	0.74
WB255D0	496.84	497.5	116.0	38.3	10.4	0.97
WB255D0	497.5	497.95	116.6	45.9	8.6	1.05
WB255D0	497.95	498.63	171.9	80.6	10.7	0.66
WB255D0	499.7	500	154.3	64.9	10.6	0.94
WB255D0	500	500.5	474.5	187.5	16.6	0.60
WB255D0	500.5	500.88	116.0	48.3	13.1	1.45
WB255D0	500.88	501.67	105.3	34.6	6.6	0.61
WB255D0	501.67	502.02	157.7	47.9	12.0	1.50
WB255D0	502.02	502.5	105.9	44.0	10.0	0.50
WB255D0	502.5	503	194.4	58.6	14.1	0.43
WB255D0	503	503.5	119.2	46.9	10.2	0.98
WB255D0	503.5	504	117.0	47.3	11.8	0.76
WB255D0	504	504.56	111.3	40.7	7.8	0.64
WB255D0	505	505.53	108.9	36.3	12.1	0.33
WB255D0	506.5	506.89	93.1	43.2	7.8	0.90
WB255D0	506.89	507.5	67.9	26.1	7.8	0.38
WB255D0	508	508.5	119.8	47.3	9.3	1.18
WB255D0	508.5	508.77	108.3	37.1	8.8	1.70
WB255D0	508.77	509.1	94.7	31.6	12.6	0.16
WB255D0	509.5	510	231.2	163.0	11.4	0.26
WB255D0	510	510.5	294.6	111.6	26.8	0.22
WB255D0	510.5	511	60.2	45.1	22.6	0.13
WB255D0	511	511.74	120.7	51.3	9.0	0.33
WB255D0	511.74	512	82.3	37.7	5.5	1.46
WB255D0	512	512.5	142.3	53.4	13.3	1.12
WB255D0	512.5	513	182.1	110.3	5.3	1.32
WB255D0	513	513.5	161.3	30.5	9.0	0.56
WB255D0	513.5	514	139.9	73.4	12.2	0.57
WB255D0	514	514.52	159.2	60.6	15.6	1.16
WB255D0	514.52	515	145.4	52.3	11.4	0.61
WB255D0	515	515.5	102.2	39.0	11.1	0.54
WB255D0	515.5	516	295.1	113.2	52.1	0.79
WB255D0	516	516.5	106.7	57.3	11.9	0.51
WB255D0	516.5	517	102.4	37.2	8.3	0.97
WB255D0	517	517.5	95.6	43.4	8.7	0.35
WB255D0	517.5	518	239.6	92.9	18.0	0.33
WB255D0	518.5	519	90.0	42.0	6.0	0.17

WB255D0	519	519.5	184.8	86.5	17.9	0.34
WB255D0	519.5	520	213.4	65.3	12.6	0.40
WB255D0	520	520.51	69.0	26.9	5.1	0.59
WB255D0	520.51	521	66.8	27.3	4.6	0.66
WB255D0	521	521.5	82.5	34.5	5.8	0.52
WB255D0	521.5	522	109.6	43.6	7.9	0.76
WB255D0	522	522.5	169.1	78.8	13.4	0.52
WB255D0	522.5	523	192.0	76.8	15.0	0.60
WB255D0	523	523.5	143.6	62.1	10.7	0.47
WB255D0	523.5	524	160.4	74.7	11.0	0.46
WB255D0	525	525.5	101.0	62.7	7.0	0.29
WB255D0	527.5	528	159.0	61.4	8.4	0.72
WB255D0	530.5	531	54.0	22.8	4.2	0.48
WB255D0	531	531.5	95.7	43.5	6.5	0.46
WB255D0	531.5	532.15	87.6	39.8	8.0	0.38
WB255D0	532.15	532.45	198.9	89.9	13.5	1.26
WB255D0	532.45	533	129.2	61.2	13.6	0.15
WB255D0	533	533.5	24.3	32.4	8.1	0.12
WB255D0	533.5	534	55.1	36.7	6.1	0.16
WB255D0	535	535.5	74.8	36.0	5.5	0.36
WB255D0	537.5	538	78.7	30.7	5.8	0.52
WB255D0	538	538.5	98.5	40.2	9.1	0.77
WB255D0	538.5	539	100.9	41.5	10.1	0.89
WB255D0	539	539.5	74.1	30.9	6.2	0.65
WB255D0	539.5	540	66.2	21.3	4.7	0.42
WB255D0	540	540.25	108.1	42.5	9.6	0.52
WB255D0	540.25	541	111.4	37.1	7.4	0.40
WB255D0	541	542	73.7	25.8	3.7	0.27
WB255D0	542	542.61	59.2	22.6	5.6	0.35
WB255D0	542.61	543	8.7	1.2	1.2	1.60
WB255D0	543	544	49.6	18.6	5.2	0.97
WB255D0	544	545	11.1	4.7	1.6	0.63
WB255D0	545	546	8.8	1.6	0.8	1.25
WB255D0	546	547	3.4	3.4	3.4	0.29
WB255D0	547	548	4.3	4.3	4.3	0.23
WB255D0	548	549	4.1	4.1	4.1	0.25
WE144D0	438.5	439	384.0	178.1	13.9	0.94
WE144D0	439	439.5	525.4	248.9	39.4	1.02
WE144D0	439.5	440	225.3	107.1	17.3	3.12
WE144D0	440	440.5	224.9	103.8	15.2	2.90
WE144D0	440.5	441	173.7	82.5	10.2	2.74
WE144D0	441	441.5	205.5	92.3	16.4	1.53
WE144D0	441.5	441.94	163.3	63.9	7.6	2.50
WE144D0	441.94	442.5	271.3	118.4	15.2	0.99
WE144D0	442.5	443	313.1	153.5	127.2	0.50
WE144D0	443	443.57	294.5	117.1	24.8	0.85
WE144D0	443.57	444	251.5	116.7	18.1	0.39
WE144D0	444	444.45	170.1	128.5	18.9	0.26

WE144D0	444.45	444.85	285.2	134.7	28.7	1.01
WE144D0	444.85	445.1	204.4	145.5	15.1	0.80
WE144D0	445.1	445.5	112.5	49.7	7.4	2.85
WE144D0	445.5	446	65.4	29.0	9.0	2.44
WE144D0	446	446.34	112.0	54.4	7.4	2.15
WE144D0	446.34	446.84	113.7	58.0	5.9	1.35
WE144D0	446.84	447.5	92.9	43.8	10.6	0.75
WE144D0	447.5	448	81.9	33.6	4.4	0.68
WE144D0	448	448.5	77.7	31.4	6.1	1.15
WE144D0	448.5	449.11	84.3	36.9	7.9	0.38
WE144D0	449.11	449.51	88.4	44.2	8.8	0.23
WE144D0	449.51	450	53.7	36.9	10.1	0.30
WE144D0	450	450.5	118.5	74.1	14.8	0.13
WE144D0	450.5	451	58.3	18.6	6.0	2.85
WE144D0	451	451.5	224.1	165.0	15.3	0.98
WE144D0	451.5	452	35.7	15.3	5.1	0.78
WE144D0	452	452.5	46.2	18.5	4.9	1.62
WE144D0	452.5	453	26.1	12.1	3.1	2.23
WE144D0	453	453.5	31.6	19.0	1.7	1.74
WE144D0	453.5	454	49.7	23.6	3.9	0.76
WE144D0	454	454.5	215.4	127.1	37.2	0.65
WE144D0	454.5	455	64.9	29.5	9.3	1.19
WE144D0	455	455.5	149.2	69.8	9.7	0.62
WE144D0	455.5	456	113.0	48.2	13.0	0.54
WE144D0	456.72	457	80.7	33.3	6.1	2.64
WE144D0	457	457.37	82.9	29.6	3.7	2.94
WE144D0	457.37	458	175.2	77.2	29.0	2.07
WE144D0	458	458.5	85.3	56.0	5.4	2.22
WE144D0	458.5	459	82.8	37.5	6.2	0.64
WE144D0	459	459.5	63.1	37.5	6.8	1.17
WE144D0	459.5	460	1.9	3.9	1.9	0.52
WE144D0	460	460.5	1.9	3.9	1.9	0.52
WE144D0	460.5	461	97.5	59.6	10.8	0.18
WE144D0	461	461.29	575.2	253.9	10.4	0.58
WE144D0	461.29	462	343.4	161.5	17.0	0.59
WE144D0	462	462.5	184.5	99.6	9.8	0.61
WE144D0	462.5	463	96.5	37.5	8.6	0.69
WE144D0	463	463.5	74.3	30.5	6.6	0.75
WE144D0	463.5	464.2	70.4	33.4	8.8	0.57
WE144D0	464.2	465	44.6	23.3	3.7	3.48
WE144D0	465	465.5	109.0	60.0	7.4	2.17
WE144D0	465.5	466	183.7	114.6	15.7	1.14
WE144D0	466	466.5	145.4	84.5	10.8	2.59
WE144D0	466.5	467.07	142.1	61.2	10.8	3.41
WE144D0	467.07	467.5	125.1	62.0	9.9	2.73
WE144D0	467.5	468	203.6	91.3	12.5	1.76
WE144D0	468	468.5	99.5	40.3	6.3	2.06
WE144D0	468.5	469	89.2	36.1	13.6	1.77

WE144D0	469	469.5	121.3	54.9	14.6	1.64
WE144D0	469.5	470	52.9	22.9	7.9	1.13
WE144D0	470	470.5	24.3	9.7	4.4	2.06
WE144D0	470.5	471	192.1	109.0	10.0	0.70
WE144D0	471	471.5	110.0	55.3	5.7	1.39
WE144D0	471.5	472	88.6	41.5	6.4	2.34
WE144D0	472	472.5	29.0	13.7	3.5	2.55
WE144D0	472.5	473	58.4	28.9	5.6	3.05
WE144D0	473	473.5	48.2	19.9	6.4	2.51
WE144D0	473.5	474	67.3	35.2	7.0	3.58
WE144D0	474	474.5	54.1	19.7	4.6	1.98
WE144D0	474.5	475	50.9	20.8	7.4	2.16
WE144D0	475	475.5	112.7	37.3	1.5	1.31
WE144D0	475.5	476	138.3	49.8	6.5	1.08
WE144D0	476	476.5	86.3	38.8	8.6	2.32
WE144D0	476.5	477	3.4	3.4	1.1	0.89
WE144D0	477	477.5	13.7	6.0	1.7	1.17
WE144D0	477.5	478	38.3	15.7	1.7	0.57
WE144D0	478	478.5	24.8	12.4	10.3	0.48
WE144D0	478.5	479	10.1	5.0	1.7	1.78
WE144D0	479	479.5	3.6	1.4	0.4	2.77
WE144D0	479.5	480	4.5	2.5	0.4	2.42
WE144D0	480	480.5	7.3	3.6	0.5	1.93
WE144D0	480.5	481	6.7	3.6	2.1	1.93
WE144D0	481	481.34	38.9	20.7	1.7	1.16
WE144D0	481.34	482	215.9	106.6	2.6	0.38
WE144D0	482	482.42	305.7	184.8	23.7	0.42
WE144D0	482.42	482.87	323.2	94.3	6.7	0.15
WE144D0	482.87	483.5	304.9	266.0	4.9	0.62
WE144D0	483.5	484	43.3	19.4	9.0	1.34
WE144D0	484	484.5	58.8	29.6	6.2	2.26
WE144D0	484.5	485	87.2	34.9	23.8	0.63
WE144D0	485	485.5	78.7	36.5	5.0	3.84
WE144D0	485.5	486	110.2	61.9	8.7	2.86
WE144D0	486	486.5	74.9	39.4	6.2	2.56
WE144D0	486.5	487	171.8	82.8	8.1	1.61
WE144D0	487	487.58	19.6	10.4	2.6	0.77
WE144D0	487.58	488.13	104.1	82.3	2.9	1.37
WE144D0	488.76	489.15	123.0	53.1	6.9	3.03
WE144D0	489.15	489.5	45.6	22.4	5.6	2.67
WE144D0	489.5	490	91.3	44.5	7.8	1.80
WE144D0	490	490.5	55.0	27.8	3.2	1.55
WE144D0	490.5	491.18	24.7	12.0	2.1	1.41
WE144D0	491.18	491.5	134.5	70.7	4.1	0.74
WE144D0	491.5	492	159.1	78.7	17.7	0.62
WE144D0	492.5	493	43.5	32.6	10.9	0.28
WE144D0	493	493.5	117.7	52.6	10.3	0.88
WE144D0	493.5	494.16	128.6	59.6	13.0	2.46

WE144D0	494.16	494.66	122.0	54.9	26.4	1.40
WE144D0	494.66	495	145.8	120.4	18.2	2.08
WE144D0	495	495.5	13.0	4.3	47.8	0.23
WE144D0	495.5	496	87.4	41.7	28.8	1.01
WE144D0	496	496.5	167.9	76.1	15.7	0.45
WE144D0	496.5	497	153.9	83.8	15.8	0.44
WE144D0	497	497.5	116.9	54.5	13.0	0.39
WE144D0	497.5	498	248.9	161.1	14.3	0.56
WE144D0	498	498.5	155.7	88.0	13.5	0.30
WE144D0	499.5	500	188.7	71.6	16.3	0.31
WE144D0	500	500.5	96.6	39.0	5.3	2.46
WE144D0	500.5	501	109.1	56.1	11.2	0.98
WE144D0	501	501.4	8.6	5.7	2.9	0.35
WE144D0	501.4	502	64.4	37.1	5.0	0.40
WE144D0	502	502.26	79.1	43.9	3.2	1.85
WE144D0	502.26	502.56	5.4	5.4	1.8	0.55
WE144D0	502.56	503	3.0	3.0	3.0	0.34
WE144D0	503.5	504	96.5	43.4	9.6	0.21
WE144D0	506	506.5	19.2	11.5	3.8	0.26
WE144D0	506.76	507.02	116.7	43.9	8.0	1.00
WE144D0	507.02	507.3	111.0	87.4	1.4	0.72
WE144D0	507.85	508.5	35.3	19.9	4.4	0.45
WE144D0	508.5	509	72.8	31.8	5.5	2.17
WE144D0	509	509.5	85.9	38.3	6.2	0.97
WE144D0	509.5	510	87.6	3.2	6.5	0.31
WE144D0	511.28	511.85	68.3	41.1	3.7	1.88
WE144D0	511.85	512.2	65.2	12.9	1.6	1.24
WE144D0	512.2	512.5	40.3	17.3	3.7	1.61
WE144D0	512.5	513	40.2	18.2	3.1	1.59
WE144D0	513	513.5	66.0	28.4	4.1	1.73
WE144D0	514.28	514.72	58.6	30.0	4.7	1.50
WE144D0	514.72	514.98	58.3	24.2	5.8	1.73
WE144D0	515.5	516	31.7	11.3	4.5	0.44
WE144D0	516.31	517	88.8	33.3	8.3	0.36
WE144D0	517	518	37.5	7.5	2.5	0.40
WE144D0	518	519	72.3	25.5	59.5	0.71
WE144D0	519	520	96.0	46.3	6.1	1.15
WE144D0	520	521	125.3	69.8	23.3	0.56
WE061D0	404.57	404.95	95.2	51.2	11.0	0.27
WE061D0	404.95	405.2	7813.8	4735.6	80.5	0.42
WE061D0	405.2	405.72	2559.1	1364.3	151.8	0.57
WE061D0	405.72	406.16	369.3	167.5	10.1	0.50
WE061D0	406.16	406.96	1243.5	519.6	84.4	0.23
WE061D0	406.96	407.5	331.3	165.7	23.3	1.16
WE061D0	407.5	407.86	261.9	156.2	24.3	1.52
WE061D0	407.86	408.5	180.8	103.3	51.6	0.04
WE061D0	408.5	408.84	203.1	82.0	32.1	0.28
WE061D0	408.84	409.5	259.9	133.5	31.2	0.70

WE061D0	409.5	410	174.8	99.9	27.8	2.08
WE061D0	410	410.5	267.4	96.5	19.3	1.04
WE061D0	410.5	410.92	207.8	89.9	24.9	1.25
WE061D0	410.92	411.21	475.9	203.3	32.3	1.49
WE061D0	411.21	411.7	152.8	66.2	11.5	3.05
WE061D0	411.7	412.21	145.6	71.3	13.9	2.40
WE061D0	412.21	412.9	131.2	60.7	13.3	1.12
WE061D0	412.9	413.37	91.5	75.2	3.5	1.09
WE061D0	413.37	413.84	118.3	52.0	7.7	3.65
WE061D0	413.84	414.5	152.4	106.6	15.7	1.66
WE061D0	414.5	415	149.7	74.3	14.6	0.89
WE061D0	415	415.69	255.2	132.2	17.2	0.87
WE061D0	415.69	415.94	106.0	40.4	7.4	2.42
WE061D0	415.94	416.5	156.2	61.1	11.6	1.29
WE061D0	416.5	417	153.7	56.7	10.1	0.79
WE061D0	417	417.4	220.4	88.8	28.0	0.61
WE061D0	417.4	418	173.7	68.6	17.0	3.24
WE061D0	418	418.5	100.7	45.6	11.1	3.07
WE061D0	418.5	419	116.4	50.6	8.7	2.75
WE061D0	419	419.31	110.9	53.3	6.6	2.27
WE061D0	419.31	419.64	124.7	52.3	8.4	0.59
WE061D0	419.64	420.13	111.5	50.7	8.2	4.05
WE061D0	420.13	420.6	196.0	145.0	54.1	0.98
WE061D0	420.6	421	251.1	95.7	15.9	0.75
WE061D0	421	421.5	234.6	105.2	19.8	1.16
WE061D0	421.5	422.1	221.2	86.8	17.8	0.84
WE061D0	422.1	422.5	70.0	26.9	5.4	0.37
WE061D0	422.5	423	75.6	29.6	6.6	0.61
WE061D0	423	423.5	50.0	20.7	3.4	0.58
WE061D0	423.5	424.07	68.1	26.8	6.5	1.23
WE061D0	424.07	424.5	359.1	113.2	16.2	0.62
WE061D0	424.5	425	280.0	83.8	19.1	0.42
WE061D0	425	425.6	380.1	99.6	14.2	1.91
WE061D0	425.6	426	130.4	59.0	12.3	2.44
WE061D0	426	426.5	240.0	113.9	12.9	1.47
WE061D0	426.5	427	376.3	168.9	25.2	1.35
WE061D0	427	427.5	543.1	264.1	22.1	1.13
WE061D0	427.5	428	434.8	233.3	19.8	1.16
WE061D0	428	428.5	232.6	103.2	15.9	3.02
WE061D0	428.5	429	338.8	154.1	16.3	2.26
WE061D0	429	429.5	537.8	256.9	25.5	1.33
WE061D0	429.5	430	271.6	118.4	12.6	1.35
WE061D0	430	430.38	304.5	117.1	31.2	0.38
WE061D0	430.38	430.64	160.6	99.5	9.8	3.38
WE061D0	430.64	431.02	491.1	251.2	25.0	0.80
WE061D0	431.02	431.54	130.4	71.5	7.6	3.82
WE061D0	431.54	432	101.0	37.6	6.3	2.21
WE061D0	432	432.5	80.6	36.2	7.7	1.82

WE061D0	432.5	433	83.8	35.6	9.9	1.52
WE061D0	433	433.5	129.2	73.7	8.4	1.32
WE061D0	433.5	434	144.7	65.1	10.7	1.78
WE061D0	434	434.59	67.2	36.8	6.1	2.96
WE061D0	434.59	434.87	49.8	23.0	4.6	3.69
WE061D0	434.87	435.5	121.9	49.3	10.9	1.93
WE061D0	435.5	436	163.8	69.5	11.2	1.25
WE061D0	436	436.3	65.1	26.8	6.0	5.14
WE061D0	436.3	436.76	63.1	30.2	4.3	4.20
WE061D0	436.76	437.27	90.0	38.4	9.1	1.98
WE061D0	437.27	437.52	199.3	101.7	14.2	0.49
WE061D0	437.52	438.09	263.4	107.3	24.4	0.62
WE061D0	438.09	438.34	280.9	130.8	24.2	0.21
WE061D0	438.34	439	398.4	165.5	29.7	0.88
WE061D0	439	439.25	147.5	70.8	14.9	2.89
WE061D0	439.25	440	166.7	60.4	17.4	2.58
WE061D0	440	440.5	32.0	13.5	3.7	0.81
WE061D0	440.5	441	15.1	11.6	1.0	1.99
WE061D0	441	441.5	54.9	16.2	4.5	1.11
WE061D0	441.5	442	47.6	20.6	3.8	1.85
WE061D0	442	442.5	186.8	73.3	17.2	0.87
WE061D0	442.5	443.19	141.0	58.7	11.0	2.54
WE061D0	443.19	443.8	205.6	98.2	11.7	1.19
WE061D0	443.8	444.35	155.0	75.5	12.1	0.99
WE061D0	444.35	445	171.7	70.3	11.7	2.47
WE061D0	445	445.38	151.7	60.3	11.2	1.61
WE061D0	445.38	445.63	77.2	35.2	9.0	2.33
WE061D0	445.63	445.92	211.4	84.7	15.3	1.24
WE061D0	445.92	446.5	85.3	36.1	6.4	3.94
WE061D0	446.5	447	97.1	45.2	4.7	3.87
WE061D0	447	447.5	232.3	163.1	26.6	1.50
WE061D0	447.5	448	257.3	125.4	19.6	1.68
WE061D0	448	448.5	328.0	141.9	19.5	0.77
WE061D0	448.5	448.78	345.2	135.8	26.0	0.88
WE061D0	448.78	449.03	240.1	54.8	15.8	2.02
WE061D0	449.03	449.29	134.7	57.1	8.8	2.15
WE061D0	449.29	449.86	290.9	110.6	28.9	0.59
WE061D0	449.86	450.11	282.3	136.2	22.6	1.51
WE061D0	450.11	450.5	156.6	69.6	17.4	0.23
WE061D0	451	451.43	315.1	162.3	26.3	0.42
WE061D0	451.43	452	150.5	69.8	8.8	2.74
WE061D0	452	452.56	139.5	66.6	9.1	2.21
WE061D0	452.56	452.81	221.0	129.3	21.6	0.19
WE061D0	452.81	453.12	167.4	79.8	12.7	1.66
WE061D0	453.12	453.53	196.2	82.9	10.9	0.46
WE061D0	453.53	453.91	248.4	141.3	21.4	0.23
WE061D0	453.91	454.2	340.9	155.5	25.3	1.07
WE061D0	454.2	454.8	268.9	122.2	19.0	0.37

WE061D0	455.37	456.07	209.5	102.1	16.1	0.37
WE061D0	456.07	456.72	73.2	25.3	5.6	0.71
WE061D0	456.72	457.15	118.9	61.1	14.1	1.49
WE061D0	457.15	457.4	81.1	38.0	7.6	0.39
WE061D0	457.4	458	175.8	73.1	16.7	0.78
WE061D0	458	458.45	242.2	151.3	60.5	0.03
WE061D0	458.45	459	132.1	64.8	9.8	0.82
WE061D0	459	459.65	50.7	23.0	5.8	0.87
WE061D0	459.65	460.03	30.1	18.0	6.0	0.33
WE061D0	460.03	460.5	65.1	26.0	6.5	0.46
WE061D0	460.5	461	87.6	39.8	8.0	0.38
WE061D0	461.5	462	12.9	6.5	3.2	0.31
WE061D0	462	462.5	208.7	61.2	25.0	0.88
WE061D0	462.5	463	132.4	68.7	3.4	4.99
WE061D0	463	463.5	64.7	20.3	5.5	1.08
WE061D0	463.5	463.85	154.6	72.1	11.5	0.96
WE061D0	463.85	464.2	46.1	20.3	20.3	0.54
WE061D0	464.2	464.9	92.2	43.6	8.0	2.00
WE061D0	465.5	466	14.9	3.0	3.0	0.34
WE061D0	466	466.34	43.1	11.3	4.5	0.44
WE061D0	466.34	466.77	194.8	47.7	19.9	0.25
WE061D0	466.77	467.5	111.2	63.5	6.6	3.31
WE061D0	467.5	468	162.8	73.2	12.8	2.67
WE061D0	468	468.5	137.1	56.3	9.9	1.51
WE061D0	469	469.5	125.1	62.6	10.9	0.64
WE061D0	469.5	470	90.3	34.7	6.9	0.43
WE061D0	470	470.5	151.1	48.4	14.0	1.86
WE061D0	470.5	471.17	178.6	99.2	8.5	2.12
WE061D0	471.17	471.93	89.5	50.7	9.0	0.34
WE061D0	471.93	472.5	155.4	80.4	14.3	0.91
WE061D0	472.5	473	131.6	75.3	13.5	1.63
WE061D0	473	473.37	97.6	54.3	10.1	2.17
WE061D0	473.37	473.62	113.4	63.9	7.2	1.39
WE061D0	473.62	474	199.4	86.7	17.3	0.46
WE061D0	475.08	475.5	202.1	93.4	20.5	0.78
WE061D0	475.5	476.26	87.5	36.6	6.1	1.97
WE061D0	476.26	477	314.6	243.3	20.1	0.55
WE061D0	477	477.5	275.4	156.1	45.9	0.44
WE061D0	477.5	477.94	48.0	41.1	116.5	0.15
WE061D0	477.94	478.5	249.0	140.5	19.2	0.94
WE061D0	478.5	479.06	154.6	76.4	10.5	2.28
WE061D0	479.06	479.37	76.6	46.0	684.2	0.20
WE061D0	479.37	479.66	66.7	30.6	7.1	2.68
WE061D0	480.23	480.92	228.3	89.1	26.0	1.00
WE061D0	481.5	482.13	162.7	67.3	11.2	0.36
WE061D0	482.13	482.5	93.4	43.8	8.1	0.87
WE061D0	482.5	483	74.8	19.7	8.6	2.43
WE061D0	483	483.5	102.0	55.9	7.0	0.72

WE061D0	483.5	483.94	162.2	75.9	14.6	1.44
WE061D0	485.95	486.5	82.7	43.6	12.1	1.74
WE061D0	486.5	486.96	77.9	30.2	5.4	3.15
WE061D0	486.96	487.5	177.7	56.9	12.2	1.88
WE061D0	487.5	488	107.9	53.6	9.1	1.33
WE061D0	488	488.5	75.7	42.7	13.8	0.73
WE061D0	488.5	489	62.2	24.1	4.7	1.29
WE061D0	489	489.5	91.5	42.4	5.0	1.20
WE061D0	489.5	490	89.4	33.2	29.8	1.48
WE061D0	490	490.55	79.5	34.2	8.6	0.82
WE061D0	490.55	490.8	39.2	20.2	5.8	2.57
WE061D0	491.5	492	149.3	67.1	7.1	2.12
WE061D0	492	492.5	108.5	32.0	5.6	1.59
WE061D0	492.5	493	85.9	36.8	11.7	1.63
WE061D0	493	493.5	81.2	36.3	8.2	2.20
WE061D0	493.5	494	71.5	36.3	13.9	0.94
WE061D0	494.5	495	111.2	23.6	127.0	0.89
WE061D0	495.5	496	150.7	59.3	12.4	1.21
WE061D0	496	496.5	99.0	55.9	25.5	1.41
WE061D0	496.5	497	62.1	27.0	5.3	2.08
WE061D0	497	497.5	33.2	16.6	5.2	1.15
WE061D0	497.5	498	26.2	7.5	7.5	0.27
WE061D0	498	498.51	79.5	35.2	5.0	0.99
WE145D0	428.5	429	361.9	417.1	38.7	2.25
WE145D0	429	429.5	156.4	57.0	17.0	3.58
WE145D0	429.5	430	294.0	119.7	28.7	1.67
WE145D0	430	430.5	251.1	122.3	15.8	1.71
WE145D0	430.5	431.17	156.8	71.3	15.5	2.45
WE145D0	431.17	431.7	190.2	51.7	11.7	3.15
WE145D0	431.7	432.14	121.3	66.5	9.6	1.97
WE145D0	432.14	432.52	108.4	68.5	13.7	0.88
WE145D0	432.52	433	238.0	122.1	18.8	0.32
WE145D0	433	433.5	250.0	130.5	16.2	1.54
WE145D0	433.5	434.1	134.0	51.4	9.5	1.89
WE145D0	434.1	434.5	143.7	45.2	6.2	1.46
WE145D0	434.5	435	56.9	26.5	2.5	0.79
WE145D0	435	435.5	129.3	57.8	9.4	1.69
WE145D0	435.5	435.94	167.1	79.2	13.1	1.15
WE145D0	435.94	436.34	203.1	101.2	11.8	1.44
WE145D0	436.34	436.65	522.8	417.8	24.2	1.36
WE145D0	436.65	437	173.4	80.9	15.0	0.87
WE145D0	437	437.38	173.8	77.0	12.2	1.06
WE145D0	437.38	437.63	180.3	78.3	14.2	0.84
WE145D0	437.63	438	203.7	81.5	12.5	0.88
WE145D0	438	438.38	205.6	120.9	14.8	1.22
WE145D0	438.38	439.07	165.7	77.5	11.2	1.88
WE145D0	439.07	439.5	147.9	71.1	8.4	1.79
WE145D0	439.5	440	76.8	37.3	4.2	4.05

WE145D0	440	440.5	166.6	74.0	10.5	1.24
WE145D0	440.5	441	43.8	19.5	4.9	0.21
WE145D0	441	441.5	34.3	27.5	6.9	0.15
WE145D0	441.5	442.1	183.1	63.4	10.6	0.28
WE145D0	442.1	442.7	127.0	65.2	10.2	1.18
WE145D0	442.7	443.19	153.2	86.5	11.1	1.62
WE145D0	443.19	443.6	85.1	45.7	5.4	1.12
WE145D0	443.6	444	136.9	66.0	4.8	0.62
WE145D0	444	444.75	64.1	31.9	6.2	3.04
WE145D0	444.75	445.27	115.2	52.8	6.2	1.46
WE145D0	445.27	446	249.5	106.6	23.2	1.08
WE145D0	446	446.5	147.0	58.4	10.8	1.39
WE145D0	446.5	447	130.9	57.4	10.4	1.73
WE145D0	447	447.6	166.0	72.7	10.7	1.21
WE145D0	447.6	448.27	182.7	81.4	32.0	1.66
WE145D0	448.27	449	96.2	41.9	11.2	2.41
WE145D0	449	449.5	109.2	49.7	7.1	2.25
WE145D0	449.5	449.93	87.0	39.4	5.5	1.80
WE145D0	449.93	450.27	145.2	59.3	14.3	0.49
WE145D0	450.27	450.72	71.8	30.6	5.0	2.38
WE145D0	450.72	451.45	94.2	38.7	6.3	2.07
WE145D0	451.45	451.77	117.7	44.6	6.3	3.03
WE145D0	451.77	452.35	117.1	51.1	12.5	2.07
WE145D0	452.35	453	126.4	60.4	9.5	1.57
WE145D0	453	453.25	74.7	42.9	4.9	2.45
WE145D0	453.25	453.91	150.2	58.2	14.9	0.74
WE145D0	453.91	454.28	258.5	120.4	21.8	0.96
WE145D0	455.03	455.6	103.8	44.7	7.4	2.57
WE145D0	455.6	456	64.0	27.9	6.1	4.41
WE145D0	456	456.44	211.9	94.6	16.9	1.36
WE145D0	456.44	457.17	128.4	59.6	18.3	0.44
WE145D0	457.17	457.49	404.6	193.5	29.3	0.17
WE145D0	457.49	457.8	598.5	303.0	34.8	0.40
WE145D0	457.8	458.06	495.4	184.8	48.2	0.37
WE145D0	458.06	458.5	450.7	198.3	36.1	0.06
WE145D0	458.5	458.9	162.2	72.1	18.0	0.06
WE145D0	458.9	459.35	137.7	67.1	8.4	2.01
WE145D0	459.35	459.79	59.8	30.2	5.1	3.51
WE145D0	459.79	460.4	154.8	71.4	9.9	1.01
WE145D0	460.4	461.08	323.2	161.6	24.7	0.61
WE145D0	461.08	461.5	36.8	17.0	2.8	0.71
WE145D0	461.5	461.93	51.6	23.5	3.4	1.49
WE145D0	461.93	462.18	210.6	126.0	13.1	2.22
WE145D0	462.18	462.5	102.2	50.0	9.7	1.76
WE145D0	462.5	462.87	183.1	81.8	12.4	0.56
WE145D0	462.87	463.5	90.0	39.2	4.9	2.24
WE145D0	463.5	464	137.5	67.2	12.4	2.26
WE145D0	464	464.5	183.7	104.9	11.2	1.88

WE145D0	464.5	465	181.2	87.6	11.6	2.33
WE145D0	465	465.42	154.6	70.3	7.8	1.93
WE145D0	465.42	465.7	46.9	24.7	1.9	4.86
WE145D0	465.7	466.26	74.3	31.7	13.1	1.29
WE145D0	466.26	466.51	60.3	40.2	24.1	0.25
WE145D0	466.51	467	136.9	53.3	1.7	2.35
WE145D0	467	467.5	82.3	32.9	2.5	2.43
WE145D0	467.5	468	59.4	26.9	1.7	2.31
WE145D0	468	468.5	22.1	9.3	2.5	2.36
WE145D0	468.5	469	24.5	12.3	2.6	1.96
WE145D0	469	469.5	16.0	7.8	2.2	2.31
WE145D0	469.5	470	21.9	10.2	2.2	2.74
WE145D0	470	470.54	23.7	9.9	3.1	2.23
WE145D0	470.54	471	21.0	13.4	0.4	2.24
WE145D0	471	471.6	43.6	20.6	1.2	1.65
WE145D0	471.6	472.28	34.3	17.7	2.1	0.96
WE145D0	472.48	472.73	17.4	6.8	1.0	2.93
WE145D0	472.73	473.1	69.3	15.6	0.8	5.27
WE145D0	473.1	473.55	31.5	15.0	1.6	1.27
WE145D0	473.55	473.8	16.0	9.7	0.6	3.31
WE145D0	473.8	474.4	13.6	5.7	0.8	2.64
WE145D0	474.4	475	13.7	7.2	0.7	2.78
WE145D0	475	475.28	17.5	6.8	0.8	2.52
WE145D0	475.28	475.56	4.8	2.4	0.4	2.52
WE145D0	475.56	476.19	17.4	5.5	0.3	2.93
WE145D0	476.19	476.7	95.8	42.8	4.7	2.36
WE145D0	476.7	477.24	40.0	20.5	3.5	2.87
WE145D0	477.24	478.05	50.4	22.4	3.0	2.32
WE145D0	478.05	478.3	30.0	15.3	2.0	1.97
WE145D0	478.3	478.55	2.2	1.7	0.6	1.80
WE145D0	479	479.34	48.9	24.5	1.6	0.61
WE145D0	479.34	479.67	41.0	21.6	2.3	0.88
WE145D0	479.67	480.41	45.1	11.3	3.2	0.62
WE145D0	480.41	480.86	3.5	2.1	0.7	1.43
WE145D0	480.86	481.5	3.7	7.5	3.7	0.27
WE145D0	481.5	482	42.2	404.0	28.1	0.28
WE145D0	486.43	487	7.8	3.9	2.0	0.51
WE145D0	487.5	488	3.6	1.8	1.8	0.55
WE145D0	488	488.4	10.7	4.0	1.3	0.75
WE145D0	488.69	489	18.0	9.7	3.5	1.45
WE145D0	489	489.5	9.1	5.4	1.8	0.55
WE145D0	489.5	490	4.6	2.3	2.3	0.43
WE145D0	490	490.5	11.4	3.8	3.8	0.26
WE145D0	490.5	491	16.7	5.6	2.8	0.36
WE145D0	496	496.5	3.4	1.7	3.4	0.58
WE145D0	499.5	500	11.9	15.8	4.0	0.25
WE145D0	501.75	502.11	26.1	8.4	0.8	1.30
WE145D0	502.11	502.8	9.4	3.1	1.6	0.64

WE145D0	502.8	503.4	254.4	101.0	22.4	0.27
WE145D0	503.4	504	41.7	25.1	5.7	1.75
WE145D0	504	504.5	44.7	15.3	4.4	0.92
WE145D0	504.5	505	29.2	19.5	2.0	2.46
WE145D0	505	505.5	66.2	30.7	6.5	0.62
WE145D0	505.93	506.5	168.9	62.2	8.9	0.22
WE145D0	506.5	507	119.4	15.8	4.5	0.44
WE145D0	507	507.5	138.7	37.2	14.5	1.10
WE145D0	507.5	508	163.8	98.3	14.7	0.89
WE145D0	510	510.5	13.8	6.9	6.9	0.14
WE145D0	510.5	511	9.3	4.7	4.7	0.21
WE145D0	511.5	512	6.7	3.3	3.3	0.30
WE145D0	514.79	515.04	43.8	20.4	4.7	0.64
WE145D0	515.45	515.7	83.7	29.7	5.5	1.45
WE145D0	515.7	516.24	47.8	16.7	2.4	0.42
WE145D0	519.1	519.5	8.6	3.5	3.5	2.32
WE145D0	519.5	520.5	74.8	21.9	7.3	0.55
WE145D0	520.5	520.75	74.3	22.5	4.3	1.16
WE145D0	520.75	521.17	68.9	27.2	12.7	0.55
WE120D0	384.71	385.31	166.1	63.8	12.2	1.07
WE120D0	385.31	385.81	138.1	61.5	10.0	0.80
WE120D0	385.81	386.31	134.1	55.9	9.9	0.81
WE120D0	386.31	386.81	131.2	69.6	12.0	0.75
WE120D0	387.31	387.81	109.7	58.5	12.2	0.41
WE120D0	388.31	388.81	77.1	45.9	4.2	0.48
WE120D0	389.81	390.31	132.6	92.0	5.4	0.37
WE120D0	390.31	390.81	127.5	64.6	11.6	0.60
WE120D0	393.31	393.81	144.7	83.7	8.2	1.10
WE120D0	393.81	394.31	162.2	55.4	8.8	1.93
WE120D0	394.31	394.66	167.5	72.7	13.2	1.90
WE120D0	394.66	395.16	192.1	76.6	13.0	1.38
WE120D0	395.16	395.8	185.4	70.6	13.5	1.86
WE120D0	395.8	396.4	207.8	64.3	19.2	2.13
WE120D0	396.4	396.9	166.3	65.3	14.8	1.29
WE120D0	396.9	397.4	187.8	66.9	16.2	2.47
WE120D0	397.4	397.95	189.8	76.3	12.6	2.31
WE120D0	397.95	398.5	206.0	85.3	21.2	1.70
WE120D0	398.5	399	238.8	104.0	16.7	1.50
WE120D0	399	399.5	194.0	71.4	12.1	2.23
WE120D0	399.5	400	205.5	72.3	13.8	2.03
WE120D0	400	400.5	225.7	92.3	14.9	1.07
WE120D0	400.5	401	241.4	101.0	18.1	0.94
WE120D0	401	401.5	155.0	75.4	12.4	0.97
WE120D0	401.5	402.11	121.1	52.7	8.9	2.48
WE120D0	402.11	402.82	191.2	74.1	14.2	1.97
WE120D0	402.82	403.13	158.7	66.6	10.6	2.46
WE120D0	403.13	403.63	239.6	89.8	21.1	1.28
WE120D0	403.63	404.13	156.5	50.4	14.3	2.10

WE120D0	404.13	404.63	233.3	66.8	27.0	2.04
WE120D0	404.63	405.13	225.0	78.7	22.1	0.72
WE120D0	405.13	405.63	242.3	99.1	19.3	1.09
WE120D0	405.63	406.13	229.9	79.7	16.5	1.52
WE120D0	406.13	406.63	214.3	65.1	16.4	1.52
WE120D0	406.63	407.13	126.7	42.6	10.9	1.74
WE120D0	407.13	407.73	151.7	50.0	10.9	1.74
WE120D0	407.73	408.23	198.1	79.7	14.2	1.83
WE120D0	408.23	408.73	145.8	52.5	12.8	2.65
WE120D0	408.73	409.23	98.7	32.2	5.3	2.27
WE120D0	409.23	409.73	217.4	83.0	13.0	1.38
WE120D0	409.73	410.57	224.6	83.9	11.5	1.39
WE120D0	410.57	411.07	209.2	76.8	5.1	0.99
WE120D0	411.07	411.57	246.6	58.6	15.7	1.47
WE120D0	411.57	412.07	194.5	68.5	22.2	1.53
WE120D0	412.07	412.57	186.0	73.2	28.5	0.98
WE120D0	412.57	413.19	61.1	26.7	6.7	1.05
WE120D0	413.19	413.69	131.7	47.7	10.4	1.82
WE120D0	413.69	414.19	108.8	42.8	8.6	2.32
WE120D0	414.19	414.69	114.4	51.4	7.7	2.35
WE120D0	414.69	415.3	111.6	33.2	8.1	2.59
WE120D0	415.3	415.8	166.9	41.0	8.2	3.42
WE120D0	415.8	416.3	162.9	57.0	12.5	3.19
WE120D0	416.3	416.8	160.2	56.8	11.9	3.85
WE120D0	416.8	417.3	132.8	50.4	12.8	2.82
WE120D0	417.3	417.8	132.8	45.5	10.3	2.92
WE120D0	417.8	418.55	139.9	49.3	11.5	2.35
WE120D0	418.55	419.05	152.0	50.1	10.8	1.86
WE120D0	419.05	419.55	131.7	51.7	10.9	2.01
WE120D0	419.55	419.93	131.7	46.0	11.7	1.28
WE120D0	419.93	420.44	86.9	31.0	5.6	1.61
WE120D0	420.44	420.94	127.6	46.7	12.1	2.23
WE120D0	420.94	421.44	142.5	52.9	9.5	2.42
WE120D0	421.44	421.93	132.4	48.6	9.6	1.36
WE120D0	421.93	422.43	166.8	59.3	15.5	1.16
WE120D0	422.43	422.93	188.5	68.4	16.0	1.37
WE120D0	422.93	423.44	187.8	67.6	17.8	1.12
WE120D0	423.44	423.94	181.1	76.9	17.5	1.43
WE120D0	423.94	424.44	106.3	38.2	7.5	1.60
WE120D0	424.44	424.94	131.7	49.8	9.9	2.03
WE120D0	424.94	425.44	136.9	52.4	10.7	2.61
WE120D0	425.44	425.94	134.7	50.3	9.3	1.29
WE120D0	425.94	426.44	139.6	51.3	10.4	1.05
WE120D0	426.44	426.94	108.6	43.8	10.0	1.00
WE120D0	426.94	427.44	131.6	51.2	8.7	1.72
WE120D0	427.44	427.94	109.2	36.8	9.2	0.76
WE120D0	427.94	428.44	121.5	46.2	9.7	1.23
WE120D0	428.44	428.94	128.1	47.6	7.6	2.37

WE120D0	428.94	429.44	86.6	31.1	6.7	1.19
WE120D0	429.44	429.94	100.3	36.9	5.8	1.89
WE120D0	429.94	430.44	116.8	46.7	10.8	0.56
WE120D0	430.44	430.94	137.7	55.1	8.7	1.38
WE120D0	430.94	431.44	147.0	49.3	15.7	0.95
WE120D0	431.44	431.94	97.0	45.0	10.4	0.29
WE120D0	431.94	432.44	83.6	29.5	4.9	0.81
WE120D0	432.44	432.94	113.0	41.4	7.2	1.52
WE120D0	432.94	433.44	148.4	51.3	13.0	1.46
WE120D0	433.44	433.94	147.8	61.0	10.0	2.29
WE120D0	433.94	434.44	134.6	44.1	18.0	2.61
WE120D0	434.44	434.94	155.5	61.4	8.9	1.68
WE120D0	434.94	435.44	105.7	34.3	6.9	3.06
WE120D0	435.44	435.94	85.4	34.5	7.0	3.71
WE120D0	435.94	436.44	131.3	50.6	11.8	1.86
WE120D0	436.44	436.94	169.9	66.0	13.2	1.29
WE120D0	436.94	437.55	95.4	35.2	3.7	2.16
WE120D0	437.55	438.05	123.4	47.7	10.3	1.36
WE120D0	438.05	438.55	120.9	41.7	6.3	1.92
WE120D0	438.55	439.05	134.0	50.1	8.7	2.07
WE120D0	439.05	439.55	137.6	51.9	8.7	1.72
WE120D0	439.55	440.05	158.8	59.3	17.0	1.77
WE120D0	440.05	440.55	152.2	55.3	11.0	2.46
WE120D0	440.55	441.05	185.2	70.8	14.3	1.54
WE120D0	441.05	441.55	172.3	28.3	6.2	3.85
WE120D0	441.55	442.05	106.2	35.7	6.5	1.23
WE120D0	442.05	442.55	183.6	30.6	3.5	3.17
WE120D0	442.55	443.05	91.5	36.8	5.3	2.45
WE120D0	443.05	443.55	33.1	11.3	4.2	2.84
WE120D0	443.55	444.05	64.1	23.1	2.7	3.72
WE120D0	444.05	444.55	41.0	13.7	1.8	3.93
WE120D0	444.55	445.05	57.6	23.2	7.1	2.24
WE120D0	445.05	445.55	80.5	34.3	6.2	1.60
WE120D0	445.55	446.05	41.2	13.7	3.2	1.89
WE120D0	446.05	446.83	35.8	9.1	5.2	1.54
WE120D0	446.83	447.13	46.6	16.2	3.8	1.05
WE120D0	447.13	447.63	20.2	8.3	1.6	8.52
WE120D0	447.63	448.13	19.8	5.2	0.4	2.67
WE120D0	448.13	448.63	2.6	0.9	0.9	1.17
WE120D0	448.63	449.13	10.4	2.3	1.2	0.87
WE120D0	449.13	449.63	17.0	10.9	0.9	2.12
WE120D0	449.63	450.13	16.2	4.6	2.3	0.43
WE120D0	450.13	450.63	10.9	2.3	0.8	1.28
WE120D0	450.63	451.13	5.6	1.3	1.3	2.30
WE120D0	451.63	452.13	11.5	3.8	3.8	0.26
WE120D0	452.13	452.63	31.2	15.6	15.6	0.06
WE120D0	452.63	453.13	3.9	3.9	3.9	0.25
WE120D0	453.13	453.63	22.3	11.2	11.2	0.09

WE120D0	453.63	454.13	20.4	7.5	0.8	1.33
WE120D0	454.13	454.63	27.7	2.4	1.2	0.83
WE120D0	454.63	455.13	12.6	12.6	12.6	0.08
WE120D0	455.13	455.63	9.3	9.3	9.3	0.11
WE120D0	455.63	456.13	11.3	5.6	5.6	0.18
WE120D0	456.13	456.63	19.6	3.0	0.4	2.70
WE120D0	456.63	457.13	10.3	3.3	0.2	13.14
WE120D0	457.13	457.63	14.7	2.3	2.3	0.89
WE120D0	457.63	458.13	23.3	3.9	1.7	1.80
WE120D0	458.63	459.13	11.4	11.4	11.4	0.09
WE120D0	459.13	459.63	6.1	6.1	6.1	0.17
WE120D0	459.63	460.13	19.8	2.3	0.8	3.99
WE120D0	460.13	460.63	5.4	5.4	5.4	0.18
WE120D0	460.63	461.13	15.0	3.0	0.7	10.90
WE120D0	461.13	461.63	10.9	1.7	0.7	4.03
WE120D0	461.63	462.13	7.2	1.3	0.7	1.52
WE120D0	462.13	462.63	6.2	6.2	6.2	0.16
WE120D0	462.63	463.13	11.5	3.8	1.9	0.52
WE120D0	463.13	463.65	9.1	2.6	0.9	6.50
WE052D0	465.01	465.43	34.7	34.7	21.7	0.23
WE052D0	466	466.63	125.6	73.3	7.0	0.29
WE052D0	466.63	467	202.0	90.7	8.6	0.93
WE052D0	467	467.5	390.6	166.2	34.9	0.60
WE052D0	467.5	468	280.4	107.9	22.5	1.83
WE052D0	468	468.5	235.0	97.4	18.7	1.71
WE052D0	468.5	469	244.5	96.9	20.5	2.29
WE052D0	469	469.5	244.6	86.8	17.3	2.09
WE052D0	469.5	470.06	185.2	69.7	12.8	2.42
WE052D0	470.34	471	260.0	82.2	21.2	1.18
WE052D0	471	471.5	212.6	70.9	17.5	2.00
WE052D0	471.5	471.81	48.4	16.4	4.7	3.22
WE052D0	471.81	472.67	183.5	74.6	15.0	1.86
WE052D0	472.67	473	32.6	12.5	2.8	2.89
WE052D0	473	473.49	198.3	70.5	13.6	1.69
WE052D0	473.49	474	106.1	37.3	6.1	2.31
WE052D0	474	474.5	175.1	66.7	12.5	1.20
WE052D0	474.5	474.8	38.4	12.6	2.7	3.33
WE052D0	474.8	475.6	222.3	92.4	19.6	1.28
WE052D0	475.6	476.08	133.8	55.1	9.7	2.89
WE052D0	476.08	476.4	238.5	67.4	27.8	1.19
WE052D0	476.4	477.08	71.3	23.8	4.8	3.32
WE052D0	477.08	477.5	138.1	83.0	14.9	1.07
WE052D0	477.5	478	172.5	51.0	11.0	2.37
WE052D0	478	478.5	234.8	90.7	19.3	0.88
WE052D0	478.5	479	47.5	14.8	5.5	1.28
WE052D0	479	479.5	104.5	64.1	11.0	0.55
WE052D0	479.5	480	161.8	51.4	13.3	1.58
WE052D0	480	480.5	144.9	44.7	10.2	2.06

WE052D0	480.5	481	161.2	63.4	12.2	1.80
WE052D0	481	481.5	158.4	74.0	17.8	1.46
WE052D0	481.5	482	237.2	79.9	23.7	0.80
WE052D0	482	482.5	230.8	83.2	19.8	1.21
WE052D0	482.5	483	203.6	97.2	15.8	1.20
WE052D0	483	483.5	207.7	154.1	20.1	1.49
WE052D0	483.5	484	142.0	50.6	11.4	1.23
WE052D0	484	484.5	132.4	52.1	10.2	0.88
WE052D0	484.5	485	42.1	16.4	3.4	2.38
WE052D0	485	485.5	58.2	8.5	5.7	0.70
WE052D0	485.5	486	164.2	61.9	11.5	1.39
WE052D0	486	486.5	229.3	96.2	14.2	1.62
WE052D0	486.5	487	204.3	55.7	20.4	1.42
WE052D0	487	487.5	181.0	59.0	19.3	1.56
WE052D0	487.5	488	226.3	66.5	14.1	1.56
WE052D0	488	488.5	140.1	47.0	23.5	1.23
WE052D0	488.5	489	266.3	98.8	23.3	0.86
WE052D0	489	489.5	270.4	88.5	23.9	1.01
WE052D0	489.5	490.14	184.5	64.0	11.1	1.08
WE052D0	490.44	491.16	91.0	37.9	6.1	0.66
WE052D0	491.16	492	146.6	47.4	11.8	0.68
WE052D0	492	492.48	118.0	49.3	10.7	0.47
WE052D0	492.48	493.24	114.6	52.6	9.3	0.65
WE052D0	494.14	494.44	168.7	60.4	16.2	1.42
WE052D0	494.44	495	143.5	60.8	10.3	0.77
WE052D0	495	495.5	221.2	90.7	14.2	0.71
WE052D0	495.5	496	203.8	82.5	16.2	1.24
WE052D0	496	496.5	191.6	72.1	13.7	1.10
WE052D0	496.5	497	184.9	76.4	13.1	0.84
WE052D0	497	497.5	183.7	75.4	13.1	0.61
WE052D0	497.5	498	167.2	66.2	12.0	0.83
WE052D0	498	498.5	153.7	61.5	12.3	0.65
WE052D0	498.5	499.04	164.3	62.1	13.1	1.14
WE052D0	499.04	499.5	160.9	62.3	12.6	1.35
WE052D0	499.5	500	166.1	65.2	13.3	0.67
WE052D0	500	500.31	159.2	60.9	12.5	0.72
WE052D0	500.71	501.23	64.3	27.0	7.5	1.07
WE052D0	501.23	502	74.8	30.3	7.1	1.12
WE052D0	502	502.5	134.5	64.9	51.6	2.56
WE052D0	502.5	503	84.9	50.4	18.6	0.38
WE052D0	507.5	508	115.0	61.9	5.9	0.34
WE052D0	508	508.51	75.4	40.8	2.0	0.49
WE052D0	508.51	509.09	105.0	44.3	9.3	1.40
WE052D0	509.09	509.55	71.7	34.5	5.4	1.48
WE052D0	509.55	510.1	122.7	48.7	5.0	1.19
WE052D0	510.1	510.4	103.2	44.9	5.5	1.27
WE052D0	510.4	510.9	178.0	67.6	13.8	0.72
WE052D0	510.9	511.21	80.7	30.1	5.8	1.56

WE052D0	511.44	512	27.1	18.1	3.0	0.33
WE052D0	512	512.5	76.7	31.8	5.3	0.38
WE052D0	512.5	513.1	43.1	17.8	2.5	0.39
WE052D0	513.1	513.37	466.0	211.9	31.6	0.76
WE052D0	513.37	513.78	114.6	37.2	6.2	0.65
WE052D0	513.78	514.27	179.9	70.1	13.2	2.20
WE052D0	514.27	515	226.0	85.3	14.4	2.44
WE052D0	515	515.5	234.5	88.4	16.6	1.63
WE052D0	515.5	516	212.2	75.5	13.2	2.04
WE052D0	516	516.3	204.5	78.0	16.0	2.00
WE052D0	516.3	516.76	222.5	73.4	18.9	2.53
WE052D0	516.76	517.61	207.3	78.5	14.3	1.89
WE052D0	517.61	518	171.2	76.9	13.8	1.95
WE052D0	518	518.5	382.3	165.5	28.7	1.32
WE052D0	518.5	519	415.8	191.4	30.8	0.88
WE052D0	519	519.5	469.8	186.3	31.9	0.75
WE052D0	519.5	520	160.6	67.9	10.6	1.61
WE052D0	520	520.5	204.8	143.1	15.0	2.14
WE052D0	520.5	521	240.6	83.2	14.7	1.23
WE052D0	521	521.5	225.0	87.5	17.5	1.54
WE052D0	521.5	522	173.2	66.3	14.0	1.28
WE052D0	522	522.5	173.6	66.5	11.9	1.01
WE052D0	523.5	524	220.8	79.8	15.3	1.57
WE052D0	524	524.5	194.4	89.6	14.6	1.85
WE052D0	524.5	525	178.8	61.5	24.7	1.74
WE052D0	525	525.5	154.3	55.8	10.6	2.27
WE052D0	525.5	526	168.6	65.7	12.2	2.21
WE052D0	526	526.5	139.1	50.8	9.0	2.78
WE052D0	526.5	527	254.4	105.4	24.1	0.87
WE052D0	527	527.5	172.0	53.8	13.2	1.97
WE052D0	527.5	528	200.0	67.8	12.6	0.87
WE052D0	528	528.5	14.6	6.6	1.3	0.75
WE052D0	528.5	529	165.8	75.7	17.5	1.25
WE052D0	529	529.5	81.0	30.3	3.6	1.12
WE052D0	529.5	530	105.1	39.1	6.7	0.89
WE052D0	530	530.32	183.9	77.8	11.8	0.85
WE052D0	530.32	531	250.5	88.1	26.3	0.87
WE052D0	531	531.5	215.8	84.9	13.0	0.85
WE052D0	531.5	532.2	349.1	136.7	22.6	0.75
WE052D0	532.2	533	225.0	81.4	15.8	0.88
WE052D0	533	533.5	208.4	80.5	15.5	1.03
WE052D0	533.5	534	195.8	73.2	14.4	1.60
WE052D0	534	534.5	215.4	78.8	19.1	2.25
WE052D0	534.5	535	203.5	80.4	13.3	1.88
WE052D0	535	535.5	176.9	73.9	13.7	0.58
WE052D0	536.5	537	197.9	80.3	14.0	1.28
WE052D0	537	537.5	261.7	96.8	20.0	1.50
WE052D0	537.5	538	180.2	72.6	16.4	0.43

WE052D0	538	539	273.0	101.0	20.0	1.00
WE052D0	539	539.5	196.3	67.8	13.6	1.84
WE052D0	540	540.3	257.7	100.5	15.6	0.71
WE052D0	540.3	540.6	160.3	50.6	16.9	0.24
WE052D0	541.65	542	255.1	115.1	17.6	1.25
WE052D0	542	542.5	208.1	79.0	12.9	0.62
WE052D0	542.5	543	244.0	88.9	19.4	0.88
WE052D0	543	543.5	195.8	74.8	15.1	1.12
WE052D0	543.5	543.87	214.5	89.1	9.3	0.97
WE052D0	543.87	544.5	300.4	117.5	17.7	0.96
WE052D0	544.5	545	203.2	77.1	10.6	1.70
WE052D0	545	545.5	150.9	58.7	9.4	0.95
WE052D0	546	546.5	208.4	89.1	9.6	0.73
WE052D0	547.27	548	193.2	51.4	8.9	1.69
WE052D0	548	548.5	237.5	83.3	14.8	0.88
WE052D0	548.5	549	214.6	85.9	9.3	0.86
WE052D0	549.5	550.1	213.9	85.0	15.2	0.66
WE052D0	551.38	552	217.7	96.3	12.6	0.72
WE052D0	552	552.5	246.9	97.1	16.4	0.85
WE052D0	552.5	553	215.7	77.0	27.3	0.84
WE052D0	553.5	554.06	201.2	99.4	14.6	1.30
WE052D0	554.63	555	311.9	97.5	17.7	1.13
WE052D0	555	555.5	239.9	95.1	14.4	0.90
WE052D0	555.5	556	252.2	98.2	18.6	1.13
WE052D0	556	556.5	171.9	70.4	9.8	0.61
WE052D0	556.5	556.98	191.1	77.9	9.4	0.42
WE052D0	556.98	557.5	271.2	115.5	14.4	0.97
WE052D0	557.5	558.16	191.7	68.1	12.7	0.87
WE052D0	558.16	558.5	248.2	93.3	17.6	1.14
WE052D0	558.5	559	258.2	94.2	14.6	1.31
WE052D0	559	559.5	286.3	120.9	19.2	1.82
WE052D0	559.5	560	262.7	92.5	24.3	1.28
WE052D0	560	560.5	289.7	105.0	20.2	0.99
WE052D0	560.5	560.97	221.4	81.1	14.4	1.32
WE052D0	560.97	561.5	201.9	71.7	13.9	1.37
WE052D0	561.5	562.18	220.4	73.5	17.1	1.52
WE052D0	562.18	562.55	211.7	76.2	16.9	0.59
WE052D0	562.55	563	248.8	90.4	19.1	0.94
WE052D0	563	563.74	233.3	87.0	17.4	0.29
WE052D0	563.74	564.4	141.9	52.4	13.1	0.46
WE052D0	564.4	565.25	222.1	79.9	16.4	0.91
WE052D0	565.25	566	269.1	97.1	23.0	1.35
WE052D0	566.5	567	272.6	100.0	24.2	0.62
WE052D0	567	567.36	360.5	132.8	23.5	0.98
WE052D0	568	568.69	272.1	99.3	16.1	1.24
WE052D0	568.69	569	154.6	55.0	12.8	0.78
WE052D0	569	569.5	138.9	49.2	12.6	1.58
WE052D0	569.5	570	147.3	53.1	11.2	1.34

WE052D0	570	570.5	392.3	53.4	21.0	1.24
WE052D0	570.5	571	253.2	93.9	26.2	0.84
WE052D0	571	571.5	178.3	69.8	27.1	0.26
WE052D0	571.5	572	178.7	60.2	14.6	0.55
WE052D0	572	572.5	179.2	63.4	12.2	0.82
WE052D0	572.5	573	156.8	55.5	13.1	0.61
WE052D0	573	573.5	208.6	80.2	14.9	1.41
WE052D0	573.5	574	188.8	65.2	13.4	0.60
WE052D0	574	574.5	216.7	74.0	10.6	0.76
WE052D0	574.5	575	121.3	47.5	10.5	0.19
WE052D0	575	575.5	129.4	53.5	11.9	0.67
WE052D0	575.5	576	146.4	56.3	10.7	1.12
WE052D0	576	576.5	143.5	57.6	10.9	0.92
WE052D0	576.5	577	172.5	73.9	14.2	1.06
WE052D0	577	577.5	188.8	74.9	15.0	0.33
WE052D0	577.5	578	81.4	33.0	8.8	0.45
WE052D0	578	578.46	148.3	61.2	10.9	0.74
WE052D0	578.46	579	148.1	64.6	10.8	0.37
WE052D0	579	580	29.6	8.5	4.2	0.24
WE052D0	580	581	11.1	5.6	5.6	0.18
WE052D0	583.34	584	126.0	47.8	8.7	0.23
WE052D0	584	585	50.6	21.7	7.2	0.14
WE052D0	585	585.41	5.7	5.7	5.7	0.17
WE052D0	585.41	586	15.0	15.0	15.0	0.07
WE052D0	588	589	95.7	53.2	10.6	0.09
WE052D0	589	590	152.9	53.7	12.4	0.73
WE052D0	590	591	177.8	69.5	14.3	0.49
WE052D0	591.36	592.26	83.4	27.8	13.9	0.07
WE052D0	592.26	593	3.2	1.6	1.6	0.62
WE052D0	593	594	12.4	49.4	12.4	0.08
WE052D0	594	595	51.2	19.2	6.4	0.16
WE052D0	599	600	123.2	56.0	7.5	0.54
WE052D0	600	601	105.5	52.8	5.9	0.17
WE052D0	602	603	83.0	35.6	11.9	0.08
WE052D0	603	604	272.6	97.6	16.3	0.25
WE052D0	604	605	68.4	30.4	7.6	0.13
WE052D0	605	606	181.0	69.0	17.2	0.23
WE052D0	606	607	227.3	66.8	10.8	0.55
WE052D0	607	608	336.0	127.9	29.7	0.34
WE052D0	608	608.52	170.8	69.4	16.0	0.19
WE052D0	608.52	609.51	47.5	47.5	47.5	0.02
WE054D0	346	347	149.8	77.9	12.0	0.33
WE054D0	348	348.7	172.9	67.5	12.7	0.47
WE054D0	348.7	349	265.4	97.8	19.6	0.36
WE054D0	349	349.5	188.1	71.6	14.0	0.71
WE054D0	349.5	350	124.6	45.8	7.9	0.63
WE054D0	350	350.5	229.8	92.3	15.1	0.53
WE054D0	350.5	351	153.5	73.2	9.4	0.42

WE054D0	351	351.5	187.3	69.8	12.9	0.54
WE054D0	351.5	352	187.5	74.3	11.8	0.59
WE054D0	352	352.5	202.0	76.6	13.9	0.72
WE054D0	352.5	353	250.5	97.7	21.3	1.27
WE054D0	353	353.5	265.4	102.8	23.9	0.42
WE054D0	353.5	353.91	414.6	222.1	25.2	1.11
WE054D0	353.91	354.45	214.3	84.6	22.6	0.35
WE054D0	354.45	355.04	183.2	65.0	13.3	1.51
WE054D0	355.04	355.4	243.8	245.8	30.7	0.49
WE054D0	355.4	355.8	466.2	223.1	30.8	0.55
WE054D0	355.8	356.2	160.4	56.3	10.1	0.69
WE054D0	356.2	356.61	175.9	83.6	11.0	0.45
WE054D0	356.61	357	194.2	97.1	19.4	0.31
WE054D0	357	357.5	162.2	60.3	15.1	0.27
WE054D0	357.5	358.1	344.7	124.4	24.9	0.28
WE054D0	358.1	358.6	137.1	58.8	11.2	0.36
WE054D0	358.6	359	199.6	89.7	13.0	0.69
WE054D0	359	359.5	111.7	57.4	9.1	0.33
WE054D0	359.5	360	125.1	69.2	8.9	0.45
WE054D0	360	360.5	91.6	43.1	8.1	0.37
WE054D0	361	361.5	185.3	71.7	14.9	0.33
WE054D0	361.5	362	254.9	92.8	20.5	1.37
WE054D0	362	362.5	234.2	88.9	16.3	0.92
WE054D0	362.5	363	232.4	80.4	16.1	1.12
WE054D0	363	363.5	196.3	74.7	13.9	1.00
WE054D0	363.5	364	142.5	62.5	10.4	0.29
WE054D0	364	364.5	189.9	85.7	14.9	0.27
WE054D0	364.5	365	165.5	71.6	11.2	0.45
WE054D0	365	365.5	269.4	106.1	18.0	0.61
WE054D0	365.5	365.92	266.1	112.0	31.5	0.29
WE054D0	365.92	366.4	179.3	68.4	15.5	0.78
WE054D0	366.4	366.9	211.2	85.9	14.6	0.69
WE054D0	366.9	367.24	221.0	89.6	12.3	1.22
WE054D0	367.24	367.76	277.9	109.9	16.4	1.16
WE054D0	367.76	368.2	181.9	75.0	11.8	1.44
WE054D0	368.2	368.6	344.7	149.1	22.8	0.97
WE054D0	368.88	369.4	306.2	81.4	20.7	0.82
WE054D0	369.4	369.84	363.4	147.9	26.8	0.71
WE054D0	369.84	370.5	125.4	52.7	9.1	0.55
WE054D0	370.5	371	173.5	61.9	13.8	2.68
WE054D0	371	371.5	221.5	118.2	11.1	1.35
WE054D0	371.5	372	260.0	89.4	24.6	1.34
WE054D0	372	372.5	240.8	87.7	15.5	2.06
WE054D0	372.5	372.84	95.5	32.3	7.4	3.37
WE054D0	372.84	373.43	165.5	61.5	12.4	2.02
WE054D0	373.43	373.7	150.4	54.9	12.0	2.75
WE054D0	373.7	374	110.2	44.7	6.8	2.37
WE054D0	374	374.5	134.0	45.5	9.8	1.63

WE054D0	374.5	375	165.5	58.1	13.7	2.05
WE054D0	375	375.5	186.1	57.8	23.1	0.78
WE054D0	375.5	376	100.9	50.7	8.4	2.27
WE054D0	376	376.29	273.2	101.0	18.3	1.04
WE054D0	376.29	377.03	310.5	109.6	24.6	1.14
WE054D0	377.03	377.5	283.5	123.3	23.1	0.65
WE054D0	377.5	378.04	288.0	110.9	20.0	0.65
WE054D0	378.04	378.5	180.1	68.7	13.6	1.69
WE054D0	378.5	378.98	211.9	83.8	14.6	1.72
WE054D0	378.98	379.5	214.1	79.2	15.9	2.01
WE054D0	379.5	380	132.9	51.7	8.0	1.63
WE054D0	380	380.26	343.6	96.4	21.4	1.31
WE054D0	380.26	380.52	407.6	168.9	26.0	0.85
WE054D0	380.52	381	324.4	119.6	17.9	0.73
WE054D0	381	381.5	211.3	82.3	13.7	1.75
WE054D0	381.5	382	320.1	138.3	26.8	0.90
WE054D0	382	382.5	254.9	102.9	19.4	0.67
WE054D0	382.91	383.41	289.4	183.2	22.3	0.99
WE054D0	383.41	383.9	200.3	94.5	15.1	0.53
WE054D0	383.9	384.51	208.7	87.2	12.0	0.58
WE054D0	384.51	385	217.1	99.1	14.2	0.64
WE054D0	385	385.5	382.7	167.1	30.4	0.66
WE054D0	385.5	386.07	326.4	122.4	21.6	0.42
WE054D0	386.4	386.84	59.5	31.2	5.7	0.35
WE054D0	386.84	387.2	145.3	69.9	8.4	0.36
WE054D0	387.2	387.7	148.8	63.4	13.8	0.36
WE054D0	387.7	388.2	147.7	59.4	11.6	0.69
WE054D0	388.2	388.69	121.8	55.8	12.4	0.48
WE054D0	388.69	389	181.2	83.5	9.0	0.78
WE054D0	389.5	390	133.2	54.7	11.9	0.42
WE054D0	390.5	391	175.9	66.8	14.1	0.28
WE054D0	392	392.5	207.0	80.9	12.9	0.62
WE054D0	392.5	393	170.2	56.1	11.0	1.00
WE054D0	393	393.48	164.7	60.6	12.0	2.16
WE054D0	393.48	394	237.1	60.2	14.7	3.67
WE054D0	394	394.5	149.3	58.8	12.2	2.06
WE054D0	394.5	395	203.8	64.5	17.3	0.87
WE054D0	395	395.5	117.4	44.8	9.3	1.29
WE054D0	395.5	396	162.0	69.8	16.8	0.36
WE054D0	396	396.5	111.9	38.2	8.2	0.73
WE054D0	396.5	396.8	73.4	26.7	8.3	0.60
WE054D0	396.8	397.2	172.2	55.8	14.0	0.21
WE054D0	397.2	397.5	199.4	104.9	8.1	0.87
WE054D0	397.5	398	99.4	82.8	8.3	0.12
WE054D0	398.5	399	21.2	42.3	10.6	0.09
WE054D0	399	399.5	54.5	38.9	15.6	0.13
WE054D0	400	400.5	25.2	25.2	12.6	0.08
WE054D0	401.5	402	11.2	16.8	5.6	0.18

WE054D0	403	403.5	7.5	22.4	7.5	0.13
WE054D0	404.5	405	18.3	18.3	9.1	0.11
WE054D0	405	405.45	44.0	8.8	8.8	0.11
WE054D0	405.45	405.76	17.2	8.6	8.6	0.12
WE054D0	405.76	406.06	21.0	9.3	1.6	1.29
WE054D0	406.06	406.32	82.5	29.9	5.1	2.34
WE054D0	406.32	406.6	84.7	25.8	4.8	2.48
WE054D0	406.6	407	67.4	22.7	3.5	2.55
WE054D0	407	407.5	82.9	27.6	5.6	1.95
WE054D0	407.5	408	88.2	33.8	9.4	0.53
WE054D0	408	408.5	37.4	13.2	4.4	0.45
WE054D0	408.5	408.76	70.2	23.4	13.2	0.98
WE054D0	409	410	233.2	94.7	14.6	0.14
WE054D0	410	411	31.2	12.5	6.2	0.16
WE054D0	411	412	20.9	8.4	4.2	0.24
WE054D0	412	413	73.3	36.6	10.5	0.19
WE054D0	413	414	103.0	179.0	5.4	0.18
WE054D0	414	415	135.4	49.5	10.4	0.38
WE054D0	415	416	83.1	31.8	4.9	0.41
WE054D0	416	417	44.5	13.2	2.4	0.83
WE054D0	417	417.39	40.9	17.1	3.4	0.59
WE054D0	417.39	418	41.7	33.3	4.2	0.24
WE054D0	418	419	32.7	9.6	1.9	0.52
WE054D0	419	420	9.3	9.3	9.3	0.11
WE054D0	420	421	27.5	16.5	5.5	0.18
WE054D0	421	422	56.2	24.1	5.3	0.37
WE054D0	422	423	90.3	30.1	5.3	0.56
WE054D0	423	424	7.8	7.8	7.8	0.13
WE054D0	424	425.15	9.0	9.0	9.0	0.11
WE054D0	425.15	425.7	66.5	18.4	4.6	0.44
WE054D0	425.7	426.38	50.9	15.3	1.7	0.59
WE054D0	426.38	427	4.9	4.9	4.9	0.21
WE064D0	271.35	271.81	1806.8	561.6	146.5	0.04
WE064D0	276.75	277.43	18.7	13.4	5.4	0.37
WE064D0	284.58	285	137.8	69.8	12.9	0.54
WE064D0	285	285.5	148.2	75.6	11.9	0.67
WE064D0	285.5	286	247.9	122.4	18.4	0.33
WE064D0	286.5	287.11	636.7	315.7	26.8	0.19
WE064D0	287.11	287.83	137.9	58.9	8.8	0.80
WE064D0	287.83	288.5	58.2	20.1	9.0	1.00
WE064D0	288.5	289	266.2	104.7	20.5	0.44
WE064D0	289	289.5	59.2	26.7	4.3	1.38
WE064D0	289.5	290	145.3	69.3	13.4	0.45
WE064D0	290	290.44	96.2	53.5	10.7	0.19
WE064D0	290.44	291	188.5	81.6	23.0	0.87
WE064D0	291	291.5	223.5	105.8	26.1	0.77
WE064D0	291.5	292	152.3	63.1	13.1	0.46
WE064D0	292	292.5	185.2	61.7	18.7	0.53

WE064D0	292.5	293	149.9	56.6	8.9	0.90
WE064D0	293	293.5	189.6	136.0	12.4	0.24
WE064D0	295.47	296	282.1	130.5	11.0	1.09
WE064D0	296	296.5	226.1	83.0	16.6	0.48
WE064D0	296.5	297	225.9	77.0	15.7	1.78
WE064D0	297	297.5	246.4	97.0	16.7	1.68
WE064D0	297.5	298	225.5	84.9	15.8	1.58
WE064D0	298.5	299	243.6	86.2	23.7	0.46
WE064D0	299	299.5	217.4	130.4	18.4	0.76
WE064D0	299.5	300	113.6	43.8	9.3	1.62
WE064D0	300	300.5	179.1	70.8	13.9	1.44
WE064D0	300.5	300.75	132.4	47.9	9.6	1.15
WE064D0	300.75	301.5	176.3	56.6	13.3	0.30
WE064D0	301.5	302	281.8	95.9	12.0	0.50
WE064D0	302	302.5	183.3	89.4	22.4	0.22
WE064D0	302.5	303.19	111.7	52.5	10.9	0.46
WE064D0	303.19	303.44	93.7	39.7	8.0	2.11
WE064D0	303.44	303.85	227.2	91.9	17.9	0.39
WE064D0	303.85	304.2	239.8	131.2	17.6	0.97
WE064D0	304.45	305	210.3	160.3	46.2	0.78
WE064D0	305	305.5	80.0	34.9	4.8	1.46
WE064D0	305.5	306	108.1	41.9	9.2	1.19
WE064D0	306	306.5	88.4	36.0	9.4	1.28
WE064D0	306.5	307	50.4	19.8	7.8	1.67
WE064D0	307	307.5	72.9	31.6	5.4	1.84
WE064D0	307.5	307.92	65.2	24.1	5.4	2.78
WE064D0	307.92	308.5	140.7	51.6	10.3	0.77
WE064D0	308.5	309	142.7	46.4	8.9	0.56
WE064D0	309	309.5	60.4	28.7	2.9	0.35
WE064D0	309.5	310	162.1	83.6	12.2	0.57
WE064D0	310	310.5	133.7	49.1	11.0	0.82
WE064D0	311.5	312	69.5	24.4	5.6	0.53
WE064D0	312	312.5	83.5	22.5	5.6	1.07
WE064D0	312.5	313	103.4	51.7	9.4	0.21
WE064D0	313	313.5	109.9	37.5	8.7	0.80
WE064D0	313.5	314	112.8	42.7	7.6	0.66
WE064D0	314	314.5	78.3	25.9	5.3	1.89
WE064D0	314.5	315	93.7	32.5	9.1	1.54
WE064D0	315	315.42	86.9	27.3	5.1	0.59
WE064D0	315.42	316	141.8	44.5	4.2	0.47
WE064D0	316	316.5	139.3	34.8	6.5	0.46
WE064D0	317	317.5	23.7	11.9	11.9	0.08
WE064D0	317.5	318	32.4	14.7	2.9	0.68
WE064D0	318	318.5	151.8	60.5	6.4	0.78
WE064D0	318.5	319	81.9	28.4	8.4	0.60
WE064D0	319	319.5	48.4	18.4	3.9	2.07
WE064D0	319.5	320	58.3	25.0	4.2	0.24
WE064D0	320	320.5	44.9	16.7	2.6	0.78

WE064D0	321	321.35	146.7	50.4	4.6	0.22
WE064D0	321.35	321.8	61.0	38.5	3.2	0.31
WE064D0	321.8	322.5	23.4	9.4	9.4	0.21
WE064D0	322.5	323	7.9	7.9	7.9	0.13
WE064D0	323	324	10.0	10.0	10.0	0.10
WE064D0	324	325	10.1	10.1	10.1	0.10
WE064D0	325	326	10.7	10.7	10.7	0.09
WE064D0	326	327	9.9	9.9	9.9	0.10
WE064D0	327	328	3.1	3.1	9.2	0.32
WE064D0	328	328.25	3.6	3.6	7.2	0.28
WE064D0	328.25	329	4.9	4.9	4.9	0.20
WE064D0	329	330	5.4	5.4	5.4	0.19
WE064D0	330	331	0.9	0.9	0.9	1.12
WE064D0	331	332	1.4	1.4	1.4	0.70
WE064D0	332	333	4.8	4.8	4.8	0.21
WE064D0	333	334	8.9	8.9	8.9	0.11
WE064D0	334	335	1.3	1.3	1.3	0.79
WE064D0	335	336	0.7	0.7	0.7	1.52
WE064D0	336	337	0.5	0.5	2.3	2.18
WE064D0	337	338	1.2	1.2	1.2	0.81
WE064D0	338	339	1.4	1.4	2.9	0.70
WE064D0	339	339.79	0.8	0.8	0.8	1.22
WE117D0	247	248	51.8	88.1	5.2	0.19
WE117D0	248	248.5	16.7	13.4	3.3	0.30
WE117D0	248.5	249	18.2	14.5	3.6	0.27
WE117D0	249	249.5	153.3	58.8	11.6	1.21
WE117D0	249.5	249.87	167.3	64.6	13.6	1.18
WE117D0	249.87	250.38	147.5	51.4	14.1	1.21
WE117D0	250.38	251	147.3	49.4	12.6	1.20
WE117D0	251	251.5	156.8	61.8	16.0	0.87
WE117D0	251.5	252.06	190.1	60.6	13.8	0.73
WE117D0	252.06	252.49	230.0	66.1	8.8	1.70
WE117D0	252.49	252.74	45.4	23.4	4.8	3.54
WE117D0	252.74	253	73.4	27.1	5.1	3.95
WE117D0	253	253.5	229.9	59.6	73.8	1.19
WE117D0	253.5	253.8	303.5	83.0	27.2	1.58
WE117D0	253.8	254.05	212.0	85.9	15.4	2.34
WE117D0	254.05	254.5	202.9	72.2	14.3	2.10
WE117D0	254.5	255	204.2	83.3	11.8	1.86
WE117D0	255	255.25	181.2	67.2	10.5	2.68
WE117D0	255.25	255.5	167.9	68.2	8.2	1.33
WE117D0	255.5	256	202.6	75.7	17.0	0.53
WE117D0	256	256.5	354.0	84.4	48.8	1.21
WE117D0	256.5	257	267.2	92.2	18.9	0.95
WE117D0	257	257.5	249.2	83.8	13.6	0.44
WE117D0	257.5	257.86	335.1	90.8	124.1	0.78
WE117D0	257.86	258.2	177.0	66.2	14.5	0.97
WE117D0	258.2	258.5	57.0	19.0	5.9	0.84

WE117D0	258.5	259	154.1	56.5	13.7	0.66
WE117D0	259	259.6	88.1	34.0	8.0	0.50
WE117D0	259.6	260	145.4	57.2	10.1	1.29
WE117D0	260	260.5	21.2	12.1	1.5	0.66
WE117D0	263.5	263.84	19.3	15.4	3.9	0.26
WE117D0	263.84	264.1	107.1	133.9	26.8	0.15
WE117D0	264.1	264.73	132.4	80.2	18.1	0.50
WE117D0	264.73	265	57.0	41.4	5.2	0.39
WE117D0	265.5	266	77.4	48.9	4.1	0.25
WE117D0	266	266.5	129.0	73.7	3.7	0.27
WE117D0	266.5	267	44.6	67.0	3.7	0.27
WE117D0	267	267.5	82.7	48.8	3.8	0.27
WE117D0	267.5	268	63.7	37.5	3.7	0.27
WE117D0	268	268.5	10.7	6.1	1.5	1.31
WE117D0	269.5	270	120.9	50.9	6.4	0.63
WE117D0	270	270.5	158.6	48.1	12.5	0.56
WE117D0	271	271.5	237.3	69.3	21.3	0.75
WE117D0	271.5	272	172.3	70.2	15.2	1.98
WE117D0	272	272.5	151.0	51.9	9.2	2.29
WE117D0	272.5	273	191.4	83.9	10.7	1.31
WE117D0	273	273.45	100.8	36.3	4.8	1.24
WE117D0	274.5	275	221.2	95.6	15.0	0.53
WE117D0	275	275.48	194.4	88.6	10.0	1.69
WE117D0	275.48	276	139.7	62.5	10.0	1.30
WE117D0	276	276.5	238.3	109.0	17.1	0.94
WE117D0	276.5	277	128.5	69.6	8.9	0.56
WE117D0	279.9	280.2	180.1	50.8	13.9	0.22
WE117D0	280.2	281	83.2	45.2	4.8	0.84
WE117D0	281	281.5	85.1	35.0	6.1	0.66
WE117D0	281.5	282	143.4	58.1	17.1	0.59
WE117D0	282	282.5	175.8	63.5	10.9	1.37
WE117D0	282.5	283	204.2	69.3	10.2	1.08
WE117D0	283	283.5	236.1	75.7	18.4	1.47
WE117D0	283.5	284	199.4	78.6	12.5	0.88
WE117D0	284	284.6	197.2	77.6	15.3	1.96
WE117D0	284.6	285	143.5	54.8	7.8	1.92
WE117D0	285	285.5	145.4	79.8	9.3	1.62
WE117D0	285.5	286	147.3	64.5	10.6	1.04
WE117D0	286	286.5	176.1	61.2	11.0	0.82
WE117D0	286.5	287	170.8	66.7	10.2	2.65
WE117D0	287	287.5	150.1	60.6	11.0	1.45
WE117D0	287.5	288	167.7	75.0	10.6	1.97
WE117D0	288	288.5	192.9	82.0	11.4	2.11
WE117D0	288.5	289	181.6	73.8	10.8	1.76
WE117D0	289	289.5	167.7	73.6	10.7	2.05
WE117D0	289.5	290	146.1	73.4	10.2	1.57
WE117D0	290	290.5	136.3	54.0	16.2	0.74
WE117D0	290.5	291	134.0	60.9	11.0	1.54

WE117D0	291	291.5	170.3	71.3	4.9	1.84
WE117D0	291.5	292.09	136.1	32.4	7.9	1.39
WE117D0	292.09	292.35	139.5	57.9	11.4	0.97
WE117D0	292.35	293	140.3	27.1	11.2	0.63
WE117D0	293	293.5	126.0	28.7	6.7	1.50
WE117D0	293.5	293.75	167.8	51.7	9.3	2.15
WE117D0	293.75	294.11	256.1	71.5	7.0	1.85
WE117D0	294.11	294.5	137.0	45.4	7.7	1.17
WE117D0	294.5	295	124.9	47.2	8.4	0.95
WE117D0	295	295.68	124.2	63.8	10.5	2.38
WE117D0	295.68	296	163.9	62.2	10.4	1.06
WE117D0	296	296.5	90.9	33.0	4.5	1.12
WE117D0	296.5	297	164.8	53.8	11.0	0.91
WE117D0	297	297.5	115.7	68.3	6.6	1.05
WE117D0	297.5	298	115.1	45.1	12.0	2.08
WE117D0	298	298.5	76.5	28.7	10.4	1.25
WE117D0	298.5	299	211.6	85.0	12.1	0.58
WE117D0	299	299.5	154.1	57.2	9.9	0.40
WE117D0	299.5	300	171.2	66.9	13.4	0.37
WE117D0	300	300.5	52.1	19.6	6.5	0.15
WE117D0	300.5	301	147.8	61.2	10.2	0.39
WE117D0	301	301.5	49.0	4.5	8.9	0.22
WE117D0	301.5	302	88.7	30.1	6.0	0.67
WE117D0	302	302.5	139.6	34.9	15.5	0.26
WE117D0	302.5	303	57.8	14.0	6.0	0.50
WE117D0	303	303.5	9.9	9.9	9.9	0.10
WE117D0	303.5	304	5.4	5.4	5.4	0.18
WE117D0	304	304.5	89.6	36.9	5.3	0.95
WE117D0	304.5	305	102.6	44.8	1.8	2.85
WE117D0	305	305.5	46.5	19.7	5.4	0.56
WE117D0	305.5	306	47.9	37.3	8.1	1.23
WE117D0	306	306.5	63.3	10.2	3.4	0.88
WE117D0	306.5	307.07	74.5	27.0	5.7	1.22
WE117D0	307.07	307.5	54.6	25.3	4.9	1.23
WE117D0	307.5	308	60.2	26.6	5.6	0.71
WE117D0	308	308.5	79.2	31.3	6.0	1.50
WE117D0	308.5	309	66.6	25.7	6.4	1.25
WE117D0	309	309.5	89.4	34.5	6.4	0.78
WE117D0	309.5	310	71.7	21.5	7.2	0.28
WE117D0	310	310.5	67.9	26.0	6.0	0.50
WE117D0	310.5	311	196.4	75.6	15.1	0.33
WE117D0	311	311.5	51.4	19.2	4.0	0.99
WE117D0	311.5	311.86	62.8	23.2	18.4	1.04
WE117D0	311.86	312.65	1.1	1.1	1.1	0.90
WE117D0	312.65	313	26.2	9.4	3.7	0.53
WE117D0	313	313.5	75.7	26.8	4.8	1.04
WE117D0	313.5	314	62.8	24.9	8.3	0.84
WE117D0	314	314.5	90.5	33.6	5.1	0.98

WE117D0	314.5	315	85.6	31.8	6.6	0.91
WE117D0	315	315.54	75.3	28.7	7.2	0.28
WE117D0	315.54	316	62.1	21.9	5.5	0.55
WE117D0	316	316.5	42.9	21.5	7.2	0.14

Appendix 4

T Zone lateral tenor variations (Average)																		
BHID	YTP	XPT	ZPT	T0_Pd	T0_Pt	T0_Au	UPA_Pd	UPA_Pt	UPA_Au	T1_Pd	T1_Pt	T1_Au	LPA_Pd	LPA_Pt	LPA_Au	T2_Pd	T2_Pt	T2_Au
WB222D1	-2587817	-11892.1	1006.126	84	52	11										203	100	52
WB221D0	-2587755	-11830.5	1007.437	41	41	19										163	94	65
WB213D0	-2587691	-11765.3	1009.136				69	56	31	99	70	29	60	26	25	47	79	84
WB215D0	-2587565	-11641.3	1013.448				154	91	55	79	61	31	203	123	60			
WB237D0	-2587591	-11667.6	1012.974				273	182	67	93	52	30	167	98	68	99	78	73
WB228D0	-2587692	-12015.9	1007.254	23	17	17							397	186	47	193	106	77
WB230D0	-2587692	-11888.8	1008.598	197	86	39							179	76	41	287	106	64

F Zone lateral tenor variations (Average)									
BHID	YTP	XPT	ZPT	FP_Pd	FP_Pt	FP_Au	FH_Pd	FH_Pt	FH_Au
WB280D0	-2585943	-9830.92	1046.884				340	138	21
WB259D0	-2585940	-9767.46	1046.116	364	166	23	283	128	20
WB257D0	-2585941	-9640.8	1044.763	133	51	15	240	97	15
WB276D0	-2586004	-9955.57	1047.55				275	111	18
WB264D1	-2585940	-9892.76	1047.81	266	115	18	278	119	21
WB261D0	-2585814	-9643.27	1047.3				343	149	23
WB255D0	-2584754	-8955.17	1063.047	135	55	11	172	73	18
WB254D0	-2584816	-8891.09	1061.188	90	38	7	146	68	13
WE144D0	-2583748	-8641.59	1076.735				113	56	10
WE145D0	-2583785	-8611.49	1075.56				124	64	10
WE061D0	-2583758	-8577.11	1075.209				237	116	20
WE052D0	-2582761	-8060.74	1061.556	189	73	14	186	73	15
WE054D0	-2582790	-7836.24	1056.2	173	70	13	208	90	16
WE064D0	-2582800	-7699.84	1053.123	147	61	12	194	91	14
WE117D0	-2582818	-7639.67	1051.799	131	50	9	147	60	14
WE120D0	-2582939	-8014.53	1060.149	102	37	8	178	72	14

All the coordinates are in WGS84 LO29 format.

Appendix 5

UmS (F Zone) Cu/Pd ratios_Lateral variations (Average)

BHID	YTP	XPT	ZPT	FH Cu/Pd	FP Cu/Pd	TGA Cu/Pd
WB280D0	-2585943	-9830.92	1046.884	61.8		
WB259D0	-2585940	-9767.46	1046.116	166.35	30.51	
WB257D0	-2585941	-9640.8	1044.763	64.5	59.15	58.36
WB276D0	-2586004	-9955.57	1047.55	87.12		
WB264D0	-2585940	-9892.76	1047.81	51.61	45.28	
WB261D0	-2585814	-9643.27	1047.3	68.68		
WB255D0	-2584754	-8955.17	1063.047	107.4	94.36	
WB254D0	-2584816	-8891.09	1061.188	182.51	123.15	
WE144D0	-2583748	-8641.59	1076.735	119.51		
WE145D0	-2583785	-8611.49	1075.56	60.75	177.17	
WE061D0	-2583758	-8577.11	1075.209	72.72		
WE052D0	-2582761	-8060.74	1061.556	65.69	53.08	
WE054D0	-2582790	-7836.24	1056.2	50.7	129.85	
WE064D0	-2582800	-7699.84	1053.123	75.27	99.5	
WE117D0	-2582818	-7639.67	1051.799	74.65	104.54	
WE120D0	-2582939	-8014.53	1060.149	50.04	65.82	

T Zone Cu/Pd ratios_Lateral variations (Average)

BHID	YTP	XPT	ZPT	T0 Cu/Pd	T2 Cu/Pd	LPA Cu/Pd
WB222D1	-2587817	-11892.1	1006.126	519.59	94.83	
WB221D0	-2587755	-11830.5	1007.437	475.66	175.94	
WB213D0	-2587691	-11765.3	1009.136	732.08	310.95	
WB215D0	-2587565	-11641.3	1013.448	161.12		255.04
WB237D0	-2587591	-11667.6	1012.974	79.44		235.28
WB228D0	-2587692	-12015.9	1007.254	693.31	100.5	
WB230D0	-2587692	-11888.8	1008.598	104.17	297.72	

All the coordinates are in WGS84 LO29 format.

Appendix 6

Data for metal balance (metal basket) within Bushveld Complex

	Pt	Pd	Au	Rh	4E	%Pt	%Pd	%Rh	%Au	
LMZ	2.73	5	0.49		8.22	33	61	0	6	HW024
						%Pt	%Pd	%Rh	%Au	
UMZ	0.87	0.51	2.33		3.71	23	14	0	63	HW029
						%Pt	%Pd	%Rh	%Au	
T ZONE	1.23	2.1	0.82	0.02	4.17	29	50	0.5	20	
						%Pt	%Pd	%Rh	%Au	
F ZONE	0.91	2.01	0.15	0.05	3.12	29	64	1.6	5	
						%Pt	%Pd	%Rh	%Au	
Unit 1	0.09	0.07	0.00	0.00	0.16	54	43	0.4	3	P15
						%Pt	%Pd	%Rh	%Au	
Upper min	0.304	0.312	0.298	0.00149	0.92	33	34	0.16	33	P11
						%Pt	%Pd	%Rh	%Au	
Turfspruit	1.68	1.7	0.28	0.11	3.77	45	45	3	7	
		The assay data is not known. Only metal percentages data by Kinnaird (2005) was obtained.				%Pt	%Pd	%Rh	%Au	
UG2						59	29	11	1	
						%Pt	%Pd	%Rh	%Au	
Merensky						63	28	4.5	4.5	
						%Pt	%Pd	%Rh	%Au	
Mogalakwena						44.26	47.24	3.6	4.9	